Immunisation with recombinant polymorphic membrane protein D elicits robust protection against sexually transmitted *Chlamydia trachomatis* infection

Implications for the development of novel chlamydial vaccines

William Neville Wayne Paes

University of York

Department of Biology

September 2015

Abstract

Chlamydia trachomatis (*Ct*) is the most common sexually transmitted bacterial pathogen worldwide, responsible for ~90 million new cases of disease each year, with asymptomatic infections giving rise to sequelae such as pelvic inflammatory disease, ectopic pregnancy and infertility in women. Aggressive 'seek and treat' public health measures have not stemmed the rise of *Ct* infections, leading to proposal of the 'arrested immunity' hypothesis, where herd immunity within a population is blunted following earlier treatment with antibiotics. This suggests vaccination as the next key step in potentially eliminating *Ct* infections. Due to the paucity of robust clinical data, protective immune parameters have largely been derived from studies in mice, where pathogen-specific Th1-type immunity involving CD4$^+$ T cells has been the focus of preclinical vaccine development. Our study represents the first preclinical characterization of a novel, rationally designed second-generation lipid adjuvant (SLA) in combination with the highly conserved recombinant *Ct* polymorphic membrane protein D (rPmpD) antigen. We demonstrate robust protection against urogenital *Ct* infection in the C57BL/6 murine model, characterized by significantly enhanced resistance to infection and reduction in mean bacterial load. However, enhanced Th1-type immunity was not found to correlate with relative protection, which rather coincided with the presence of robust rPmpD-specific serum and cervico-vaginal IgG titres. Prior to our study, the only convincing evidence of neutralizing antibodies effecting protection against chlamydial infection *in vivo* has emerged from studies employing the antigenically variable *Ct* MOMP as a vaccine immunogen. We propose that anti-rPmpD antibodies may play a significant role in vaccine-induced protection against urogenital *Ct* challenge, and that the role of antibodies warrants further investigation in future *Ct* vaccine development.

Table of contents

4. Chapter 4: Biophysical characterization of *Chlamydia trachomatis* polymorphic membrane protein D – a candidate vaccine antigen

5. Chapter 5: Investigation of the putative function of PmpD as a chlamydial adhesin *in vitro*

List of figures

Chapter 4: Biophysical characterization of *Chlamydia trachomatis* polymorphic membrane protein D – a candidate vaccine antigen

Chapter 5: Investigation of the putative function of PmpD as a chlamydial adhesin *in vitro*

Chapter 6: Investigation of a novel second-generation lipid adjuvant (SLA) in combination with rPmpD as a preclinical *Ct* vaccine

List of tables

Acknowledgements

Author's declaration

All data presented in this thesis are original and performed by myself, unless stated otherwise. This work has not previously been presented for an award at this, or any other University. All sources are acknowledged as References. Publications associated with this thesis include the following manuscripts that have been accepted or are under review:

Alexander Badamchi-Zadeh; Paul F McKay; Martin J Holland; **Wayne Paes**; Andrzej Brzozowski; Charles Lacey; Frank Follmann; John S Tregoning; Robin J. Shattock (2015) Intramuscular immunization with chlamydial proteins induces *Chlamydia trachomatis* specific ocular antibodies **PlosOne**

Under review
Wayne Paes, Naj Brown, Andrzej Brzozowski, Rhea Coler, Steve Reed, Darrick Carter, Martin Bland, Paul M. Kaye, Charles J.N. Lacey (2016) Immunisation with recombinant PmpD elicits robust protection against intra-vaginal *Chlamydia trachomatis* infection **Journal of Immunology**

Chapter 1: General Introduction

1.1 *Chlamydia trachomatis*

Chlamydia trachomatis (*Ct*) is a Gram-negative obligate intracellular bacterial pathogen of humans, and the causative agent of sexually transmitted disease and blinding trachoma. Indeed, the first reliable mentions of ocular disease were documented in the Ebers papyrus as early as 1553-1550 BC (Clarke, 2011). However, despite these early records, little is known about the origins of *Ct*, and no evidence of a common ancestor has been isolated from primates, our closest living relatives. These observations indicate that *Ct* is an ancient pathogen, likely to have co-evolved solely with humans for millennia.

Halberstaedter and von Prowazek first described these organisms in 1907 through examination of trachoma patient isolates (Clarke, 2011). Staining revealed that *Ct* elementary bodies (EBs) were cloaked within a membranous compartment in host cells. Assuming these organisms to be protozoan, the discoverers originally named them 'chlamydozoa', after the Greek word 'χλαμύδα' meaning 'cloak'. However, a seminal breakthrough occurred in 1957, when propagation of *Ct* in hens' eggs by T'ang and colleagues allowed for preservation and culture of the *Chlamydia*, when it was subsequently observed that *Ct* possessed a cell wall, and further showed susceptibility to antibiotics, resulting in classification as a distinct species within a unique bacterial phylum now known as the *Chlamydiales* (Moulder, 1966).

1.2 Life Cycle of the *Chlamydiales*

The *Chlamydiales* all undergo a unique biphasic developmental cycle, and nearly all related species possess a distinctive outer membrane complex (COMC) that differs

entirely in composition from all other bacteria (Everett and Hatch, 1995). Infectious elementary bodies (EB) are metabolically inactive (~0.3μm in diameter), and contain an exclusively cysteine-rich (Cys-rich) disulphide-linked COMC that is thought to confer extracellular osmotic stability as the functional equivalent of peptidoglycan (Hatch, 1996).

Following internalization, the EB membrane then undergoes disulphide reduction and expansion within the intracellular chlamydial inclusion as the bacterium differentiates into metabolically active and larger (~1μm) reticulate bodies (RB) that multiply through binary fission (Hatch, Allan and Pearce, 1984). After replication within the inclusion, RBs differentiate back into EBs and egress through cell lysis or extrusion to infect neighboring cells (**Fig.1.1**). In addition to the two classical EB and RB morphological phenotypes, *Ct* RBs have also evolved to combat host defence strategies through development of a persistent form. These are observed in the presence of antibiotic treatment *in vitro*, and in response to the production of host IFN-γ that leads to intracellular tryptophan starvation (Beatty et al., 1994). Following removal of IFN-γ or antibiotic treatment *in vitro*, these persistent morphotypes re-differentiate back in to infectious elementary bodies that can infect new cells (Skilton et al., 2009).

Importantly, chlamydial species are also responsible for a wide range of veterinary and opportunistic zoonotic diseases. *C.pneumoniae* is associated with atherosclerosis and non-hospital acquired pneumonia, *C.psittaci* with psittacosis outbreaks and *C.abortus* with abortion in pregnant women (Longbottom and Coulter, 2003). Thus, given the extremely high degree of genomic synteny between *Ct* and many other

established and emerging species of pathogenic *Chlamydiae* (Voigt, Schofl and Saluz, 2012), the outcomes of a wide array of independent or inter-related *Ct* research fields are also likely to have impact for the 'One Health Initiative' (Bidaisee and Macpherson, 2014).
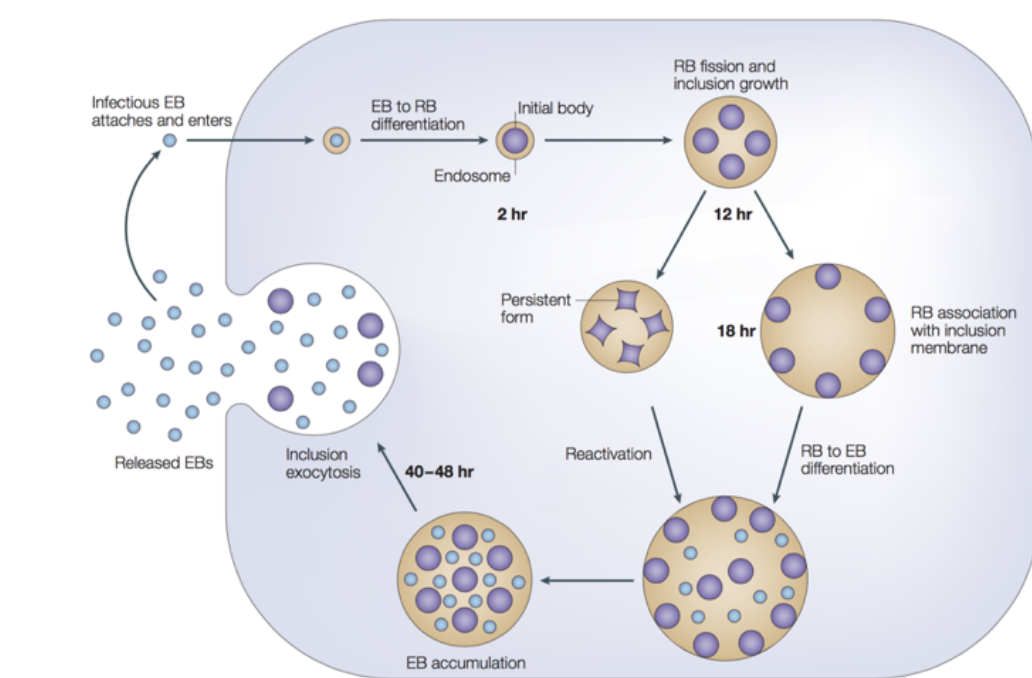
Figure 1.1: Life cycle of *Chlamydia trachomatis* (Brunham and Rey Ladino, 2005). *Chlamydia trachomatis* is an obligate intracellular pathogen of humans. *Ct* elementary bodies (EBs) infect ocular conjunctival (serovars A-C) or epithelial cells of the genital mucosa (serovars D-L3). Infectious EBs transform in to metabolically active reticulate bodies (RBs) that modify the early endosomal compartment to prevent fusion with the lysosome. Depending on the serovar, at 48-72 hours, RBs re-differentiate back in to EBs and infect neighbouring cells through extrusion or cell lysis. In addition, aberrant persistent forms of *Ct* are known to occur in the presence of extracellular stressors such as antibiotics or innate immunity.

1.3   *Chlamydia trachomatis* disease phenotypes

Ct strains have historically been divided into three major clades that cause radically different pathologies. However, despite >98% overall genomic synteny and identity across the entirety of the ~1.04Mbp genome, key factors that lead to distinct pathology and tropism remain unknown (Carlson et al., 2005). *Ct* serovars A-C primarily infect human conjunctival epithelial cells, causing inflammation of ocular

mucous membranes. If left untreated, repeated infections typically lead to trichiasis and corneal opacities, followed by subsequent blindness. Serovars D-K are responsible for the majority of non-invasive urogenital infections that show tropism for the single cell columnar epithelium of the ectocervix of women and the male urethra (Brunham and Rappuoli, 2013). LGV serovars are the most invasive *Ct* serotype, and sexually transmitted infections lead to systemic dissemination of bacteria, causing swelling and ulceration of lymph nodes; more characteristic of bubonic diseases such as plague (Brunham and Rappuoli, 2013). More recently however, an atypical outbreak of LGV has arisen in Europe, primarily in men who have sex with men (MSMs). This is characterized by a non-classical manifestation of the disease, as the associated L2b strain exhibits a predominantly rectal tropism, presenting clinically with proctitis (Thomson et al., 2008).

Genital and LGV strains are the most common sexually transmitted bacterial pathogens, responsible for ~90 million new cases of disease each year (Marrazzo and Suchland, 2014). It is important to note that urogenital infections are asymptomatic in 30-50% of men and 70-90% of women (Peipert, 2003). Hence, major complications occur predominantly in women, and arise from untreated ascending infections that infiltrate the endometrium and fallopian tubes causing pelvic inflammatory disease (PID), ectopic pregnancy and infertility (**Fig.1.2**). An additional complication known as Fitz-Hugh-Curtis syndrome may arise more rarely, involving liver capsule inflammation (Peter, Clark and Jaeger, 2004).

In addition, because *Ct* is an immunizing as well as immune-sensitizing infection, and pathology is often immune-mediated (Rekart et al., 2013), the careful choice of

antigen and adjuvant are likely to be crucial factors in the successful development of prophylactic or therapeutic vaccines. Thus, the delineation of immune correlates of protection in preclinical models of *Ct* infection is of paramount importance.
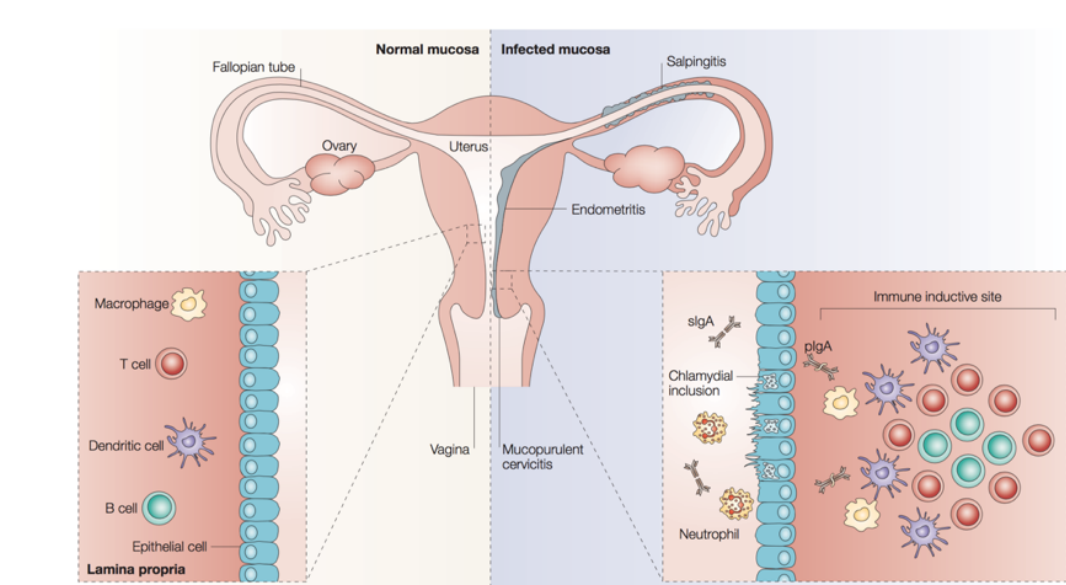
Figure 1.2: Pathology of sexually transmitted *Ct* infections (Brunham and Rey Ladino, 2005). Sexually transmitted *Chlamydia trachomatis* infections are the cause of significant morbidity in women, where about 70-90% of infections are asymptomatic. Post-infection sequelae such as fibrosis, salpingitis and pelvic inflammatory disease are thought to be the result of the formation of immune inductive sites elicited by prolonged cytokine and chemokine production by persistently infected epithelial cells. Untreated infections can also lead to infertility and life-threatening ectopic pregnancy. In men, the frequency of asymptomatic infections is less frequent, and complications such as epididymitis and infertility occur less frequently.

1.4   Immunobiology of *C.trachomatis* infection

The immunobiology of genital chlamydial infection has been extensively studied using two closely related chlamydial species - *C.muridarum* and *C.trachomatis*. Most studies have been undertaken in murine models of infection, although fundamental differences in bacterial virulence, tropism and pathogenesis between these two species in their natural hosts limit direct extrapolation of some of these findings to human infection. Firstly, *Cm* is a mouse pneumonitis strain, and does not show natural tropism for the female reproductive tract. Secondly, when infected intra-vaginally,

most murine strains generally clear *Cm* and *Ct* within four weeks, whereas *Ct* infection in humans is a chronic disease (Darville et al., 1997). Thus, while insight on the immune response to acute *Ct* infection may be gained from the study of murine models, it is likely that observed mechanisms of pathogenesis might not be representative of that in humans.

Animal models have clearly established that control and resolution of natural infection with *Chlamydia* spp. correlates with and is dependent upon on CD4^{+} effector T cells of the Th1 subtype. Nude mice fail to control infection, but adoptive transfer of CD4^{+} or CD8^{+} *Chlamydia*-specific T cells allows these mice to control infection (Ramsey and Rank, 1991; Rank, Soderberg and Barron, 1985). In the *Cm* infection model, adoptive transfer of *Cm*-specific CD4^{+} Th1- but not Th2-cell clones led to significant protection against genital tract infection (Hawkins, Rank and Kelly, 2002). Furthermore, it has become apparent that CD4^{+} T cells secreting IFN-γ are crucial for the control of *Cm* infection, as mice deficient in MHC Class II molecules (Morrison, Feilzer and Tumas, 1995), CD4 marker (Morrison et al., 2000), IL-12 (Perry, Feilzer and Caldwell, 1997), IFN-γ (Wang et al., 1999) or IFN-γ receptor (Johansson et al., 1997) all fail to control *Cm* infection when compared to wild-type controls.

The role for CD8^{+} T cells and B cells in the resolution of primary infection remains less categorical and rather more circumstantial, as mice deficient in key CD8^{+} T cell cytolytic effector molecules (perforin and FAS) show no significantly diminished ability to control or clear *Cm* infection (Perry et al., 1999). In addition, B cell deficient mice are also found to show similar clearance kinetics and control of *Cm* infection as wild-type controls (Ramsey, Soderberg and Rank, 1988). However,

studies conducted on the resolution of secondary infection have revealed an important role for B cells in subsequent Ct clearance following depletion of CD4^{+} and CD8^{+} T cells (Morrison and Morrison, 2001; Morrison et al., 2000), while in the Cm model of infection, Fc-receptor knockout mice display more severe secondary infection than their wild-type counterparts, which points to a role for B cells and antibodies in the promotion and enhancement of effective T cell responses (Moore et al., 2002).

Taken together, *in vivo* studies of natural infection in the most commonly used murine models of Ct and Cm infection reveals a crucial role for antigen-specific CD4^{+} effector T cell function in resolution of primary infection, and a possible synergistic role for antibodies and B cells in control of secondary infections. These latter effects are likely mediated through direct neutralization of bacterial infection in the lower genital tract, increased antigen presentation to T cells and possible antibody-dependent cell-mediated cytotoxicity (Igietseme et al., 2004; Moore et al., 2003). This is summarized in **Fig.1.3**.

1.4.1 Cellular and immunological hypotheses of *C.trachomatis* pathology

While the immune responses to natural infection have been useful in guiding the development of preclinical Ct vaccines, investigation of the mechanisms of pathogenesis are less well understood, and evidence from human studies remains largely correlative. However, following an array of clinical observations in humans and studies in mice, two theories have been proposed for the pathogenesis of Ct infection: the 'immunological' and 'cellular' hypotheses. However, these are not mutually exclusive.
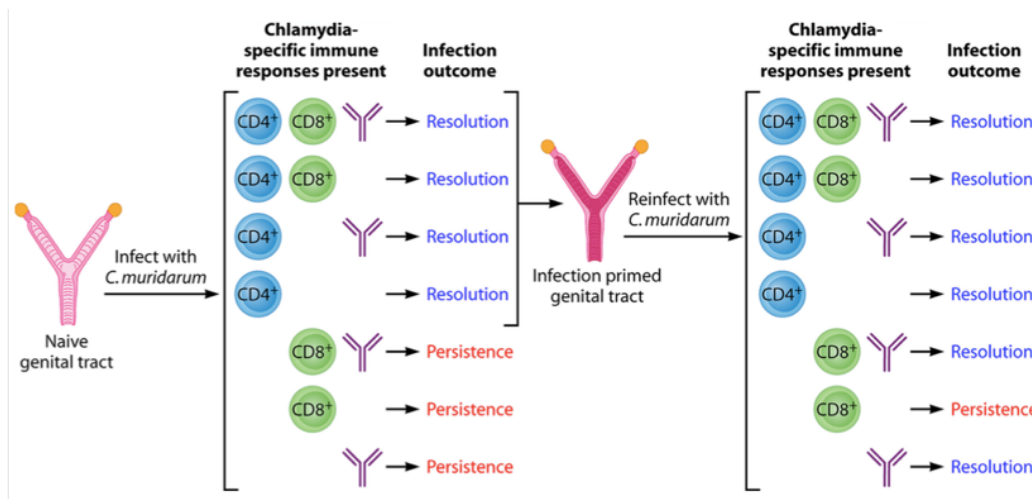
Figure 1.3: Immune correlates of protection against primary and secondary infections from the *Chlamydia muridarum* **murine model of infection (Farris and Morrison, 2011).** T and B cell depletion studies investigating the resolution of *C.muridarum* infections in mice have highlighted the indispensable requirement of CD4+ T cells in the resolution of primary infection, while antibodies are considered to play an important role in the clearance of secondary infection. The role of CD8+ T cells remains unclear.

The immunological hypothesis is founded on the premise that immune responses to persistent *Ct* infection lead to tissue damage that manifests as clinical disease (fibrosis and scarring). Interestingly, studies have found that HSP60, a chlamydial antigen, is recognized by T and B cells in humans and nonhuman primates, and predisposes individuals to an increased risk of PID and delayed-type hypersensitivity reactions (Lichtenwalner et al., 2004; Peeling et al., 1997; Yi, Yang and Brunham, 1997). A role for autoreactive CD4+ and CD8+ T cells that arise following *Ct* infection have been implicated in the aetiology of post-infection sequelae such as reactive arthritis, and are thought to be the result of molecular mimicry leading to the development of cross-reactive T cell clones (Goodall et al., 2001; Hassell et al., 1993). Furthermore, it has been observed that Th2-type responses that may develop during infection correlate with persistence, and may temper protective Th1-type responses, which also corroborate findings in IL-10 gene knockout mice that show enhanced Th1-type

protective immune responses following *Cm* infection (Holland et al., 1996; Igietseme et al., 2000; Yang et al., 1999).

The cellular hypothesis maintains that cytokines and chemokines secreted by infected epithelial cells lead to the recruitment and priming of antigen-specific immune cells, and hence, the ensuing exacerbation of pathology following persistent or repeated infection (Stephens, 2003). This hypothesis was proposed following observations that *Ct*-infected epithelial cells secrete IL-8, granulocyte macrophage colony-stimulating factor (GM-CSF), IL-1α and IL-6 *in vitro* (Rasmussen et al., 1997). This further extends to *C.pneumoniae*, where infected endothelial cells are observed to secrete IL-8, indicating similarities in chlamydial pathology at the genus level (Molestina et al., 1999). Overall, it is thought that chlamydial infection is likely to lead to the development of lymphoid follicles with both antigen-specific and non-specific effector functions, and that persistence of infections through chlamydial immune evasion strategies leads to cyclical chemokine secretion and amplification of the immune response that exacerbates pathology. This is illustrated in **Fig.1.4**.

This link between the immunological and cellular hypotheses may also lead to observed pathological phenotypes such as tissue remodeling and scarring in both genital and ocular disease. Studies have shown that *Ct*-infected epithelial cells also secrete IL-11, a cytokine known to be involved in tissue fibrosis (Dessus-Babus et al., 2002), and infected mammalian cells were also found to show up-regulation of fibroblast growth factor, endothelial growth factor and connective tissue growth factor (Coombes and Mahony, 2001; Hess et al., 2001). This evidence suggests a key role

for cellular mechanisms of pathogenesis initiated by variable cytokine and chemokine secretion profiles of epithelial cells during chlamydial infection.
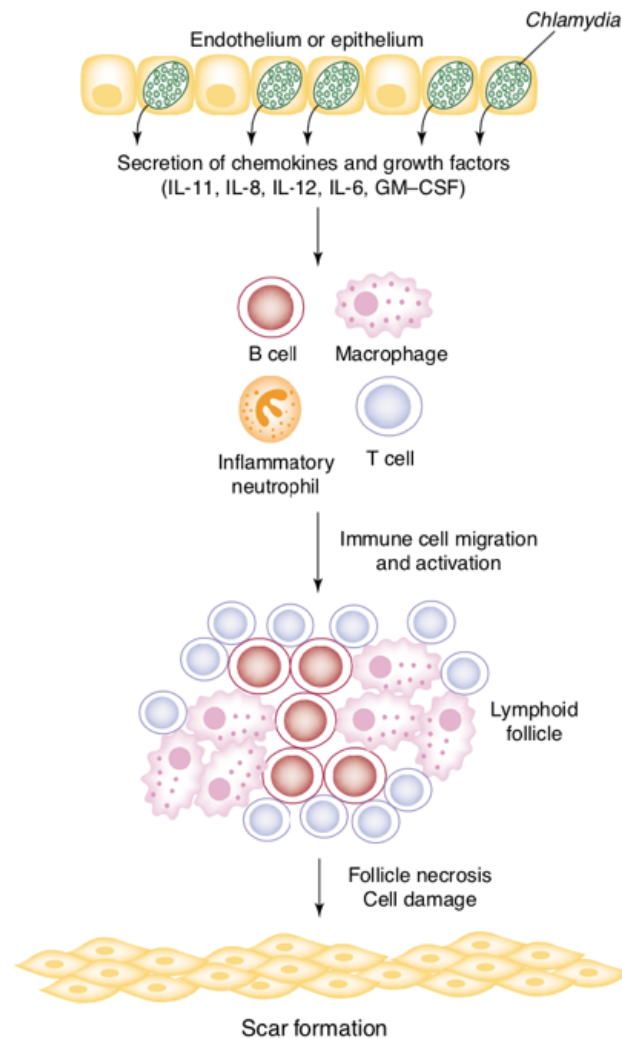
Figure 1.4: The cellular hypothesis of chlamydial pathogenesis (Stephens, 2003). The prolonged secretion of cytokines and chemokines by persistently infected epithelial cells leads to the development of lymphoid follicles through the recruitment and activation of immune cells. Pathogenesis following persistent or repeat infections is thought to occur due to the secretion of growth factors and immune modulators secreted by newly recruited immune cells that result in the ensuing fibrosis and scarring. Thus, tissue remodeling is thought to be mediated through both non-specific and antigen-specific autocrine and paracrine responses of both the innate and adaptive immune systems to infection, rather than *Ct* antigen-specific hypersensitivity or autoimmune mechanisms.

The two paradigms have important implications for the design of future vaccines, especially where the selection of protective versus immunopathogenic antigens is of primary importance. It is also increasingly appreciated that a greater understanding of immunogenetics within the human population may provide clues on rational chlamydial vaccine design by using cohort comparison studies with isolation and high throughput screening of T cells from patients that show resistance or susceptibility to

pathology following infection. This may further inform the rational selection of broadly protective *Ct* antigens for incorporation in to multicomponent vaccines.

1.5   Progress in *C.trachomatis* vaccinology

Treatment of chlamydial infections is currently accomplished through administration of doxycycline or azithromycin (Wetten et al., 2015). While antibiotics are thought to be efficacious at clearance of primary infection, they are not effective at preventing reinfection, which exacerbates pathology (Brunham and Rey-Ladino, 2005). Although not widely studied, it is becoming increasingly apparent that some chlamydial infections are recalcitrant to antibiotic treatment, and failures have been reported in the clinic, particularly with regard to ano-rectal and urogenital repeat infections (Hocking et al., 2015; Kong et al., 2015). This has largely been attributed to factors such as differential drug pharmacokinetics, autoinoculation from rectum to cervix in women and major differences in the genital microbiome (Kong et al., 2015). Furthermore, although anatomically proximate, immune priming of the rectal and genital tracts varies during natural infection and is dependent on vaccination route (Mestecky, Moldoveanu and Russell, 2005). Although an obligate intracellular lifestyle was initially thought to prevent extensive lateral gene transfer and likely acquisition of antibiotic resistance, recent evidence shows that there are no absolute barriers to recombination within and between *Ct* serovars despite this intracellular niche (Harris et al., 2012), and that these bacteria do possess the ability for the transfer of tetracycline resistance *in vitro* (Suchland et al., 2009).

Public health measures to control *Ct* infections since the early 1990s have largely promoted a 'seek and treat' approach at the community level. However, screening and

antibiotic regimens represent a substantial cost and burden to public health resources in both developed and developing countries. The UK National Chlamydia Screening Programme expenditure reached an excess of £100M between 2003-2009, while treatment, diagnosis and screening expenditure exceeded $2billion p.a. in the US (Donovan, 1997; Riha et al., 2011). Interestingly, following a study of *Ct* infection in women aged between 15-39 years in British Columbia, it has recently been proposed that while cases of reported PID have dropped substantially since 1995, *Ct* infection rates continue to rise (Brunham and Rekart, 2008).

This led the authors to propose the hypothesis of 'arrested immunity', which postulates that early detection and treatment of *Ct* infection blunts the acquisition of naturally acquired immunity to infection within individuals, which in turn abrogates herd immunity within a population. Indeed, a study in mice showed that early treatment with doxycycline blunts the development of protective immunity (Su et al., 1999). Epidemiological evidence supporting the acquisition of naturally acquired immunity in humans was obtained from clinical studies of a cohort of sex workers in Nairobi (Kenya), where resistance to *Ct* infection was found to be proportional to the duration of prostitution irrespective of age (Brunham et al., 1996). However, in humans, it has also been found that immunity takes a long time to develop (Molano et al., 2005), most likely due to immune evasion strategies employed by *Ct*. Phase variation of polymorphic outer membrane proteins (Pmps), chimerism of the major protective antigen MOMP, and a predominantly intracellular environmental niche are the main strategies employed by the pathogen to evade immune surveillance. This has led researchers to propose rationally designed vaccines as the next step in controlling

Ct infections. However, a greater understanding of a plethora of key components will be required for chlamydial vaccine development. These include:

(i)   An increased understanding of the applicability of commonly used animal models to study human chlamydial disease

(ii)   Furthering our understanding of the unique immunological properties of the genital tract mucosa for enhancement of vaccine-mediated mucosal immunity

(iii)   Prioritizing the design of a new generation of novel adjuvants to elicit T cell-mediated immune responses for optimum prevention or resolution of *Ct* infection

(iv)   Developing an informed knowledge of the mechanisms of attachment and pathogenesis of *Ct*, in order to facilitate antigen prioritization for vaccine development

These four key areas will be discussed in the following section.

1.5.1   Animal models of chlamydial infection

The four main species employed to study genital chlamydial infection comprise the macaque, guinea pig, domestic pig and murine models. Each model presents with its individual advantages and drawbacks, although no model perfectly replicates the anatomical features or endocrinology of the human reproductive tract (De Clercq, Kalmar and Vanrompay, 2013).

The pig-tailed macaque (*Macaca nemestrina*) is perhaps the most representative model for studying human *Ct* genital tract infections, as anatomy and physiology

closely mimics that of the human reproductive tract, with similar vaginal microflora and a 28-30 day menstrual cycle (Patton et al., 1996; Patton, Sweeney and Paul, 2009). Furthermore, no pretreatment with progesterone to initiate a productive infection (as required in murine models) is necessary in this species, which shows natural susceptibility to *Ct* infection (Patton, Sweeney and Paul, 2009). Two separate models have been developed to study *Ct* infections in the pig-tailed macaque, the *in situ* model and the subcutaneous pocket model (Patton et al., 1983; Patton et al., 1987). However, the expense, ethical approval and expertise required to work with nonhuman primates precludes widespread use of this model.

Another very useful model for studying chlamydial infection is the guinea pig, which acquires *C.caviae* infection that manifests as inclusion conjunctivitis, and is hence known as the guinea pig inclusion conjunctivitis (GPIC) model (Murray, 1964). Easier handling, cheaper costs and maintenance of these animals allow for larger preclinical studies for evaluation of vaccines. Most notably, infection in guinea pigs can be sexually transmitted (Mount, Bigazzi and Barron, 1973), and perinatal infection has been observed in neonates, similar to human infections (Mount, Bigazzi and Barron, 1972). The female reproductive tract is also much more similar to that of humans than other commonly used small rodents such as mice (Vanrompay, Lyons and Morre, 2006).

Importantly, the domestic pig (*Sus scrofa domesticus*) has also highlighted significant advantages in modeling of *Ct* infections, and more importantly, in addition to investigation of the immunobiology of *Ct* infection, also offers the advantage of studying pathogenesis of *Ct* infection, as urogenital *Ct* serovars E/Bour or E/468 lead

to ascending infection following intravaginal inoculation of 16-week old specific pathogen-free pigs (Vanrompay et al., 2005). This model has further been utilized to test the efficacy of preclinical recombinant subunit vaccines. *Ct* PmpG and SctC showed protective immunity against experimental genital infection, characterized by reduced bacterial shedding (Schautteet et al., 2011). Importantly, porcine reproductive tract tissue shows remarkably similar gene expression to the human genital tract (Dawson et al., 2013), and comparison of the porcine, murine and human immune systems has found that ~80% of the porcine immune system parameters investigated were more similar to humans than their murine equivalents. Finally, pigs are naturally susceptible to a wide array of chlamydial organisms including *C.abortus*, *C.pecorum*, *C.psittaci*, and *C.suis*. *C.suis* further shares a high degree of genomic identity and synteny with *C.trachomatis* (Suchland et al., 2009). However, despite the numerous inherent advantages of the aforementioned models, for practical reasons, which include the availability of specific knockout strains, a wide range of readily available immunological reagents, low cost, high experimental numbers and ease of maintenance and housing, the murine model is still most widely used to investigate *Ct* infections, and will therefore be discussed here in more detail.

1.5.2   Murine model of chlamydial infection and pathogenesis

As previously discussed, both human and murine strains (*C.muridarum* and *C.trachomatis*) have been used to study chlamydial immunobiology and correlates of immune protection *in vivo*. With regard to investigation of human urogenital infections, neither model represents all aspects of pathogenesis and infection well enough, although immune correlates of the resolution of acute chlamydial infection

may hold greater relevance to human disease for guiding preliminary design and investigation of vaccines.

C.muridarum was originally isolated from the lungs of mice (Nigg, 1942), and when used to study genital infections, is employed in an anatomically distinct eco-niche that is physiologically quite different from the respiratory mucosa for which it shows natural tropism. Most *Cm* intravaginal infections rapidly ascend to the uterine horns and ovarian bursa, eliciting classic symptoms of hydrosalpinx, fibrosis, and ensuing infertility (de la Maza et al., 1994; Shah et al., 2005). However, mice typically clear infection within about 4 weeks with secondary *Cm* infections also much more short-lived, indicating the acquisition of long-lived adaptive immunity that does not always occur in humans following primary *Ct* genital infection (Barron et al., 1981; Morrison, Feilzer and Tumas, 1995).

Conversely, the human pathogen *Ct* elicits mostly a mild genital infection in mice, which is usually unable to ascend to the upper genital tract, although some strains have been shown to infect the endometrium and ovarian bursa (Carmichael et al., 2013; Sturdevant et al., 2010). While typical inoculating doses for establishment of productive *Cm* infections consist of ~1500 inclusion forming units (IFU), most noninvasive urogenital *Ct* strains require both a much higher inoculating dose (~10^6-10^8 IFU), as well as pretreatment of mice with progesterone to optimize bacterial infections. This limits investigation of hormonal contributions and the influence of the menstrual cycle on the acquisition of *Ct* infection in both murine models, although progesterone pretreatment may be dispensable for achieving productive *Cm* infections depending on inoculating dose (Ramsey et al., 1999). Because of the inability of *Ct*

infections to frequently infiltrate the upper genital tract, post-infection sequelae can only be studied when *Ct* bacteria are inoculated directly in to the uterine horns.

Although confounding, it has been observed that *Ct* infections in mice can resolve in the absence of adaptive immunity, whereas adaptive immunity is indispensable for resolution of *Cm* infections (Morrison et al., 2011; Tuffrey, Falder and Taylor-Robinson, 1982). Interestingly, although phylogenetically most closely related, subtle genetic differences between the two species may determine virulence *in vivo*. The *Cm* biovar lacks allelic variation of MOMP (a major *Ct* immune evasion strategy) and the immunological effects of the cytokine IFNγ differ between human and mouse models for the respective strains (O'Meara, Andrew and Beagley, 2014).

In *Ct*, non-invasive urogenital serovars possess the *trpBA* operon that counteracts the effects of IFNγ-mediated tryptophan starvation. However, in mice, these effects are not observed, as IFNγ is thought to upregulate interferon regulated genes (IRGs) that reduce sphingolipid trafficking to the chlamydial inclusion and cause lipid starvation (Nelson et al., 2005). This may explain the rapid clearance and lack of ascending infections in the murine model of *Ct* infection for most serovars, as innate immunity may be sufficient to control lower genital tract infection. Intra-vaginal infection with *Cm* typically leads to ascending infection and pathology as bacteria infiltrate the endometrium and uterine horns causing hydrosalpinx (Carey et al., 2009). It has been suggested that in mice, *Cm* may have evolved to counteract disparate IFN-γ-mediated effects through inactivation of host cell IRGs, although this hypothesis requires further interrogation (Van Voorhis et al., 1997).

Of notable interest is the expression of three functional orthologs of the CT166 cytotoxin in *Cm*, whereas noninvasive urogenital *Ct* strains have one functional copy, with ocular and LGV strains possessing truncated versions of the gene (Carlson et al., 2004; Lo et al., 2012). Thus, the unknown role of this putative glycosyltransferase may also influence the observed differential outcomes of pathogenesis in mice between the two chlamydial biovars. However, it is still unclear as to which of the two murine models of infection are more representative of human infection. Indeed, it could be argued that the *Ct* model, which results in an acute self-limiting infection, is in fact more representative of natural primary infections in humans. Equally, the *Cm* model elicits more virulent ascending infection to the upper genital tract, with accompanying pathology representative of post-infection sequelae in women, but the infection is not chronic and usually cleared within a month. While subtle differences in *Ct* strains within mouse models can dictate infection outcome, differences in the genetic background of individual mouse strains further predisposes to the severity of disease outcomes, and this will be discussed next.

1.5.3   Mouse strain variation in chlamydial infection and pathogenesis

Differences in the course and outcome of chlamydial infections have been studied in three of the most commonly used mouse strains used to investigate pathogenesis (Darville et al., 1997; Darville et al., 2001b). These comprise C57BL/6, Balb/c and C3H/HeN mice. It was initially observed that differences in cytokine profiles of these three mouse strains was found to correlate with both duration of infection and incidence of pathology following primary intravaginal infection with the *Cm* mouse pneumonitis biovars (Darville et al., 1997).

C57BL/6 mice cleared bacteria most quickly, showing on average a 22-day course of infection. The Balb/c strain showed similar shedding kinetics, clearing *Cm* infection by day 25 following infection, while C3H/HeN mice showed markedly increased duration of shedding, with bacterial clearance achieved 38 days post challenge. Interestingly, the incidence of upper genital tract pathology was also markedly different between the three strains, with less than 50% of C57BL/6 (14/30) animals showing severe oviduct dilation, while 80% (24/30) and 97% (29/30) of the C3H/HeN and Balb/c mice (respectively) showing hydrosalpinx 42 days post infection with *Cm* (Darville et al., 2001b).

Inspection of cervico-vaginal secretions revealed significantly elevated TNFα and IL1β in all C57BL/6 and Balb/c mouse strains when compared to C3H/HeN mice. Importantly, the level of murine macrophage inflammatory protein MIP-2 (the putative functional equivalent of human chemokine IL-8) was found to be sustained in C3H mice relative to the other two strains one week post-infection, most likely due to the increased duration of the infection, but Balb/c mice showed significantly elevated levels of MIP-2 compared to both other mouse strains at early time points during infection (days 2-5). MIP-2 is found to be responsible for recruitment and activation of neutrophils to the genital tract (Cacalano et al., 1994). These observations suggest that inter-strain variations in the kinetics of specific cytokine profiles dictate the course of infection and may also influence pathology that is likely immune-mediated.

This lends credence to both the cellular and immunological paradigms of chlamydial pathogenesis, as prolonged infection is mirrored by secretion of MIP-2 that likely

leads to enhanced recruitment and sustained activation of neutrophils, with concomitant pathology (hydrosalpinx). Indeed, this has been shown to occur in *Chlamydia*-infected epithelial cells *in vitro* (Rasmussen et al., 1997). However, due to the pleiotropic nature of many cytokines, dissection of cytokine-specific mechanisms of pathogenesis are difficult to study *in vivo*, and other cytokines postulated to be involved in resolution or persistence of chlamydial infection such as IL-12, IL-10, IL-4 and IFNγ were not investigated here.

In a separate study, it has been shown that *Cm* utilized in a mouse pneumonitis model of infection caused increased mortality and prolonged infection in Balb/c mice versus their C57BL/6 counterparts (Yang, HayGlass and Brunham, 1996). Investigation of antigen-specific responses revealed a marked increase in IL-10 in Balb/c compared to C57BL/6 mice, with an inverse correlation observed for the IFNγ response. However, in the study by (Darville et al., 2001b), no mortality or significant difference in rate of clearance of genital *Cm* infection between Balb/c and C57BL/6 mice is observed. This not only illustrates differences in strain-specific immune responses between mice, but also highlights the important pathological differences when chlamydial organisms are deployed at sites anatomically disparate to their natural route of infection.

Although the mechanisms governing the differential production of Th1-type cytokine profiles in different mouse strains remain unknown, (Jacob, Lee and Strassmann, 1996) showed that identical numbers of macrophages obtained from different mouse strains also showed differential secretory levels of TNFα when stimulated with LPS or IFNγ. As C57BL/6, Balb/c and C3H mouse strains each contain a different

haplotype H-2^b, H-2^d, H-2^k (respectively), the authors proposed that TNFα production might be linked to major histocompatibility complex alleles. MHC haplotypes are incredibly diverse within the outbred human population, and further investigation is required to establish whether any correlates between *Ct* infections and pathogenesis exist within patient cohorts.

It is now also known that a plethora of anatomical and physiological factors may govern infectivity and ensuing degrees of immune-mediated pathology at sites of infection. These are not limited to, but may include: differential lymphocyte homing receptor expression in disparate tissues (Johansson et al., 1999), differential tissue-specific abundance and type of innate immune cells such as dendritic cells and macrophages in respective animal models, and even the timing of infection within the context of the menstrual cycle and pathogen dose (Carey et al., 2009). Thus, the use of *Cm*, a mouse pneumonitis biovar to infect the murine genital or respiratory tracts (a non-native pathogenic niche) may lead to differential immune responses and mechanisms of pathogenesis in each respective environment.

This is quite clearly illustrated in a recent study investigating the *Cm* antigen TC0582 as a vaccine candidate for *Cm* infections. This immunodominant antigen was discovered following examination of a proteome microarray used to test sera from infected mice (Jacob, Lee and Strassmann, 1996). TC0582 is a highly conserved V-type ATP synthase subunit, and possesses ~40% sequence homology to its eukaryotic orthologs. Moreover, TC0582 was preferentially recognized by serum from mice that developed hydrosalpinx when infected intravaginally with *Cm*, suggesting a correlation with immunopathology rather than protection (Zeng et al., 2012). Thus,

studies investigating potential protective efficacy of this antigen were conducted in respiratory tract *Cm* models of infection (Cheng et al., 2014). Here, it was found that mice immunized with TC0582 showed significant protection from intranasal challenge with *Cm*, evidenced by lower recoverable IFU in the lungs and percentage change in body weight relative to controls. Furthermore, cross-reactive autoantibodies directed against the murine V-type ATP synthase were not detected, indicating potential safety of the vaccine. Interestingly, CT308, the *Ct* gene ortholog of TC0582 was not recognized by serum from women presenting with tubal factor infertility, showing no direct immune correlate to disease in humans (Budrys et al., 2012; Rodgers et al., 2011).

This evidence highlights important nuances and caveats in the use of the *Cm* biovar for investigation of vaccine efficacy and pathogenesis in different environmental niches within the host, where an antigen may be protective in one setting, but also demonstrate an enhanced proclivity to initiate deleterious effects at another anatomically or immunologically distinct site. As previously discussed, it is likely that these differences may also be mediated by the genetic profiles of the host to a large extent. However, another major challenge that precludes effective design of vaccines against many sexually transmitted pathogens is the immunological uniqueness of the human genital tract, which is primed differently to the common mucosal immune system, and is thought to require combined systemic and mucosal (primarily intranasal) immunization to elicit optimal protection.

1.5.4 Immunology of the reproductive tract

The human genital tract is anatomically and immunologically distinct from the so-called 'common' mucosal immune system that comprises the oral, intestinal and respiratory mucosae (Mestecky, Moldoveanu and Russell, 2005). Major differences between reproductive tract immunology and that of anatomically disparate mucosal sites include:

(i) The lack of immune inductive sites within male and female genital tract tissues such as the organized lymphoid structures known as Peyer's patches in the gut mucosa (Yeaman et al., 1997)

(ii) A predominance of IgG rather than secretory IgA within genital tract semen and cervico-vaginal fluid (Russell and Mestecky, 2002)

(iii) The influence of fluctuating hormonal levels within the female reproductive tract during the menstrual cycle (Kozlowski et al., 2002)

These features may thus influence the immune response to natural infection as well as vaccines designed to combat sexually transmitted infections such as HIV, *N.gonorrhoeae* and *C.trachomatis*. For instance, the lack of specialized lymphoid structures within the genital epithelium leads to weak humoral immune responses to natural infection or immunization at sites distal to genital infection, especially in the absence of potent adjuvants (Russell and Mestecky, 2002). A vaccination route that enables the acquisition of robust immunity within both the genital and common mucosal systems may be important when considering immunization strategies for coverage of a broad array of chlamydial infections, given the highly divergent tropism

of ocular, urogenital and LGV serovars, which show appetence for the conjunctival mucosa, genital tract and monocytes (respectively).

Furthermore, with the recent emergence of the new L2b epidemic, the causative agent of proctitis in high-risk MSM populations, a potentially attractive experimental strategy that may combat a wider array of pathogenic *Ct* strains would be the development of per-rectal immunization strategies, as the lower intestinal and genital tracts possess shared lymphatic drainage due to their anatomical proximity (Mestecky, Moldoveanu and Russell, 2005). Nonhuman primate models and early clinical trials have further demonstrated the efficacy of this immunization route for the bacterial pathogen *Salmonella typhi* (Crowley-Nowick et al., 1997; Eriksson et al., 1998; Kantele et al., 1998; Nardelli-Haefliger et al., 1996)

In contrast to the human genital mucosa, the presence of organized lympho-epithelial structures like tonsils and Peyer's patches ensure that oral and per-rectal immunization lead to generalized immune responses within the common mucosal system characterized predominantly by antigen-specific secretory IgA (sIgA) responses. Interestingly, while systemic immunization leads to weak intestinal humoral responses, this route has been found to elicit high titres of IgG as the dominant immunoglobulin subtype in cervico-vaginal secretions (Bouvet et al., 1994; Russell and Mestecky, 2002). This is demonstrated in experimental models of HIV infection, where passive protection against vaginal HIV-1 or simian immunodeficiency virus (SIV) is conferred by systemically administered neutralizing monoclonal antibodies (Baba et al., 2000; Mascola et al., 2000).

However, intranasal vaccination remains the most effective route for eliciting high titre genital tract antibodies and cell-mediated immune responses (Di Tommaso et al., 1996; Johansson et al., 1998; Russell et al., 1996). Most preclinical studies have employed cholera toxin B subunit (CTB) as a mucosal adjuvant, or other versions of this heat-labile enterotoxin, which are potent stimulants that may not be readily amenable for use in human vaccine development. Subsequent safety studies have indicated potential side effects of these ganglioside-binding toxins that may result in pathology following retrograde neuronal transport of antigens (Mutsch et al., 2004; van Ginkel et al., 2000).

Another potential advantage of intranasal immunization is that high titres of vaginal IgA and IgG are elicited irrespective of the phase of the menstrual cycle, whereas the strength of local immune responses following intravaginal immunization showed phase-dependence during menstruation (Johansson et al., 2001; Kozlowski et al., 2002). However, the influence of sex hormones on reproductive tract immunology still remains poorly understood, but may be critical for the development of future *Ct* vaccines. This further highlights the need for the development of novel antigen-adjuvant combinations with a broad therapeutic index that elicit robust mucosal immunity and are safe to administer via clinically established parenteral routes. The role of adjuvants in the development of next-generation T cell based vaccines will be discussed next.

1.5.5   Adjuvants

Adjuvants are key substituents of nearly all licensed vaccines, and are defined as components that are capable of either enhancing or shaping the immune response to

specific antigens. However, even the mechanisms of action of aluminium salts, some of the oldest adjuvants first employed in the 1920s, still remain poorly characterized or entirely unknown (Marrack, McKee and Munks, 2009). Hence, to facilitate transition from preclinical trials to licensing, the development of new adjuvant classes for an array of infectious diseases seeks to both understand the mechanisms of action of novel immunostimulatory molecules in order to better define safety and tolerability profiles, while further filling crucial gaps in modern vaccinology, which include:

(i)　　Antibody response broadening - to target pathogens such as influenza, HIV, *Plasmodium falciparum* or *Chlamydia* spp. which display inter-strain variability in key immunogens or antigenic drift

(ii)　　Enhanced potency and durability of responses - which may result in antigen dose sparing to increase global vaccine supply

(iii)　　Vaccines for the elderly to counteract senescence of the immune system

(iv)　　New T cell vaccines to combat intracellular pathogens such *Chlamydia* spp., *Mycobacterium tuberculosis* or *Leishmania* spp.

Clinically approved adjuvants licensed for use in human vaccines primarily comprise the aluminium salts, modified derivatives of bacterial lipopolysaccharide (LPS), and liposomal formulations. These can be formulated with various additives such as saponins or oils in either aqueous or oil-in-water emulsions (MF59, AS03, AF03) and AS04 (monophosphoryl lipid A (MPL) plus aluminium salts) (Reed, Orr and Fox, 2013). Thus, broadly speaking, adjuvants generally consist of two main components: (i) immunomodulatory molecules that interact directly with the host immune system (such as TLRs, or NOD- and RIG-like receptors) and (ii) delivery systems (such as

liposomes or virosomes) that may enhance antigen presentation to the immune system.

Combination systems are those that incorporate a mixture of both immunomodulatory and delivery components, and most licensed adjuvants or those undergoing Phase III clinical trials represents this class. For instance, the recently licensed Cervarix (*GlaxoSmithKline*) and Fendrix (*GlaxoSmithKline*) vaccines, used to combat HPV and hepatitis B (respectively) employ the proprietary AS04 combination system comprising MPL (an immunostimulatory TLR4 agonist) and aluminium salts (putative delivery system with intrinsic adjuvanticity) (Draper et al., 2013; Levie et al., 2002), while the RTS,S malaria vaccine recently evaluated in a Phase III clinical trial is composed of the AS01 formulation containing MPL and QS21, which also contains a liposomal delivery vehicle (Agnandji et al., 2011).

Other vaccines based on delivery systems that enhance antigen presentation include the virosome-based Inflexal V influenza vaccine and the hepatitis A Epaxal vaccine manufactured by Crucell, and likely function through encapsulating native viral particle structure combined with multimeric antigen presentation and fusogenic activity of lipids (Reed, Orr and Fox, 2013). Thus, the functionality of adjuvants is dependent not only on the identity of the immunostimulatory molecule, but also on formulation, and the intricacies of formulation-dependent effects of adjuvants in vaccine design will be discussed next.

1.5.6 Formulation-dependent effects of adjuvants in vaccine design

Formulation-dependent variables of adjuvants and their effect on the quality of the immune response and vaccine efficacy are numerous, and will not be discussed in detail here, although several reviews highlight the importance of engineering constituent nanoparticles to achieve specific particle size distribution, surface charge and chemical structure (Bachmann and Jennings, 2010; Hubbell, Thomas and Swartz, 2009; Oyewumi, Kumar and Cui, 2010). Several clinical and preclinical trials document the formulation-dependent effects of adjuvants on vaccine efficacy, epitomised by the recent development of the RTS,S malaria vaccine candidate (Stoute et al., 1997).

Studies showed that formulation of the *P.falciparum* circumsporozoite antigen with AS02 (an oil-in-water emulsion plus MPL and QS21) protected 6/7 recipients from malarial infection, while formulation with AS04 (MPL and aluminium hydroxide) and AS03 (emulsion only) elicited protection in 1/8 or 2/7 recipients (respectively) (Mettens et al., 2008). Furthermore, in both preclinical and early phase clinical trials, it was subsequently realized that switching from an oil-in-water emulsion (AS02) to a liposomal formulation (AS01) significantly enhanced Th1-type cell-mediated immunity as well as antibody titres (Kester et al., 2009; Owusu-Agyei et al., 2009; Polhemus et al., 2009). These studies neatly illustrate the individual and combinatorial impact that immunostimulatory molecules (such as the TLR agonist MPL) and delivery vehicles (liposomes) may have on the quality of the immune response.

In addition to the AS01-AS04 formulations, MF59 is another licensed adjuvant used in Fluad and Pandemrix vaccines, also widely tested in preclinical studies (O'Hagan et al., 2012). Here, addition of TLR ligands (the TLR9 agonist CpG or TLR4 agonist E6020) to the MF59 emulsion has been shown to result in a Th1-skewed immune response, although antibody titres remained the same (Baudner et al., 2009). More interestingly, however, the nature of the ensuing immune response for a given adjuvant formulation may also be heavily dependent on the antigen incorporated in the vaccine. Addition of TLR ligands to adjuvant formulations show added benefit when the vaccine antigen is a recombinant protein (Singh et al., 2012), while limited benefit in magnitude or quality of the immune response is observed when inactivated pathogens with intrinsic immunogenicity are added (Rumke et al., 2013). In addition to formulation- and antigen-dependent effects on adjuvant potency, key additional caveats lie in the physiological disparities in preclinical animal models, which may result in poor efficacy or adverse effects in clinical trials.

1.5.7   Animal models in adjuvant design

General caveats are inherent when investigating the translational potential of adjuvants screened in preclinical animal models, particularly with regard to TLR agonists as used in our study. The intricacies of TLR4 signaling will be discussed in more detail in Chapter 5, which describes the first preclinical study of a second-generation lipid adjuvant (SLA). SLA is a novel, rationally designed TLR4 agonist used in combination with *Ct* rPmpD as a vaccine in a murine model of chlamydial infection. However, it is worth noting that murine TLR4 is more promiscuous at interacting with a variety of modifications on both natural and synthetic TLR4 ligands than is human TLR4. Importantly, expression patterns of TLRs differ substantially

between species. For instance, TLR8 is not expressed in murine cells, while the TLR9 expression pattern varies between humans and rodents, thus compounding the significance and interpretation of the immunological effects of certain TLR agonists in preclinical studies (Hemmi et al., 2002; Jurk et al., 2002; Klinman et al., 2004).

Differences also exist in the type of vaccination regimen employed. For instance, DNA immunization is far less immunogenic in humans than in mice, preexisting immunity to certain viral vectors within the human population limits the efficacy of viral-vectored vaccines that may show promise in preclinical rodent or primate models (Li, Saade and Petrovsky, 2012; Saxena et al., 2013). However, rare side effects of adjuvant-antigen combinations may still not be detectable in insufficiently powered preclinical or even large-scale Phase III trials in humans.

This is epitomised by reports of narcolepsy in children and young people receiving both the Pandemrix (GSK) and Focetria (Novartis) H1N1 influenza vaccines (Miller et al., 2013; Partinen et al., 2012; Wijnans et al., 2013). Interestingly, both the adjuvants and antigens employed in each vaccine were remarkably different, Pandemrix consisting of an inactivated split virus vaccine with the AS03 (squalene, α-tocopherol and polysorbate 80) adjuvant, with Focetria composed of purified hemagglutinin and neuraminidase subunits with MF59 (squalene, polysorbate 80 and sorbitan trioleate) (Reed, Orr and Fox, 2013). These studies illustrate key uncertainties that the field of adjuvant biology is fraught with, particularly as the cellular and molecular interactions of many adjuvants and their formulation constituents are poorly understood.

Nonetheless, despite these inherent drawbacks, preclinical models must form the basis of investigation for initial assessment of adjuvant safety and efficacy, and an increased understanding of physiological differences and similarities with humans is of paramount importance in the field. In addition to understanding their molecular mechanisms of action, key future requirements for next-generation adjuvants within the context of sexually transmitted diseases, include defining the best formulation and route of administration to elicit robust and durable immunity within the genital tract mucosa. Drawing links between measurable protective efficacy of certain adjuvants (such as enhanced T or B cell responses) and their initial cellular immune signatures through exploiting advances in transcriptional profiling, may also help to identify key correlates that are predictive of specific profiles of immunity. This approach has been adopted in the analysis of the yellow fever vaccine YF-17D, where, for instance it was shown that a robust $CD8^+$ T cell response correlated with expression of eukaryotic translation initiation factor 2 alpha kinase 4 (Querec et al., 2009). This may allow for more rational screening of adjuvants at an earlier phase of development.

Thus, in light of the potential shift away from whole cell and live-attenuated *Ct* vaccines (which possess intrinsic immunogenicity) as well as the need to enhance robust antigen-specific T cell priming within the genital tract to target intracellular *Ct* infections, it is likely that novel adjuvants will have a profound influence on the future development of *Ct* vaccines. While the expansion of preclinical chlamydial vaccine candidates has been incremental over the past few decades, it is likely to grow exponentially in the coming years. This is largely expedited with the advent of new technological approaches which enable the judicious choice of antigens primed to

elicit protective T cell as well as humoral responses, and the very recent development of a complementary genetic toolkit that has finally made this obligate intracellular pathogen amenable to genetic manipulation (Kari et al., 2011; Nguyen and Valdivia, 2012; Wang et al., 2011). The repertoire of chlamydial vaccine candidates investigated to date will be discussed next.

1.5.8 Antigens

Vaccine development against chlamydial infections was initiated in the 1950s, where whole-cell inactivated EBs were used to immunize nonhuman primates in an infection model of ocular trachoma, and further included the first Taiwanese trachoma vaccine human field trial (Collier et al., 1967; Wang, Grayston and Alexander, 1967; Woolridge et al., 1967). However, manifestations of immuno-pathogenesis were detected following reinfection in some individuals, while others showed reduced disease and measurable short-term protection. Adverse immune events were categorized as delayed-type hypersensitivity reactions and the use of whole-cell organisms was subsequently replaced in favour of the MOMP subunit that comprised the mainstay of chlamydial vaccinology research for the better part of the following two decades. A plethora of MOMP-based immunization strategies were employed in a variety of animal models (Batteiger et al., 1993; Tan et al., 1990), using variations in administration routes (Su, Parnell and Caldwell, 1995; Taylor et al., 1988), prime-boosting and antigen-adjuvant combinations (Dong-Ji et al., 2000). As expected, this diverse array of studies reported variable results of vaccine efficacy, and it was not until the early 21st century that technological advances in genomics have shed light on the intricacies and caveats of MOMP vaccination.

MOMP has been found to be a hotspot for genetic recombination within and between *Ct* serovars, and consists of four variable domains (VD1-VD4) (Harris et al., 2012). Extensive recombination of *ompA* (the gene encoding MOMP) within and between *Ct* strains thus confounds conventional clinical serotyping and further masks true phylogenetic relationships between serovars that are more clearly revealed through whole-genome sequencing of clinical strains (Harris et al., 2012). MOMP is the dominant constituent of the chlamydial outer membrane complex, comprising ~65% of the COMC (Hatch, Allan and Pearce, 1984). Although the function of MOMP is unknown, antigenic variation in MOMP may act as a major immune evasion strategy for *Ct*, as anti-MOMP antibodies have been shown to neutralize *Ct* infections *in vivo* (Pal et al., 2001; Tuffrey et al., 1992). However, the use of MOMP in combination with OmcB as a multi-subunit recombinant vaccine expressed in a *Vibrio cholerae* ghost (VCG) delivery vehicle, was found to elicit a greater population of antigen-specific IFNγ-secreting T cells, resulting in enhanced protection against *Ct* serovar D/UW3/Cx infection, suggesting the likely importance and cooperative effect of other COMC proteins in eliciting chlamydial clearance through the generation of robust Th1-type cellular immune responses (Eko et al., 2004).

Thus, the last 10-15 years have seen an increased focus on the identification and prioritization of novel chlamydial antigens that elicit cell-mediated immune responses, concomitant with technological advances in proteomics. Such novel approaches have examined chlamydial proteins preferentially loaded on to MHC class I or II molecules following pulsing of dendritic cells (DCs) with live or UV-inactivated *Cm* (Karunakaran et al., 2008; Yu et al., 2011), or employed high throughput screening of sera and splenocytes from infected patients or animal models

to identify chlamydial antigens preferentially recognized by antibodies as well as CD4$^+$ T cells (Finco et al., 2011). Importantly, these methodologies hold great importance for the development of novel vaccines against intracellular pathogens, and a summary of the findings of these and other studies outlining several of the main chlamydial vaccine candidates in conjunction with preclinical *in vivo* protection data is presented in **Table 1.1**.

Table 1.1: Chlamydial vaccine candidates (*Rey-Ladino et.al*, 2014)				
Antigen	**Chlamydial localisation**	**Adjuvant**	**Protection**	**Immune response**
CT043	Membrane	DNA/Protein	2.6-log reduction in lungs	Th1 type response
ArtJ	Periplasm	ND	ND	Neutralizing Abs *in vitro*
CrpA	Inclusion membrane	Vaccinia virus	Partial protection	CD8$^+$ T cell expansion
CPAF	Cytosol	IL-12	Reduction in vaginal bacterial load	Abs and IFNγ
Tarp	Cytosol	CpG and IFA	Reduction in vaginal bacterial load	Th1-type response
PmpG	Membrane	Protein pulsed DCs	60% reduction in vaginal IFU	T cells producing IFNγ
PmpE	Membrane	Protein pulsed DCs	50% reduction in vaginal IFU	T cells producing IFNγ
RplF	Ribosome	Protein pulsed DCs	50% reduction in vaginal IFU	T cells producing IFNγ
PmpD	**Membrane**	**ND**	**ND**	**Neutralizing Abs *in vitro*, human CD4$^+$ T cell recognition**
MOMP	Membrane	FA, CpG, OspA, rVCGs	70% reduction in vaginal IFU	Th1-type response with IFNγ production
NrdB	ND	Cholera toxin, CpG	Partial protection	CD4$^+$ T cells

To account for genetic variation in MHC haplotypes, Karunakaran et al. (2008) utilized bone-marrow derived dendritic cells (BMDCs) from C3H and C57BL/6 mice with distinct MHC alleles (H2^k and H2^b respectively) pulsed with either live *Ct* or *Cm* for 12 hours, and subsequently employed cell lysis and monoclonal antibody purification of MHC-peptide complexes. In this study, it was found that MHC allelic selection is crucial in determining protein recognition, and this may play a more significant role in determining the outcome of infection and pathogenesis in an outbred human population. Peptide fragments of 17 proteins from the *Cm* proteome were purified on MHC II of C57BL/6 mice, while only 11 were isolated from the C3H mouse strain. Interestingly, the only overlapping peptides between the two mouse strains were from the PmpG and PmpF orthologs, and moreover, MOMP, and Pmps E, F and G generated multiple MHC class II-binding epitopes. This may indicate roles in immune evasion within hosts, particularly as recently identified hotspots for genetic variation in Pmps correspond to epitopes predicted to bind MHC (Gomes et al., 2007). Overall, when trialled as subunit vaccines, PmpG was found to elicit the greatest levels of protection, which also correlate with its immunodominance in the *Cm* model of infection (Johnson et al., 2012; Li and McSorley, 2013).

Yu et.al (2011) further showed that intranasal immunization with live *Cm* EBs elicited significantly greater levels of protection than did immunization with UV-inactivated EBs (UVEBs), which further correlated with the number and types of peptides loaded on to MHC class II. The authors isolated 45 peptides from 13 different proteins following DC pulsing with live *Cm* EBs *in vitro*, while only 6 peptides belonging to 3 different proteins were loaded on to MHC class II following pulsing with UVEBs. A

further correlate of protection was the increased number of multifunctional T cells elicited by live *Cm* infection secreting IFNγ and TNFα with or without IL-2, relative to UVEBs. Moreover, the antigens entering the MHC class II pathway following DC pulsing by live EBs included the Pmps E, F, and G, while surprisingly, none of the three proteins (RplF, FabG, AtpE) following UVEB pulsing of DCs consisted of outer membrane constituents. Preferential loading of Pmps on to MHC class II suggests possible targets for T cell based vaccines. Moreover, the observation that Pmps are preferentially processed and loaded on to MHC class II molecules during live infection but not following UV-inactivation, further suggests likely roles in pathogenesis or intracellular function.

Finco et.al (2011) employed a two-pronged approach to identify chlamydial antigens that elicited both humoral and cellular immune responses using high throughput screening of 120 *Ct* serovar D recombinant proteins in a protein array to screen human sera from *Ct*-infected patients, and stimulate splenocytes from *Ct*-infected mice. Five antigens that were both recognized by human sera and resulted in significantly enhanced antigen-specific IFNγ-secretion in murine splenocytes were identified – IncA, CT372, OmcB, MOMP and CT823. Here again, key components of the COMC were identified, as well as an inclusion membrane protein expressed during mid-cycle development, highlighting a broader range of putative vaccine candidates. However, the use of recombinant proteins in immobilized arrays may result in non-native conformations and hence, a number of viable candidates containing conformational-dependent epitopes may have been overlooked in the screening of patient sera. However, some studies investigating the antibody signatures of *Ct* ocular infections have avoided this by using intrinsically radiolabelled

Chlamydiae in a radio-immunoprecipitation assay (Kari et al., 2013), and such novel approaches may be a way of circumventing loss of sensitivity in antibody epitope recognition.

Thus, the surface-exposed nature of chlamydial Pmps (Crane et al., 2006), their postulated role as adhesins in *Ct* and other chlamydial species (Becker and Hegemann, 2014; Molleken, Becker and Hegemann, 2013), as well as the presence of multiple T cell epitopes on these highly immunogenic proteins (Yu et al., 2014), may result in robust cell-mediated immunity and neutralizing antibody responses when incorporated in to chlamydial vaccines. However, the precise role these proteins play in *Ct* infection and pathogenesis remains enigmatic, and no cellular interaction partners have been identified for any *Ct* Pmp. Existing knowledge on this family of proteins in *Ct* will be the subject of discussion in the following section.

1.6   Secretion systems in Gram-negative bacteria

In many bacterial pathogens, virulence and adhesion are mediated by a plethora of secreted or surface-exposed proteins, which are able to perform an array of diverse functions to manipulate host cell machinery. In order for secretion and translocation to occur, specialized secretory pathways are utilized. These are grouped in to seven major classes (Thanassi and Hultgren, 2000). Types II, IV, V and chaperone/usher secretion systems rely on a Sec-dependent transportation mechanism across the inner membrane, where recognition of a short, cleavable N-terminal signal sequence (~30 amino acids) on the protein leads to transport from the cytoplasm across the inner membrane of the bacterium via the Sec apparatus - an evolutionarily conserved system for protein transport in bacterial and eukaryotic phyla (Stephenson, 2005).

Type II secretion may also be mediated through the twin-arginine translocation (Tat) secretory system (Sargent et al., 1998). In contrast, type I and type III secretion systems are Sec-independent (Beeckman and Vanrompay, 2010), and the discovery of a new secretion mechanism in *Pseudomonas aeruginosa* extended the classification to include a Type VI secretory system (Mougous et al., 2006), indicating a rich diversity of mechanisms by which virulence factors are secreted in Gram-negative bacteria.

Types I-IV and Type VI secretion systems comprise large modular complexes that either span the inner and outer membranes, or contain multiple protein components variously associated with both membranes (Beeckman and Vanrompay, 2010). *Chlamydiales* possess a type III secretion system, of which several components and substrates have been identified. However, perhaps more striking is the presence of an expanded family of polymorphic membrane proteins (Pmps) that belong to the Type V autotransporter secretion system (T5ATs), and comprise roughly 13% of the total genomic coding capacity in *Ct* (Grimwood and Stephens, 1999). *Ct* possesses nine Pmps (Pmp A-I) within its genomic repertoire. The maintenance of such a large family of Pmps in a bacterial phylum that has undergone evolution by genomic reduction, suggests crucial or redundant roles for these proteins in the life cycle of the bacterium. However, the functional roles of Pmps during infection and biphasic development in *Ct* remain unclear.

Proteins secreted by the T5AT mechanism possess a general unifying composition of motifs consisting of (i) an N-terminal leader sequence recognized by the Sec apparatus (ii) a functional passenger domain and (iii) C-terminal β–barrel pore. This is illustrated in **Fig1.5**. The extreme inter- and intra-species sequence variation of T5AT passenger domains is likely indicative of differing functional roles, while the β–barrel

pore remains largely conserved (Henderson, Navarro-Garcia and Nataro, 1998). Using this conserved modular structure as a template, T5ATs have been identified through genomic analysis in a wide range of pathogens, and are thought to comprise the largest family of secreted proteins in Gram-negative bacteria (Wells et al., 2007). However, for the majority of T5ATs, precise roles in virulence or host cell interactions remain putative or unknown. Selected T5ATs in key sexually transmitted or intracellular pathogenic Gram-negative bacteria are discussed next.
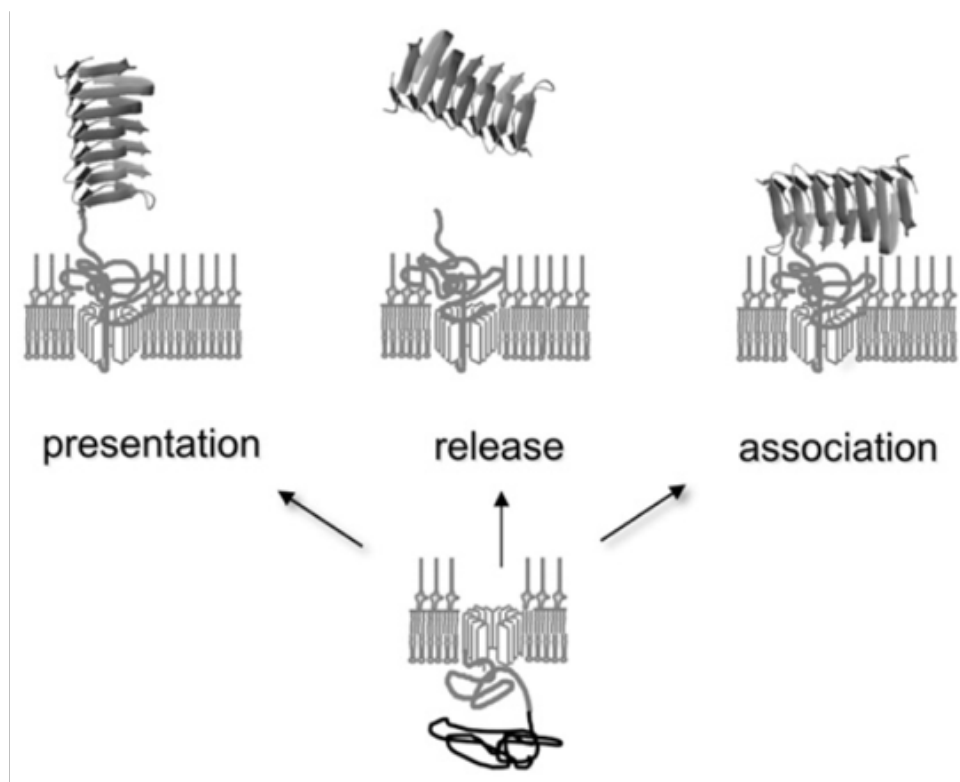
Figure 1.5: The type V autotransporter system (Benz and Schmidt, 2011). Type V autotransporters (T5AT) comprise the largest family of secretion systems in Gram-negative bacteria. Translocation of the protein across the inner membrane occurs via recognition of an N-terminal signal sequence by the Sec-apparatus, followed by insertion of the C-terminal β–barrel in the outer membrane. Once translocation is achieved, the passenger domain mediates effector function through interactions with host cells, and may either remain attached to the bacterial membrane or cleaved and secreted.

1.6.1 Type V autotransporters in pathogenic Gram-negative bacteria

The IgA1 protease of *Neisseria gonorrhoeae* was the first identified T5AT (Pohlner et al., 1987). These proteins cleave secretory IgA1 at the hinge region (Kilian et al., 1996), although IgA1 protease mutants were not defective in establishing infection in either the male urethra (Johannsen et al., 1999) or female genital tract (Hedges et al., 1998). However, roles beyond IgA1 cleavage have been identified for the *N.gonorrhoeae* IgA1 protease, most notably, cleavage of the lysosomal integral membrane glycoprotein LAMP1 (Hauck and Meyer, 1997), (Lin et al., 1997). Furthermore, the ability to contribute to pathogenesis through eliciting the production of pro-inflammatory cytokines is another important function identified for the *N.gonorrhoeae* IgA1 protease (Lorenzen et al., 1999). Interestingly, this suggests multifunctional roles for a single T5AT correspondent to both extra- and intracellular survival, which would enable conservation of genomic space and metabolic requirements.

Another well-studied pathogen of humans that displays T5AT toxin multi-functionality is *Helicobacter pylori*, identified as a causative agent of gastritis (Kuipers et al., 1995), gastric adenocarcinoma (Parsonnet et al., 1991) and mucosa-associated lymphoid tissue (MALT) lymphoma (Wotherspoon et al., 1991). *H.pylori* vacuolating toxin (VacA) is a T5AT expressed as a 140kDa pro-toxin that undergoes N- and C-terminal processing to an 88kDa secreted protein (Cover, Hanson and Heuser, 1997). This further undergoes partial proteolytic digestion to soluble 33kDa and 55kDa fragments (Nguyen, Caprioli and Cover, 2001). VacA is responsible for a panoply of effects in gastric epithelial cells including swelling of endosomal compartments (Pagliaccia et al., 1998), mitogen activated protein kinase activation

(Nakayama et al., 2004), and disruption of epithelial barrier permeability (Papini et al., 1998). In addition, VacA has been shown to exert both anti-proliferative effects on T cells (Boncristiano et al., 2003), (Gebert et al., 2003) as well as pro-inflammatory cytokine production *in vitro* (Supajatura et al., 2002).

In addition to VacA, *H.pylori* possesses another T5AT associated with clinical pathology. The blood-group antigen binding adhesin (BabA) is responsible for epithelial attachment within the gastric mucosa, and may be a site of extensive recombination or mutation (Aspholm-Hurtig et al., 2004). In a German population, clinical isolates revealed a strong association between the *babA2* gene and gastric adenocarcinoma (P-val=0.033), and strains triple-positive for *babA2*, *vacAs1* and a Type III secretion effector-encoding gene *cagA* showed a significantly higher correlation with ulcer formation and adenocarcinoma (P-val=0.014) (Gerhard et al., 1999).

Another monophyletic group within the α-*Proteobacteriaceae* known to possess T5ATs are the *Rickettsiales*. Like the *Chlamydiales*, *Rickettsiae* are obligate intracellular bacteria, sub-divided into two groups (typhus or spotted fever) based on differential antigenicity, outer membrane proteins and resulting pathology (Anacker, Mann and Gonzales, 1987). Within the *Rickettsiales*, a study revealed a family of genes encoding surface cell antigens that were differentially fragmented or absent between species (Blanc et al., 2005). Four of the genes have been identified as T5ATs – *ompA*, *ompB*, *sca1* and *sca2* (Blanc et al., 2005). In *R.conorii*, Sca1, Sca2 and OmpB all have been shown to mediate adherence to host cells (Cardwell and Martinez, 2009; Chan et al., 2009; Riley et al., 2010), and OmpB was found to elicit

protective immunity (Feng et al., 2004a; Feng et al., 2004b). In addition, OmpA was recently shown to mediate adhesion through interaction with $\alpha_2\beta_1$ integrin in non-phagocytic human endothelial cells *in vitro* (Hillman, Baktash and Martinez, 2013).

Given their widespread distribution and roles in adhesion and virulence in a number of pathogenic organisms, T5ATs are promising candidates for vaccine development. For instance, in addition to whole-cell vaccines against whooping cough caused by the pathogen *Bordetella pertussis*, acellular vaccines have been developed that include, amongst other antigens, the T5AT pertactin (Cherry et al., 1998). High-titre humoral responses to pertactin have been found to have the strongest correlation to reducing the likelihood of acquiring pertussis disease (Hewlett and Halperin, 1998; Storsaeter et al., 1998). However, the physiological role pertactin plays in pathogenesis remains contentious, while conflicting studies on adhesion to various cell types is reported (Everest et al., 1996; van den Berg et al., 1999), an immunoprotective epitope comprising the C-terminal $(PQP)_5$ motif has been identified (Charles et al., 1991). In addition, pertactin was the first T5AT for which the 3D-structure was obtained, which revealed a 16-stranded parallel β-helix (Emsley et al., 1996). This enables detailed inspection of the molecular nature of putative binding motifs and immunoprotective epitopes.

Most recently, the Bexsero vaccine (Novartis), developed to combat *Neisseria meningitidis* serogroup B infections, was the first clinically approved vaccine to be developed by reverse vaccinology. Bexsero contains the *Neisseria* adhesin A (NadA) T5AT as one of the three recombinant protein antigens (Serruto et al., 2012). Large-scale genomic comparisons were used to identify virulence factors and potential

vaccine candidates *in silico*, across a broad range of strains. Preclinical *in vivo* studies identified NadA as a protective antigen in rats, able to induce bactericidal antibodies (Comanducci et al., 2002), while *in vitro* studies using heterologous expression in non-invasive *Yersinia enterocolitica* indicate a putative role for NadA as a bacterial adhesin (Capecchi et al., 2005; Nagele et al., 2011). Thus, T5ATs are an important class of proteins present in a wide range of *Proteobacteria* that are able to exert a plethora of distinct and often multifunctional effects to manipulate a variety of host cell types. Importantly, the range of oligomeric or monomeric states exhibited may exert distinct functional roles, which may in turn vary depending on the environmental niche of the pathogen. Interestingly, despite adaptation to an intracellular lifestyle through 'evolution by reduction', the *Chlamydiaceae* preserve a large number of T5ATs within their genomic repertoire. However, the structural and functional characterization of these proteins still remains rudimentary.

1.7 The polymorphic membrane proteins (Pmps) of *Chlamydia trachomatis*

By 2012, completion of the genome sequences of all known pathogenic and zoonotic *Chlamydiaceae* revealed an expanded family of Pmps within this diverse family. *C.pneumoniae* (21 Pmps), *C.pecorum* (16 Pmps), *C.abortus* (18 Pmps), *C.caviae* (17 Pmps), *C.psittaci* (21 Pmps), *C.felis* (20 Pmps). *Ct* possesses a family of nine polymorphic membrane proteins (Pmps A-I) which all belong to the T5AT family. These proteins comprise roughly 13.6% of the total genomic coding capacity (Grimwood and Stephens, 1999). However, the precise role of this large family of proteins within the context of chlamydial infection is yet to be fully established, although certain clues are emerging through studies of small patient cohorts and recent advances in genetic manipulation of *Ct*.

The expression profiles of *Ct* Pmps have been extensively studied at both the mRNA and protein levels in the 18 laboratory reference strains that comprise ocular, urogenital and LGV serovars (Gomes et al., 2006; Nunes et al., 2007). Six out of the nine *pmp* genes clustered according to tissue tropism (Gomes et al., 2006). The study showed that degrees of polymorphism between *Ct* Pmps were highly variable, although this did not necessarily reflect changes in amino acids, evidenced by the ratio of non-synonymous to synonymous mutations (dN/dS). *pmpF* and *pmpH* were the most polymorphic but remained conserved at the protein level (dN/dS = 0.23 and 0.14 respectively), indicating possible conserved function. In contrast, *pmpB* possessed the highest level of protein variation (dN/dS=1.59) that may be suggestive of horizontal gene transfer or host immune pressure. This is also reflected in *pmpE*, *pmpF* and *pmpH* genes, which showed a non-random distribution of polymorphisms, and in a separate study, *pmpF* was found to have a cluster of non-synonymous mutations at locations of predicted MHC epitopes (Carlson et al., 2005).

Polymorphic variation in these regions may be a strategy to affect MHC-T cell interactions and antigen presentation. Of note, the two most clinically prevalent *Ct* serovars E and F phylogenetically diverged from the other urogenital serovars for Pmps B, C, D, H and I, which was distinct from a comparison of interrelatedness using the *ompA* gene encoding the chimeric MOMP protein, where serovars E and F were more closely related to other serovars (Millman, Tavare and Dean, 2001). This points to a possible role for polymorphisms in Pmps conferring selective ecological advantages in certain strains, as well as in mediating tissue specific tropism.

A subsequent study by the same group sought to compare *pmp* expression between clinical (E and L2) and reference (E/Bour and L2/434) strains (Nunes et al., 2007). All *pmp* genes were expressed at 2 hours post infection, with *pmpF* showing the highest peak levels of gene expression in all strains, and *pmpA* the lowest. Subsequently, sera from 39 female adolescents presenting with *Ct* infection in clinics in Oakland were used to assess reactivity to recombinant Pmps D and F, where mixed infections were ruled out *apriori* using sequencing of *ompA* in cervical samples. Interestingly, 57.7% of sera reacted to rPmpD, while no patient serum was reactive to rPmpF in immunoblots. Furthermore, sera from patients infected with serovars E, F, Ba and K all recognized rPmpD, while those infected with serovars D, Ia, J, and G were non-reactive. Importantly, this may reflect differing levels of *in vivo* expression or immunodominance of MOMP or Pmps in different *Ct* serovars within the context of human infection, and further work is required to elucidate whether any correlations may be drawn with regard to serovar-specific Pmp immunogenicity and infection clearance or pathology.

To investigate the heterogeneity in humoral responses to the nine-member *Ct* Pmp family, four separate patient cohorts were selected representing sexually, pathologically and geographically distinct populations (Tan et al., 2009). Women presenting with PID from Pittsburgh, adult male patients from Baltimore and adolescent females from Oakland and Little Rock with confirmed *Ct* infection were included. Pmps B, C, D and I were the major Pmps recognized by immune sera, indicating that these may be likely surfaced-exposed or expressed in abundance during *Ct* infection. Expression of Pmps may also be highly regulated during genital infection, and host-specific differences in epitope recognition may also play a part in

preferential recognition. In addition, geographical disparity of patient groups may mask epidemiological variations in serovar distribution that in turn may influence specific anti-Pmp serological profiles. However, in this study, 73% of patient sera recognized rPmpD, a highly immunogenic *Ct* antigen.

To complement genomic profiling of *pmp* expression in *Ct*, Pmp expression was investigated using a panel of highly cross-adsorbed polyclonal antibodies directed against *Ct* Pmps A-I (Tan et al., 2010). Here, it was found that all Pmps are surface-exposed, and that varying numbers of inclusions within a single infection do not express a given Pmp subtype. An 'off rate' for a given Pmp was defined as the percentage of inclusions that were homogenously negative for Pmp staining relative to those that were positive. Fixing and staining was conducted 42 hours post infection. Pmps A and D had the lowest 'off' rate (<1%), which may indicate important roles in RB development or RB to EB transition. Pmps F and H showed slightly elevated off rates (1-2%), while Pmps B, C and E displayed 'off' rates of 5-10%.

Interestingly, two types of PmpF were recognized in differential staining patterns (homogenous and punctate) by two separate anti-PmpF pAbs, which also reacted differently in immunoblotting, reflecting different epitope recognition. This suggests that PmpF polymorphism may also be occurring *in vitro*. Interestingly, a single cell harbouring two distinct inclusions displayed PmpB expressing inclusions at one pole but not at the other, indicating the on-/off-rates of Pmps are not likely governed by the metabolic or developmental state of the infected cell. Co-immunofluorescence for Pmps revealed that expression of a given Pmp was found to be shut off independently

of Pmps that were both genetically linked (i.e. in the same operon) or genetically disparate.

The presence of such a large family of orthologous genes in the *Chlamydiales* is indicative of a trait common to several obligate intracellular pathogens that have evolved to adapt to an intracellular lifestyle through genomic reduction. These bacterial pathogens comprise the *Rickettsiae*, *Ehrlichiae* and spirochetes, whose entire genomes are about one third the size of *E.coli* (Palmer, 2002). The *Ct* genome was found to contain ~859 genes, with ~28% showing no similarity to proteins deposited in GenBank (Stephens et al., 1998). Adaptation to an intracellular lifestyle precludes the need for many genes involved in metabolic pathways, and gene deletion often occurs through progressive loss-of-function mutations. In the sexually transmitted pathogen *Treponema pallidum*, the causative agent of syphilis, more than 50% of the open reading frames encode proteins of no known function (Fraser et al., 1998), and the loss of genes involved in metabolic pathways has also been observed in the genomes of *Rickettsia prowazekii* and *C.trachomatis* (Andersson et al., 1998; Stephens et al., 1998).

Interestingly, it has further been postulated that paralogous gene families encoding outer membrane proteins (such as the chlamydial Pmps) may play a role in immune evasion (Palmer, 2002). Studies conducted on the animal pathogen *Anaplasma marginale* identified and addressed the putative function of an expanded family of gene paralogs in this species termed major surface proteins (*msp2*) (Palmer et al., 1994). It is known that *A.marginale* can replicate for years within immunocompetent hosts to facilitate the likelihood of transmission (Eriks et al., 1989; Kieser, Eriks and

63

Palmer, 1990). This is accomplished by MSP-2 variants that arise cyclically to cause waves of bacteremia (Palmer, Brown and Rurangirwa, 2000).

Variants are generated by recombination of multiple pseudogenes with hypervariable central regions in to the *msp2* expression site (Brayton et al., 2001). Orthologs of the *msp2* family are also found and expressed in *A.phagocytophila*, the causative agent of human granulocytic ehrlichiosis (Zhi, Ohashi and Rikihisa, 1999). The strategy of antigenic phase variation to evade the host immune system is also employed by a protozoan eukaryotic pathogen of humans – *Trypanosoma brucei* (El-Sayed et al., 2000), where waves of undulating parasitemia are observed following changes in the variant surface glycoproteins. That a number of bacterial pathogens with comparatively small genomes such as the *Chlamydiaceae* may also implement this strategy to facilitate survival and transmission, may be of significant importance when considering vaccine development in tandem with the immune evasion strategies of *Ct*, especially in light of its elaborate repertoire of Pmps. Furthermore, it is now well-established that *Ct* possesses the ability to undergo genomic recombination and antigenic polymorphism, particularly within the *ompA* gene and certain Pmps, but also within the cryptic plasmid which can also be exchanged between serovars (Gomes et al., 2006; Harris et al., 2012). These surface-exposed antigens represent both challenges and opportunities for the future development of prophylactic or therapeutic chlamydial vaccines.

1.8   Concluding remarks

To date, chlamydial vaccine development has focused on the prioritization of vaccination strategies that elicit robust pathogen-specific CD4$^+$ Th1-type responses,

usually quantified by monitoring of splenic lymphocyte populations secreting IFNγ. However, the role of antibodies is becoming increasingly important as a correlate of vaccine-induced protection against infection, and so far, the only robust evidence documenting the *in vivo* efficacy of neutralizing antibodies has arisen from employing the antigenically variable chlamydial MOMP as an immunogen (Olsen et al., 2015; Pal et al., 2001). Thus, given the limited application of chimeric antigens such as MOMP, there is a need for broadening preclinical vaccine studies towards assessing an array of other chlamydial outer membrane proteins that may act as targets for neutralizing antibodies due to their surface-exposed nature. The Pmp family of proteins comprises a judicious choice of candidates.

Pmps have been regarded as promising vaccine candidates due to a high number of predicted T cell epitopes, and immunoproteomics approaches using tandem mass spectrometry have also found these proteins to be preferentially loaded on to MHC class II (Karunakaran et al., 2008; Karunakaran et al., 2015; Yu et al., 2014). Based on these findings, preclinical vaccine studies incorporating Pmps E, F, G and H have been conducted *in vivo* in heterologous mouse strains (Yu et al., 2014), demonstrating differential haplotype-dependent immunodominance, correlating with the variable humoral responses to Pmps in clinical studies (Tan et al., 2009). However, a recent bioinformatics analysis of these Pmps show that Pmps E and F are highly polymorphic between LGV and noninvasive urogenital strains, with differences in the number of GGA(I,L,V) and FXXN motifs and Cys residues, likely indicating differences in adhesion profiles or functionality. Indeed, polymorphisms in these Pmps have also been shown to reside in regions of the proteins corresponding to predicted T cell epitopes, suggesting a role in immune evasion (Gomes et al., 2007;

Nunes et al., 2015). Interestingly, the *pmpG* gene has also been implicated in phase variation, following the identification of regulatory sequences within the gene (Nunes et al., 2015).

Thus, we have chosen to employ the *Ct* PmpD as a preclinical vaccine candidate. PmpD is the most highly conserved Pmp across all known *Ct* serovars (>99.15%), is surface-exposed, and is known to contain a broad array of T cell epitopes (Crane et al., 2006; Swanson et al., 2009). This fulfills key prerequisites in the development of an effective chlamydial vaccine, which include: (i) coverage of a broad array of circulating strains (ii) ability to provide heterotypic antibody-mediated neutralization against *Ct* infection (iii) ability to elicit robust CD4$^+$ Th1-type cellular immunity.

In addition to the judicious choice of antigen, it is likely that adjuvants will play a key role in the success of future chlamydial vaccines, particularly due to the previously outlined regulatory and safety requirements for well-defined molecular mechanisms of action, the ability to demonstrate effective translational potential from preclinical models to clinical trials (in view of anatomical and physiological disparities between humans and mice), and the need to elicit robust pathogen-specific cell-mediated immunity predominantly reliant on memory and effector CD4$^+$ T cells (Reed, Orr and Fox, 2013; Su and Caldwell, 1995). To this end, we have performed the first preclinical study using a novel, rationally designed TLR4-based second-generation lipid adjuvant (SLA), that has previously undergone evaluation of potency and efficacy on both human and murine primary and cultured cell lines *in vitro*, and has been documented to elicit a robust Th1-biased immune response evidenced by cytokine and chemokine profiles (Darrick Carter, personal communication).

Moreover, given the deployment of MPL in the licensed Cervarix vaccine (GSK) for the prophylaxis of prevalent HPV transmission and infection, the wealth of information describing the safety and efficacy of TLR4 agonists would expedite the translation of this molecule to early phase clinical trials (Draper et al., 2013).

1.9   Aims of the project

Several inter-related areas were addressed in this project, with the primary aim of assessing and documenting the efficacy of rPmpD and SLA in the development of future chlamydial vaccines. In addition, we conduct the first biophysical characterization studies of rPmpD and the T3SS virulence factor CT694, two important effector proteins implicated in *Ct* adhesion and invasion. Biophysical characterization of CT694 will be discussed first, as this investigation was a subsidiary objective conducted as an adjunct to the main focus of the thesis, which comprises a more detailed investigation of rPmpD as a chlamydial adhesin and a highly efficacious vaccine immunogen.

1.9.1   Biophysical characterization of *Ct* CT694

CT694 is a putative T3SS early effector protein unique to *Ct*, with no genetic paralogs present in closely related chlamydial species, or any significant sequence homology to genes in phylogenetically distinct bacterial genomes. To facilitate functional annotation for this protein, we have initiated early biophysical characterization studies with the eventual goal of obtaining a 3D molecular representation of the structure using X-ray crystallography. This is the focus of Chapter 3.

1.9.2   Biophysical characterization of *Ct* rPmpD

In light of the requirement for the preservation of native protein structure in vaccine development and future structural studies, we provide the first biophysical characterization of a chlamydial Pmp using an array of biochemical and analytical techniques, and propose a model that illustrates a likely role for PmpD during biphasic chlamydial development within the context of our own and others' previous work. This is presented in Chapter 4.

1.9.3   *In vitro* investigation of *Ct* rPmpD as a chlamydial adhesin

The second area of study comprises a preliminary investigation of the putative function of *Ct* rPmpD as a chlamydial adhesin. Neutralization and competitive inhibition assays are employed, providing preliminary evidence implicating *Ct* rPmpD as a chlamydial adhesin. This implies a functional role for PmpD in mediating chlamydial attachment to host cells, suggesting that this highly conserved chlamydial antigen may be a judicious target for incorporation in to future chlamydial vaccines. These findings are discussed in Chapter 5.

1.9.4   *In vivo* efficacy of rPmpD in combination with a novel, rationally designed TLR4 agonist for use in preclinical *Ct* vaccines

Finally, we characterize the efficacy of *Ct* rPmpD as a chlamydial vaccine candidate, and conduct the first preclinical investigation on the immunogenicity and efficacy of a novel, rationally designed TLR4 agonist in combination with rPmpD. This study demonstrates the protective efficacy of vaccines incorporating rPmpD in both the presence and absence of SLA in a murine model of *Ct* lower genital tract infection, and has further implications for the design of next-generation adjuvants in shaping

ensuing immune responses. In addition, we highlight an important role for pathogen-specific antibodies at eliciting protection against sexually transmitted *Ct* infections. These data are presented in Chapter 6.

Chapter 2: Materials and Methods

2.1   Protein production and biophysical characterisation

This section describes the procedures used in cloning, expression, purification and biophysical characterization studies of recombinant *Ct* PmpD and CT694 proteins described in Chapters 3 and 4.

2.1.1 Polymerase Chain Reaction (PCR)

Prior to PCR, *Ct* serovar E/Bour genomic DNA (ATCC) was amplified using the GenomiPhi DNA amplification kit (GE Healthcare). All *Ct* genes were subsequently amplified using PCR from resulting DNA. Primer sequences are listed in **Table 2.1**. The PCR cycle conditions employed for amplification of each gene fragment are listed in **Table 2.2**, and the composition of each PCR mix in **Table 2.3**. Phusion High-Fidelity DNA Polymerase (NEB) was used to perform PCR reactions. Reactions were incubated in a BIOER LifeEco Thermocycler in 200µl thin-walled PCR tubes. After addition of loading dye, 20µl reactions were run on a 1% agarose gel and purified using the QIAQuick Gel Extraction Kit (QIAGEN) according to the manufacturer's protocol. Each PCR product was eluted in 50µl of nuclease-free water and the concentration (ng/µl) determined using a NanoDrop ND-1000 Spectrophotometer. PCR products were stored at -20°C until use.

2.1.2 Cloning and generation of plasmids using restriction enzymes

All reagents were purchased from New England Biolabs (NEB). Gel-purified PCR products of the target genes and vector backbones (**Fig.2.1**) were digested using the respective restriction enzymes overnight at 37°C. (**Table 2.5**). Antarctic shrimp phosphatase was added to vector digests to de-phosphorylate the 5'-end of the vector

to minimize spontaneous re-ligation. After addition of loading dye, 25µl of the vector

Table 2.1: Forward and reverse primers	
Gene Name	**Forward primer (F) and Reverse primer (R)**
pmpD (F1)	F:AGTTGCCATGGTAGATCTTCATGCTGGAGGACAGTCTGTAAATGAGC R:ATCTACTCGAGTTCCATACGCTGAGCAGTGAGATTATGAGC
pmpD (F2)	F:ATCTTCCATGGATAGTCAGGCTGAAGGACAGTATAGG R:ATTGACTCGAGTTTAAAACCATAACTACATAATGTAGCTCC
pmpD (F3)	F:ATCTTCCATGGATAGTCAGGCTGAAGGACAGTATAGG R:ATCGTCTCGAGACGTAAGCAAGAAATAGCACC
ct694	F:ATCGTCCATGGCAAGTATTCGACCTACTAATGGGAGTGG R:CGCGGGTCGACGTCTAAGAAAACAGAAGAAGTTATGACAGTTAGTGTTTGG
ΔN-ct694	F:ACGCGCCATGGATATTTATCATCCGACTATTTCTGGACAAGG R:GCCGTCTCGAGGTCTAAGAAAACAGAAGAAGTTATGACAGTTAGTGTTTGG
T7 Primers	F:TAATACGACTCACTATAGGG R:GCTAGTTATTGCTCAGCGG

Table 2.2: Polymerase chain reaction (PCR) cycle conditions						
PCR Cycle	**Initial Denaturation**	**Denaturation**	**Annealing**	**Extension**	**No. Cycles**	**Final Extension**
pmpD	98°C, 30s	98°C, 30s	55°C-75°C, 30s	72°C, 3mins and 30s	30	72°C, 6mins
ct694	98°C, 30s	98°C, 30s	55°C-75°C, 30s	72°C, 2mins and 40s	30	72°C, 6mins

Table 2.3: Polymerase chain reaction mix	
Component	**Volume (µl)**
5x Phusion polymerase buffer	5
10mM dNTPs	0.5
10mM 5'F primer	1.25
10mM 5'R primer	1.25
Phusion DNA polymerase	0.5
Template DNA	2
Nuclease-free water	14.5

Table 2.4: Ligation Reactions	
Component	**Volume (µl)**
10x ligase buffer	2
100mM DTT	2
10mM ATP	1
Insert:Vector (Molar Ratio)	(3:1)
T4 DNA ligase	1
Nuclease-free water	to 20µl

double digest reactions were run on a 1% agarose gel and purified using the

QIAQuick Gel Extraction Kit (QIAGEN) according to the manufacturer's protocol.

Ligation reaction conditions are listed in **Table 2.4**. Prior to ligation with gene inserts, inactivation of Antarctic Shrimp Phosphatase contained in the vector digest reaction was achieved by heating at 65°C for 15 minutes. Following isolation of digested insert DNA using the QIAquick PCR Purification Kit (QIAGEN), insert was added to the vector in 3:1 molar excess and incubated at 16°C overnight. All genes inserted into the multiple cloning site of all pET-vectors possessed a non-cleavable C-terminal His$_6$-tag (**Fig.2.2**).

Table 2.5: Restriction Enzyme Double Digest Reactions			
Insert		**pET Vector**	
Component	**Volume (µl)**	**Component**	**Volume (µl)**
*Nco*I (*ct694*, ΔN-*ct694* and *pmpD*)	1	*Nco*I	1
*Xho*I (ΔN-*ct694* and *pmpD*)	1	*Xho*I	1
*Sal*I (*ct694)*	1	10x Buffer 4	3
10x NEB Buffer 4	3	pET vector	10
Gene Insert	10	Antarctic Shrimp Phosphatase	1
Nuclease-free water	15	10x Antarctic Shrimp Phosphatase Buffer	3
		Nuclease-free water	11

2.1.3 Plasmid transformation and amplification

2-5µl of ligation reaction mixture was added to 50µl of chemically competent NovaBlue Single *E.coli* cells (Novagen) and transformed via heat shock. The mixture was incubated for 5mins on ice, transferred to a heating block at 42°C for 30s and immediately placed back on ice for 10mins. 250µl of sterile SOC Media (Novagen) was added to the cells and incubated with gentle shaking at 37°C for 1-2hrs, and then plated on to LB agar containing 50µg/ml kanamycin sulphate (Sigma Aldrich). Colonies were obtained after incubating the agar plates at 37°C overnight.
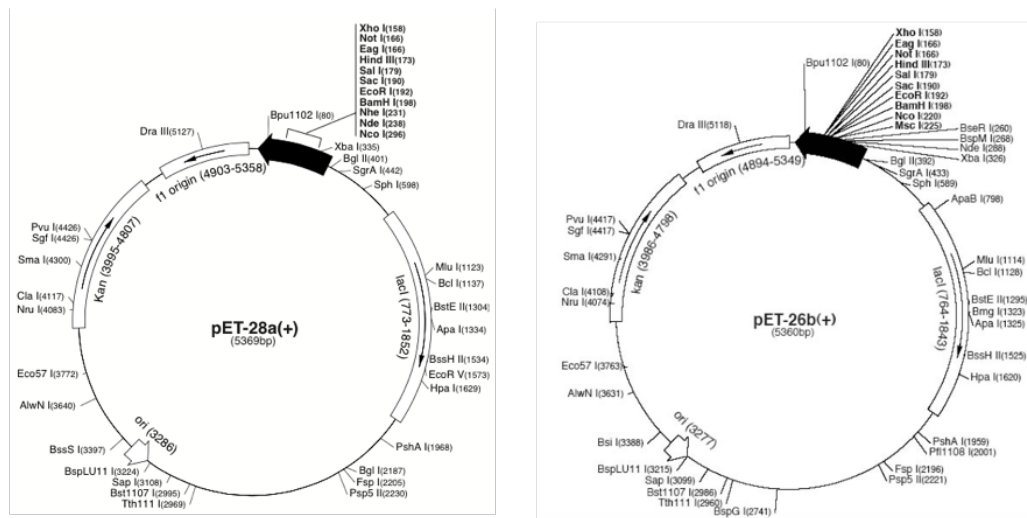
Figure 2.1: pET vector schematic. Schematic of the pET vectors (Novagen) showing the kanamycin antibiotic resistance gene, lacI promoter region and restriction enzyme sites. *pmpD* and *CT694* gene fragments were initially cloned in to the pET-28(b) vector. The pET-26(b) vector possessing the N-terminal pelB leader sequence designed to initiate periplasmic transport of the protein was also used for cloning and expression of PmpD passenger domain fragments, as T5AT proteins are typically translocated across the inner membrane of the bacterium (**Fig.1.5**). Gene fragments were inserted in to the multiple cloning site (black) using restriction enzyme digests and ligation (**Tables 2.4 and 2.5**).
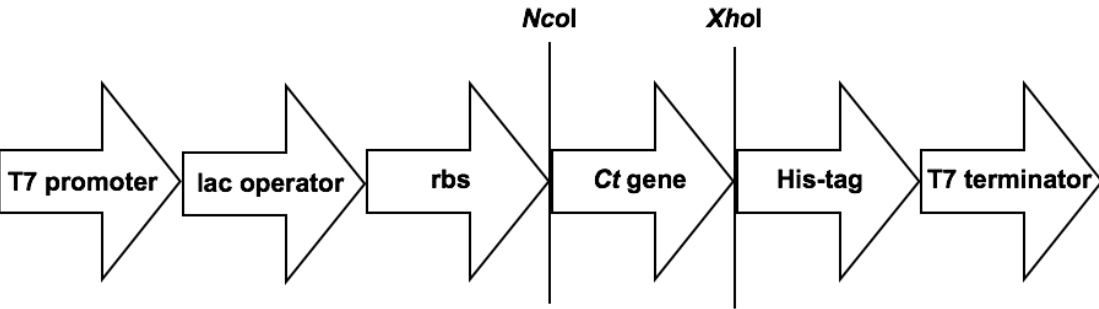
Figure 2.2: Schematic of the multiple cloning site showing insertion of *Ct* genes. The *pmpD* and *CT694* genes were inserted between the ribosome binding sequence (rbs) and the C-terminal hexa-histidine tag. Plasmid sequencing was carried out using forward and reverse primers corresponding to the T7 promoter and T7 terminator regions (respectively).

Verification of plasmid uptake was conducted using colony PCR with the same primers used for initial gene amplification, and relevant colonies were picked and grown in 5-10ml LB media containing kanamycin (50µg/ml) at 37°C for 5-8hrs. Plasmids were isolated using the QIAprep Spin Miniprep Kit (QIAGEN), eluted in 50µl of nuclease-free water and stored at -20°C. The fragments were resolved by agarose gel electrophoresis and visualised using SybrSafe DNA gel stain (Sigma

Aldrich) under UV-light. All plasmids were sequenced to screen for correct in-frame ligation and potential mutations using primers recognizing the T7-promoter and T7-terminator regions in the multiple cloning site of the pET-vector. Where feasible, successful cloning of respective genes was also confirmed by restriction enzyme double digest analysis.

LB-medium (volume = 1L): 10g tryptone (Fisher Scientific), 5g yeast extract (Fisher Scientific), 10g NaCl (Fisher Scientific), deionised water

LB-agar (volume = 1L): 10g tryptone (Fisher Scientific), 5g yeast extract (Fisher Scientific), 10g NaCl, 15g agar (LAB M Ltd), deionised water

2.1.4 Analysis of the plasmids by nucleotide sequencing

The correct sequence of the recombinant plasmids was confirmed by nucleotide sequencing. T7-promoter and terminator primers, as well as internal primers complementary to the target genes were used to verify correct sequences. Plasmid sequencing reactions were performed by the Bioscience Technology Facility (York, UK) with an Applied Biosystems 3130XL sequencer. Analysis of sequence chromatograms was performed using the ABI Vector NTI program. All genes were amplified correctly from genomic DNA as verified by Clustal Omega sequence alignments.

2.1.5 Over-expression of the recombinant PmpD and CT694 protein fragments

For small scale expression tests, competent *E.coli* BL21 (DE3), Origami 2 (DE3), Rosetta 2 (DE3) and C41(DE3) cells were transformed and induced. The recombinant genes from *Chlamydia trachomatis* serovar E/Bour DNA (ATCC) were

overexpressed in the BL21 (DE3) *E.coli* strain (Novagen). For large scale expression, strain *E. coli* BL21 (DE3) (Novagen) was used for the production of all recombinant proteins used in this study. In each case, transformed cells were grown at 37°C in lysogeny broth supplemented with kanamycin sulphate antibiotic (50μg/ml) to an optical density of 0.6, induced with 1mM isopropyl β-d-1-thiogalactopyranoside and then cultured overnight at 37°C. To purify rPmpD and CT694, cells were harvested by centrifugation, resuspended in extraction buffer consisting of 20mM TrisHCl pH 8.0, 50mM NaCl, 10mM imidazole, to which an EDTA-free protease-inhibitor cocktail tablet (Roche Diagnostics, USA) had been added, and lysed by sonication. For recombinant CT694, cell lysate supernatants containing soluble protein were carried forward for affinity purification. For rPmpD, inclusion body isolation, denaturation and refolding was carried out prior to purification.

2.1.6 Inclusion body preparation

For preparation of inclusion bodies, bacteria were induced at OD of between 0.6-1.0, as protein yield can often be enhanced at higher OD. Following expression overnight at 37°C, bacteria were lysed by sonication in the following lysate buffer: 20mM Tris-HCl, pH 8.0 50mM NaCl, 5mM EDTA , 0.5% Triton-X100 and 0.1mM PMSF. Reducing agents were avoided so as to not interfere with potential intramolecular disulphide bonding. Cells from 4 litres of culture were lysed in 250ml of lysate and sonicated for a total of 10-15 minutes on ice in 10s bursts with 10s intervals. Following sonication, 10mM $MgSO_4$ was added to chelate EDTA, and lysozyme (0.1mg/ml) subsequently added to the lysate and incubated at RT for 20min to facilitate cell lysis. The lysate was centrifuged (6000 rpm for 15 minutes) to collect inclusion bodies, and the pellet resuspended completely once more by sonication in

the lysate buffer. The final wash step was conducted using lysate buffer without Triton-X100: 20mM Tris-HCl, pH 8.0 50mM NaCl , 5mM EDTA. The washed inclusion body pellets were dispersed completely by sonication and then dissolved overnight at 4°C by stirring vigorously, in 20mM Tris buffer (pH 8.0) containing 6M GdHCl. 100 mL for 2 L of culture was used at this dissolution stage. The following day, the solution was centrifuged (6000 rpm for 20 minutes) to remove any insoluble particulates, and refolding of the rPmpD was conducted using step-wise dialysis by altering the concentration of GdHCl from 6M to 4M to 2M to 1M over the course of 3 days at 4°C.

2.1.7 Protein purification

Recombinant CT694 or rPmpD were purified using a nickel-affinity chromatography column (GE Healthcare) pre-equilibrated with binding buffer (20mM TrisHCl pH 8.0, 50mM NaCl, 10mM imidazole), and protein was eluted under a linear imidazole gradient (10–500mM). Eluted fractions were analysed by SDS–PAGE and those containing overexpressed protein (approximately 90% pure) were pooled and concentrated and then applied onto a 16/60 S75 Superdex gel-filtration column (GE Healthcare) which was pre-equilibrated with 20mM TrisHCl pH 8.0, 50mM NaCl. Eluted fractions containing pure CT694 protein (appearing as a single band on SDS–PAGE) were concentrated to approximately 20–40 mg/ml protein and stored at −80°C.

2.1.8 Circular Dichroism

Circular-dichroism (CD) spectra were recorded at 20°C with a Jasco J-180 CD

spectrophotometer using a 0.1 cm path-length quartz cell. Experiments were carried out in 20mM Tris/HCl buffer pH 8.0. The protein concentrations in the samples were 0.2 mg ml^{-1}. Random error and noise were reduced for each spectrum by averaging three scans in the wavelength range 260–195 nm. The signal acquired for the buffer used for dilution of the proteins was subtracted from the spectra acquired for the proteins.

2.1.9 Dynamic Light Scattering

The polydispersity of rPmpD oligomeric and monomeric fractions was analysed using dynamic light scattering (DLS). Measurements were carried out at 20˚C with the protein at 1 mg/ml in size exclusion buffer using the DynaPro Dynamic Light Scattering system (Protein Solutions).

2.1.10 Protein Crystallization Screening

Crystallization was carried out in nandroplet sitting-drop vapour-diffusion format in 96-well low-profile Greiner plates and Mosquito liquid handling robot (TTP Labtech, UK). Plates were placed at 277K using sitting drops formed by mixing equal volumes (150nl) of protein and reservoir solution. All high-throughput 96-well crystallization screens were purchased from Hampton Research. These included the Hampton 1 and 2, Index, PACT, CSS 1 and 2, Peg Ion 1 and Peg Ion 2 screens. In addition, due to the likely association of both CT694 and PmpD with host and bacterial cell membranes, specialized 96-well high-throughput MemPlus and MemGold membrane protein screens (Molecular Dimensions) were also utilized. For rPmpD and CT694 proteins, concentrations of 5-20mg/ml or 10-80mg/ml were used (respectively).

2.1.11 Agarose Gel Electrophoresis

DNA was analysed using agarose gel electrophoresis. Agarose and SybrSafe DNA gel stain were purchased from Invitrogen. 1kb DNA ladder and 6× loading dye were purchased from New England Biolabs (NEB). A 1% (w/v) agarose gel consisted of 0.7g of agarose in 70ml Tris-base, acetic acid and EDTA (TAE) buffer and 1µl of 10000× SybrSafe DNA gel stain. 20µl-loading samples consisted of 83% (v/v) DNA solution and 17% (v/v) loading dye. Electrophoresis with 1% agarose gels was carried out at 100V for 40 minutes in 1× TAE buffer. DNA fragment length was estimated using 1kb DNA ladder (NEB). Detection, photography and excision of amplified DNA fragments were visualized under a Safe Lamp and excision of bands of corresponding molecular weights carried out using a scalpel.

1x Gel Loading Dye: 2.5% Ficoll-400, 11mM EDTA, 3.3mM Tris-HCl (pH 8.0), 0.017% SDS, 0.015% bromophenol blue

TAE buffer: 40mM Tris, 20mM acetic acid, 5mM EDTA, pH 8.0

2.1.12 SDS- and Native PAGE

Acrylamide solution was purchased from National Diagnostics. All running and loading buffers for Native PAGE contained no SDS. SDS-PAGE samples were denatured for 5mins in sample loading buffer at 95°C prior to gel loading. 'Broad Range Molecular Weight Marker' (BioRad) was used as a standard to estimate protein molecular weights. The marker contained myosin (200kDa), β-galactosidase (116kDa), phosphorylase B (97.4kDa), serum albumin (66.2kDa), ovalbumin (45kDa), carbonic anhydrase (31kDa), trypsin inhibitor (21.5kDa), lysozyme (14.4kDa) and aprotinin (6.5kDa).

Protein samples were analysed by loading on to 10% SDS gels and 5% native gels. A 10% resolving gel consisted of 2ml deionized water, 1.5ml buffer (1.5M Tris/HCl, 0,4% (w/v) SDS, pH 8.8), 1.65ml acrylamide solution, 25μl of 10% (w/v) APS, 4μl TEMED and 4μl bromophenol blue. A 5% native gel consisted of 2ml of deionized water, 1.5ml buffer (1.5M Tris/HCl, pH 6.8), 0.825ml acrylamide solution, 25μl of 10% (w/v) APS and 4μl TEMED. Following electrophoresis, the gels were immersed overnight in staining and then destaining solutions (see below) and photographed using the SynGene INGENIUS apparatus with GeneSnap software.

Loading buffer: 0.5M Tris, 10% (w/v) glycerol, 2% (w/v) SDS, 0.005% Bromophenol Blue, 5% (v/v) β-mercaptoethanol, pH 6.8

Running Buffer: 25mM Tris, 250mM glycine, 0.1% (w/v) SDS, pH 8.4

Staining solution: 25% (v/v) propan-2-ol, 10% glacial acetic acid, 0,2% (w/v) Coomassie Brilliant Blue

De-staining solution: 5% (v/v) propane-2-ol and 7% (v/v) glacial acetic acid

2.2   *In vitro* cell adhesion studies

This section describes the procedures used in cell adhesion experiments with rPmpD-coated polystyrene beads described in Chapter 5.

2.2.1 Bradford Assay

Eight dilutions of BSA standard (2000μg/ml, 1500μg/ml, 1000μg/ml, 750μg/ml, 500μg/ml, 250μg/ml, 125μg/ml, 25μg/ml and 0μg/ml) were prepared. Buffer containing 20mM Tris/HCl, 50mM NaCl was used as the diluent for BSA standards.

1x dye reagent was equilibrated to room temperature, and 1ml of this solution pipetted in to a disposable cuvette. 20µl of standard or protein sample of unknown concentration was pipetted in to the cuvette, mixed well, and left for 5mins at room temperature before absorbance was measured at 595nm on a UV Eppendorf Biophotometer. Unknown protein concentrations were determined from the standard curve.

Coomassie (Bradford) Protein Assay Reagent: Coomassie G-250 dye, methanol, phosphoric acid and solubilizing agents in water.

2.2.2 Endotoxin Removal and Quantification

To remove LPS from rPmpD prior to use in immunisations and adhesion assays, 1ml of rPmpD was sealed with parafilm in a sterile Eppendorf tube and incubated with 10µl of Triton-X 114 detergent (1:100 dilution) with stirring in a water bath at 4°C overnight. Sample was then incubated at 37°C for 10mins to form detergent micelles with LPS followed by immediate centrifugation at 13,300rpm and separation of supernatant aqueous (rPmpD-containing) from detergent (LPS-containing) phases. Supernatants were then analysed for endotoxin concentration using the LAL Endotoxin Chromogenic substrate kit according to the manufacturer's protocol.

All reagents were equilibrated to room temperature before use. Four vials containing endotoxin standards (1EU/ml, 0.5EU/ml, 0.25EU/ml, 0.1EU/ml) were prepared, and 50µL of each standard or unknown sample replicate into the appropriate microplate well, cover the plate with the lid and incubate for 5 minutes at 37°C. Each series of determinations included duplicate runs of rPmpD supernatant, blanks (50µL of endotoxin-free protein buffer or endotoxin-free water) and four endotoxin standards.

50μL of LAL was added to each well using a pipette and incubated at 37°C for 10 mins. 100μL of substrate solution to each well and mixed thoroughly, followed by incubation of the plate at 37°C for 6 minutes. 50μL of Stop Reagent (25% acetic acid) was added and gently shaken on a plate mixer for 10 seconds. Absorbance was read at 405nm on a plate reader VersaMax microplate reader in conjunction with the SoftMax Pro v.5.3 software (Molecular Devices, USA).

After subtraction of the average absorbance of the blank replicates from the average absorbance of all individual standard and unknown sample replicates, a standard curve was plotted with average blank-corrected absorbance for each standard versus concentration in EU/mL. Endotoxin concentration of each unknown sample was estimated using the equation for the line of best fit.

Pierce LAL Chromogenic Endotoxin Quantitation Kit, sufficient reagents to perform 50 assays of standards and samples in a microplate (i.e., 50 wells total)

Kit Contents: *Escherichia coli* (*E. coli*) Endotoxin Standard (011:B4), lyophilized, 1 vial, 15-40 endotoxin units (EU)/mL upon reconstitution **Limulus Amebocyte Lysate (LAL),** lyophilized, 2 vials, 1.4mL/vial upon reconstitution **Chromogenic Substrate,** lyophilized, 1 vial, 6.5mL/vial upon reconstitution **Endotoxin-free Water,** 1 vial, 30mL

2.2.3 Bead adhesion experiments

1 mL of 1% bead suspension in 50 mM MES pH 6.1 containing a final protein concentration of 0.25μg/ml - 50μg/ml rPmpD or BSA was used for coating the beads. A final concentration of 1mM EDAC was used to covalently link rPmpD directly to

the beads through primary amine groups on the ligand. 50µg/ml, 25µg/ml, 2.5µg/ml and 0.25µg/ml concentrations of rPmpD were used for coating beads. The mixture was incubated at 20°C with gentle shaking for 1hr and the reaction was stopped by centrifugation of the suspension, discarding the supernatant, and washing the pellet twice in in binding buffer to remove all traces of EDAC. Coupling of rPmpD protein to the beads was verified on SDS-PAGE by inspection of the reaction supernatant and boiling of coated beads at 95°C for 5mins.

2.2.4 Bead binding

Initial adhesion assays using 2µm L4530 fluorescent beads (Sigma Aldrich) were performed on layers of Hak cells (70-80% confluent) in 96-well plates. Serial dilutions of beads (1:20, 1:50 and 1:100) were added to Hak cells which were incubated for 1 h at 4°C to initiate binding. Unattached beads were removed by twice washing with PBS, and cells were fixed with methanol. Binding was quantified following Giemsa staining, by counting the number of attached beads per 50 cells in triplicate fields of view under phase microscopy. Naked (uncoated) or BSA-coated beads were used as controls.

2.2.5 Antibody neutralisation assay

Three dilutions (1:20, 1:50 and 1:100) of a 1% solution of L4530 fluorescent beads were separately pre-incubated with three dilutions (1:50, 1:100, 1:200) of heat-inactivated pre-immune or anti-rPmpD immune serum (obtained from immunized C57BL/6 mice) for 1h at 37°C with gentle shaking to enable binding of antibodies to

the beads. Bead-serum mixtures were then added to layers of Hak cells (70-80% confluent) in 96-well plates, and incubated for 2h at 4°C to allow for binding. Unattached beads were removed by twice washing with PBS, and cells were fixed with methanol. Binding was quantified following Giemsa staining, by counting the number of attached beads per 50 cells in triplicate fields of view under phase microscopy. Naked (uncoated) or BSA-coated beads were used as controls.

2.2.6 Competitive inhibition assay

Monolayers of Hak cells (70-80% confluent) in 96-well plates were pre-incubated with four dilutions (50μg/ml, 25μg/ml, 2.5μg/ml and 0.25μg/ml) of soluble rPmpD for 1hr at 4°C to allow for binding. Following two washes in PBS to remove unbound protein, three dilutions (1:20, 1:50 and 1:100) of a 1% solution of L4530 fluorescent beads were added and incubated for 2h at 4°C to allow for binding. Unattached beads were removed by twice washing with PBS, and cells were fixed with methanol. Binding was quantified following Giemsa staining, by counting the number of attached beads per 50 cells in triplicate fields of view under phase microscopy. Naked (uncoated) or BSA-coated beads were used as controls.

Beads: Fluorescent carboxylate-modified beads of several mean particle size distributions were purchased from Sigma Aldrich - L3210 (0.5μm), L4655 (1μm) or L4530 (2μm).

Coupling buffer: Covalent coupling to carboxylate-modified beads was performed by reaction with 1mM *N*-Ethyl-*N′*-(3-dimethylaminopropyl)carbodiimide hydrochloride (EDAC) (Sigma Aldrich) in 50 mM MES pH 6.1.

Binding buffer: 100mL of binding buffer was composed of 10mL (10x RPMI), 10% BSA (w/v), 1mL 1M HEPES (pH7.5) and 89mL deionized water. Buffer was sterile-filtered prior to use.

Giemsa stain solution

Giemsa stain solution consisted of 3.6ml Sorensen A [9.5g/l $NaHPO_4$ (Sigma)], 1.4ml Sorensen B [9.07g/l KH_2PO_4 (Sigma)], 45ml de-ionized water and 5.55ml Giemsa stain (VWR International).

2.3 *In vivo* vaccinology studies

This section describes the procedures used in *in vivo* vaccinology studies (described in Chapter 6) using monomeric 65kDa rPmpD (**Fig.4.2**) in combination with three different formulations of a second-generation lipid adjuvant (SLA) in a mouse model of *Ct* infection.

Buffers and Solutions

Phosphate buffered saline

1x phosphate buffer saline (PBS) consisted of 10mM PO_4^{3-}, 137 mM NaCl, and 2.7 mM KCl made up in distilled water.

Gey's solution

Individual solutions consisted of:

Solution A (1L): 35g NH_4Cl (Sigma-Aldrich), 1.85g KCl (VWR International), 0.63g Na_2HPO_4 (Sigma-Aldrich), 0.12g KH_2PO_4, 5g Glucose

Solution B (100mL): 0.42g $MgCl_2.6H_2O$ (Sigma-Aldrich), 0.14g $MgSO_4.7H_2O$ (Sigma-Aldrich), 0.34g $CaCl_2$ (Sigma-Aldrich)

Solution C (100mL): 2.25g $NaHCO_3$ (Sigma-Aldrich)

Gey's working stock (1x): Solution A: 20 parts, Solution B: 5 parts, Solution C: 5 parts, Distilled water: 70 parts

Buffers for Enzyme-Linked Immunosorbent Assay (ELISA)

Coating buffer consisted of 0.1M Na_2CO_3, 0.1M $NaHCO_3$, pH 9.6. Blocking buffer and diluent consisted of 1x PBS with 0.05% Tween-20 (Sigma-Aldrich) and 0.1% BSA (Sigma-Aldrich). 0.01% sodium azide (Sigma-Aldrich) was added to blocking buffer only. Wash buffer consisted of 1x PBS with 0.05% Tween-20 (Sigma-Aldrich).

2.3.1 Animals

Female C57BL/6 mice were obtained from a locally maintained colony (University of York, York, UK). Female Balb/c mice were obtained from Harlan Laboratories (Wisconsin). Both mouse strains were used from 6-8 weeks of age and housed under specific pathogen-free conditions. Experimental procedures were administered in accordance with the UK Home Office regulations.

2.3.2 Animal Samples

Blood samples were obtained by tail snip. Up to 50µl of blood was stored in Eppendorf vials on ice or at 4°C until processing. Total blood volume was taken via cardiac puncture using a 25G needle after death. Mice were killed by carbon dioxide asphyxiation followed by cervical dislocation. The spleen was dissected and kept at 4°C. in 1x RPMI (Gibco) until processing. Each spleen was homogenized using a 50µm cell strainer. 10ml of sterile 1x RPMI medium (Sigma Aldrich) was used to wash splenocytes through the strainer into the Falcon tube. These were centrifuged at 1300rpm for 10mins at 4°C.

2.3.3 *Chlamydia trachomatis* strains

C.trachomatis E/Bour strain and genomic DNA were obtained from ATCC. Clinical isolates E9/Soton and F1/Soton were obtained from Professor Ian Clarke (University of Southampton) and serovar D/UW3/Cx from Imperial College, London (propagated in the Shattock Laboratory, originally from Rey Carabeo).

2.3.4 Cell culture and propagation of *Chlamydia trachomatis* strains

C.trachomatis isolates were propagated in mycoplasma-free McCoy cells (ATCC) in 96-well, 24-well, 6-well plates (Sigma) or 75-cm^2 polystyrene culture flasks (Corning). McCoy cells were grown in Dulbecco's modified Eagles' medium (DMEM) supplemented with 10% fetal calf serum (FCS). Cell seeding densities were determined using Tryphan Blue staining and haemocytometer counts. Cells were infected with *C.trachomatis* strains by centrifugation of the inoculum at 1800rpm for 30mins-1hour at room temperature or 37°C in DMEM containing cycloheximide (1µg/ml) and gentamicin (25µg/ml). After completion of the biphasic developmental cycle, cells were harvested using a cell scraper and centrifuged at 3500rpm. For storage, the *C.trachomatis*-infected pellet was resuspended in a 1ml solution of ice-cold 4-sucrose phosphate buffer (16mM Na$_2$HPO$_4$, pH 7.1 and 0.4M sucrose, abbreviated as 4SP) and 10% PBS (mixed in a 1:1 ratio). The cells were transferred into a bijoux tube with sterile glass beads and lysed by vortexing for 2 mins. Cell debris was removed by centrifugation at 1500rpm for 5 mins and the supernatant collected and stored at -80°C.

2.3.5 *Chlamydia trachomatis* UV-inactivation

C.trachomatis serovars E9/Soton or E/Bour elementary bodies were inactivated by UV irradiation at a distance of 15cm under a UV-lamp for 60 minutes. Viability was validated by inoculation on to McCoy cell monolayers and immunofluorescence staining 48 hrs post infection.

2.3.6 Second Generation Lipid Adjuvant Formulations

Second-generation lipid adjuvant (SLA) was synthesised by Avanti Polar Lipids (Alabaster, AL), Corden Pharma (Liestal, Switzerland), or in collaboration with Dr. Robert William's lab at Colorado State University. Squalene and cholesterol were purchased from Sigma-Aldrich (St. Louis, MO). Poloxamer 188 and glycerol were obtained from Spectrum Chemical (Gardena, CA). Buffer components purchased from J.T. Baker (San Francisco, CA). Dioleoyl phosphatidylcholine (DOPC) was obtained from Lipoid LLC (Newark, NJ). Dimyristoyl phosphatidylcholine (DMPC) and dipalmitoyl phosphatidylcholine (DPPC) were obtained from Avanti Polar Lipids or Lipoid.

Aqueous suspensions of SLA (SLA-AF) were manufactured by mixing DPPC and the TLR4 ligand at a 2:1 DPPC:SLA molar ratio in chloroform, which was then evaporated. Ultra pure water was added to the resulting dried film, and the mixture was sonicated in a VWR 75D (West Chester, PA) or Crest Powersonic CP230D (Trenton, NJ) sonicating water bath at 60°C until the formulation was translucent.

Oil-in-water emulsion formulations of SLA (SLA-SE) were manufactured by high-speed mixing a buffered aqueous phase (containing poloxamer 188, glycerol, and

ammonium phosphate buffer) and an oil phase (containing squalene, DMPC, and SLA) at 7,000-10,000 rpm for 10 minutes followed by microfluidization for 10-12 passes at 30,000 psi as described previously with minor modifications (Misquith et al., 2014).

The liposome formulation (SLA-LSQ) was manufactured by the thin film technique, with the lipid excipients (DOPC:cholesterol 4:1 weight ratio) together with SLA were initially mixed in chloroform. Following evaporation of the solvent, the lipid film is hydrated in 25 mM ammonium phosphate buffer (pH ~5.7) and briefly sonicated in a water bath to remove the film from the glass flask. This crude liposome mixture is then processed by high-pressure homogenization at 20,000 psi for five cycles to achieve a monodisperse particle size ~80 nm, which is then mixed with aqueous QS21 solution and sterile-filtered through a 0.2 μm membrane.

2.3.7 Mouse immunisations

Six-eight week old C57BL/6 mice were obtained from local colonies (York BSF) and housed in specific pathogen-free conditions. Animals were immunised subcutaneously (s.c.) at the base of the tail on day 0 with 100μl of sterile PBS containing 5μg/dose SLA adjuvant (SLA-AF, SLA-SE SLA-LSQ) with 5μg/dose rPmpD or 2×10^{7} IFU of UV-inactivated *Ct* serovar E/Bour EBs. Mice were boosted s.c. with the same doses on days 21 and 42. Additional groups of mice received rPmpD or PBS alone as controls.

2.3.8 *Chlamydia trachomatis* intra-vaginal challenge, bacterial swabbing and quantification

Mice were anaesthetised with isofluorane (Abbott, Maidenhead, UK) in a dedicated inhalation chamber prior to Depo-Provera administration and challenge. All animals received a subcutaneous injection of 2.5mg of medroxyprogesterone acetate (Depo-Provera, Pfizer) in the scruff of the neck one week prior to challenge. After testing for lack of a reflex, when in a light sleep, the animals were held upwards from the base of the tail and 10µl of *Chlamydia trachomatis* urogenital serovar D/UW3/Cx containing 4.5×10^8 IFU (obtained from Prof. Rey Carabeo) was pipetted into the vaginal vault using a Microman Precision Microliter Pipette with rounded-tip capillary pistons (Gilson).

Cervicovaginal swabs were obtained on days 1, 3, 7, 14 and 22 post-challenge. Swabs were vortexed in 500µl sterile PBS with glass beads and stored at -80°C until titration. Enumeration of recoverable *Ct* bacteria was conducted in Hak cells (ATCC) using serial dilutions of swab samples centrifuged on to cell monolayers by immunofluorescence 48hrs post infection. The total number of inclusions per well were counted at 10x magnification using fluorescence microscopy, and quantified as inclusion forming units per ml (IFU/ml).

2.3.9 Cervico-vaginal washes

Cervico-vaginal washes were carried out under the same conditions of anaesthesia. 100µl of sterile-filtered 1x PBS was pipetted up-and-down the vaginal cavity ten times using a Microman Precision Microliter Pipette with rounded-tip capillary pistons. To prevent protein degradation, 25x Protease Inhibitor Cocktail (Sigma-

Aldrich) was added to the PBS. Cervico-vaginal washes were stored at -80°C until use.

2.3.10 ELISA

Serum was obtained on days 0, 14, 35, 56 and 105. Cervico-vaginal washes were obtained on days 34 and 55 post initial immunization. Blood samples were left at 4°C overnight to facilitate clotting. The following day, samples were centrifuged at 24,000 x g at 4°C for 15 minutes to separate serum from cells. Sera and washes were stored at -20°C until required. 96-well Assay plates (Costar) were coated with 50µl rPmpD (1µg/ml) or UV-inactivated *Ct* E/Bour UVEBs (5.8×10^6 IFU/ml) at 4°C overnight in coating buffer (0.1M Na_2CO_3, 0.1M $NaHCO_3$, pH 9.6). Plates were washed four times with wash buffer (300µl/well). All subsequent washing steps were carried out using the same number of washes and volume of wash buffer per well with a SkanWasher 400 (Molecular Devices, USA). Blocking buffer was added (200µl/well) and plates incubated for 2hr at room temperature prior to addition of serial dilutions of serum (100µl/well) in diluent from (1/10 to 1/10,000,000) and serial dilutions of cervico-vaginal wash (neat to 1/625). After incubation for 2 hours at 37°C, plates were washed and then incubated with HRP-conjugated goat anti-mouse IgG, IgG1 or IgG2c antibodies (AbD Serotec) at 37°C for 30 minutes. After the final wash step, 50µl/well of ,3',5,5'-tetramethylbenzidine (TMB) substrate solution (Sigma-Aldrich) was added. Colour development was stopped after 5 minutes with 1M H_2SO_4 (KPL, USA) and plates were read immediately at 450nm (OD_{450}) with a VersaMax microplate reader in conjunction with the SoftMax Pro v.5.3 software (Molecular Devices, USA). Reciprocal serum dilutions corresponding to 50% maximal binding were used to obtain titres.

2.3.11 ELISpot

For initial immunogenicity studies, animals were euthanized 15 days after the final immunization, spleens collected, and single cell suspensions made. For the challenge study, animals were euthanized 8 weeks following final immunization (5 weeks post challenge). Enzyme-linked immunospot (ELISpot) assays were performed immediately following splenic harvest. Briefly, 96-well MultiScreen plates filtration plates (Millipore) were coated overnight at 4°C with IFNγ, IL-2, IL-5 or IL-10 monoclonal capture antibodies (Mabtech). Splenocytes ($2.5x10^5$) were added to the plate in the presence of 1μg/ml rPmpD. After incubation at 37°C with 5% CO_2 for 20h, plates were washed and incubated with respective biotinylated detection antibodies according to manufacturer's protocol (Mabtech). This was followed by incubation with streptavidin-alkaline phosphatase (1hr, RT) and addition of BCIP/NBT-plus substrate until distinct spots emerged. Plates were washed and dried overnight and spot forming units enumerated by eye.

2.3.12 Western Blot

Whole cell lysates of *Ct* serovar D/UW3/Cx were fractionated by SDS-PAGE and transferred to a polyvinylidene difluoride (PVDF) membrane using a transfer apparatus according to the manufacturer's protocols (Bio-Rad). After incubation with 5% BSA in Tris-buffered saline and Tween-20 (TBST - 10mM Tris, pH 8.0, 150mM NaCl, 0.5% Tween 20) for 60 min, the membrane was washed once with TBST and incubated with either preimmune serum, or d56 serum obtained from C57BL/6 mice immunized with rPmpD or UVEBs at 4°C overnight. Membranes were washed three times in TBST for 10 min and incubated with a 1:1000 dilution of HRP-conjugated anti-mouse antibody for 2h. Blots were washed with TBST three times and developed

with the ECL reagents (Amersham Biosciences) according to the manufacturer's protocols.

2.3.13 Immunofluorescence

Cells were fixed by incubating in 100% methanol (chilled at -20°C) at room temperature for 5 min. After decanting the methanol, blocking buffer was added for 30 min at room temperature to prevent unspecific binding of the antibodies. Cells were subsequently incubated with primary antibody (1:50) in dilution buffer for 1hr at room temperature and washed three times in PBS (5 min per wash) prior to addition of corresponding secondary antibodies (1:300) in the dark. After two 5mins washes, DAPI solution diluted (1:5000) in blocking buffer was added for 5mins and coverslips were subsequently dipped in deionized water and mounted in mounting medium on glass slides (ThermoFisher).

Immunofluorescence antibodies and buffers

1× Phosphate Buffered Saline (Sigma-Aldrich), Methanol (Fluka), Blocking and Dilution Buffer (1x PBS/0.2% BSA), **Primary antibodies**: Mouse anti-*Ct* LPS (ab54377 - abcam), Mouse anti-*Ct* MOMP (sc51837 - Santa Cruz), **Secondary Antibodies**: Donkey anti-mouse Alexa-Fluor 555 (Invitrogen), Goat anti-rabbit Alexa-Fluor 488 (Invitrogen), 4',6-diamidino-2-phenylindole – DAPI (Invitrogen), **Mounting medium**: Add 2.4 g of Mowiol 4-88 was added to 6 g of glycerol. 18 mL of 0.2 M Tris-Cl (pH 8.5) was added and heated to 50°C for 10min with occasional mixing. Following dissolution of the Mowiol, DABCO was added to 2.5% (w/v) to reduce fading. 1mL aliquots were stored at −20°C.

2.4   Statistical Analysis

Unless otherwise stated, groups were compared using an unpaired t-test assuming non-uniform variance, and all statistical analyses performed using the GraphPad Prism5 software. For vaccinology studies measuring resistance to infection and mean bacterial load, Professor Martin Bland performed the statistical analysis using the Stata data analysis and statistical software package. Groups were compared using one-way analysis of variance (ANOVA). If the data did not fit the model of normal distributions with uniform variance, a transformation was used. Visual inspection of the transformed data and Bartlett's test for equal variances were used to verify the assumptions.   Following one-way ANOVA, pairs of groups were compared using Sidak's multiple comparison method. P-values ≤ 0.05 were considered significant.

Chapter 3: Biophysical characterization CT694, an early type-three secretion system effector of *Chlamydia trachomatis*

3.1   Introduction

In addition to the Type V autotransporter secretion system (T5AT) that comprises the nine Pmps, *C.trachomatis* also possesses a Type III secretion system (T3SS), of which several substrates have been identified, and shown to interact with an array of host proteins. These include members of Inc family of proteins which associate with the *Ct* inclusion membrane (Rockey et al., 2002), and the well studied effector known as Tarp (translocated actin-recruiting phosphoprotein). Tarp is an early *Ct* effector known to be involved in remodelling of the host cytoskeleton and interactions with cell signaling proteins (Jewett et al., 2008; Jewett et al., 2006). Manipulation of the cytoskeletal machinery and signaling pathways is often a key prerequisite in the successful invasion of non-phagocytic cells by pathogenic bacteria (Dautry-Varsat, Subtil and Hackstadt, 2005).

Genomic transcriptional analysis during the *Ct* developmental cycle has been conducted (Belland et al., 2003). Here, microarrays were used to determine upregulation of genes associated with early (EB to RB) and late (RB to EB) stages of chlamydial development. Typically, it was found that immediate-early genes are associated with metabolism, and one gene was discovered to be a homolog of human early endosomal antigen-1 (CT147), associated with the chlamydial inclusion. Genes transcribed later in development typically encoded proteins involved in membrane assembly such as the cysteine-rich outer membrane proteins OmcA and OmcB (CT444 and CT443), Pmps G and H (CT871 and CT872) and aforementioned

thioredoxin disulphide isomerases (CT780 and CT783), are likely associated with correct disulphide bond formation in the COMC.

Interestingly, a predicted T3SS effector unique to *C.trachomatis* (CT694) was also found highly upregulated late in development. Genes transcribed late in development during RB to EB transition are hypothesized to be packaged away as effector proteins primed for invasion (Fields et al., 2003). Until very recently, due to the lack of a tractable genetic manipulation system for *Ct*, several T3SS substrates have been identified through the use of chemical inhibitors and heterologous expression systems in *Yersinia* and *Salmonella* (Fields and Hackstadt, 2000; Muschiol et al., 2006; Subtil, Parsot and Dautry-Varsat, 2001; Wolf et al., 2006).

CT694 and the adjacent CT695 gene were secreted by *Yersinia pseudotuberculosis*, but not by the T3SS null mutant (Δ*yscS*) *Yersinia pseudotuberculosis* (Hower, Wolf and Fields, 2009). Interaction partners for CT694 were identified using a *Saccharomyces cerevisiae* yeast-two-hybrid screen, with full-length CT694 fused to the *gal4* binding domain and expressed in an AH109 strain, which was mated with a Y187 strain expressing a HeLa cell cDNA library fused to the *gal4* activation domain. Recovered plasmids revealed interaction with residues 891-1055 of human AHNAK, a 700kDa protein known to bind actin (Haase et al., 2004; Hohaus et al., 2002). Further experiments also revealed that a CT694 ΔC-terminal truncated protein (CT694ΔC) failed to interact with AHNAK indicating involvement of this region in host cell interactions.

Ectopic expression of CT694 in HeLa cells revealed colocalization of GFP:CT694 with endogenous AHNAK. In contrast, GFP:CT694ΔC was found to associate with the plasma membrane, but failed to associated with AHNAK. Furthermore, ectopic expression of GFP:CT694 in HeLa cells resulted in decreased abundance of actin fibres stained by phalloidin, indicating possible effects on cytoskeletal remodeling by CT694 (Hower, Wolf and Fields, 2009). To investigate the hypothesis that the N-terminus of the protein contains a domain that may be involved in membrane localization, subsequent studies generated a range of GFP-fusion constructs to identify protein localization and binding partners during ectopic expression and yeast-two-hybrid (Y2H) screens (Bullock, Hower and Fields, 2012).

Fig.3.1 (reproduced from Bullock, Hower and Fields (2012)), shows the different truncations used to study the subcellular localization of the N- and C-terminal domains of CT694. The authors found that full-length CT694 associated with AHNAK as well as plasma membranes, but that a construct deficient in the N-terminal region corresponding to amino acid residues 40-80 is deficient for membrane localization. CT694 has thus been classified as a multi-domain T3SS effector, and is postulated to function in concert with Tarp during the invasion process, most likely in cytoskeletal remodeling. The presence of an N-terminal membrane localization domain may be important in targeting effector molecules to specific host cell compartments, while the distal C-terminal domain involved in AHNAK interaction and morphological changes may confer effector function.

A

	Designation	Ahnak binding	Membrane localization
1— [====] —322	694-FL	+	+
1— [====] —284	694-Δ39	–	+
1— [====] —221	694-Δ101	–	+
1— [===] –130	694-Δ192	–	+
1— [==] –79	694-Δ243	–	+/–
43— [====] —322	Δ42-694	+	+/–
1— [=]—[===] —322	694-Δ40-80	+	–

Figure 3.1: CT694 fusion constructs (Bullock et al., 2009). CT694 GFP fusion constructs generated to study the subcellular localization of the T3SS effector. CT694 consists of a multi-domain modular protein structure that possesses a lipophilic N-terminal membrane localisation domain in addition to a putative AHNAK binding C-terminal effector domain.

Recently, a *Ct* molecular chaperone Slc1 has been identified in complex with both CT694 and CT695, suggesting that CT695 is also a *Ct* effector, the function of which is yet to be fully elucidated (Pais et al., 2013). In addition, CT694 has been used as a diagnostic antigen in the monitoring of trachoma programs (Goodhew et al., 2012; Martin et al., 2015), suggesting immunogenicity during the course of natural infection, and its implied effector function may warrant its use as an antigen in future multicomponent *Ct* vaccines. Our investigations aim to elucidate the biophysical characteristics of this *Ct*-specific T3SS effector, using a range of methodologies similar to those employed for the study of rPmpD.

3.2   Results

3.2.1   Generation of the plasmids encoding CT694

Ct serovar E/Bour genomic DNA (ATCC) was amplified using the GenomiPhi DNA amplification kit (GE Healthcare) to generate increased amount of DNA for PCR reactions. This resulted in a range of DNA fragments of varying molecular weights **(Fig.3.2)**.
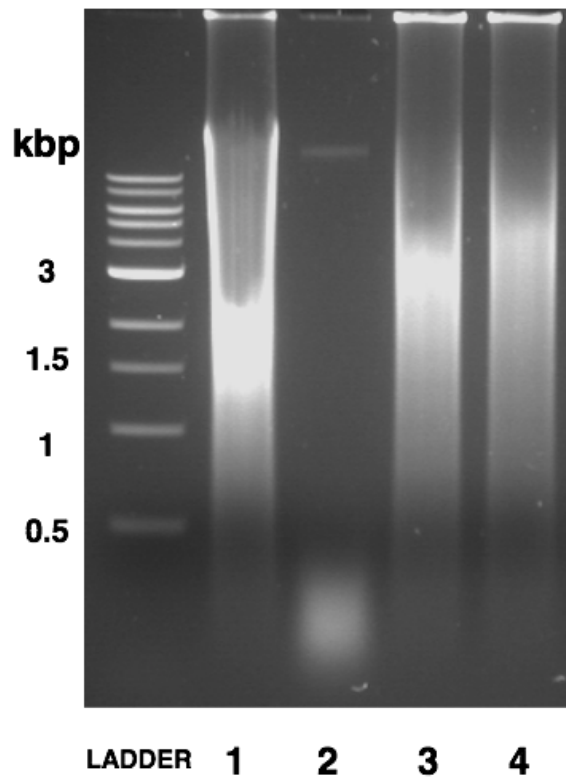
Figure 3.2: Whole genome amplification. *Ct* serovar E/Bour DNA amplification was implemented using the GenomiPhi amplification kit (GE Healthcare) to increase the amount of DNA available for PCR reactions (Lane 1). As controls, *L.major* (Lane 3) and *P.falciparum* (Lane 4) DNA were also subjected to identical reaction conditions. Non-amplified *Ct* E/Bour DNA (Lane 2) is also shown for comparison. DNA fragments encompassing a range of molecular weights are generated in all amplification reactions.

3.2.2 Analysis of plasmids for correct gene insertion using PCR and DNA sequencing

Following ligation, transformation and plasmid amplification in NovaGigaSingle cells, PCR amplification of the isolated plasmids was conducted using initial primers used for gene amplification (**Table.2.2**). DNA fragments were resolved using agarose gel electrophoresis and visualization with SybrSafe stain under UV-light (**Fig.3.3**). This revealed the expected fragment size for ligated inserts. DNA sequencing was used to verify the correct sequence of all plasmids following cloning (**Appendix**). Due to the presence of a *Xho*I restriction enzyme site (CTCGAG) within the CT694 gene, plasmids encoding the full-length gene were generated from the pET-28 (b) vector backbone using *Nco*I and *Xho*I restriction enzyme digest of the vector, and *Nco*I and *Sal*I restriction enzyme digest of the gene fragment amplified from *Ct* serovar E/Bour DNA (**Fig.3.3**). *Sal*I possesses the same complementary overhang

[TCGA] as *Xho*I, so ligation can still be carried out using the T4-DNA-ligase. For cloning of the ΔN-CT694 gene, both vector and fragment were cloned and ligated using *Nco*I and *Xho*I restriction enzyme digests followed by incubation with T4 DNA-ligase. Genes cloned using this restriction enzyme combination result in a C-terminal His$_6$ tag. After ligation of the vector and insert, gene fragments were located between the ribosome binding sequence and the His$_6$ tag (**Fig.2.2**).
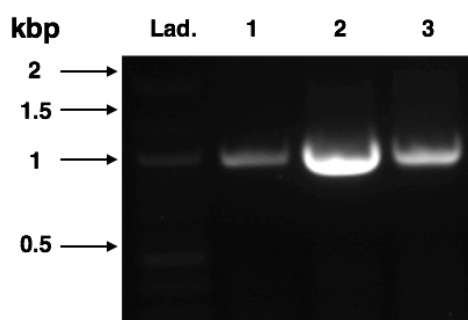
Figure 3.3: PCR of CT694 gene from *Ct* serovar E/Bour DNA. The CT694 gene was amplified from *Ct* serovar E/Bour DNA at three different annealing temperatures in a BIOER LifeEco Thermocycler machine (Lane 1). Following separate gene fragment and vector digestion with respective restriction enzymes (**Table 2.5**), ligation in to the pET28(b) vector for cytosolic expression was performed as described in Materials and Methods. PCR of two colonies was conducted to confirm plasmid uptake and ligation of the CT694 gene (Lanes 2 and 3). The expected gene size with appended C-terminal hexa-histidine tag (972bp) is observed in each case.

3.2.3 Overexpression of *Chlamydia trachomatis* recombinant CT694 full-length protein

Full-length (~35kDa) CT694 was overexpressed and purified in the soluble cytosolic fraction in *E.coli* BL21 (DE3) cells. Overexpressed full-length protein was purified using a three-step Ni-MAC, SEC and IEC procedure and analysed using both 5% native gel electrophoresis and 12% SDS-PAGE. Representative Akta traces are shown for typical purification steps (**Fig.3.4-3.5**). CT694 elutes as two well-defined peaks, with a mixture of oligomers eluting at the void volume of the column, and monomeric 35kDa CT694 protein eluting as the second peak. Purity was confirmed using SDS-PAGE and native gel electrophoresis.
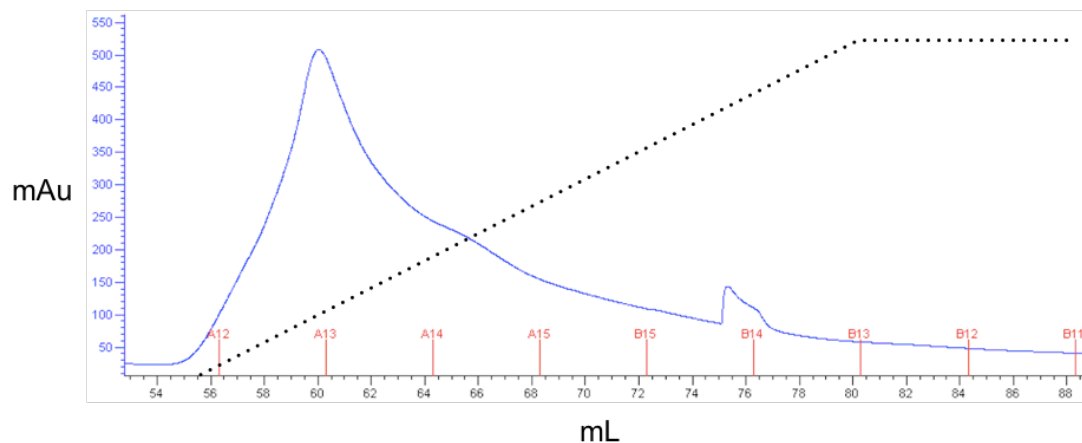
Figure 3.4: Metal affinity chromatography elution profile for CT694. Soluble CT694 expressed with a C-terminal His$_6$-tag was purified using nickel affinity chromatography from the cytosolic supernatant fractions following sonication, lysis and gradient centrifugation of *E.coli* BL21(DE3) cell lysates. Recombinant protein bound to the Ni-column was eluted using an imidazole gradient (dotted line).
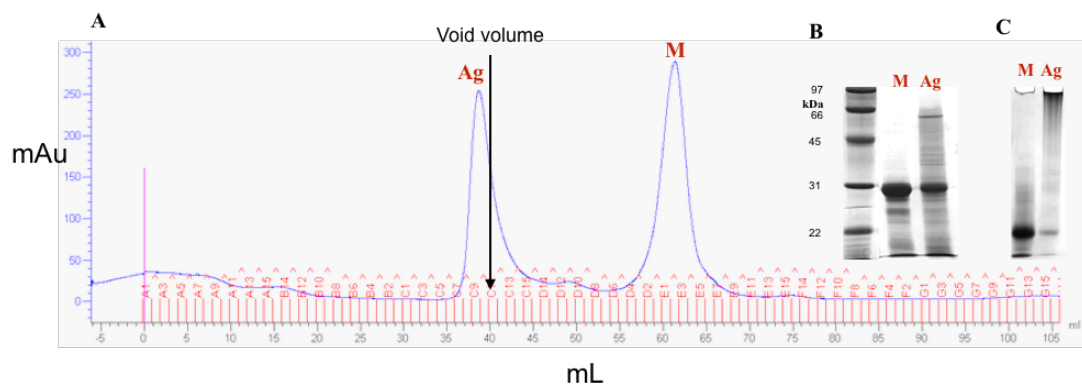
Figure 3.5: Fast protein liquid chromatography of CT694. Soluble CT694 purified using nickel metal affinity chromatography (**Fig.3.4**) with a C-terminal His$_6$-tag was further fractionated according to size distribution on S75 16/60 Superdex gel filtration columns. CT694 elutes as a mixture of soluble higher molecular weight aggregates ('Ag'- at the void volume of the column) and monomeric protein ('M'). A representative trace of a typical purification run is shown (**A**). Purity was confirmed by SDS- and Native-PAGE (**B** and **C**, respectively). Protein concentration was determined using the Bradford assay as described in Materials and Methods.

SDS gels show significant proteolysis of full-length recombinant CT694 over time. This breakdown pattern is shown in **Fig.3.6(A)**, as full-length protein degrades to a well-defined fragment after four months at 4°C. N-terminal sequencing of this breakdown product revealed the sequence: DIYHPTIFGQGAQPIVSTGDKKLD (**Fig.3.6(B)**), although no data were obtained for the C-terminal sequencing. Interestingly, the N-terminal sequence begins at amino acid residue 80 of the protein, suggesting the putative membrane localization domain identified in the study by

100

(Bullock, Hower and Fields, 2012) is labile or auto-catalytically cleaved. We have named this ~27kDa fragment ΔN-CT694.

A. CT694 proteolysis *in vitro* (4°C)

MW (kDa)

66
45
31
22
14

t=0   +3m   +4m

B.

MSIRPTNGSGNGYPSINPSNDNQDGLVQSTSGPNYGG
HTVSSRGGFQGICVRIADLFRNCFSRNRGTTTPSRPVIT
QADIYHPTIFGQGAQPIVSTGDKKLDSAIIQADLRAQNK
QTLATHIQSKLGSMEGQSPQDYKAGAYSALRLMLFTP
GETTVSSERERQACVTGRDLWEQAAGDLATNGNTDG
LMLMANLSVGGKHVPAGHLREYMNIVKGTFTDENEAT
DPTVDAILDLAAKIDATEFSSPGSGPVILNYIGNCGQVV
LENEKMNQLVLEDQNGQDPQRVQDNSKELQKLLENA
RKTDPELYFQTLTVITSSVFLD

Figure 3.6: Proteolysis of CT694 and N-terminal sequencing. Soluble full length CT694 undergoes proteolysis when stored at 4°C *in vitro* over a period of up to 4 months (**A**). This results in a stable fragment of MW ~27kDa. Sequencing of the proteolytic fragment reveals truncation of the N-terminus up to amino acid residue 80 (highlighted in red) (**B**). This portion is identified by Bullock et al. (2009) (**Fig.3.1**) as the membrane localization domain of CT694, and may be required for membrane association *in vivo*, but subsequently cleaved off as the C-terminal domain mediates effector function. This fragment (ΔN-CT694) was cloned as described in Materials and Methods, and expressed in exactly the same fashion as full-length protein showing a similar size exclusion profile (**Fig.3.5**).

3.2.4 Overexpression of *Chlamydia trachomatis* recombinant ΔN-CT694 fragments

ΔN-CT694 was successfully cloned in to the pET-28 (b) vector for cytosolic expression (**Fig.3.7**) using primers designed as described in Materials and Methods (**Table 2.1**).

Ladder (kbp)

3
1.5
1
0.5

739bp
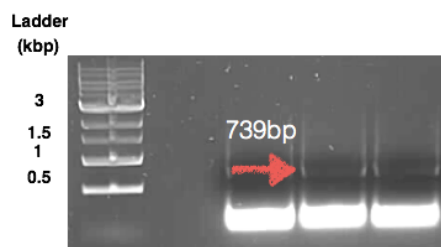
Figure 3.7: CT694 colony PCR. Colony PCR was utilised to screen for plasmid uptake. Insertion of the CT694 gene was confirmed. Sequencing using primers correspondent to the T7 promoter and T7 terminator domains showed correct sequence and ligation in to the multiple cloning site of the pET28(b) vector.

Overexpression of ΔN-CT694 reveals a similar SEC elution profile as full-length CT694 (**Fig.3.5**). Manual annotation of the N-terminal sequencing data following

MALDI-MS is shown in **Fig.3.8**. This is confirms the three most prevalent N-terminal sequences observed in the sample.
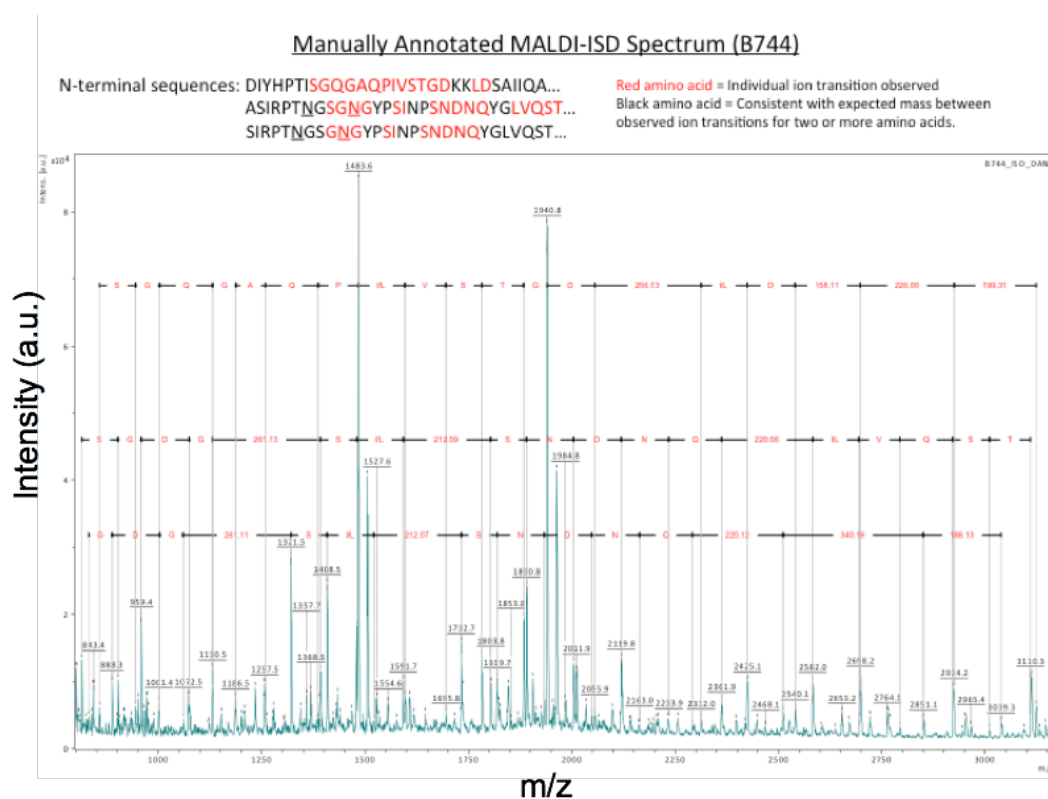
Figure 3.8: MALDI analysis of ΔN-CT694 proteolytic fragment. The proteolytic ΔN-CT694 product (~27kDa) was analysed for N- and C-terminal sequencing using MALDI-MS analysis. Although no data was reliably obtained for the C-terminal portion of the fragment, N-terminal sequencing shows truncation of the first 79 amino acid residues.

ΔN-CT694 is found to be stable at 4°C at the 6 week time point, but shows proteolysis when incubated for the same time period at 17°C and 20°C (**Fig.3.9(A)**). This may be due to slight contamination and increased activity of cytosolic *E.coli* proteases at higher temperatures, and the diminishing effects of protease inhibitor cocktails used in protein purification over time. ΔN-CT694 was retrieved from crystallization drops form Greiner plates incubated at 4°C for 6 weeks in native and SDS gels under both reducing and non-reducing conditions. No indications of disulphide-mediated intermolecular interactions are observed here, as ΔN-CT694 enters and migrates to the predicted molecular weight irrespective of the presence of β–ME in 12% SDS-PAGE (**Fig. 3.9 B and C**). Likewise, there is no evidence for

differential migration in native gels with or without the presence of reducing agents. This indicates the likelihood of an intramolecular disulphide bond formed between the two Cys residues contained within this fragment that stabilize the protein fold. All further crystallization experiments were thus carried out at 4°C.
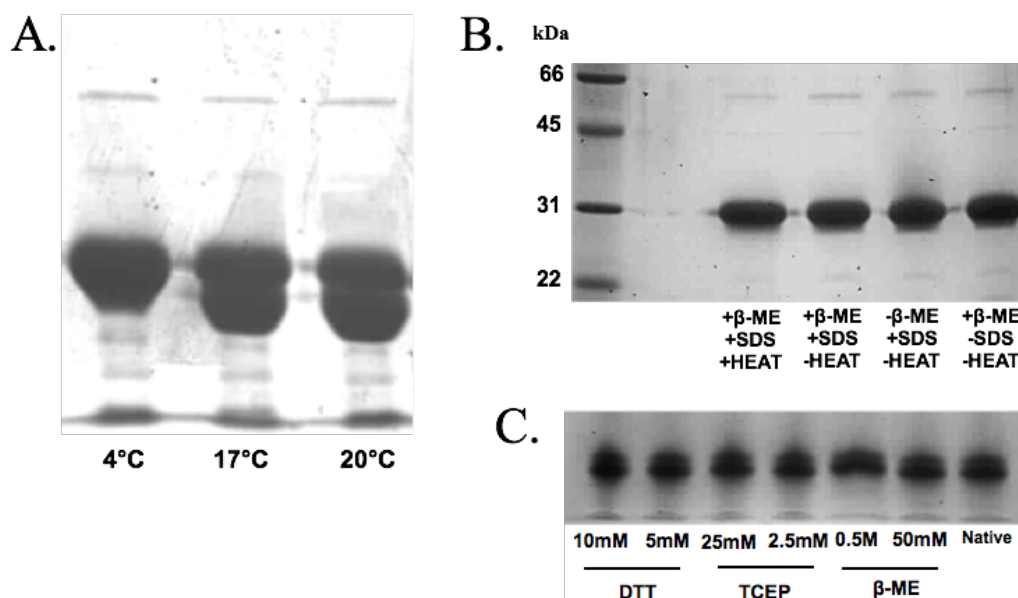
Figure 3.9: Crystallization screening of ΔN-CT694. ΔN-CT694 crystallization screens were set up at 4°C, to prevent protein degradation observed at 17°C and 20°C (**A**). Although no crystals have yet been obtained, drops were aspirated 6-8 weeks post set-up to verify integrity of the recombinant protein. Reducing and non-reducing SDS- and Native PAGE gels (**B** and **C**, respectively) show no indication of intermolecular disulphide-bonding or protein degradation.

To assess the likely secondary structure of ΔN-CT694, circular dichroism was conducted. This shows likely structured, folded protein, and a characteristically α–helical profile (**Fig.3.10**), as predicted by secondary structural prediction algorithm PSIPRED (**Fig.3.11**).
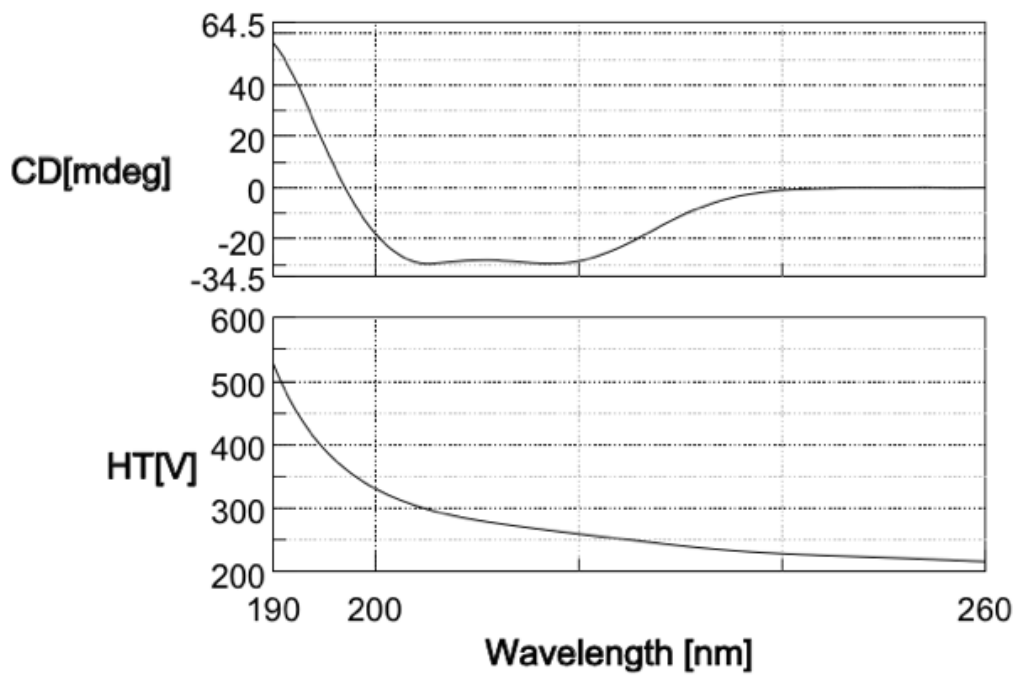
Figure 3.10: Circular dichroism of ΔN-CT694. Soluble monomeric ΔN-CT694 was analysed using circular dichroism. Spectra are characteristic of predominantly α-helical secondary structure.
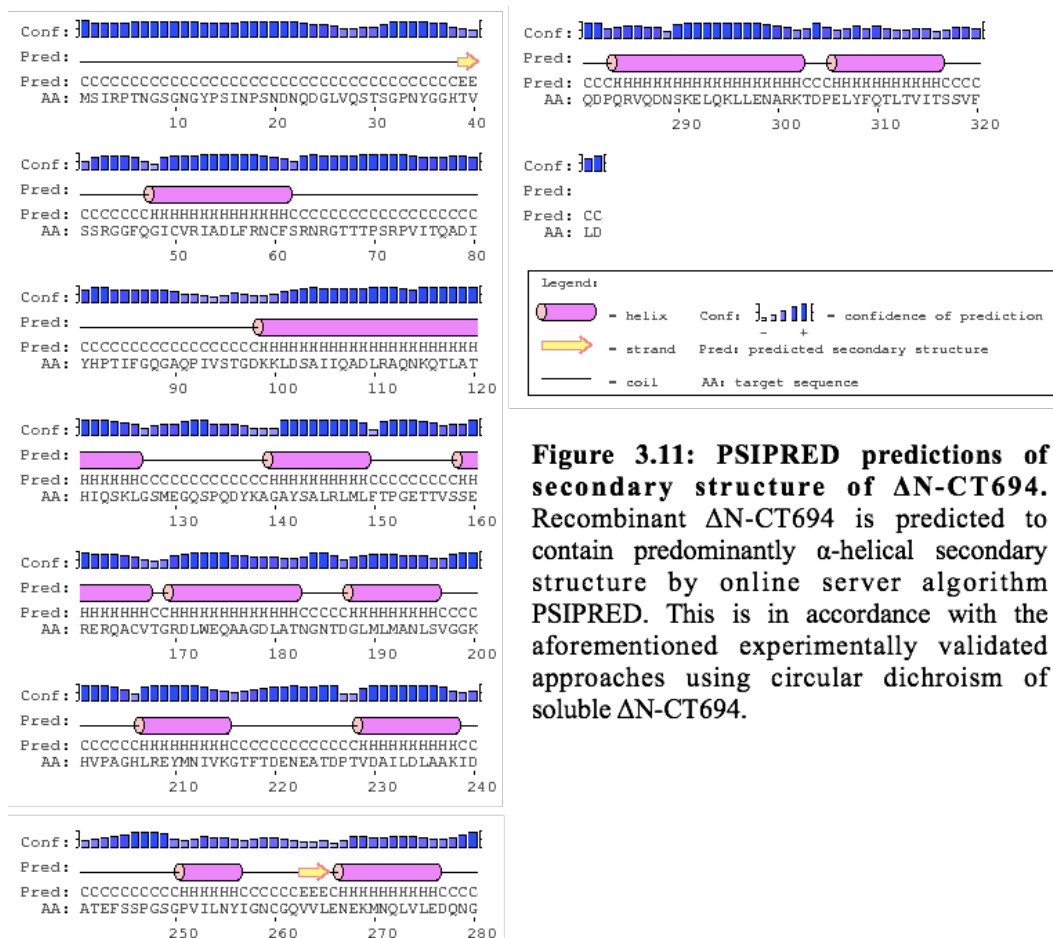
Figure 3.11: PSIPRED predictions of secondary structure of ΔN-CT694. Recombinant ΔN-CT694 is predicted to contain predominantly α-helical secondary structure by online server algorithm PSIPRED. This is in accordance with the aforementioned experimentally validated approaches using circular dichroism of soluble ΔN-CT694.

104

3.2.5 I-TASSER tertiary structural modeling of CT694

As an adjunct to ongoing crystallisation screens, an attempt was made to gain likely insight in to ΔN-CT694 tertiary structure and topology by *ab initio* modeling using the iterative threading assembly refinement (I-TASSER) server (Roy, Kucukural and Zhang, 2010). This methodology has previously been employed and validated for the modeling of hypothetical *Ct* protein CT296 (Kemege et al., 2011). Interestingly, the I-TASSER predicted model very closely matched the experimentally verified structure of CT296 solved by X-ray crystallography (RMSD of Cα atoms ~2.72-angstroms). Furthermore, these structural descriptions challenged previous experimental findings within the field, and validated the efficacy of *ab initio* modeling in predicting the structure, and hence function of a hypothetical protein (Kemege et al., 2011).

Because CT694 shows no primary sequence homology to any known protein outside *Ct* or the closely related *Cm* biovars, it was decided to employ I-TASSER modeling to deduce likely secondary structure (**Fig.3.12**). Importantly, the predicted α–helical structure corresponds to experimentally validated secondary structure using circular dichroism (**Fig.3.10**). The majority of solved protein structures within the PDB that possessed most significant homology to the predicted CT694 model as generated by I-TASSER belonged to the karyopherin superfamily of nuclear importins. Karyopherins are responsible for binding to specific cytosolic proteins bearing a classic nuclear localization sequence (NLS) (Lee et al., 2006), followed by translocation across the nuclear membrane (Kobayashi and Matsuura, 2013).

Furthermore, the stable proteolytic product observed following expression of full-length CT694 corresponds with complete cleavage of the membrane localization domain (MLD) between residues 79/80 (Bullock, Hower and Fields, 2012).

Figure 3.12: I-TASSER predictions of the tertiary structure of CT694. The I-TASSER tertiary structural predictions for the full-length (37kDa) hypothetical protein CT694 are shown. The almost exclusively α-helical structure depicted was verified experimentally by circular dichroism (**Fig.3.10**). The majority of the ten closest structural analogs identified by I-TASSER in the PDB comprise the transportin superfamily of proteins (such as karyopherins) that mediate nuclear import of a wide array of cytosolic proteins including transcription factors and cell cycle regulators (Kobayashi and Matsura, 2013).

Given that CT694 does not fractionate with membranes during late-cycle development (Bullock, Hower and Fields, 2012), it may be likely that the MLD is required only for interaction with host cell membranes during *Ct* adhesion and invasion, but is subsequently cleaved off during later stages, suggesting possible alternative cytosolic effector functions for the CT694 C-terminal domain in RBs.

Hower, Wolf and Fields (2009) do not rule out the possibility of GTPase activating protein (GAP) activity for CT694 directed towards a plethora of host cell proteins. However, if CT694 is indeed a karyopherin-like protein as predicted by I-TASSER

106

modeling, it is tempting to speculate that it may be responsible for nuclear translocation of certain host cell or injected *Ct* proteins during the early stages of infection, and during biphasic development. For instance, PmpD possesses a nuclear localization sequence, and the passenger domain is co-purified with host cell cytosolic proteins (Swanson et al., 2009). Other *Ct* effectors may also possess characteristic NLS.

Furthermore, following carboxymethylation of CT694, we have identified at least one of the four Cys residues (Cys_{50}) at the N-terminus of the protein is unpaired and hence able to partake in intermolecular interactions. The ΔN-CT694 domain contains two of the four Cys residues (Cys_{167} and Cys_{261}) (assumed to be paired), given that no intermolecular aggregation is observed in non-reducing SDS gels. Native gels run under reducing and non-reducing conditions also indicate no changes in biophysical state (**Fig.3.9 (B), (C)**).

3.3 Discussion

Ct has only very recently become readily amenable to genetic manipulation (Nguyen and Valdivia, 2012; Wang et al., 2011). Prior to this, over the last 6-8 years, insight in to mechanisms of pathogenesis of *Ct* infections has been obtained through advances in pharmacological or genetic manipulation of host cell pathways and observation of the effects of these modifications on cellular phenotypes. However, the temporal, spatial and functional roles that specific *Ct* proteins play in orchestrating cellular phenotypes or cell signaling pathways is much less clear during the course of *Ct* infection of host cells. Many observable phenotypes are likely due to the ~80 or so predicted T3SS effectors, most of which have unknown function.

A problem that has become endemic within the field of intracellular pathogen biology in the absence of tractable genetic manipulation is models derived from correlative data, where an observed cellular effect due to (e.g. ectopic expression) has been directly correlated with an observed cellular phenotype. While advances in cell biology techniques such as ectopic expression and yeast-two-hybrid screens may provide a good starting point from which to probe effector protein function, they are by no means definitive, as cell signaling events are usually context-dependent and part of a complex network of interacting pathways that may provide negative or positive feedback loops which are not well represented by overexpression *in vitro*. Furthermore, whether these proteins are actually translocated in to the host cell *in vitro* remains to be confirmed for many effectors. The most concrete means of directly correlating observed T3SS effector function with a cellular phenotype has been through microinjection of antibodies in to cells, where anti-Tarp antibodies have been shown to lead to a reduction in infection, and anti-IncA antibodies result in a fragmented inclusion phenotype (Hackstadt et al., 1999; Jewett et al., 2010).

In the latter case, this also reflects the observed phenotype in a clinical strain defective for *incA* expression (Johnson and Fisher, 2013), indicating the importance of future whole genome sequencing to represent a variety of clinical strains and its potential utility in elucidating genotype-phenotype relationships. T3SS effectors act throughout the developmental cycle of *Ct*, and have also been observed to play a role in the acquisition of lipid precursors and in bacterial exit pathways. A Y2H screen for interaction partners of the Inc protein CT228 revealed an interaction with the myosin light chain phosphatase (MYPT1), which is heavily regulated by phosphorylation, and

is thought to play a role in myosin-dependent extrusion of inclusions late in the infectious cycle (Lutter et al., 2013). Here again, genetic validation of a likely role for this interaction is provided by a naturally occurring clinical strain *Ct* B/Jali20 serovar (Lutter et al., 2013). This serovar has a truncated CT228 gene, which fails to recruit MYPT1 to the inclusion membrane.

Crucially, the advent of genetic manipulation of *Ct* has allowed more rigorous analysis of T3SS effectors, and this has helped to interrogate the function of specific genes at different stages of *Ct* development (Saka et al., 2011). Recently, a mutant strain lacking the T3SS effector Tepp, enabled the delineation of phosphorylation events on host protein recruitment, and these effects were importantly validated by plasmid transformation of the mutant strain that showed restoration of Tepp function (Chen et al., 2014). Most recently, the function of CPAF has been elucidated using advances in genetic manipulation (Snavely et al., 2014).

Although CT694 has been identified to interact with human AHNAK, the functional consequence of this interaction remains circumstantial (Hower, Wolf and Fields, 2009), and will most likely require complementation of a *CT694* null mutant to verify purported interactions. With the required toolkit now available to manipulate endogenous proteins in *Ct*, experimental validation of observed cellular phenotypes can be rigorously tested *in vitro*. However, a caveat of this approach is that if the gene is essential for bacterial survival, it may not be possible to observe a cellular phenotype, although an observed reduction in infection is most likely, given the presumed role of CT694 as early T3SS effector (Belland et al., 2003). Thus, structural approaches hold significant advantages in functional annotation of hypothetical

chlamydial proteins that may be integral to bacterial invasion or intracellular replication. The biophysical characterization of PmpD, a putative chlamydial adhesin subsequently employed as a candidate vaccine immunogen in our study, will be discussed in the following chapter. Structural integrity of recombinant vaccine antigens may play an important role in the ensuing immune response, particularly with regard to recognition of native antigenic epitopes, but is also crucial for downstream structural studies and protein crystallization.

Chapter 4: Biophysical characterization of *Chlamydia trachomatis* polymorphic membrane protein D – a candidate vaccine antigen

4.1   Introduction - PmpD

Purification of the *Ct* outer membrane complex was first carried out in 1981 following treatment of isolated EBs with an array of non-ionic, dipolar and anionic detergents (Caldwell, Kromhout and Schachter, 1981). Early studies on the COMC showed that *Ct* EBs and RBs from both *C.psittaci* and *C.trachomatis* LGV-434 species were not solubilised by the anionic detergent SDS, unless reducing agents were present (Hatch, Allan and Pearce, 1984). *Ct* EBs consist primarily of MOMP and two major cysteine-rich outer membrane proteins (CRPs) - known as OmcA (12kDa) and OmcB (60kDa) in *C.trachomatis* (Hatch, Allan and Pearce, 1984). In addition, COMCs in chlamydial species have been shown to harbor varying numbers of polymorphic membrane proteins (Pmps) (Tanzer, Longbottom and Hatch, 2001). The Pmps comprise a large and diverse family of Type V autotransporter (T5ATs) proteins within the *Chlamydiaceae*. While the total number of *pmp* genes varies between species, all possess a single *pmpD* ortholog (Wheelhouse et al., 2012). In addition, PmpD is the most highly conserved Pmp in *Ct*, with 99.15% sequence identity between the 18 *Ct* reference serovars (Carlson et al., 2005). This suggests a likely crucial or conserved role for *pmpD* in the life cycle of *Ct*.

Early studies using convalescent sera from patients with trachoma, lymphogranuloma venereum (LGV), cervicitis and urethritis all recognized a ~155kDa species-specific antigen (Caldwell, Kuo and Kenny, 1975). Several years later, this immunogenic protein was subsequently identified as PmpD, and shown to be surface-exposed on *Ct* elementary bodies (Crane et al., 2006). Furthermore, polyclonal anti-PmpD serum

demonstrated pan-neutralising activity against ocular, genital and LGV strains *in vitro*, and the authors further postulated that pre-existing antibodies to *Ct* MOMP or LPS blocked the ability of anti-PmpD antibodies to neutralise *Ct* infection (Crane et al., 2006). Examination of the PmpD protein sequence reveals 26 cysteine residues (the highest of any *Ct* Pmp), with 17 GGA(I,L,V) and 19 FXXN tetrapeptide repeat motifs – a feature shown to be characteristic of the chlamydial autotransporter passenger domains, and markedly over-represented in Pmps relative to the rest of the chlamydial proteome (**Fig.4.1**) (Craneet al., 2006).
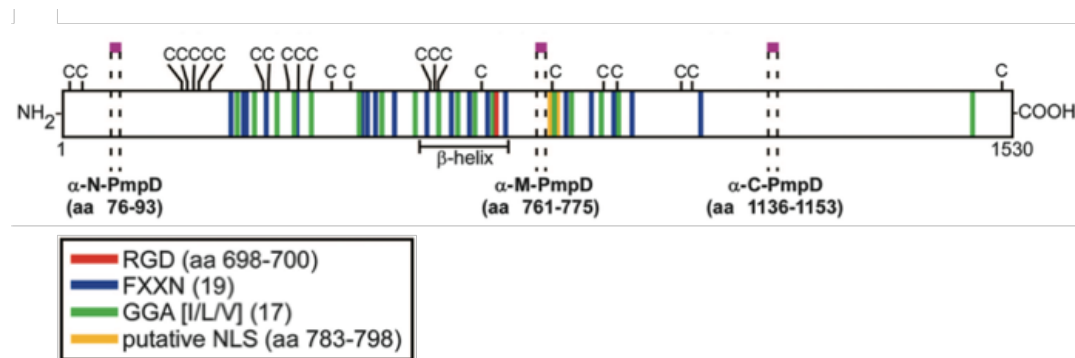
Figure 4.1: Schematic of *Ct* polymorphic membrane protein D (Swanson et al., 2009). PmpD is the most cysteine-rich Pmp in *Ct*, possessing 26 Cys residues in addition to 17 GGA(I,L,V) and 19 FXXN tetra-peptide repeat motifs, which are over-represented in chlamydial Pmps relative to the rest of the proteome. The GGA(I,L,V) motif (green) is only found in 10 proteins (one copy per protein) across all chlamydial proteomes, while the FXXN motif (blue) appears an average of 13.6 times in *Ct* Pmps and 11.3 times in *C.pneumoniae* Pmps, with an average of less than one copy per protein across both species' genomes. These epitopes may play key roles in the biological function of Pmps. The putative nuclear localization (yellow) and RGD binding motifs (red) are also shown.

The chlamydial outer membrane is unique when compared to all other known Gram-negative phyla, due to the presence of an extensively oxidized disulphide-linked outer membrane complex (COMC) in EBs, which shows increased fluidity, plasticity and differential protein composition and function as the infective forms transform in to metabolically active RBs through reduction of outer membrane proteins (Bavoil, Ohlin and Schachter, 1984; Hatch, Allan and Pearce, 1984). Although the cues for

regulation of biphasic development are not known, this reduction and re-oxidation of the COMC is thought to be crucial to enable vital infectious and metabolic processes which are key to intracellular survival, such as the initiation of entry and attachment (Abromaitis and Stephens, 2009), the insertion of the T3SS apparatus (Betts-Hampikian and Fields, 2011), and porin function of the chlamydial major outer membrane porin (MOMP) that comprises ~65% of the COMC, and is thought to be responsible for nutrient acquisition (Bavoil, Ohlin and Schachter, 1984; Sun et al., 2007). Given their uncharacteristic abundance within the chlamydial genome, it is highly likely that Pmps play pivotal roles in this biological transformation both extracellularly and possibly during intracellular metabolic activity.

During biphasic development, membrane composition has been shown to alter substantially, with RBs possessing little or no cysteine-rich proteins (CRPs) (Hatch, Allan and Pearce, 1984). In addition, most of the MOMP protein was shown to exist in monomeric form within RBs, with membranes more readily dissociable using anionic detergents, while EBs possess a large proportion of disulphide-linked trimeric MOMP (Sun et al., 2007). Earlier studies also employed the use of exogenous reducing agents to address the biological properties of both *C.psittaci* and *C.trachomatis* LGV-434 EBs (Hackstadt, Todd and Caldwell, 1985). It was observed that treatment of EBs with DTT resulted in decreased infectivity, increased glutamate oxidation and changes in Machiavello staining properties. However, reducing agents alone were not able to elicit a true RB transition, as electron microscopy revealed no changes in bacterial size or electron density, indicating irreversible disruption of key structural motifs required for membrane remodeling. These observations indicate that reduction of outer membrane proteins within the COMC may elicit metabolic and

structural changes, likely due to conformational changes in MOMP, although the contribution of other proteins (such as Pmps) to these morphological changes cannot be excluded.

Bavoil, Ohlin and Schachter (1984) used reduction and alkylation of MOMP within EBs to implicate the involvement of MOMP in pore-forming activity in the *Ct* COMC. Retention of carbol fuchsin dye suggested increased membrane permeability, and the abrogation of infectivity may reflect the disruption of key inter- and intramolecular bonding in extensively cysteine-rich outer membrane proteins that may function as adhesins, yielding a disordered and sub-optimal membrane structure. The mechanisms of reductive cleavage or re-oxidation of the COMC *in vivo* are still not understood, although MOMP has been shown to be reduced to its monomeric form within 1hr of EB entry in to host cells and CRPs are detected 20-22hrs post infection (Hatch, Miceli and Sublett, 1986). This suggests that changes in either the oxido-reductive states within the host cell inclusion or metabolism of the bacterium may effect transformation.

Of note is the presence of an RGD motif (aa698-700), (also shared by PmpF) and hypothesized to partake in adhesion via integrin binding, as well as a putative nuclear localization sequence (aa783-aa798). Two recent studies investigating PmpD processing reveal a variety of proteolytic species using antibodies generated against peptide fragments from the N-terminal, passenger and C-terminal domains (Kiselev, Skinner and Lampe, 2009; Swanson et al., 2009). Swanson et al. (2009) report a variety of membrane-associated and soluble forms of PmpD. Flower-like oligomeric structures (~23nm) are observed on EBs (**Fig.4.2**), and comprise full length (155kDa)

114

and processed (73kDa and 82kDa) forms of PmpD. A secondary, late-stage processing step results in a soluble 111kDa proteolytic fragment that subsequently undergoes cleavage to 73kDa and 30kDa soluble products that remain localized within the inclusion lumen (Swanson et al., 2009). However, this does not necessarily preclude potential cytosolic effects of PmpD, as proteins secreted in to the host cell cytosol at low levels may be difficult to detect by immunofluorescence.

Figure 4.2: Electron micrograph images of PmpD expression on *Ct* (Swanson et al., 2009). PmpD is expressed on both (A) intracellular (RB) (B) and extracellular (EB) developmental forms of *Ct*. PmpD also forms flower-like oligomeric structures (C) on the surface of the bacterium, suggestive of multiple oligomeric states.
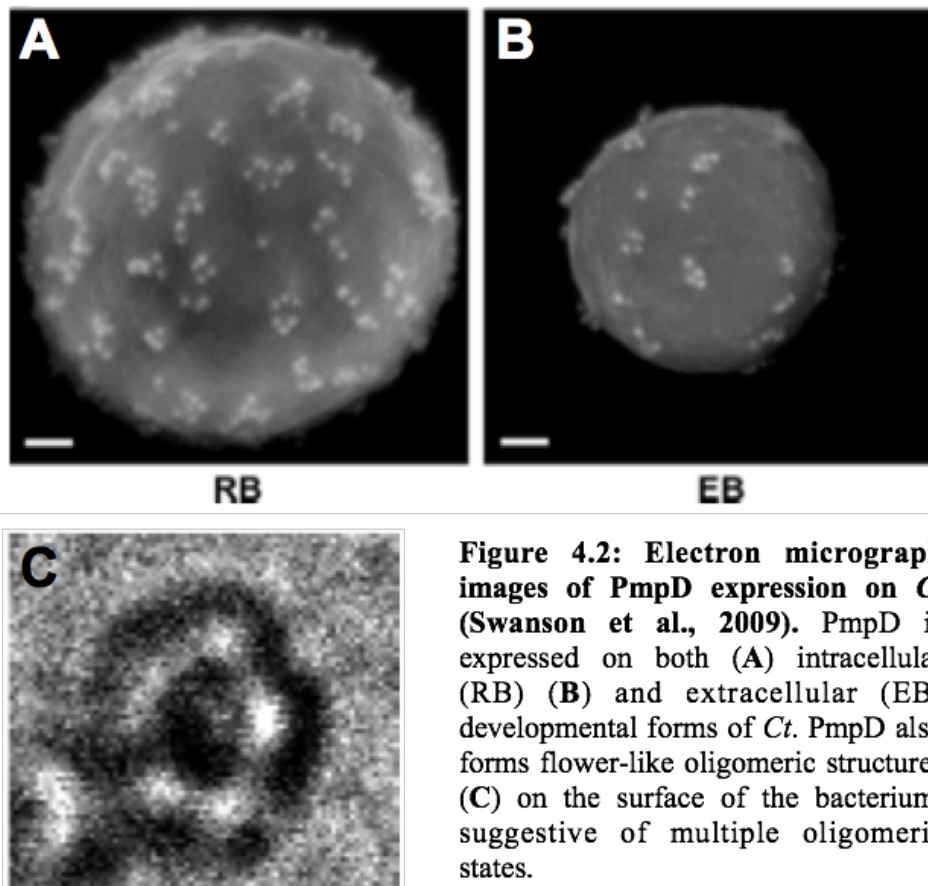
In contrast, Kiselev et.al (2009) reported earlier processing of the 157kDa passenger domain (24hpi) to 65kDa and 80kDa fragments, the latter remaining attached to the chlamydial cell wall, with the former secreted within the inclusion lumen (**Fig.4.3**) (Kiselev, Skinner and Lampe, 2009). The study also revealed similar temporal expression of the *pmpD* gene for ocular, urogenital and LGV (A, D and L2) strains,

115

and a proteolytic breakdown pattern similar to that for the PmpD ortholog (Pmp21) in *C.pneumoniae* (Wehrl et al., 2004). It was found that Pmp21 in *C.pneumoniae* is surface-exposed as well as cleaved from the mature 170kDa protein to 70kDa and 55kDa fragments. These observations are also consistent with earlier reports investigating the processing of *C.pneumoniae* outer membrane proteins (Vandahl et al., 2002).
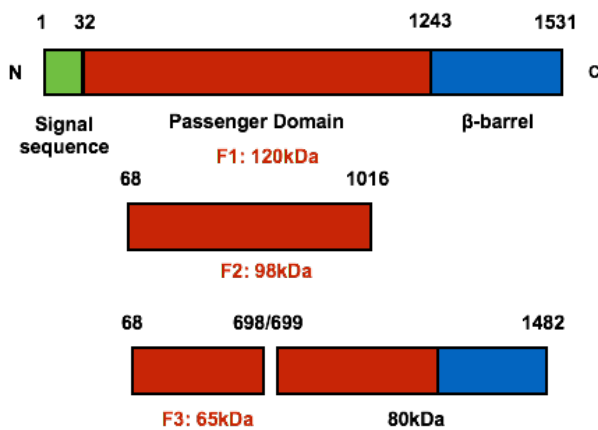
Figure 4.3: PmpD post-translational products. A schematic of PmpD post-translational products identified using mass spectrometry (Kiselev et al., 2009) of fractionated *Ct*-infected cells. *pmpD* gene segments corresponding to illustrated proteolytic fragments (F1-F3) were cloned in to pET-26(b) and pET-28(b) vectors for periplasmic and cytosolic expression (respectively) in a range of *E.coli* strains.

Furthermore, post-translational proteolysis of another PmpD ortholog has been investigated in *Chlamydia abortus*, designated Pmp18D in this species (Wheelhouse et al., 2012). *C.abortus* is the causative agent of ovine enzootic abortion (OEA), and infections comprise a substantial economic burden to the livestock industry, as well as a significant threat to pregnant women (Wheelhouse et al., 2010). Pmp18D was found to undergo processing to a 104kDa passenger domain fragment and a 48kDa protein comprising the β–barrel that remained associated with the chlamydial outer membrane (Wheelhouse et al., 2012). Akin to the proteolytic pattern of *Ct* PmpD observed by Swanson et al. (2009), the *C.abortus* Pmp18D 104kDa passenger domain fragment undergoes further cleavage to molecular weights corresponding to 84kDa, 76kDa and 73kDa, indicative of an array of putative soluble effector molecules within the inclusion lumen. These studies indicate that PmpD is expressed and undergoes

post-translational processing in a range of chlamydial species and may play a role in the extracellular as well as intracellular environmental niches of *Chlamydiaceae.*

This chapter provides the first biophysical and biochemical characterization of the *Chlamydia trachomatis* 65kDa recombinant PmpD passenger domain fragment. Evidence for the existence of rPmpD in a variety of oligomeric species is presented by conducting dynamic light scattering (DLS) on purified rPmpD fractions separated by size exclusion chromatography. In accordance with the prediction algorithm PSIPRED, we provide experimental evidence for the secondary structure of rPmpD using circular dichroism, and demonstrate that oligomeric and monomeric rPmpD display predominantly pleated β–sheet structure, further consistent with the 3D molecular descriptions of the majority of T5AT proteins from an array of Gram-negative pathogenic bacteria solved by X-ray crystallography (Henderson, Navarro-Garcia and Nataro, 1998).

In addition to differences in the relative proteolytic lability of monomeric and oligomeric rPmpD, we employ conventional redox techniques to delineate putative differences in the biochemistry of the protein. We demonstrate that oligomeric rPmpD is composed of an extensively disulphide-bonded network, as the absence of high concentrations of reducing agents fails to elicit dissociation and migration in to native and SDS gels. Anionic detergents are insufficient to cause complete dissociation into monomeric constituents. Conversely, monomeric rPmpD is very sensitive to the effects of even very low quantities of reducing agents, and increasing concentrations of TCEP, DTT, glutathione and β–ME rapidly cause intermolecular aggregation. This is suggestive of key intramolecular disulphide bonding important for tertiary

structural integrity, that when disrupted may cause exposure of hydrophobic patches that lead to intermolecular aggregation. In light of these findings, a model for PmpD within the context of chlamydial outer membrane biology and the unique biphasic developmental cycle of the *Chlamydiaceae* is proposed.

4.2   Results

4.2.1   Cloning of *pmpd* passenger domain gene truncations

Genes encoding truncated PmpD passenger domain fragments F1-F3 (**Fig.4.4**) were PCR-amplified from *Ct* serovar E/Bour genomic DNA (ATCC) using primers encoding the respective restriction enzyme sites prior to cloning in to the pET-26 (b) and pET-28 (b) vectors (**Fig.2.1**). The pET-26 (b) vector containing the pelB leader sequence was utilized to initiate translocation of rPmpD across the inner membrane to the bacterial periplasm, a typical secretory route for autotransporter proteins.
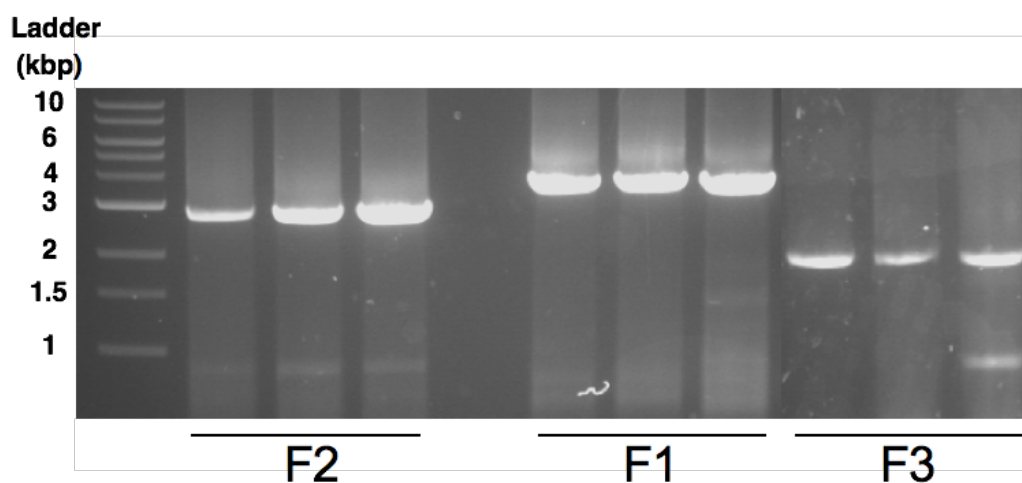
Figure 4.4: PCR of *pmpD* fragments F1-F3 from *Ct* serovar E/Bour DNA. The genes encoding the respective fragments of the PmpD passenger domain shown in **Fig. 4.3** were amplified from *Ct* serovar E/Bour DNA at three different annealing temperatures (L to R: 58.5°C, 61°C, 63.1°C) in a BIOER LifeEco Thermocycler machine. Expected gene fragment sizes are observed for each amplified product (F1=3651bp, F2=2862bp, F3=1908bp).

Following ligation, transformation and plasmid amplification in NovaGigaSingle cells, double digests of transformed plasmids were conducted using *Nco*I and *Xho*I

enzymes. DNA fragments were resolved using agarose gel electrophoresis and visualization with SybrSafe stain under UV-light (**Fig.4.5**). This revealed the expected fragment size for all genes cloned. DNA sequencing was used to verify the correct sequence of all three plasmids following cloning.
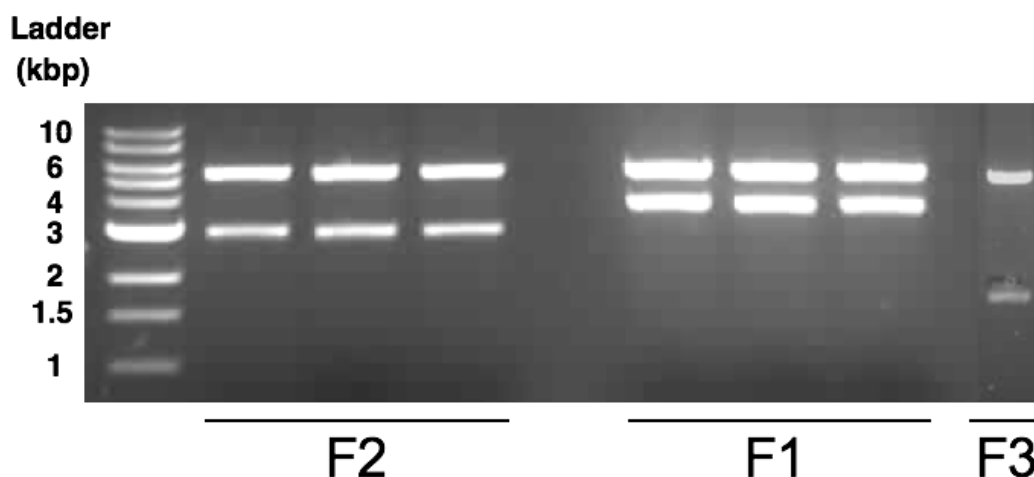
Figure 4.5: Double digest reactions showing cloned *pmpD* fragments. *NcoI/ XhoI* double digests for genes encoding full length pmpD passenger domain fragment F1 (3651bp) and proteolytic fragments F2 (2862bp) and F3 (1908bp) ligated in to pET28(b) vector (Novagen). Similar gels were obtained for the pET26(b) vector. Sequencing using primers recognising the T7 promoter and T7 terminator domains showed correct gene sequence and ligation in to the multiple cloning site of each pET vector.

4.2.2 Overexpression of *Chlamydia trachomatis* recombinant PmpD passenger domain fragments

For overexpression of the recombinant PmpD passenger domain fragments *pmpD* F1 (120kDa) and F3 (65kDa) gene fragments were cloned and expressed in a variety of *E.coli* strains at 16°C and 37°C in order to determine optimal conditions for soluble protein expression. BL21 (DE3), Origami 2 (DE3) and Rosetta 2 (DE3) strains were transformed with the relevant plasmids. To circumvent the likelihood of ribosomal translational arrest due to the presence of 52 interspersed rare codons within the rPmpD passenger domain, an *E.coli* Rosetta 2 (DE3) strain encoding eight additional rare tRNAs was also utilized. Given the cysteine-rich content of the PmpD protein (26 Cys residues), Origami 2 (DE3) strains with mutations in glutathione and thioredoxin

reductases were transformed in the attempt to facilitate cytoplasmic disulphide bonding. Expression was induced using 1mM IPTG when cultures had reached an OD_{600} of 0.6. Cell lysates were analysed using 12% SDS-PAGE.
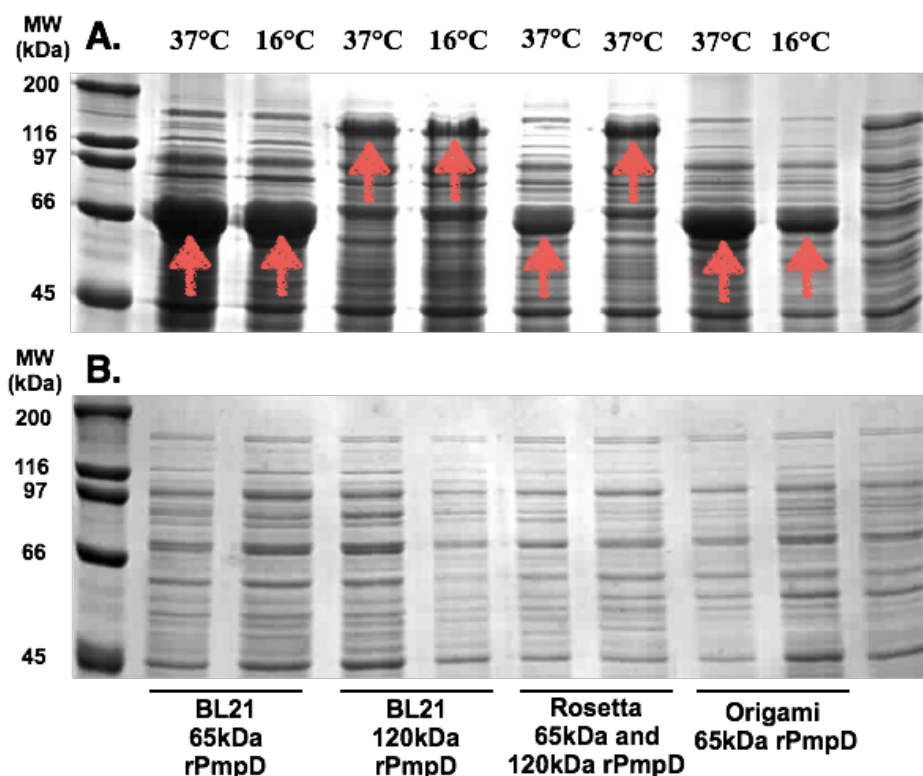
Figure 4.6: Small-scale over-expression of PmpD proteolytic fragments. PmpD F1 (120kDa) and F3 (65kDa) fragments (red arrows) were over-expressed using IPTG induction in *E.coli* expression strains – BL21(DE3), Origami 2(DE3) and Rosetta 2(DE3) transformed with the pET28(b) vector encoding the respective passenger domain fragments. Expression was conducted at 37°C and 16°C overnight and both insoluble (**A**) and soluble (**B**) lysate fractions were analysed on a 10% SDS-PAGE gel. Very little or no soluble protein was observed, with the majority of rPmpD sequestered in insoluble inclusion bodies.

Soluble cytoplasmic and insoluble fractions were analysed for F1 (120kDa) and F3 (65kDa) PmpD fragments. Higher expression levels were obtained in all cell types for the F3 fragment, while lower yields of F1 (full length passenger domain) and F2 (98kDa proteolytic fragment) were obtained and also purified (not shown). As an alternative approach to confinement of the Cys-rich rPmpD in a primarily reducing cytosolic environment, a pelB leader sequence was appended to the N-terminus of the

F1-F3-encoding *pmpd* gene fragments using the pET-26 (b) vector, in order to effect rPmpD translocation across the inner membrane into the oxidizing environment of the periplasm, a typical transportation route for T5ATs. However, no soluble periplasmic protein was obtained in any strain or growth temperature tested in small-scale expression tests with constructs harboring the pelB leader sequence, with the majority sequestered in insoluble inclusion bodies (**Fig.4.7**).
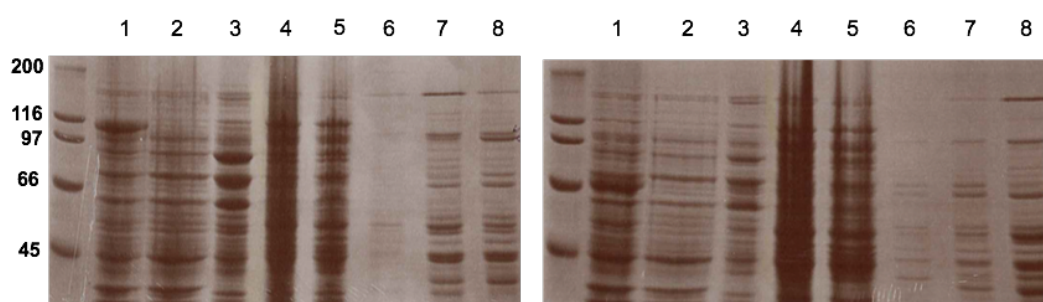
Figure 4.7: Small-scale over-expression of PmpD proteolytic fragments with pelB leader sequence. PmpD F2 (98kDa) and F3 (65kDa) fragments were over-expressed using IPTG induction in BL21(DE3) *E.coli* cells transformed with the modified pET26(b) vector containing the pelB leader sequence at both 16°C (not shown) and 37°C overnight. Lane 1: induced cell total protein (TCP); Lane 2: un-induced control TCP; Lane 3: periplasmic fraction; Lane 4: crude soluble lysate; Lane 5: unbound Ni-column eluate and Lane 6-8: soluble bound Ni-column eluate were analysed on a 10% SDS-PAGE gel. Very little or no soluble or periplasmic protein was observed at the expected molecular weight for either rPmpD fragment, with the majority of rPmpD sequestered in insoluble inclusion bodies. Black arrows indicate expression of F2 and F3 rPmpD fragments.

Because fragment F3 (**Fig.4.3**) was expressed in high abundance, this was taken forward for all subsequent *in vitro* studies and investigation of rPmpD immunogenicity and *in vivo*. BL21 (DE3) cells were used for rPmpD production, as these also resulted in highest levels of expression (**Fig.4.5**). The partition of rPmpD almost exclusively in the insoluble fraction of cell lysates necessitated the use of inclusion body solubilization and refolding by dialysis.

4.2.3 Purification of rPmpD 65kDa passenger domain

Inclusion bodies were solubilised in 6M guanidinium hydrochloride (GdHCl) dissolved in elution buffer (20mM Tris HCl, 50mM NaCl), and refolded by step-wise dialysis (6M, 3M, 1.5M) over 3 days. Insoluble aggregated protein was removed by

centrifugation, and soluble material applied to a Ni-column. The remaining GdHCl was gradually washed out following protein immobilization, and a two-step purification involving imidazole gradient elution from the Ni-column (**Fig.4.8**) and fast protein liquid chromatography (FPLC) on an S200 16/60 Superdex gel filtration column was conducted. rPmpD elutes as a broad peak consisting of a mixture of higher order oligomers, with a smaller peak comprising monomeric protein (**Fig.4.9**). The presence of oligomers is consistent with previously published electron micrograph images reported by Swanson et al. (2009) (**Fig.4.2**), where PmpD is observed to exist in clusters and rosettes of varying dimensions indicative of a broad range of oligomeric states.
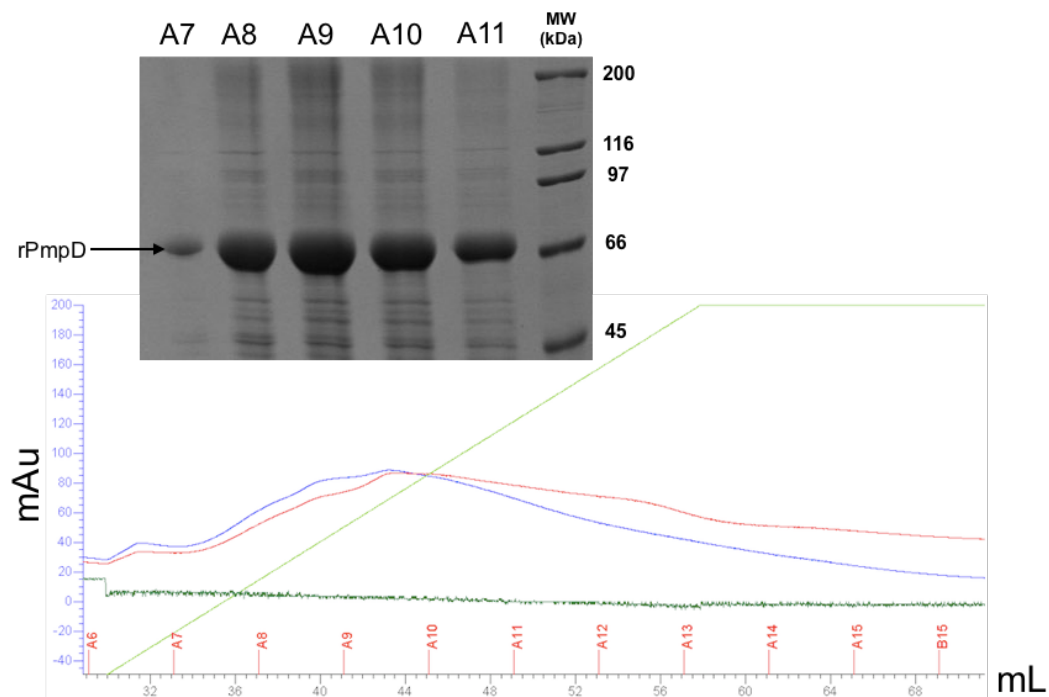
Figure 4.8: Metal affinity chromatography elution profile for rPmpD. Soluble 65kDa rPmpD expressed with a C-terminal His_6-tag was refolded from inclusion body preparations (as described in the Materials and Methods), and purified using nickel metal affinity chromatography. Blue and red traces indicate the absorbance of the elution profile at different wavelengths (280nm and 294nm respectively). Recombinant protein was eluted under an imidazole gradient (depicted in light green), and eluted fractions were inspected using SDS-PAGE.
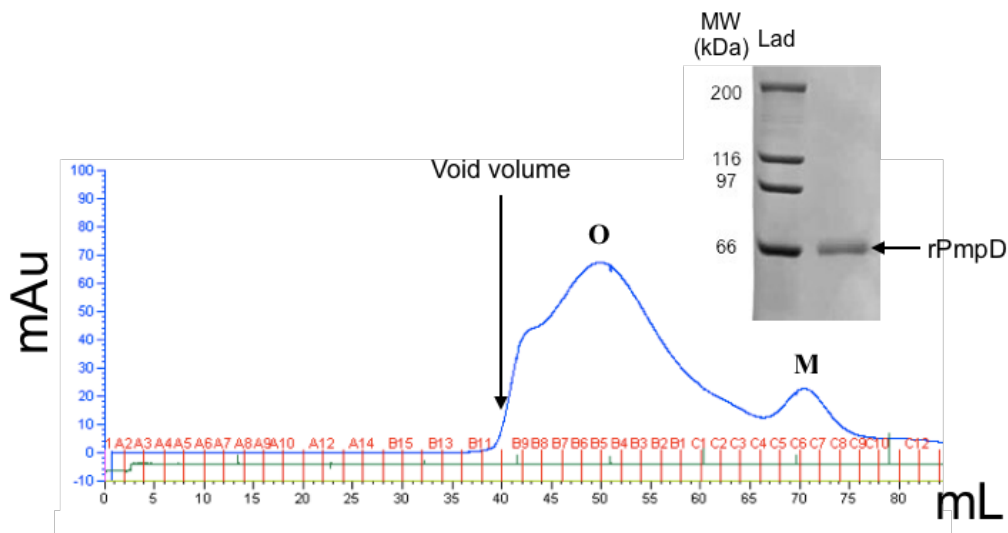
Figure 4.9: Fast protein liquid chromatography of rPmpD. Soluble 65kDa rPmpD refolded from inclusion body preparations and purified using nickel metal affinity chromatography with a C-terminal His_6-tag was further fractionated according to protein size distribution on S200 16/60 Superdex gel filtration columns. rPmpD elutes as a mixture of oligomeric species ('O') interspersed with substantially lower concentrations of soluble monomeric protein ('M'). Both oligomeric and monomeric fractions were assessed on SDS-PAGE, showing the chemical purity of the eluate. Protein concentration was determined using the Bradford assay as described in Materials and Methods.

123

MALDI-MS was further utilized to determine the identity of the 65kDa fragment eluted **(Fig.4.9)**. As expected, spectral analysis confirmed this protein as PmpD from *Ct* serovar E/Bour (**Fig.4.10**).
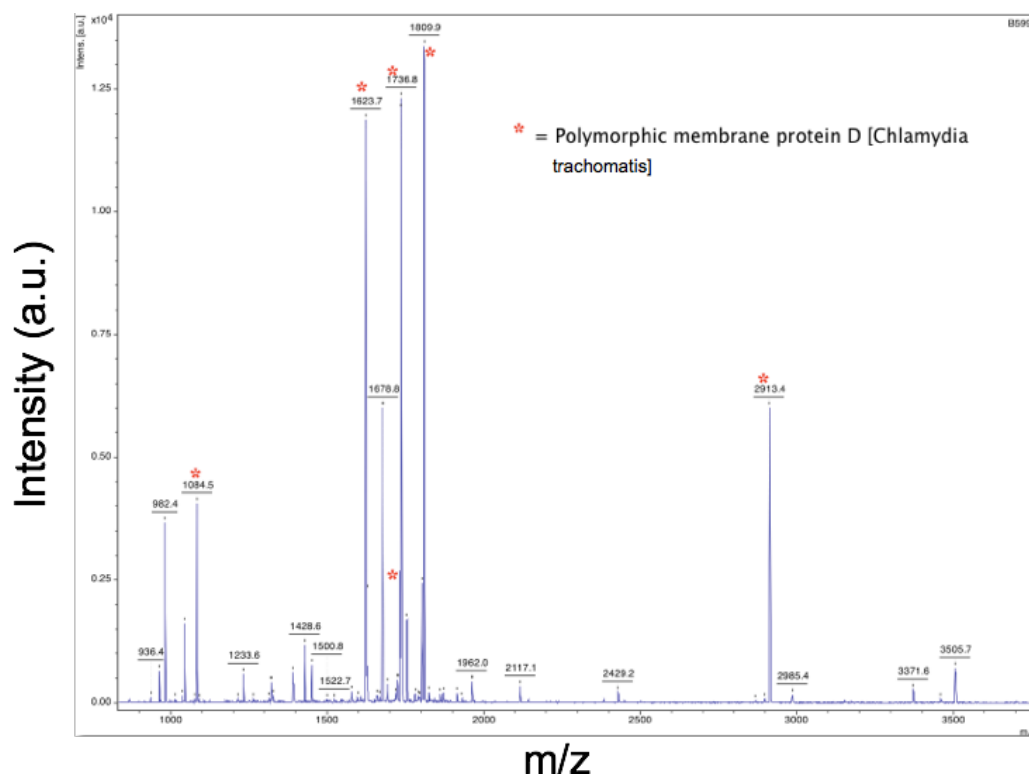
Figure 4.10: MALDI-MS spectrum for rPmpD. To further confirm the identity of the ~65kDa eluate purified using FPLC (**Fig.4.8**), MALDI-MS was implemented. Differences in spectral shifts correspond to the sequence of *Ct* E/Bour PmpD.

4.2.4 Dynamic light scattering

To assess the size distribution of species within the two fractions prior to crystallisation, dynamic light scattering was implemented. Polydispersity index (PDI) was used as a measure of sample homogeneity, and defined as the ratio of the average molecular mass to the number average molecular mass, with a PDI of 1 indicating monodispersity. Histograms plotting hydrodynamic radius (nm) against particle size distribution calculate a PDI of 0.34 for Peak 'O', indicating a complex mixture of oligomeric species, while Peak 'M' shows a PDI of 0.9, reflecting nearly complete

monodispersity, with possible slight contamination from oligomeric fractions (**Fig.4.11**).
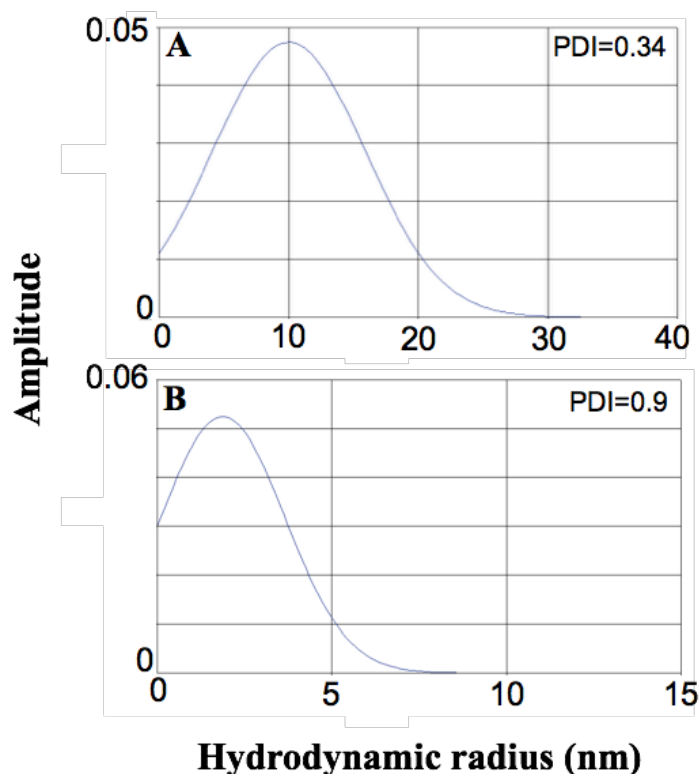
Figure 4.11: Dynamic light scattering of rPmpD. Soluble monomeric and oligomeric fractions of rPmpD were analysed using dynamic light scattering (DLS). Histograms for oligomeric (**A**) and monomeric (**B**) recombinant PmpD fractions are depicted. The polydispersity index (PDI) for the oligomeric fraction was 0.34, indicating a wide distribution of molecular weights within the fraction. In contrast, the PDI of the monomeric fraction was 0.9, indicative of a more uniformly distributed hydrodynamic radius within the monomeric fraction.

4.2.5 Circular dichroism

As rPmpD was refolded from inclusion bodies following denaturation, the yield of soluble protein was fairly low (0.2mg/ml). Furthermore, it was necessary to gain insight in to the secondary structure of the protein. This was implemented using circular dichroism. Peaks 'O' and 'M' both showed profiles characteristic of predominantly β–sheet structure (**Fig.4.12**). This is consistent with predicted secondary structures obtained using PSIPRED (**Fig.4.13**), and indeed with numerous other structures of Gram-negative T5ATs (Nishimura et al., 2010). In addition, rPmpD is found to partition almost exclusively in to the aqueous rather than the

detergent phase during TX-114 extraction of LPS from purified *E.coli* inclusion body

pellets (**Fig.4.14**), indicating predominantly hydrophilic properties.
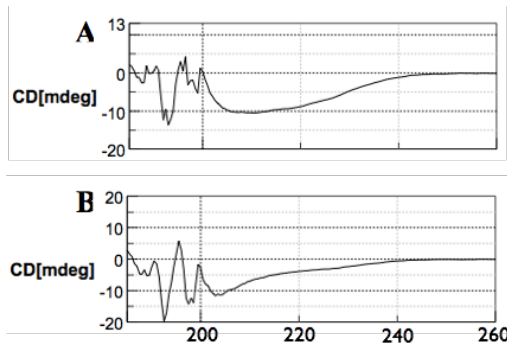
Figure 4.12: Circular dichroism of rPmpD. Soluble monomeric and oligomeric fractions of rPmpD were analysed using circular dichroism. Spectra for oligomeric (**A**) and monomeric (**B**) rPmpD fractions are indicative of mainly β-sheet secondary structure with possible mixture of random coils. Despite no significant sequence homology with the passenger domains of T5ATs from bacteria outside the *Chlamydiales*, β-sheet profile is consistent with the solved structures of a handful of these proteins in a diverse array of Gram-negative bacteria – VacA (*H.pylori*), IgA1 protease (*N.gonorrhoeae*) and pertactin (*B.pertussis*).

Figure 4.13: PSIPRED predictions of secondary structure of *Ct* PmpD. Recombinant PmpD is predicted to contain predominantly β-sheet secondary structure by online server algorithm PSIPRED. This is in accordance with experimentally validated approaches using circular dichroism of soluble oligomeric and monomeric rPmpD.
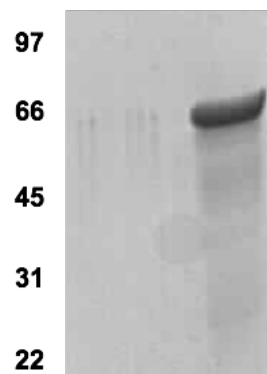
Figure 4.14: Phase separation of rPmpD. rPmpD partitions almost exclusively into the aqueous phase following incubation and phase separation with Triton X-114 detergent. This is indicative of predominantly hydrophilic properties of the rPmpD passenger domain, despite its membrane localization.

126

4.2.6 Crystallisation screens of monomeric rPmpD

The crystallization of monomeric PmpD was conducted using a range of protein concentrations and crystallization screens. These included the Hampton 1 and 2, Index, PACT, CSS 1 and 2, Peg Ion 1 and Peg Ion 2 screens. In addition, specialized 96-well high-throughput MemPlus and MemGold membrane protein screens (Molecular Dimensions) were also purchased. For rPmpD proteins, concentrations of 5mg/ml-20mg/ml were employed. **Fig.4.15** shows typical microcrystalline precipitate observed under a range of conditions in both customized and commercial screens. However, no crystals amenable to diffraction studies were obtained in our study.
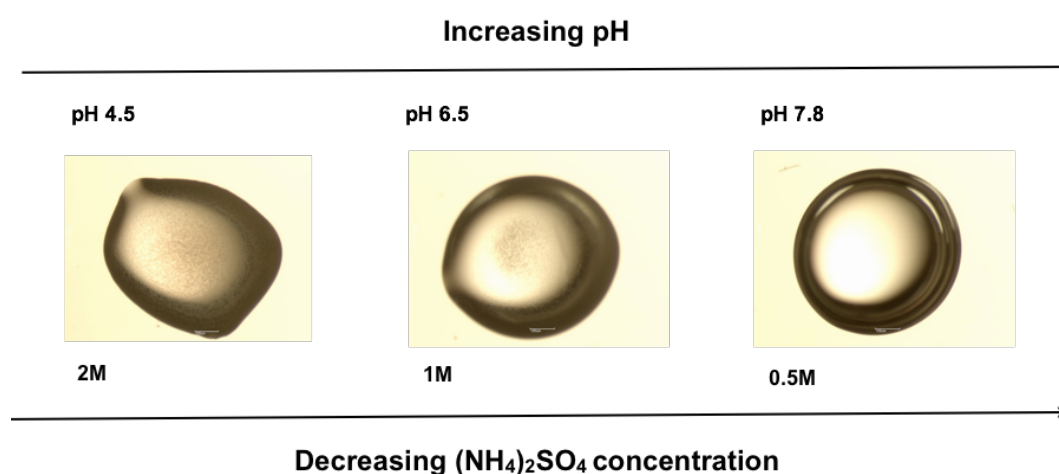
Figure 4.15: Crystallization screening of monomeric rPmpD. Soluble monomeric rPmpD, with a more homogenous particle size distribution than oligomeric fractions, was subjected to an array of crystallization screens and customized conditions (Materials and Methods). Microcrystalline precipitate was observed under several conditions in commercial and manually customised screens, usually at lower pH (consistent with the isoelectric point (pKI=4.73) of rPmpD). However, no crystals have been obtained thus far. This is likely due to disulphide-mediated intermolecular aggregation when monomeric rPmpD is concentrated to 10-20mg/ml, or to protein degradation following previously observed *in vitro* lability.

4.2.7 Redox biochemistry of rPmpD

To determine the biochemical nature of oligomeric and monomeric rPmpD, and to address the role of potential differences in disulphide bonding and ionic interactions in rPmpD, native and SDS gels were run under a variety of redox conditions

(**Fig.4.16-4.17**). **Fig.4.16** shows a 10% SDS gel with rPmpD monomer and oligomer. Monomeric rPmpD migrates alongside the 65kDa molecular weight marker under all conditions (Lanes 5-8). However, oligomeric rPmpD, a mixture of species, fails to dissociate and enter the gel completely in the absence of 0.5M β–ME in the loading buffer (Lane 4), indicating intermolecular disulphide-mediated bonding in the majority of species present within the mixture. SDS, an ionic detergent is insufficient to disrupt these intermolecular interactions.
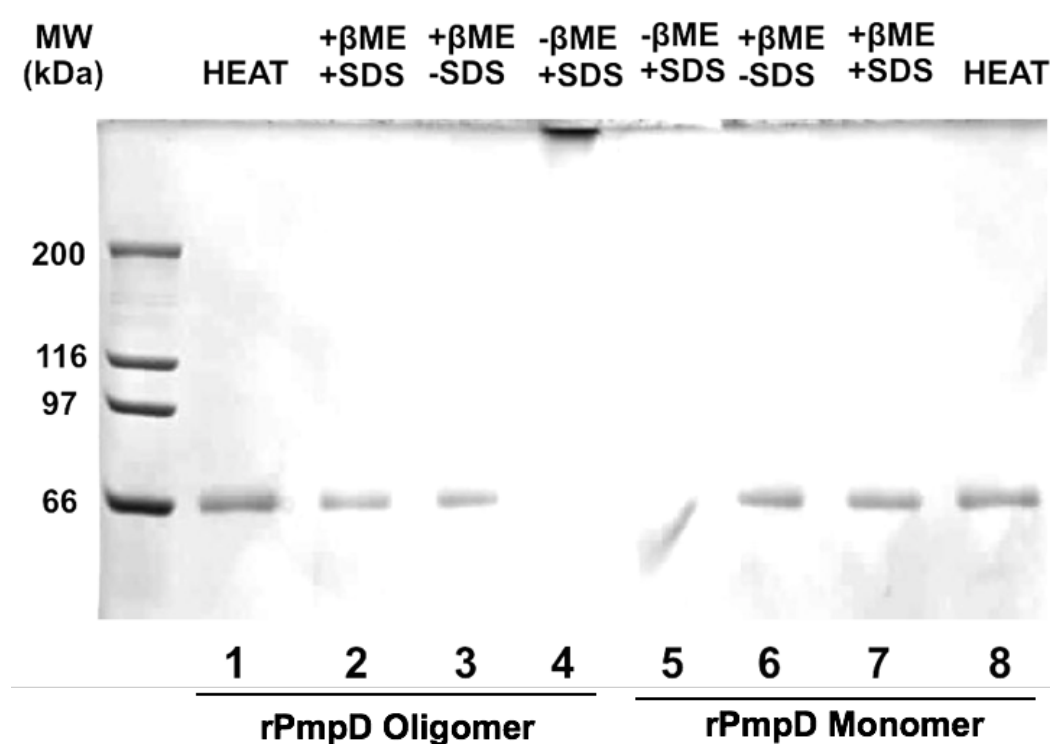
Figure 4.16: Reducing and non-reducing SDS-PAGE of rPmpD. Monomeric rPmpD enters a 10% SDS gel in the absence of 0.5M β-mercaptoethanol (Lane 5). In contrast, oligomeric rPmpD fails to completely enter and migrate into the 12% SDS gel in the absence of β-mercaptoethanol (Lane 4), indicating primarily disulphide-bonded protein complexes. Both monomeric and oligomeric rPmpD fractions enter the gel in the presence of β-mercaptoethanol and SDS.

Monomeric and oligomeric rPmpD species also behave differently in the absence of reducing agents and detergent. Under native conditions, migration of monomeric rPmpD occurs, whereas the oligomeric fraction fails to enter and migrate in to the 5%

acrylamide gel, likely due to its high molecular weight (**Fig.4.17**). Interestingly, the three different reducing agents also differentially influence the behavior of rPmpD monomer under native conditions. It was anticipated that addition of reducing agents would disrupt oligomers into their constitutive subunits, but even the addition of 0.5M β–ME fails to cause entry in to the gel. Increasing concentrations of reducing agents to recombinant monomeric rPmpD lead to a change in charge:size ratio and reduced mobility of the protein.
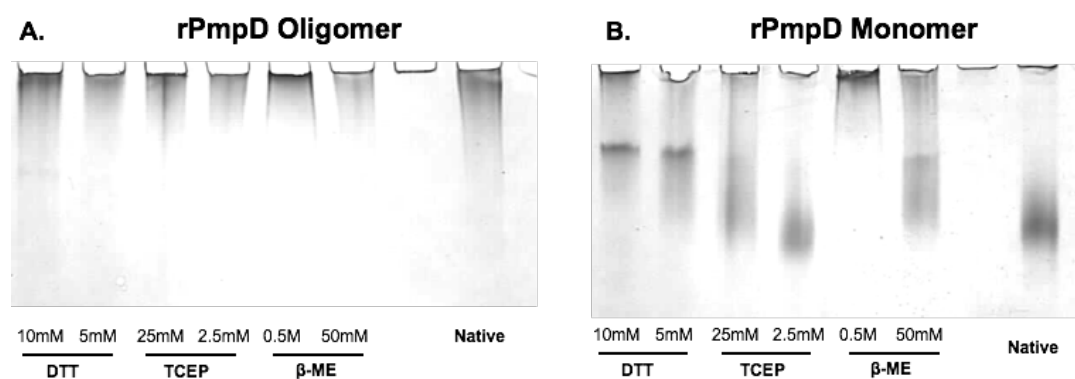
Figure 4.17: Reducing and non-reducing Native-PAGE of rPmpD. Native gels showing monomeric and oligomeric rPmpD fractions in the presence of varying concentrations of reducing agents dithiothreitol (DTT), tris(2-carboxyethyl)phosphine (TCEP) and β-mercaptoethanol (β-ME). Entry of native oligomer (**A**) in to the 5% acrylamide native gels is limited, and addition of mM quantities of reducing agents fails to enhance migration of oligomeric complexes. However, monomeric rPmpD (**B**) enters and migrates in to the native gel, and the presence of the three reducing agents have differential effects on gel entry, with increasing concentrations trending towards the formation of intermolecular aggregates that may possess different charge:size ratios. This suggests that interference with key intramolecular disulphide bonds may disrupt key secondary structural elements leading to intermolecular aggregation (presumably through non-specific hydrophobic or ionic protein-protein interactions).

Taken together, these data suggest that rPmpD exists in an array of distinct molecular species with secondary, tertiary and quaternary structures governed by a complex mixture of biochemical interactions most likely involving Cys residues. Monomeric rPmpD is sensitive to the effects of reducing agents, and it is tempting to propose that

129

this may be due to the disruption of key intramolecular disulphide bonds, which, when disrupted, may lead to denatured protein and subsequent aggregation through non-specific hydrophobic interactions, evidenced by upward shifts under native conditions (**Fig.4.17**). rPmpD oligomers are held together by intermolecular disulphide interactions, although intramolecular disulphide interactions are likely present as well.

Currently, carboxymethylation of rPmpD to dissect the positions of exposed and paired Cys residues in monomeric and oligomeric rPmpD has been carried out. It is anticipated that the use of mass spectrometry following selected proteolytic digests of the protein will enable elucidation of Cys-Cys interactions within each biochemical species, and inform rational site mutagenesis of exposed residues to prevent intermolecular aggregation and enhance the yield of a stable, monodisperse rPmpD species more amenable to crystallization optimization.

4.2.8 Proteolytic digestion

Both rPmpD monomer and oligomers were subjected to proteolytic digest using a panel of four different enzymes: clostripain, elastase, trypsin and chymotrypsin. Proteolysis was carried out at room temperature for 0.5mins, 2mins, 5mins and 30mins, and the samples immediately denatured and run on a 12% SDS gel. Clostripain and chymotrypsin failed to cause proteolysis even after 30mins. Elastase caused similar breakdown patterns for both oligomeric and monomeric rPmpD, but notable differences were observed in the presence of trypsin. The 65kDa rPmpD monomer was almost completely degraded to smaller fragments ~22kDa and ~35kDa after 30 minutes (**Fig.4.18**). In contrast, rPmpD oligomer showed a different

proteolytic pattern; with a wider range of digest fragments and some 'full length' protein still observed indicating some degree of proteolytic recalcitrance. These observations are in contrast to those observed for chlamydial MOMP, where it was found that the 67kDa MOMP trimer was completely recalcitrant to trypsin digestion even when incubated at 37°C for 20h, whereas the MOMP monomer was susceptible to cleavage by the enzyme (Sun et al., 2007).
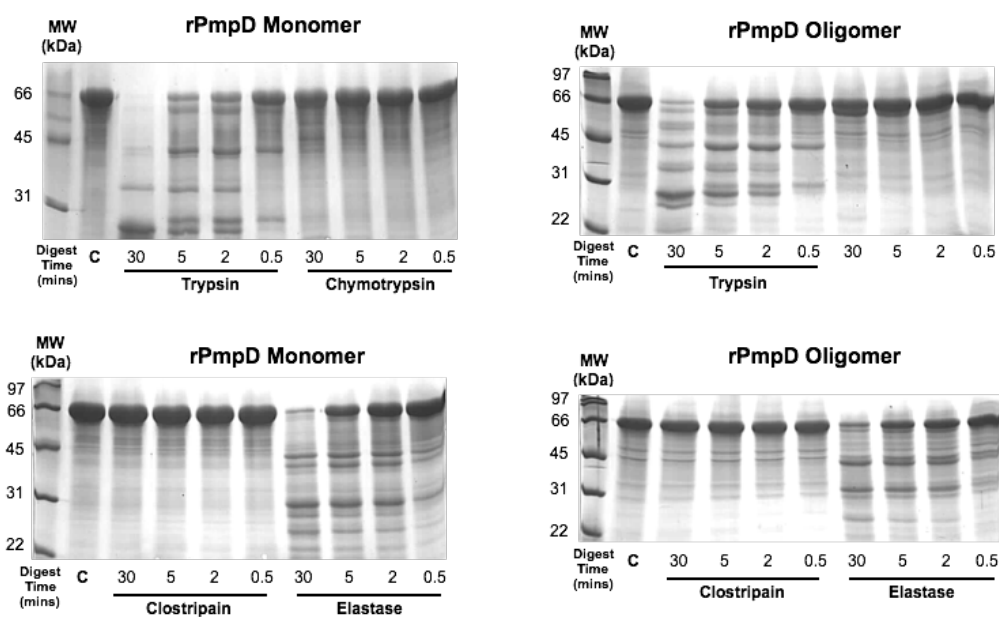
Figure 4.18: Proteolysis of rPmpD. rPmpD was incubated in the presence of four proteases for different time periods (30min, 5mins, 2mins, 30secs). Undigested control samples 'C' were run in Lane 1 of each gel. Differential proteolytic patterns are observed with each enzyme. Clostripain and chymotrypsin show no effect even at 30mins, while elastase elicits a similar breakdown pattern for both oligomeric and monomeric PmpD. Refractoriness to proteolysis is observed following tryptic digest of oligomeric but not monomeric rPmpD. The relative lability of monomeric rPmpD may reflect differing biological roles between the two species during the extra- and intracellular developmental phases of *Ct*.

Moreover, trimeric MOMP only became amenable to proteolytic cleavage following boiling, indicating that intermolecular disulphide-mediated bonding may be responsible for providing proteolytic recalcitrance. This is consistent with the properties for other outer membrane porins, and previous studies have observed that

both *E.coli* and *N.meningitidis* porins display similar proteolytic resistance (Jansen et al., 2000; Rosenbusch, 1974). However, proteolytic studies have not previously been conducted on chlamydial Pmps, and the relative lability of rPmpD may be correspondent with findings and postulated roles of PmpD passenger domain fragments of variable molecular weights during biphasic development, including secretion in to the inclusion lumen or host cell cytosol (Kiselev, Skinner and Lampe, 2009; Swansonet al., 2009).

4.2.9 Effect of pH on rPmpD dissociation

The effect of pH on dissociation of oligomeric rPmpD was also investigated under non-reducing conditions in SDS-PAGE (**Fig.4.19**). No difference in migration or dissociation was observed for rPmpD oligomer at a range of different pH levels (pH 3-10). This is in contrast to the MOMP trimer that dissociates at low (pH 3) and high (pH 10) levels. Importantly, such observations may have implications for the detection of conformational-sensitive epitopes in certain immunological assays such as ELISAs, where the pH of bicarbonate coating buffers is usually around pH 9.6, as this facilitates binding to assay plates.

However, a loss in sensitivity may be observed for native oligomeric proteins that dissociate at high pH, particularly with regard to monoclonal antibody epitope recognition. Indeed, this has been observed *in vitro* following dissociation of MOMP trimers at high pH (Sun et al., 2007). We have shown here, that rPmpD is stable at both high and low pH levels, thus mitigating loss of detection of conformational-dependent epitopes in ELISA assays. This enhanced stability may also have physiological implications for *in vivo Ct* infections. In *C.pneumoniae* infections *in*

vitro, abrogation of infectivity was demonstrated at high pH levels (Theunissen et al., 1992).
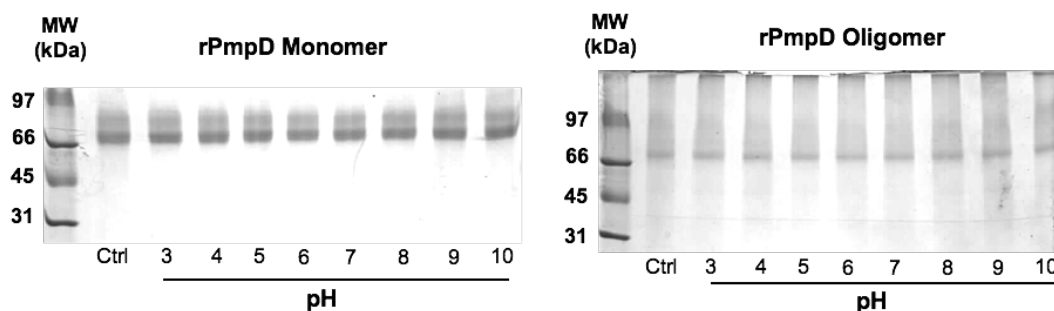
Figure 4.19: Effect of pH on dissociation of rPmpD. Oligomeric rPmpD was incubated with for 3hr at room temperature at a range of pH values. High and low pH levels have no effect on dissociation of oligomeric PmpD, although chlamydial MOMP has been shown to dissociate at pH 3 and 10. The enhanced degree of disulphide bonding in *Ct* rPmpD relative to MOMP may account for the extreme stability of the oligomer at high and low pH.

4.3   Discussion

This study is the first to investigate the biophysical properties of a chlamydial Pmp. Purification of recombinant Pmps in *E.coli* in previous studies has been conducted through recovery of insoluble protein from inclusion bodies by denaturation in chaotropic agents followed by subsequent protein refolding (Becker and Hegemann, 2014; Crane et al., 2006; Molleken, Schmidt and Hegemann, 2010). However, no study has characterized the biophysical or biochemical nature of the protein species used in subsequent immunological or *in vitro* assays. This is important, as the preservation of native structure is likely to influence sensitivity of binding assays as well as antibody recognition of native protein epitopes. Moreover, in some studies, truncated rPmpD passenger domain fragments that have not been shown to be present during the natural life cycle of *Ct* have been expressed and utilised in adhesion assays (Becker and Hegemann, 2014), making direct relevance to described physiological function slightly unrepresentative. Here, we have characterized the biochemical

133

properties of the 65kDa rPmpD passenger domain, a proteolytic fragment identified by mass spectrometry that is shown to be present in the soluble fractions of *Ct* cell lysates (Kiselev, Skinner and Lampe, 2009). We show that:

(i) rPmpD purifies as a complex mixture of extensively disulphide-linked oligomers and soluble monomeric protein, in which key intramolecular disulphides may be important in maintaining native secondary structure

(ii) Oligomeric and monomeric rPmpD consist primarily of β–sheet pleated structure, as evidenced by circular dichroism, consistent with secondary structural predictions and observed 3D molecular structures of solved T5AT proteins

(iii) Oligomeric rPmpD is more recalcitrant to proteolysis by trypsin than monomeric 65kDa rPmpD, a property likely consistent with its physiological role as a membrane protein designed to maintain *Ct* COMC structural integrity

(iv) Monomeric 65kDa rPmpD passenger domain partitions in to the aqueous phase following incubation with LPS-extraction detergent TX114, demonstrating predominantly hydrophilic properties

As previously alluded to, proteins comprising the chlamydial COMC undergo substantial changes in redox states that facilitate EB to RB transition and protein function (Hatch, Allan and Pearce, 1984). Although the precise mechanisms governing biphasic development and reduction of chlamydial membrane proteins are unknown, an alternative mechanism has been proposed for the modification of disulphides within the COMC at the host-pathogen interface. This involves active

modification through the activity of host cell protein disulphide isomerase (PDI) (Davis, Raulston and Wyrick, 2002). Biotinylated *Ct* serovar E (UW5-Cx) EBs were incubated with an endometrial epithelial cell line (HEC-1B), and matrix-assisted laser desorption ionization mass spectrometry (MALDI-MS) was used to identify protein complexes coupled to EBs following affinity purification. The 55kDa PDI protein was repeatedly identified in complex with EBs in addition to heat shock protein 60 (hsp60), actin and ATP synthase.

The significance of PDI in thiol-disulphide exchange reactions is epitomized by the cleavage of diphtheria toxin, which is an essential step for mediating host cell cytotoxicity (Ryser, Mandel and Ghani, 1991). Thiol/disulphide exchange at the host cell interface is also involved in the internalization of important viral pathogens such as HIV and Newcastle disease virus (Jain, McGinnes and Morrison, 2007; Ou and Silver, 2006). Although most PDI is located within the endoplasmic reticulum, it is also present at the cell surface, often associated with host cell receptors (Couet et al., 1996; Feener, Shen and Ryser, 1990; Klappa, Hawkins and Freedman, 1997; Landel, Kushner and Greene, 1995). To further confirm the role of PDI in facilitating productive *Ct* infection, three methodologies were used to modify chlamydial and host disulphides in addition to PDI activity (Davis, Raulston and Wyrick, 2002):

(i)   Pre-incubation with anti-PDI antibodies ~69% caused a reduction in chlamydial infectivity relative to control IgG in HEC-1B cells

(ii) Reduction in chlamydial infectivity by ~22% was observed following addition of bacitracin, a membrane-impermeable inhibitor of PDI,

previously shown to be instrumental in inhibiting attachment of human immunodeficiency virus (Ryser et al., 1994)

(iii) Reduction in *Ct* infectivity by ~30% was observed following addition of DTNB (5,5'-dithiobis[2-nitrobenzoic acid]), a membrane-impermeable thiol-alkylating agent also shown to reduce Sindbis virus entry in BHK-1 cells through interference with viral capsomere disulphide binding (Abell and Brown, 1993).

These data suggest an important role for correct disulphide bonding within the COMC in addition to the requirement for a functional host PDI in the chlamydial infection process. Furthermore, two subsequent studies using a CHO6 cell line with a defect in PDI N-terminal signal sequence processing have implicated PDI to be essential in chlamydial entry and attachment, and further demonstrate that bacitracin, when present throughout EB incubation with host cells, almost completely abrogated infection in contrast to the modest decrease in previously reported results by (Davis, Raulston and Wyrick, 2002) when the inhibitor was washed off prior to infection (Abromaitis and Stephens, 2009; Conant and Stephens, 2007). The authors attribute this difference to constitutive expression and recycling of PDI to the cell surface in CHO6 cells ectopically expressing functional PDI, and further report that enzymatic activity of PDI was found to be essential for entry. It is likely that *Ct* may bind to a receptor closely associated with PDI.

However, despite these observations, it is difficult to address experimentally whether PDI acts to modify host or bacterial surface proteins. Conventional biochemical techniques such as the pretreatment of membranes with reducing or alkylating agents

in the study of host-pathogen interactions *in vitro* may confound interpretation of results on infectivity due to rapid re-oxidation or mismatched disulphides. Hence, the use of stably transfected cell lines may be a more robust way to study interactions at the *Ct*-host cell interface. However, with the very recent advances in genetic manipulation of *Ct*, the field of research will be dramatically transformed in the near future, with the ability to interrogate the contribution of specific genes to adhesion both *in vitro* and *in vivo* (Kari et al., 2014; Nguyen and Valdivia, 2012).

Taken together, these data indicate a role for active host cell modification of COMC disulphides during the *Ct* infection process, although it is likely that several other redundant mechanisms may be involved that result in outer membrane modification. The *Ct* serovar D genome has been found to contain two PDI-encoding genes (CT780 and CT783), which contain thioredoxin domains, but bear little homology to eukaryotic PDIs (Davis, Raulston and Wyrick, 2002;Stephenset al., 1998). In addition, recent studies have also linked disulphide bonding within the chlamydial T3SS apparatus to biphasic development, detecting significant alterations in the cysteine-rich needle protein CdsF (Betts-Hampikian and Fields, 2011). Reduction of the rigid EB COMC is necessary for insertion of the T3SS apparatus into the outer membrane. The T3SS is essential for delivery of key virulence factors in *Ct* invasion, many of which initiate cytoskeletal remodeling and bacterial internalization (Hower, Wolf and Fields, 2009;Jewett et al., 2006). Cys-rich membrane proteins such as PmpD may act as a scaffold for such effector systems, particularly given the disulphide-rich nature of both PmpD and *Ct* needle proteins such as CdsF (Betts-Hampikian and Fields, 2011). It is thus tempting to speculate that a complex array of

bacterial and host cell effectors may facilitate chlamydial invasion during the early stages of infection.

Of particular relevance in chlamydial species when compared to other Gram-negative bacteria is the unique capacity to maintain a number of free thiols within periplasmic or membrane-associated proteins. The formation of disulphide bonds is usually restricted to non-cytoplasmic compartments, mainly occurring within the bacterial periplasm, and is crucial for protein stability and folding (Nakamoto and Bardwell, 2004). In *E.coli* and the majority of other Gram-negative bacterial species, disulphide bonding is mediated mainly by the oxidative folding pathway that comprises the periplasmic enzymes DsbA and DsbB that each possess a characteristic CXXC motif (Dutton et al., 2008). In addition, several species from bacteria to eukaryotes also possess enzymes that form part of a different pathway known as the disulphide isomerization pathway that is used to rectify incorrectly matched disulphides (Nakamoto and Bardwell, 2004).

Using a cysteine counting method for predicted cell envelope proteins, in combination with homology searches of DsbA and DsbB enzymes in 375 diverse bacterial genomes, (Dutton et al., 2008) found a significant bias towards even numbers of Cys residues in predicted transmembrane proteins across diverse bacterial phyla. This may be an evolutionary adaptation to avoid likely mismatching of disulphides within the periplasm. Interestingly, bacteria predicted to lack disulphide bonds consisted mainly of obligate intracellular and anaerobic organisms, including *Chlamydiae*, Deltaproteobacteria, Firmicutes and Spirochetes (Dutton et al., 2008). It was postulated that in these bacteria, intracellular redox conditions may prohibit

extensively disulphide-bonded proteins, while fermenting organisms such as *Lactobacilli* within the Firmicute phylum lack an electron transport chain, which is key to catalysis of disulphide bond formation (Dutton et al., 2008). Thus, novel mechanisms of protein folding may occur in these unique bacterial phyla. Indeed, the structural biology has elucidated the existence of a novel isopeptide mechanism of stabilization in a pilin protein of the Lactobacillus bacterium *Streptococcus pyogenes* (Kang et al., 2007).

However, the findings by Dutton et.al (2008) are clearly not representative of the *Chlamydiaceae*, as previous studies have clearly demonstrated the presence of at least one intra-molecular disulphide-bonded protein MOMP (Yen, Pal and de la Maza, 2005). Thus, it is apparent that *Chlamydiaceae* may employ a more diverse range of mechanisms to modify the disulphide bonding status of membrane-associated proteins. In addition to possessing homologs of DsbA and DsbB (CT176 and CT177), the recent discovery, structural and functional characterization of DsbH in *C.pneumoniae* has shown that this enzyme functions as a disulphide reductase, and may be responsible for maintaining reduced Cys residues within the chlamydial periplasm (Mac et al., 2008).

Given the extreme phylogenetic distance from well-characterized bacteria such as *E.coli* and *B.subtilis* (Pace, 1997), as well as their unique adaptation to intracellular environments, such discoveries are important in elucidating potential links between plasticity of the Cys-rich outer membrane and the biphasic developmental cycle of *Chlamydiales*. Indeed, it has recently been discovered that following transition to metabolically active RBs, a role for functional peptidoglycan becomes apparent

(Liechti et al., 2014; McCoy and Maurelli, 2006). DsbH is likely important in either maintaining the chlamydial periplasm in a generally reducing state depending on the metabolic stage of the bacterium, or for initiating host-pathogen interaction by reducing a subset of proteins in the supramolecular disulphide complex. Analysis of the *C.pneumoniae* and *E.coli* genomes also reveal a fourfold higher proportional representation of oxidoreductases in *C.pneumoniae* than *E.coli* (Inaba et al., 2006; Kalman et al., 1999). Interestingly, structural comparison of the active site of *C.pneumoniae* DsbH to solved structures of *E.coli* thioredoxins has revealed critical importance of the central two residues in the CXXC motif in dictating substrate specificity.

The role of disulphide reductases such as DsbH may also play even more crucial and specific roles within the context of T5AT secretion. A recent study investigated the size and conformational limits of the presence of disulphide-bonded loops in the secretion of T5AT proteins (Leyton et al., 2011). By conducting systematic site mutagenesis, increasing the distance between the Cys residues in the *E.coli* plasmid-encoded toxin (Pet), a member of the serine protease ATs of the *Enterobacteriaceae* (SPATEs), the authors were able to determine the maximum length of the disulphide-bonded loop that does not interfere with translocation of the passenger domain. This was found to be a gap of 18 amino acid residues between consecutive cysteines.

Examination of over 30 different T5ATs from a diverse range of bacterial species including (among others) *E.coli*, *S.flexneri*, *H.pylori*, *N.meningitidis*, *P.aeruginosa* and *H.influenzae* revealed a paucity of Cys residues within these proteins, with an average of 2.5 Cys residues per protein. This is in stark contrast to the 26 Cys residues

in *C.trachomatis* PmpD and 14 Cys residues in the *C.pneumoniae* ortholog Pmp20. Overall, the nine *C.trachomatis* Pmps A-I possess an average of 16 Cys residues. In addition, the average distance between Cys residues in all 31 T5ATs examined from bacterial species outside the *Chlamydiaceae* is 7.5 amino acids. This proximity, coupled with the even number of Cys residues (2 or 4) observed in all but two ATs (*E.coli* EspC and *S.flexneri* IcsA) would likely facilitate both intramolecular disulphide binding within the periplasm by the aforementioned oxidative pathway involving DsbA and DsbB enzymes, as well as enable transport through the β–barrel pore by preventing large loops from forming that may block translocation (**Fig.4.20**).
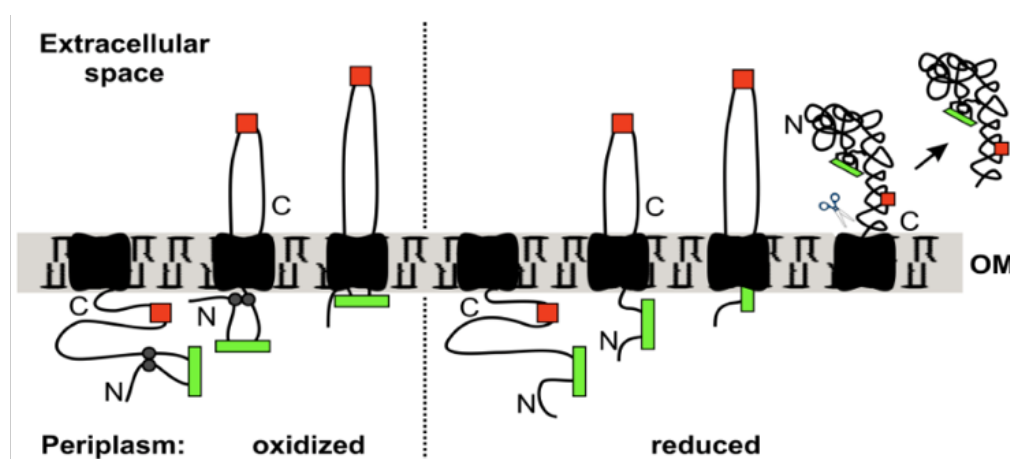
Figure 4.20: Effect of Cys residues on the translocation of bacterial autotransporter proteins (Leyton et al., 2011). Leyton et al. demonstrate that the maximum gap between Cys residues that form a periplasmic intramolecular disulphide bond that still allows for translocation of the passenger domain through the β–barrel pore is 17aa. The average gap between consecutive Cys residues forming a disulphide bond is 7aa residues in virtually all known Gram-negative bacteria, where the periplasm is a largely oxidizing environment due to the presence of DsbA and DsbB enzymes. However, it is likely that in *Ct*, a more complex redox biochemistry governing biphasic development and membrane restructuring may occur, leading to the selective maintenance of free thiols in Cys-rich passenger domains of the T5AT Pmp family within the periplasm. Depending on biphasic developmental stage, free thiols may be required for homo- or hetero-oligomerisation with other COMC proteins such as MOMP, or act as a scaffold for the T3SS apparatus. The discovery of DsbH, a chlamydial disulphide reductase, may support this hypothesis.

In *Ct* PmpD, 2 Cys residues reside in the cleavable N-terminal signal sequence, and 1 Cys residue in the C-terminal β–barrel domain, with an odd number of 23 Cys

residues present in the passenger domain of the protein. This would either necessitate the maintenance of free thiols within the periplasm or intermolecular disulphide linkage within the *Ct* outer membrane. Furthermore, the average distance between successive Cys residues contained within the passenger domain of PmpD is 39 amino acid residues. In light of the findings of (Leyton et al., 2011), transport of the full-length passenger domain through the β–barrel autotransporter domain via a proposed hairpin mechanism would be impossible under typical oxidative bacterial periplasmic environments. The fact that PmpD is secreted into the chlamydial inclusion lumen and is found in the soluble cytosolic fractions of infected cell lysates (Crane et al., 2006) suggests that inhibition of translocation does not occur, and lends further credence to the likelihood of an actively controlled redox environment within *Chlamydiaceae*, especially following the discovery of thiol-reductases DsbH (CT780) and DsbJ (CT783) (Mac et al., 2008).

Biophysical characterization of *Ct* rPmpD suggests that this protein exists in an array of oligomeric and monomeric states. This is also observed for the extensively studied *H.pylori* virulence factor VacA, which is viewed as a paradigm for toxin multifunctionality (Cover and Blanke, 2005), although a plethora of other toxins in pathogenic bacteria from *Staphylococcus aureus* alpha toxin (Bantel et al., 2001) to the A and B subunits of cholera and pertussis toxins that mediate ADP ribosyltransferase activity and host cell binding (respectively) also display multifunctionality (De Haan and Hirst, 2004; Tamura et al., 1983).

A hallmark of toxin multifunctionality is the ability to cause distinct effects in an array of different environmental niches in a temporally and spatially variable manner

both intracellularly and at the extracellular host-pathogen interface. In addition to cellular vacuolation, VacA has been implicated in cell adhesion (Garner and Cover, 1996), immune modulation (Gebert et al., 2003), mitochondrial transmembrane potential alteration (Willhite and Blanke, 2004), and cellular signal transduction pathways (Fujikawa et al., 2003). *Ct* is responsible for a diverse array of disease phenotypes, ranging from ocular trachoma, urogenital infections and lymphogranuloma venereum (LGV). PmpD is 99.15% conserved between all 18 reference serovars (A-L3) that encompass ocular, genital and LGV strains, suggesting a conserved function despite a wide range of cell tropisms from conjunctival and ectocervical epithelial cells to monocytes. In addition, PmpD has an ortholog in all other known *Chlamydiaceae* (Wheelhouse et al., 2012).

Furthermore, the ability to consolidate multiple functions within a single protein would be a likely outcome of evolution by genomic reduction exhibited by obligate intracellulars, as this results in greater conservation of genome coding capacity and metabolic resources. Oligomerisation of PmpD on the *Ct* bacterial surface may be a means of enhancing adhesion through the incorporation of a greater concentration of binding sites (**Fig.4.2**). Structural characterisation of pentameric Shiga toxin has revealed three different binding sites on each of the subunits that interact with cellular receptors, giving a total of 15 binding sites per oligomer (Ling et al., 1998). Pmps in *Ct* may employ a similar strategy.

It is also interesting to note that *Ct* PmpD has almost twice the average amount of Cys residues than all other 8 *Ct* T5ATs, and is the most Cys-rich T5AT in *C.trachomatis*, constitutively expressed throughout development (Crane et al., 2006; Tan et al.,

143

2010). Based on the assumptions of size and conformational restraints of passenger domain translocation proposed by (Leyton et al., 2011), using a maximum spacing of 17 amino acids between consecutive Cys residues required to form an intramolecular disulphide bond that can still fit through the β–barrel AT pore, inspection of the linear primary sequence indicates that PmpD may need to maintain as many as 11 reduced Cys residues within the entirety of the passenger domain for translocation, after which homo- or hetero-oligomerisation may occur. This relatively large number of free Cys residues suggests that PmpD may act as a scaffold for maintaining the structural integrity of the COMC through cross-linking with other Cys-rich membrane proteins (e.g. OmcB, Pmps and MOMP) as well as supporting other key effector proteins such as the T3SS apparatus during biphasic development. In light of our observations, we propose a model for the role of PmpD, a cysteine-rich chlamydial T5AT, within the context of previously described knowledge on the mechanisms of T5ATs, and recent insight on the intricate redox biochemistry of the chlamydial membrane (**Fig.4.21**).
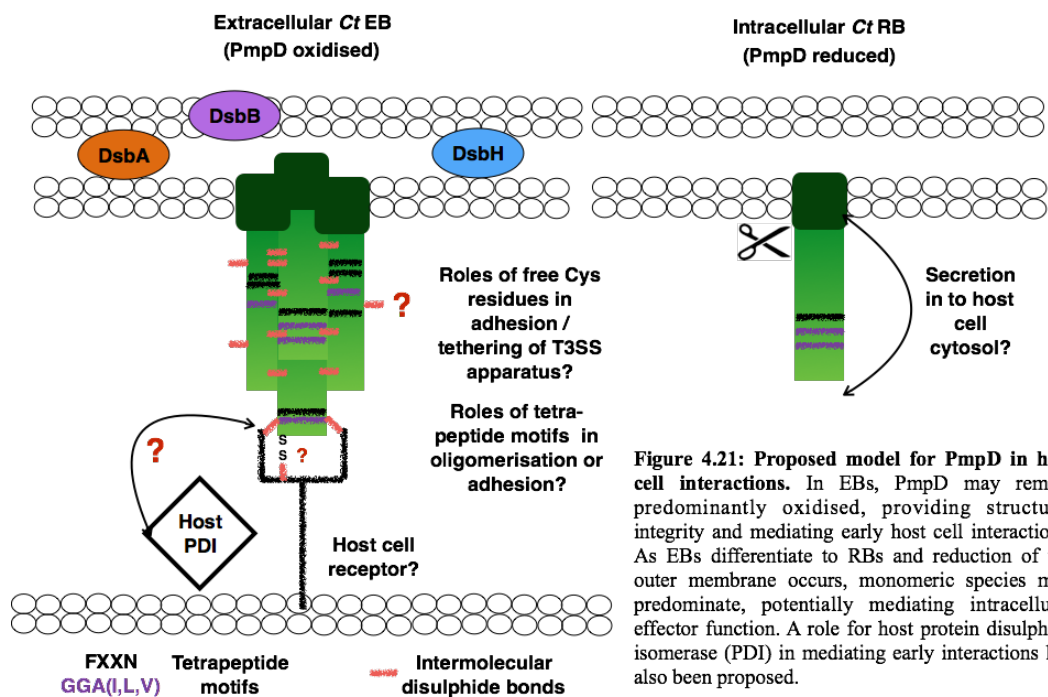
Figure 4.21: Proposed model for PmpD in host cell interactions. In EBs, PmpD may remain predominantly oxidised, providing structural integrity and mediating early host cell interactions. As EBs differentiate to RBs and reduction of the outer membrane occurs, monomeric species may predominate, potentially mediating intracellular effector function. A role for host protein disulphide isomerase (PDI) in mediating early interactions has also been proposed.

As the positions of paired and exposed free Cys residues likely to mediate homo- or hetero-oligomeric intermolecular interactions have not yet been determined, *in silico* modeling following sequence alignment of *B.pertussis* pertactin 69kDa passenger domain was implemented. The 3D molecular structure of the *B.pertussis* pertactin T5AT domain has been deposited in the PDB (Emsley et al., 1996), and *in silico* site mutagenesis of corresponding pertactin amino acid residues to Cys was performed to determine residues most likely to mediate intra- and intermolecular disulphide bonding. Despite the anticipated low sequence homology between the two passenger domains, secondary structural predictions for the two proteins are similar. As anticipated, several Cys residues were predicted to be unpaired, and protruded on loops outside the modular β–helix (**Fig.4.22**). These may be responsible for the formation of homo- or hetero-oligomeric complexes. However, two Cys pairs appear in close enough proximity to mediate intramolecular disulphide binding, likely indicating a complex array of redox states within PmpD. This modeling provides a crude template from which to employ strategic site mutagenesis of Cys residues to serine *in vitro*. It is anticipated that this may prevent intermolecular aggregation and facilitate the purification of soluble, homogenous monomeric rPmpD that may be employed in crystallization optimization studies.

Importantly, our study highlights the inherent difficulties in production of Cys-rich chlamydial bacterial membrane proteins in *E.coli*, where very low yields of soluble protein derived from insoluble inclusion bodies are obtained. It is likely that expression of modular complexes in baculovirus or mammalian expression systems with a larger repertoire of chaperones and post-translational modifications may enable

higher expression levels and correct folding of recombinant proteins that mimic native conformation. This has been achieved for many complex eukaryotic membrane proteins (Bieniossek et al., 2013; Rasmussen et al., 2007). Initial cloning and expression would employ the established MultiBac protocol (Berger, Fitzgerald and Richmond, 2004). This will allow for rapid regeneration of new or modified constructs by homologous recombination of transfer vectors to expedite optimisation of protein expression in *Sf*21 or High Five™ insect cells. Cloning may be conducted as either single or multi-gene constructs using ligation-independent *in vitro* Cre-fusion.
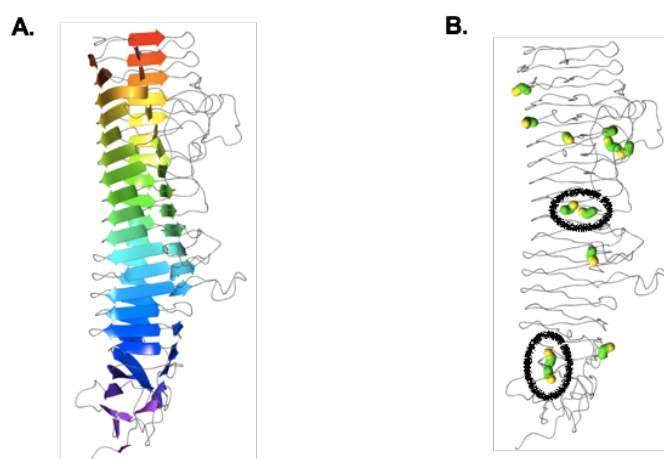
Figure 4.22: Homology modelling of the rPmpD 65kDa passenger domain with the pertactin 69kDa passenger domain. Sequence alignment was performed between the 65kDa *Ct* PmpD and *B.pertussis* pertactin 69kDa passenger domains. *In silico* site mutagenesis of the corresponding residues of the *B.pertussis* pertactin T5AT domain (**A**) (Emsley et al., 1996) to Cys residues was performed to gain insight into the positions of Cys residues most likely to mediate intra- and intermolecular disulphide bonding (**B**). Despite the low sequence homology between the two passenger domains, secondary structural predictions for the two proteins are similar. Most Cys residues are likely unpaired, and protrude on loops outside the modular β–helix. Two Cys pairs (highlighted) appear in close enough proximity to mediate intramolecular disulphide binding, likely indicating a wide array of redox states within PmpD.

For mammalian expression, generation of constructs will be conducted using the pOPIN vector suite designed by the Oxford Protein Production Facility. The majority of these vectors enable tremendous flexibility of expression in different hosts - *E.coli*,

*Sf*9 (insect), and HEK293T (mammalian) cells as well as high-throughput screening and regeneration using the In-Fusion^TM method. Moreover, all vectors contain cleavable His_6-tags to facilitate purification, crystallization or functional assays. Transient transfection protocols will offer another alternative that may enable the high-throughput screening of a large number of constructs in parallel to select and optimise rPmpD for X-ray crystallography. In addition, further validation of suitably folded protein structure following expression and purification may be performed using nuclear magnetic resonance (NMR) spectroscopy, whilst codon optimisation of *pmpD* gene fragments could be implemented to facilitate translation and prevent possible ribosomal arrest and potential misfolding.

In conclusion, we have observed biochemical differences in the oligomeric and monomeric states of rPmpD, likely consistent with differential roles in biphasic development of the bacterium at early and late stages of infection, and have further proposed a model for a possible functional role of PmpD in the context of our study and previous investigations on the chlamydial outer membrane. The next question to be addressed was whether proposed roles for PmpD as a putative chlamydial adhesin were apparent *in vitro*. This is the topic of investigation in Chapter 5.

Chapter 5: Investigation of the putative function of PmpD as a chlamydial adhesin *in vitro*

5.1   Introduction

Knowledge of the mechanisms of attachment of *Chlamydiae* to host cells remains rudimentary. Recent studies have led to proposed models of invasion involving T3SS effector proteins such as CT694 and Tarp which are also thought to facilitate internalization, including rearrangement of the actin cytoskeleton and activation of signaling pathways (Carabeo et al., 2002; Coombes and Mahony, 2002). However, receptor-ligand interactions at the host-pathogen interface remain poorly characterized, especially at the molecular level. To date, within the *Chlamydiaceae*, two main adhesin-receptor interactions have been identified in *Chlamydia pneumoniae*; the OmcB-GAG interaction (Wuppermann, Hegemann and Jantos, 2001), and the Pmp21-EGFR interaction (Molleken, Becker and Hegemann, 2013). However, the OmcB-GAG interaction is also thought to facilitate *C.trachomatis* adhesion (Moelleken and Hegemann, 2008). Existing knowledge on role of chlamydial Pmps at mediating early host cell interactions will be discussed next.

5.1.1   Pmps in early host cell interactions

Following description of the OmcB-GAG interaction, subsequent studies targeted elucidation of putative cellular receptors for *C.pneumoniae* Pmps. Chlamydial species possess varying numbers of Pmps. In *C.pneumoniae*, there are 21 members. It was found that the characteristic, repetitive short amino acid motifs found within these proteins – FXXN and GGA(I,L,V) were important for binding, and deletion experiments generating peptide fragments revealed that a minimum of two copies of

these motifs (either FXXN/FXXN or FXXN/GGA(I,L,V)) were required for adhesion (Molleken, Schmidt and Hegemann, 2010).

In the same study, it was found that pretreatment of the mammalian HEp-2 cell line with Pmp6, Pmp20 and Pmp21 all reduced infectivity of *C.pneumoniae*, with antibodies specific to Pmp21 also abrogating infection *in vitro*. Furthermore, it is likely that these motifs may indeed possess critical structural or functional properties, given their distinct over-abundance in Pmps relative to the rest of the genome. The GGA(I,L,V) sequence is only found in 10 other proteins in all known chlamydial proteomes (only at one copy per protein), while the FXXN motifs are observed an average of 13.6 times in *Ct* Pmps and 11.3 times in *Cp* Pmps, with an average of 0.73 and 0.84 times per protein (in *Ct* and *Cp* proteomes, respectively). However, no interactions between Pmps and GAGs were observed, as yeast cells expressing Pmp21 adhered equally well to GAG-expressing and GAG-deficient CHO-cell lines (Molleken, Schmidt and Hegemann, 2010), suggesting an alternative and potentially cooperative binding mechanism with *Ct* OmcB.

If the repetitive FXXN/GGA(I,L,V) tetrapeptide motifs indeed contribute to binding, the presence of multiple motifs on a single Pmp could indicate a propensity for binding to multiple different sites on either a single or multiple receptor molecule(s), or may play a role in self- or hetero-oligomerisation. Incorporation of multiple binding sites within a single molecule, in addition to oligomerisation of individual monomers dramatically increases the density of binding sites on bacterial cell membranes, and has been observed in the 3D structural description of the Shiga-like toxin I (SLT-I) binding subunit of pathogenic *E.coli* (Ling et al., 1998). Here,

pentameric assemblies of monomeric subunits that contain 3 binding sites per molecule, lead to 15 individual trisaccharide-binding sites that likely augment adhesion. Importantly, this 3D structural description of the SLT-I pentamer in complex with carbohydrate molecules has the potential to inform rational design of novel sugar-based inhibitors of the toxin that may prevent host cell adhesion.

The most comprehensive study identifying an invasin-receptor interaction within the *Chlamydiae* involved description of *C.pneumoniae* Pmp21 adhesion to HEp-2 cells using a plethora of cellular and biological approaches (Molleken, Becker and Hegemann, 2013). Pmp21-coated beads were shown to adhere to and be internalized by HEp-2 cells, and biochemical approaches using biotinylation of Pmp21 following incubation with HEp-2 cells initially revealed the EGFR-Pmp21 interaction following streptavidin affinity purification. Y2H screens were utilized to further confirm this interaction, and ectopic expression of EGFR in EGFR-negative CHO cells results in enhanced infectivity of EBs and Pmp21-coated bead binding, while activation of EGFR signaling following EB and Pmp21 binding was indirectly measured by recruitment of adaptor proteins Grb2 and c-Cbl (Molleken, Becker and Hegemann, 2013). Taken together, these data suggest that at least two distinct interactions (involving OmcB and Pmp21) are involved at the host-pathogen interface to initiate *C.pneumoniae* adhesion, and possibly invasion.

Following elucidation of Pmps as adhesins in *C.pneumoniae*, investigation of putative *C.trachomatis* Pmp interactions were recently carried out. Recently, all nine recombinant *Ct* Pmps (A-I) were used in competitive inhibition assays in HeLa, HEp-2 and HUVEC cells with infectious EB bacteria (Becker and Hegemann, 2014).

Soluble recombinant Pmps were also found to abrogate infection in both a species- and tissue-dependent manner when used in neutralization assays. PmpD and PmpG inhibited infection of *Ct* but not *Cp*, while Pmp6, Pmp20 and Pmp21 inhibited *Cp* infection, but had no significant effect in abrogation of *Ct* infectivity (Becker and Hegemann, 2014). Differences in binding to epithelial and endothelial cells were also reported for different Pmp species and subtypes. For instance, Pmp21-coated beads showed significantly increased binding to HUVEC (primary endothelial cells) than HEp-2 (cultured epithelial) cell lines, while PmpD-coated beads showed the inverse relationship, broadly consistent with distinct environmental tropism. These observations may indicate a role for Pmps in influencing tissue tropism in different chlamydial species by binding to receptors within a specific environmental niche with greater avidity.

Interestingly, phylogenetic analysis of PmpD across nine chlamydial species indicates that only *C.suis* shares 100% amino acid identity to *C.trachomatis* serovar E PmpD, and clusters with urogenital biovars in a phylogenetic tree of PmpD protein sequences, also possessing the putative RGD binding motif and nuclear localization sequence (Wheelhouse et al., 2012). PmpD orthologs in zoonotic pathogens that typically affect livestock - *C.abortus*, *C.psittaci*, *C.caviae* and *C.felis* cluster in a separate, phylogenetically distant clade from *C.trachomatis*. It is thus tempting to speculate that PmpD may have species-specific roles in infection or pathogenesis, and that the tissue type used in *in vitro* assays is important for studying protein function. These observations may further hold some degree of physiological relevance in light of the anatomical similarities of the reproductive tract between pigs and humans, and

the recent adoption of pigs as an alternative model for studying human genital *Ct* infections (Vanrompay et al., 2005).

Perhaps the most biologically relevant study of *Ct* PmpD function *in vitro* and *in vivo* arose via generation of the first ever *Ct* null mutant (Kari et al., 2014). The study employed a targeted reverse genetics approach (Kari et al., 2011) to generate a *pmpD* nonsense mutation in *Ct* serovar D/UW3/Cx. Immunofluorescence and transmission electron microscopy revealed that *pmpD* null mutants showed aberrant inclusion morphology with reduced association of RBs with the inclusion membrane, but no obvious growth defects. Furthermore, a species-specific role for PmpD in early cellular interactions was identified, with null mutants showing no significant attenuation of infectivity in murine (McCoy and primary Bm12.4) cells and in a C3H/HeJ mouse model of infection, evidenced by recoverable IFU and duration of shedding relative to the wild-type strain (Kari et al., 2014).

In contrast, the *pmpD* null mutant was significantly attenuated for virulence in immortalised human endocervical (A2EN) and conjunctival (HCjE) cells relative to the wild-type strain, showing a 70% reduction in its ability to infect or proliferate in human cells relative to the wild-type strain, evidenced by enumeration of IFU. The serovar D/UW3/Cx *pmpD* null mutant was also used in an ocular challenge model of cynomolgus macaques, where the initial chlamydial burden and clinical disease score was found to be significantly higher for the wild type strain at only two sampling time points over the first 2-3 weeks, but no significant differences in duration of shedding were observed. Peak differences in shedding were observed at 1week post infection, showing a 25-fold reduction in inclusion forming units for the *pmpD* null mutant.

Overall, these data suggest that PmpD may play a role in early interactions with host cells, possibly in adhesion and/or invasion, but also in late cycle interactions with the chlamydial inclusion, and that this function may be species-specific, and possibly fine-tuned by host-pathogen co-evolution. Indeed, the *Chlamydia muridarum* PmpD shows only 72% amino acid sequence identity to its *C.trachomatis* ortholog, where the putative RGD integrin-binding motif is substituted by a KGD motif (Kari et al., 2014). Further experimentation is required to confirm this, and would entail the study of a *C.muridarum pmpD* null mutant. While the generation of *Ct* null mutants is incredibly labour-intensive and costly, this study showcases the utility of examination of endogenous chlamydial protein function that holds greater biological relevance than heterologous or ectopic expression studies. However, the use of a non-invasive urogenital *Ct* serovar null mutant in *in vitro* assays using conjunctival cells and *in vivo* ocular infection models holds limited relevance to the natural biology of the pathogen. Furthermore, transformation of the *pmpD* null mutant with a PmpD-expressing shuttle vector was not implemented to demonstrate restoration of function, the gold-standard test in molecular biology.

In this chapter, we provide further evidence implicating PmpD as a *Ct* adhesin by implementing adhesion assays with covalent coupling of PmpD to functionalized latex bead surfaces. The 65kDa PmpD passenger domain fragment used in the adhesion study was previously identified by mass spectrometry (Kiselev, Skinner and Lampe, 2009) in *in vitro* propagated *Ct*, and is hence likely to be representative of a proteolytic species produced during the course of natural infection. Here, we show for the first time that rPmpD-coated beads show significantly enhanced adhesion to Hak

(epithelial-like) cell lines, conventionally used to culture and study antibody neutralization of *Ct*, and that anti-rPmpD immune serum abrogates the ability of rPmpD-coated beads to adhere to Hak cells. As shown in previous host-pathogen interaction studies, we also demonstrate that soluble rPmpD competitively inhibits binding of rPmpD-coated latex beads from adhering to Hak cells in a dose-dependent fashion, providing further evidence of the importance of PmpD in early host cell interactions. All work carried out in subsequent adhesion assays employs the purified monomeric 65kDa rPmpD fragment (**Fig.4.3**) unless stated otherwise.

5.2   Results

5.2.1   Coating of recombinant monomeric 65kDa PmpD to carboxylate modified polystyrene beads

Recombinant PmpD or BSA were covalently coupled to carboxylate modified polystyrene beads of different diameters (0.5μm, 1μm, 2μm) using the water-soluble coupling agent 1-ethyl-3-(3-dimethylaminopropyl) carbodiimide (EDAC) (**Fig.5.1(A)**). This coupling method has been implemented in previous immunological studies (Quash et al., 1978). BSA was selected as a control due to its similar molecular weight (~69kDa) and pI (~5.89) to the rPmpD fragment (~65kDa, pI~4.61). To confirm efficient coupling of recombinant proteins to the functionalized bead surface, supernatants were tested for the presence of recombinant protein before and after the coupling reaction, and coated beads were boiled in the presence of β–ME and SDS and tested using SDS-PAGE (**Fig.5.1(B)**). Efficient coupling of both rPmpD and BSA were observed for 0.5μm and 2μm diameter beads, but not for 1μm polystyrene particles.
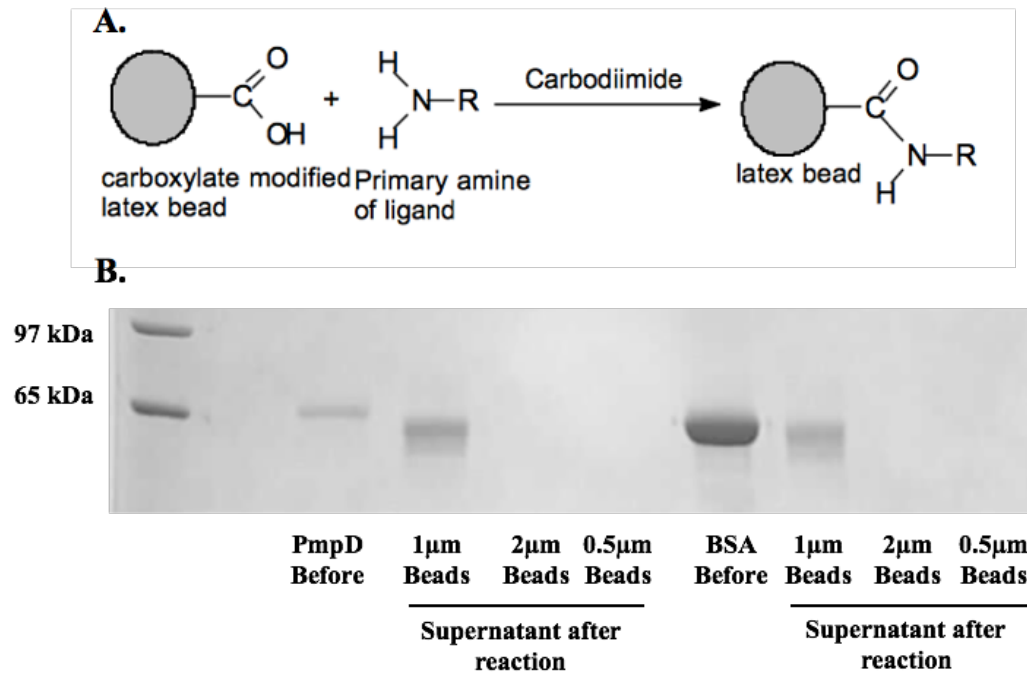
Figure 5.1: Covalent coupling of rPmpD and BSA to carboxylate modified latex beads. EDAC was used to covalently link rPmpD to carboxylate-modified beads through primary amine groups on the protein ligand (**A**). Coupling of rPmpD and BSA protein to beads of several diameters (0.5μm, 1μm, and 2μm) was verified on SDS-PAGE by inspection of the reaction supernatant before and after the reaction (**B**). Poor coupling to 1μm beads is observed. 2μm beads were used in all subsequent adhesion assays due to ease of quantification following inspection by phase microscopy.

5.2.2 Adherence of rPmpD-coated polystyrene beads to Hak and McCoy cell lines

Due to the ability to more easily visualize and reliably quantify the 2μm beads relative to the 0.5μm beads, 2μm beads were subsequently used in all adhesion assays. The naked, rPmpD- or BSA-coated beads were incubated with mammalian epithelial-like Hak and murine fibroblast McCoy cell lines. Following washing in PBS to remove unbound beads, methanol fixation and Giemsa staining, the number of beads attached to 50 cells in triplicate random fields of view was counted using phase microscopy (**Fig.5.2-5.4**). rPmpD-coated beads showed a significant increase in adhesive capacity to Hak cells relative to naked and BSA-coated beads. This experiment confirms that

rPmpD demonstrates adhesin-like properties, a finding also previously documented by (Becker and Hegemann, 2014).
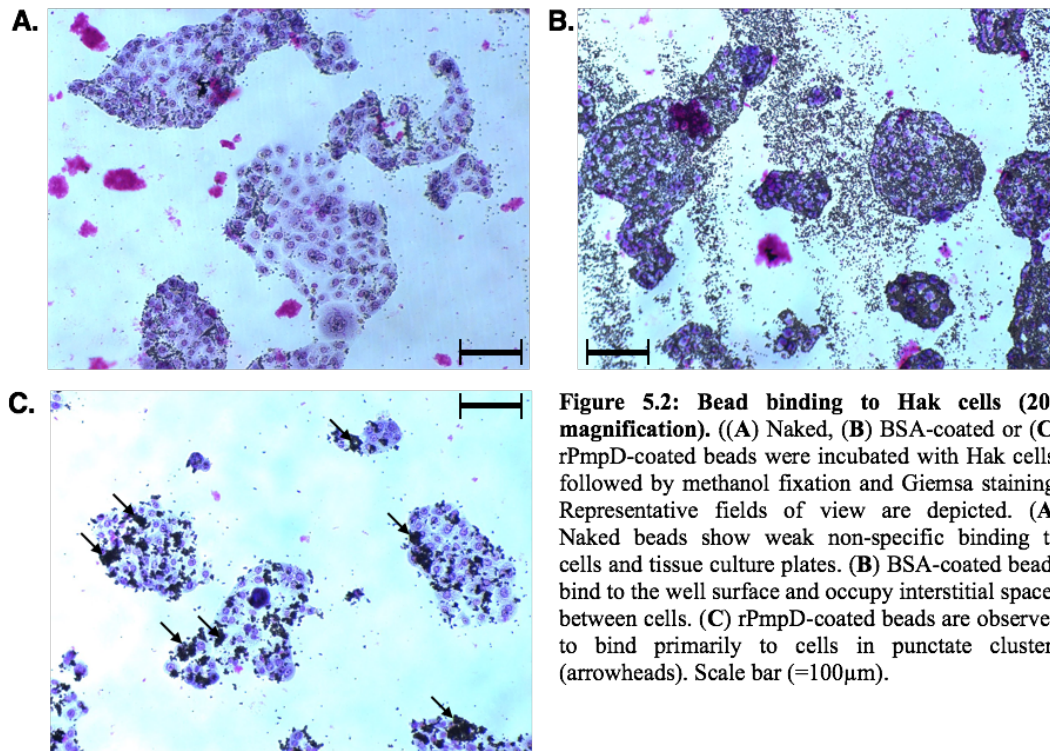
Figure 5.2: Bead binding to Hak cells (20x magnification). ((A) Naked, (B) BSA-coated or (C) rPmpD-coated beads were incubated with Hak cells, followed by methanol fixation and Giemsa staining. Representative fields of view are depicted. (A) Naked beads show weak non-specific binding to cells and tissue culture plates. (B) BSA-coated beads bind to the well surface and occupy interstitial spaces between cells. (C) rPmpD-coated beads are observed to bind primarily to cells in punctate clusters (arrowheads). Scale bar (=100μm).
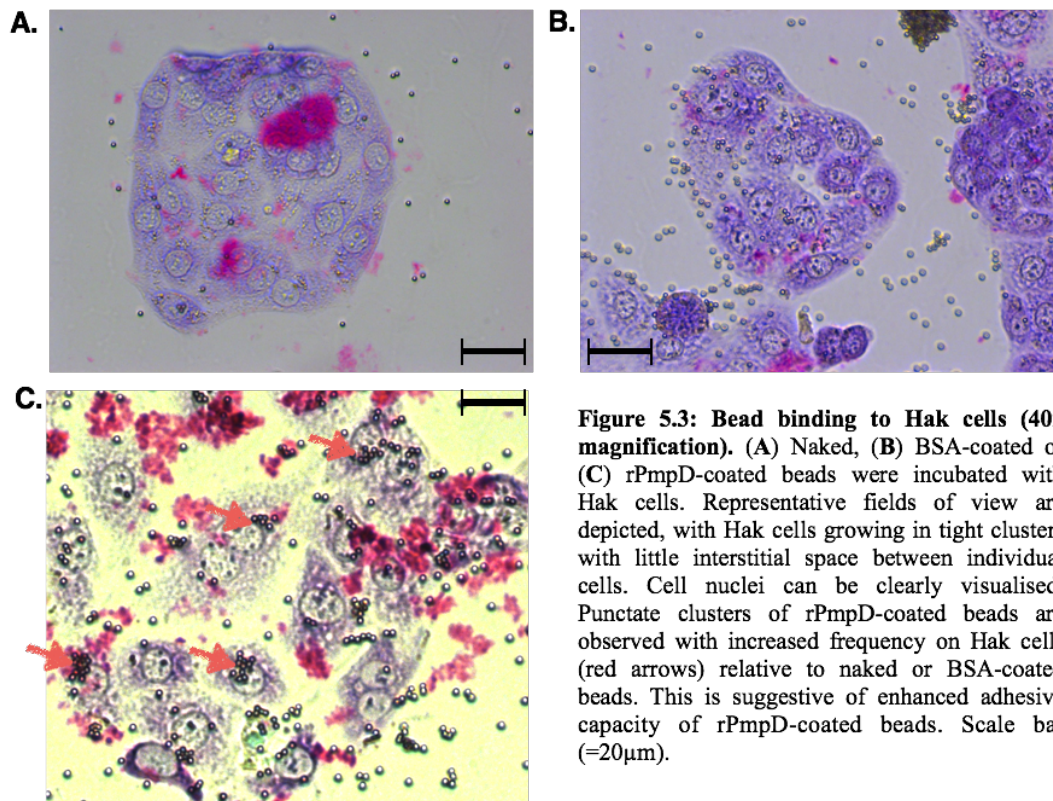
Figure 5.3: Bead binding to Hak cells (40x magnification). (A) Naked, (B) BSA-coated or (C) rPmpD-coated beads were incubated with Hak cells. Representative fields of view are depicted, with Hak cells growing in tight clusters with little interstitial space between individual cells. Cell nuclei can be clearly visualised. Punctate clusters of rPmpD-coated beads are observed with increased frequency on Hak cells (red arrows) relative to naked or BSA-coated beads. This is suggestive of enhanced adhesive capacity of rPmpD-coated beads. Scale bar (=20μm).

156
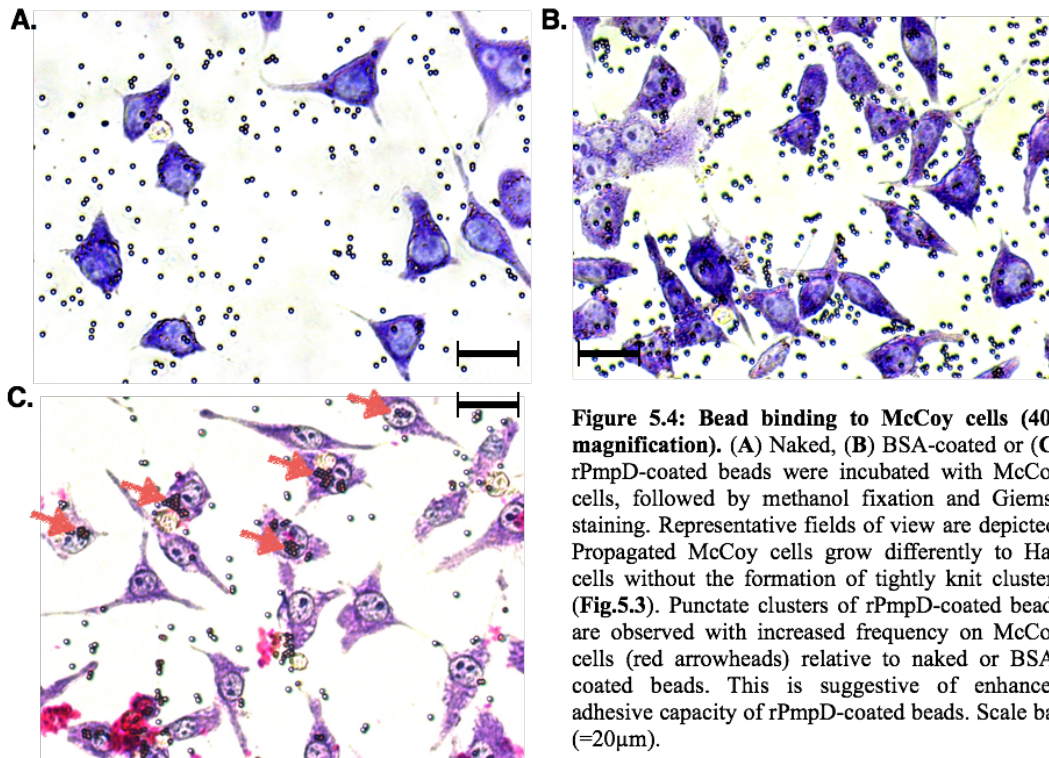
Figure 5.4: Bead binding to McCoy cells (40x magnification). (**A**) Naked, (**B**) BSA-coated or (**C**) rPmpD-coated beads were incubated with McCoy cells, followed by methanol fixation and Giemsa staining. Representative fields of view are depicted. Propagated McCoy cells grow differently to Hak cells without the formation of tightly knit clusters (**Fig.5.3**). Punctate clusters of rPmpD-coated beads are observed with increased frequency on McCoy cells (red arrowheads) relative to naked or BSA-coated beads. This is suggestive of enhanced adhesive capacity of rPmpD-coated beads. Scale bar (=20μm).

5.2.3 Titration of rPmpD coating concentrations on carboxylate modified polystyrene beads

Titration of rPmpD bead coating concentration from 50μg/ml to 0.25μg/ml was carried out, and incubation of a 1:50 dilution of a 1% solution of polystyrene beads with Hak cells revealed a concentration-dependent reduction in bead binding (**Fig.5.5**). A rPmpD-coating concentration as low as 2.5μg/ml still effected roughly four-fold greater adhesion (118±10) than beads coated with 200μg/ml of BSA control protein (29±11).
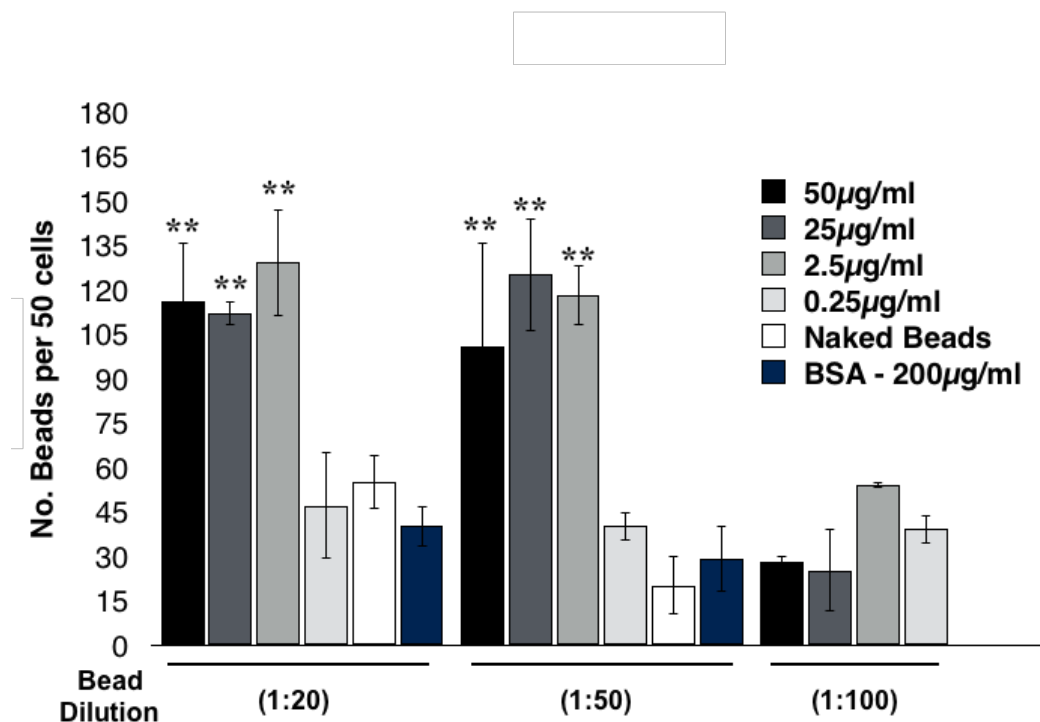
Figure 5.5: Quantification of Hak cell bead adhesion. The number of rPmpD-coated beads adherent to 50 cells within triplicate fields of view was counted and compared to control (200μg/ml naked or BSA-coated beads). rPmpD-coated beads showed significantly enhanced adhesive capacity compared to naked or BSA-coated beads (200μg/ml). * = $p \leq 0.05$, ** $p \leq 0.01$, ***$p \leq 0.001$ (relative to BSA-coated beads).

5.2.4   Analysis of infection abrogation of carboxylate modified rPmpD-coated polystyrene beads by mouse anti-rPmpD serum

To further investigate whether rPmpD was essential to Hak cell adhesion, anti-rPmpD serum from rPmpD-immunized C57BL/6 mice was pre-incubated with rPmpD-coated beads. Two different dilutions of immune serum were used (1:100 and 1:50), and incubated with beads coated with differing concentrations of rPmpD from 50μg/ml-2.5μg/ml (**Fig.5.6**). Following addition of a 1:50 dilution of a 1% solution of polystyrene beads to Hak cell monolayers, significant reduction in adhesion (four to five-fold) was observed with a 1:50 dilution of immune serum relative to the negative control (binding media).
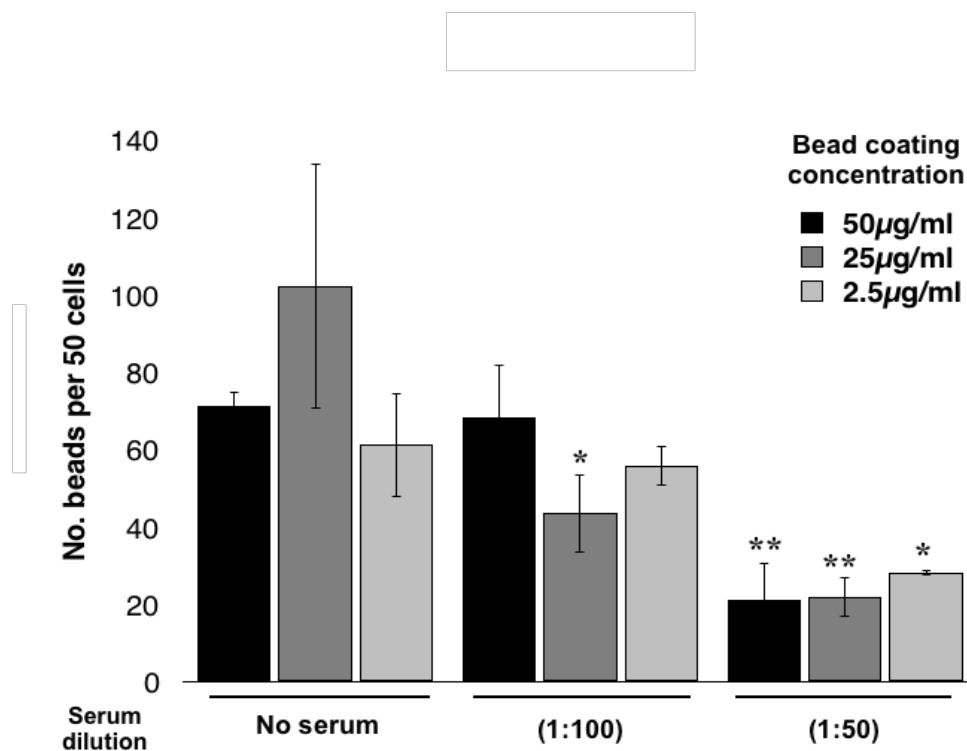
Figure 5.6: Anti-rPmpD serum abrogation of rPmpD-coated bead adhesion. Heat-inactivated anti-rPmpD serum obtained from rPmpD-immunized mice abrogates adhesion of rPmpD-coated beads in a dose-dependent fashion. Bead coating concentration of rPmpD varied from 50μg/ml -2.5μg/ml.* = p≤0.05, ** p≤0.01, ***p≤0.001 (relative to no anti-rPmpD serum).

5.2.5 Competitive inhibition of carboxylate modified rPmpD-coated polystyrene beads by soluble rPmpD

To determine whether soluble rPmpD could block rPmpD-coated bead binding to Hak cells, pre-incubation of Hak cells with soluble rPmpD (50μg/ml-2.5μg/ml), was followed by washing and incubation with beads coated with differing concentrations of rPmpD (50μg/ml-2.5μg/ml). Increasing concentrations of soluble rPmpD competitor significantly abrogate bead adhesion relative to the negative control (pre-incubation with BSA) (**Fig.5.7**).
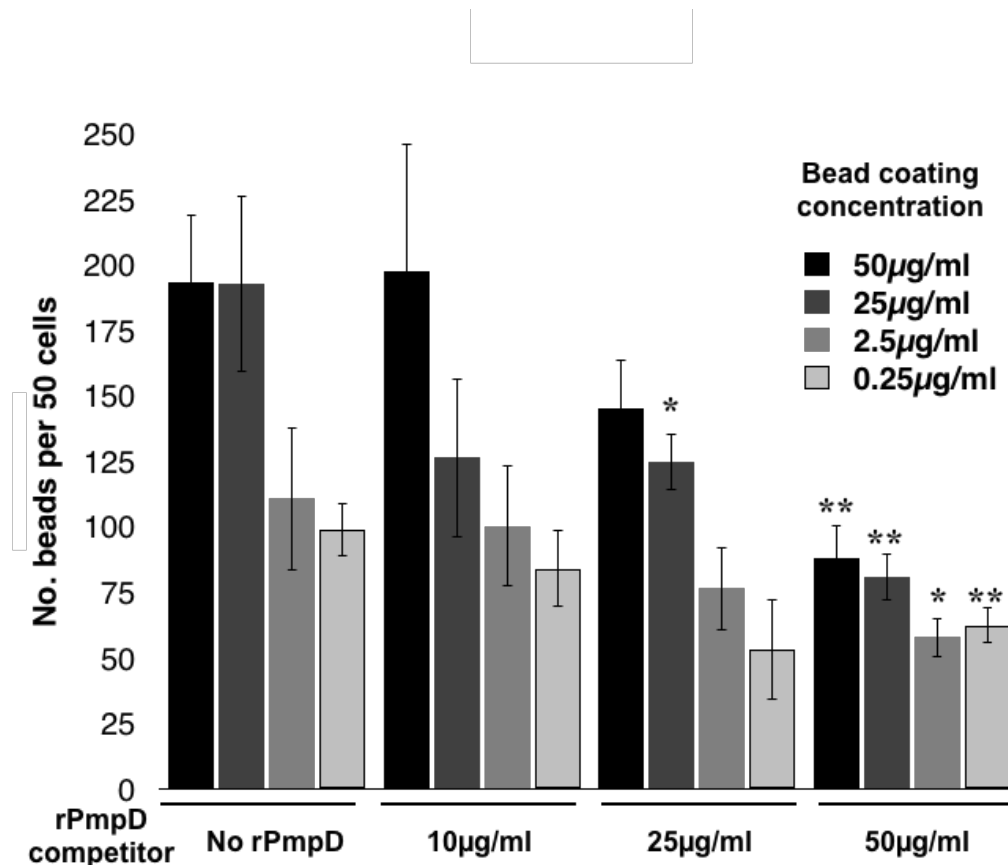
Figure 5.7: Soluble rPmpD competitive inhibition of rPmpD-coated bead adhesion. Soluble rPmpD was incubated with Hak cells for 1hr prior to addition of rPmpD-coated beads. For a given bead coating concentration, the rPmpD competitor significantly reduces adhesion of rPmpD-coated beads in a dose-dependent manner, likely indicating competitive binding of putative host cell receptor(s).* = $p \leq 0.05$, ** $p \leq 0.01$, ***$p \leq 0.001$ (relative to no rPmpD competitor).

This experiment indicates that binding of rPmpD to a putative cellular receptor or extracellular matrix component, likely competes for binding sites available for rPmpD-coated polystyrene bead adhesion.

5.3   Discussion

Whole-genome sequencing of bacterial genomes has elucidated an incredibly diverse array of putative adhesin genes in pathogenic bacteria, and it is likely that several routes to host cell adhesion and invasion exist (Brzuszkiewicz et al., 2006). Such inbuilt functional redundancy inevitably puts a large constraint on *in vitro* studies and vaccine development, and for many important bacterial pathogens such as *Ct*, elucidation of structure-function relationships and receptor-ligand interactions is crucial for informing therapeutic development. Moreover, our knowledge of the functional consequences of the expansion of Pmps in *Ct* and related chlamydial species is rudimentary.

Becker and Hegemann (2014) have recently implicated all recombinant *Ct* Pmps as chlamydial adhesins, and showed tissue-specific adhesion properties of rPmpD-coated bead binding to epithelial-like HEp-2 and HeLa cell lines, but not endothelial HUVE cells. Furthermore, (Kari et al., 2014) demonstrate that infectivity of a serovar D/UW3/Cx *pmpD* null mutant is defective for adhesion in human conjunctival (HCjE) or endocervical (A2EN) cell lines, but not in McCoy (murine fibroblast) cell lines. Our data show for the first time that the 65kDa rPmpD passenger domain proteolytic fragment, shown to be present under physiological conditions in *in vitro* cultured *Ct*, possesses adhesive properties in the mammalian epithelial-like Hak cell line, widely used for culture and study of antibody-mediated neutralization of *Ct* infections *in*

vitro, due to the lack of Fc-receptor expression which may facilitate bacterial internalization in other cell types. The rPmpD-host cell interaction was further confirmed using competitive inhibition assays and anti-rPmpD mediated neutralization of rPmpD-coated latex bead adhesion. Both anti-rPmpD serum and soluble rPmpD competitor abrogate adhesion *in vitro*. These experiments provide further evidence suggesting *Ct* PmpD may function as a chlamydial adhesin.

Possible extensions to our investigations of the function of PmpD include *in vitro* anti-rPmpD serum neutralization and soluble rPmpD competitive inhibition of live *Ct* infection. However, the identification of specific host cell interactions for adhesins remains a significant experimental challenge due to phase variability and differential expression of multiple adhesins in *Ct* that may also possess overlapping functions and binding affinities, and failure to observe abrogation of infection under such experimental conditions may not necessarily rule out Pmp effector function *in vivo*. For instance, *Ct* encodes nine different Pmps with variable expression profiles during biphasic development (Gomes et al., 2006; Nunes et al., 2007; Tan et al., 2010), with all nine proteins implicated in host cell adhesion (Becker and Hegemann, 2014). However, determining whether these proteins exert a cooperative effect, or act independently through multiple different interactions with host cell ligands will be of direct relevance to rational vaccine design.

Although no structure of a chlamydial adhesin has yet been solved, examination of the structure of outer membrane proteins of *Yersinia* spp. has indicated diverse functional roles of T5ATs. In *Yersinia*, the structures of outer membrane autotransporters have been solved by X-ray crystallography. YadA is a large, modular

trimeric autotransporter protein that possesses a head, neck, stalk and anchor domain (Hoiczyk et al., 2000). This results in a lollipop-like projection that protrudes to a distance of ~23nm from the bacterial cell surface (Koretke et al., 2006). The 3D structure of the YadA head domain has been elucidated, and implicated in neutrophil and collagen binding, as well as auto-agglutination (Hoiczyk et al., 2000). The YadA head domain demonstrates self-affinity that ultimately leads to bacterial flocculation, a process also exemplified by the *E.coli* T5AT Ag43 (Klemm et al., 2004). This is thought to mediate bacterial resistance against host antimicrobial agents and promote biofilm formation.

Ct PmpD may function in a similar manner, possibly mediated through Cys-Cys interactions or distinctive GGA(I,L,V) / FXXN tetrapeptide motifs within the passenger domain, and future work may involve investigating changes in adhesive capabilities of PmpD passenger domains with specific Cys mutations or disruptions in tetrapeptide motif sequences. (Molleken, Schmidt and Hegemann, 2010) demonstrate that at least two of these copies are required for adhesion to host cells in *C.pneumoniae*. Interestingly, YadA has also been shown to act as a scaffold for the T3SS injectisome (Visser, Annema and van Furth, 1995), and it is likely that PmpD, given its constitutive expression throughout *Ct* biphasic development in EB and RB forms (Tan et al., 2010), may play a similar role, most likely through Cys-Cys interactions with other Cys-rich *Ct* T3SS apparatus proteins such as the needle-like protein CdsF (Betts-Hampikian and Fields, 2011).

However, perhaps the most well characterized *Yersinia* adhesin is invasin. This protein shows an inverse arrangement of the T5AT system with the β–barrel at the N-

terminus of the protein, and is composed of a modular architecture consisting of four bacterial immunoglobulin-like (BIG) domains (D1-D4) and a D5 domain that possesses similar topology to the C-type lectins (Hamburger et al., 1999). Domains D4-D5 are critical and sufficient for integrin binding, as is the formation of the disulphide bond between Cys_{906} and Cys_{982}. Importantly, invasin binds integrins with greater affinity than host ligand fibronectin, and structural examination of the inter-domain interfaces reveals a larger binding interface for invasin, which likely explains this enhanced affinity (Hamburger et al., 1999). Invasin thus reveals a remarkable instance of convergent evolution of pathogenic effector molecules that not only mimic, but also outcompete host cell ligands for binding. Thus, structural approaches used to examine host-pathogen interactions are important for shedding light on functional interactions or guiding cell biology approaches to interrogate adhesin function *in vitro*.

Ongoing and future work involves identification of putative cellular interaction partners for PmpD. To identify extracellular molecular targets of rPmpD, two approaches for identifying protein-protein interactions are currently in progress. The first involves fusion of PmpD 65kDa passenger domain to a constitutively active *E. coli* biotin ligase (BirA) (Roux et al., 2012). In the presence of biotin in cell culture, BirA biotinylates proteins in close proximity. Soluble *Ct* rPmpD-BirA fusion protein added to A2EN, HCjE or Hak cell lines will then be warmed to 37ºC in the presence of biotin, allowing biotinylation of proteins in close proximity. Recombinant BirA alone will be used to generate control samples for proteomics. Both transient and stable interaction partners isolated using magnetic streptavidin beads will be identified by on-bead tryptic digestion and analysis by 1D LC/MS/MS.

A caveat to the biotinylation experiment is that the rPmpD host cell interaction partner needs to be accessible to the BirA ligase fusion protein. If the fusion construct interferes with binding or results in diminished protein expression, rPmpD will be biotinylated *in vitro* using NHS-SS-biotin and incubated with respective cell lines. Cross-linking to receptor proteins using DTSSP will be implemented, and biotinylated rPmpD-receptor complexes isolated using streptavidin affinity purification following cell lysis and elution by DTT reduction of the disulphide bond between rPmpD and NHS-SS-biotin (**Fig.5.8**). A similar approach has been used previously to identify Pmp21 interaction partners in *Chlamydia pneumoniae* (Molleken, Becker and Hegemann, 2013).
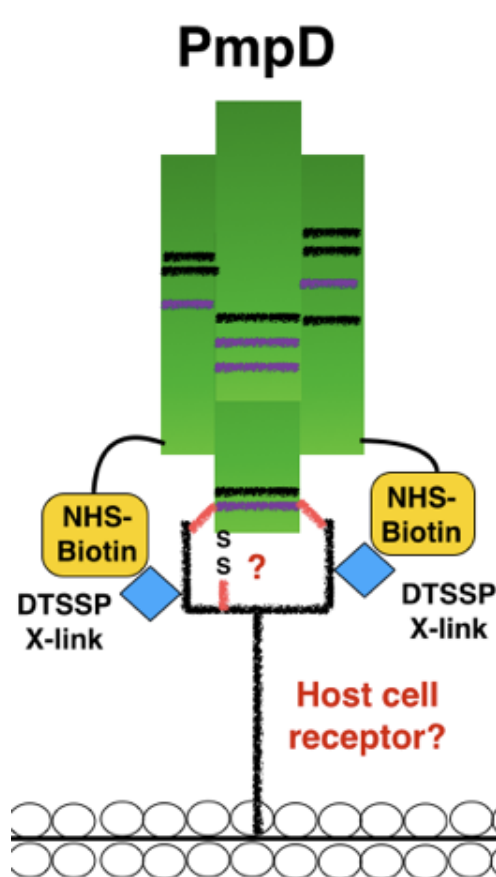
Figure 5.8: Biotinylation of rPmpD. Future work entails *in vitro* biotinylation (yellow) of soluble rPmpD (green), followed by chemical cross-linking to putative host cell receptors using DTSSP (blue). Receptor-ligand interactions will be identified using affinity purification with streptavidin beads followed by mass spectrometry of eluted proteins cleaved from the beads using DTT and resolved using SDS-PAGE.

In addition, PmpD possesses a putative nuclear localization sequence, and the *pmpd* null mutant shows atypical inclusion morphology with defective RB attachment to the

inclusion membrane (Kari et al., 2014; Swanson et al., 2009). To identify likely intracellular interactions, HEK293 cells stably expressing inducible mycBirA-rPmpD fusion construct under an inducible Tet promoter will be generated, with endogenous biotinylated proteins purified using streptavidin beads upon cell lysis. Validation of protein-protein interactions may then further be studied using siRNA knockdowns of identified targets in CHO cells and complementary Y2H assays.

In light of the evidence provided here, and in previous studies implicating Pmps and T5ATs from a diverse range of Gram-negative pathogenic bacteria in host cell adhesion, these chlamydial outer membrane proteins are promising antigenic components for the development of future chlamydial vaccines. The successful incorporation and *N.menigitidis* NadA and *B.pertussis* pertactin in the licensed Bexsero meningitis B and DPT vaccines (respectively) provides robust evidence of the importance of T5ATs in mediating protection against bacterial disease. The following chapter investigates the efficacy of *Ct* rPmpD as a chlamydial vaccine candidate in a murine model of *Ct* infection.

Chapter 6: Investigation of a novel second-generation lipid adjuvant (SLA) in combination with rPmpD as a preclinical *Ct* vaccine

6.1   Introduction

The immune response to an invading pathogen consists of two broadly characterized innate and adaptive phases. The innate immune system implements the initial non-specific pro-inflammatory response through sensing of pathogen associated molecular patterns (PAMPs) by an array of pathogen recognition receptors (PRRs) on macrophages and dendritic cells (DCs), and confers generalized protection to the host through phagocytosis and the secretion of cytokines and chemokines which also facilitate the arrival of neutrophils and other innate effector cells such as NK or NKT cells with antimicrobial properties (Banchereau and Steinman, 1998; Creagh and O'Neill, 2006). This initial inflammatory response also leads to the recruitment and priming of cells of the adaptive immune system, which are programmed and shaped to recognize pathogen-specific molecules by professional antigen presenting cells (APCs) of the innate immune system, resulting in immunological memory (Palm and Medzhitov, 2009). The importance and intricacies of innate immune signaling are now becoming increasingly appreciated within the context of adaptive immunity, particularly where vaccine development is concerned (Kasturi et al., 2011; Wiley et al., 2011).

Many live-attenuated or whole-cell vaccines now struggle to fulfill the more stringent regulatory requirements of safety and standardized manufacturability, and also carry the risk of reversion to virulent wild-type strains *in vivo*. Furthermore, although intrinsically immunogenic, these vaccines are often more costly to manufacture, and depending on the nature of the pathogen, may not be suitable for administration to

subsets of patients who are immunocompromised. Thus, for many pathogens, antigenic components manufactured as recombinant proteins are considered a safer, cheaper and more robust alternative. However, in the absence of a plethora of immunogenic surface-exposed PAMPs in whole-cell or live-attenuated vaccines (e.g. bacterial lipopeptides, lipopolysaccharides, flagellins), recombinant protein vaccines are weakly immunogenic. This necessitates the development of adjuvants able to elicit a potent and durable antigen-specific immune response. However, because the mode of action of even the most widely used adjuvants in currently licensed vaccines such as the aluminium salts and MF59 are poorly characterized (Marrack, McKee and Munks, 2009; O'Hagan et al., 2012), a shift in focus towards understanding and defining the molecular mechanisms of new adjuvants in both preclinical models and human trials has been identified as a crucial step to fulfilling both regulatory statutes and existing unmet medical needs (Reed, Orr and Fox, 2013).

One of the most pressing clinical requirements for next-generation adjuvants in the field of infectious diseases is the development of new T cell based vaccines to combat intracellular pathogens that cause substantial mortality or morbidity worldwide. Malaria, tuberculosis and HIV are among the most widely investigated, but several other neglected tropical diseases such as the spectrum of leishmaniases, ocular trachoma and sexually transmitted chlamydial infections comprise this category. An array of judicious targets for novel adjuvants is represented by the wide array of innate immune receptors that mediate PAMP recognition within the host, and are able to differentially program the ensuing pro-inflammatory response through specific signaling cascades.

The family of PRRs known as Toll-like receptors (TLRs) will briefly be discussed below, followed by a major focus on TLR4 and the first preclinical characterization of a novel, rationally designed TLR4 agonist employed as an adjunct to *Ct* rPmpD for use in the development of future chlamydial vaccines. This second generation lipid adjuvant (SLA) was designed and formulated by the Infectious Disease Research Institute (IDRI), and has previously undergone preliminary characterization in *in vitro* assays through analysis of cytokine and chemokine profiles following stimulation of human and murine cells (IDRI, personal communication). We provide the first preclinical study utilizing rPmpD as a chlamydial vaccine antigen, and demonstrate the *in vivo* efficacy of the SLA-rPmpD combination in significantly enhancing both resistance to *Ct* infection and reduction in bacterial load.

6.1.1   Toll-like receptors

TLRs constitute a family of 10 transmembrane PRRs in humans, which are differentially expressed on variable APC subsets that also vary in population density at disparate anatomical sites (Ueno et al., 2011). Indeed, much attention has been devoted to the study of these subsets and their physiological abundance *in vivo*, with particular focus on the use of TLR-based adjuvants to target specific DC subsets for an optimal immune response (Reed, Orr and Fox, 2013). TLRs 1, 2 and 6 are surface-expressed, and possess the ability to hetero-dimerize with predominant recognition of lipidated peptides, while TLR5 is responsible for the recognition of bacterial flagellin. TLRs 3, 7, 8 and 9 are expressed intracellularly, and mediate innate immune recognition of dsRNA (TLR3), ssRNA (TLRs 7 and 8) or unmethylated CpG DNA (TLR9). TLR4, perhaps the most well-characterized PRR in the field of adjuvant development, is also expressed on the surface of APCs, and mediates immune

signaling through sensing of an array of structural variants of bacterial lipopolysaccharides (LPS), signaling predominantly through the MyD88 and TRIF-dependent pathways (Bowen et al., 2012). The rational design and *in vivo* characterization of a novel TLR4 agonist for use in future chlamydial vaccines will be the focus of this chapter.

6.1.2   TLR4: an exploitable target for adjuvant development

TLR4 is an attractive innate immune receptor upon which to base the design of next-generation adjuvants, particularly in light of a wealth of safety and immunogenicity data provided by previous clinical trials using TLR4 agonists, and a detailed description of the molecular mechanisms of LPS interaction with the TLR4 receptor (Hajjar et al., 2002; Ohto et al., 2012). Indeed the only approved TLR agonist licensed for use in vaccine development to date is 3D-MPL, a synthetic derivative of LPS developed by Ribi ImmunoChem and Corixa Corporation (Baldridge et al., 2004; Ulrich and Myers, 1995), and now a main constituent of the AS04 adjuvant formulation currently in use in the HPV vaccine, Cervarix (GSK) (Didierlaurent et al., 2009; Giannini et al., 2006).

Recent studies have provided a much clearer picture of the molecular basis of TLR4 signaling in response to activation by an array of structural variants of LPS. Indeed, the 3D description of the structure of the TLR4-MD2 complex through X-ray crystallography was a seminal discovery that has subsequently guided the rational design of ligands to target this molecule (**Fig.6.1**) (Park et al., 2009). Signaling through TLR4 involves loading of LPS on to the myeloid differentiation factor 2 (MD2) molecule with the aid of the helper protein CD14 (Lu, Yeh and Ohashi, 2008).

This is followed by dimerization of the LPS-MD2 complex with the TLR4 receptor (Ohto et al., 2012).
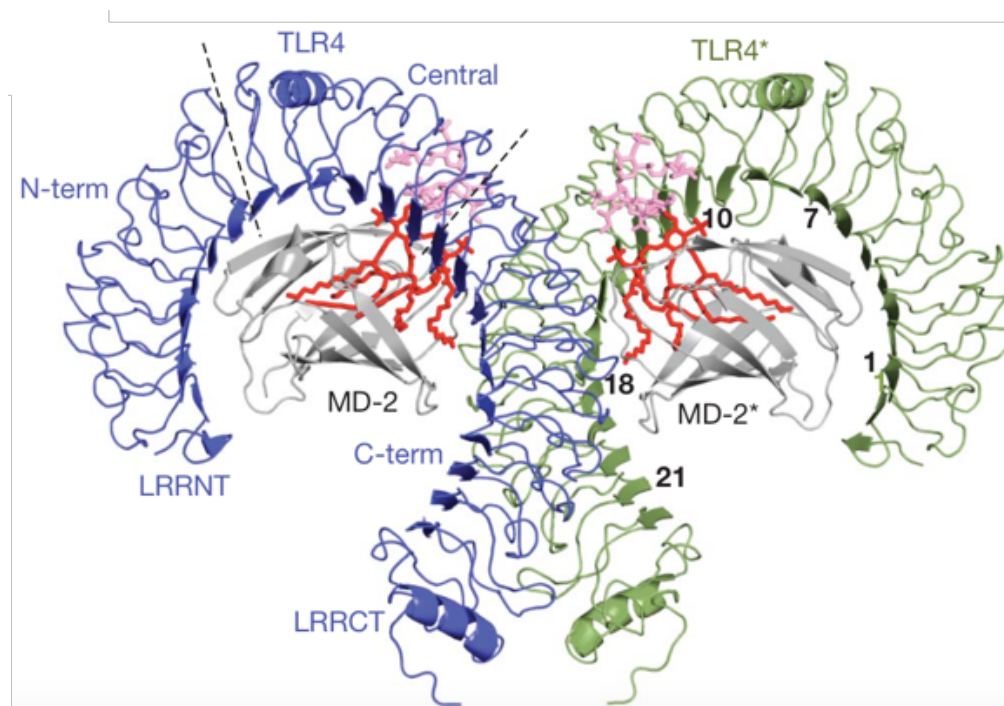
Figure 6.1: Molecular description of the TLR4-MD2 interaction (Park et.al, 2009). Structure of TLR4-MD-S-LPS complex solved by X-ray crystallography (Park et al., 2009). The binding of LPS results in formation of the binding interface and subsequent dimerisation. The lipid A component of LPS is coloured red, and the inner core carbohydrates of LPS coloured pink with individual subunits of the TLR4 dimer in blue and green.

It is now widely acknowledged that TLR4 is a major transducer of intracellular signaling cascades that lead to the maturation of APCs and initiation of the acute inflammatory immune response (Beutler, 2000). Evidence for this has been provided in both animal models and human genome-wide studies, where hypo-responsiveness to LPS is observed in C3H/HeJ and C57BL/10ScCr mice with mutations in the TLR4 gene (Poltorak et al., 1998). In contrast, mice deficient in TLR2, once implicated in LPS signaling, show no differences in the immune response to LPS (Hoshino et al., 1999).

A main premise for the development of TLR4 ligands as innate immune adjuvants was the observation that pathogenic bacteria (such as *Salmonella* and *Pseudomonas*) altered the acylation state of their lipid A surface components in order to modulate host-mediated innate immune responses (Ernst et al., 1999; Guo et al., 1997). Importantly, subtle changes in the structure of bacterial LPS can also lead to the differential modulation of the inflammatory response. This was elegantly demonstrated in a study comparing clinical and laboratory isolates of *P.aeruginosa* - a Gram-negative pathogen of humans (Hajjar et al., 2002).

Laboratory-adapted strains of *P.aeruginosa* possess a predominantly penta-acylated LPS structure, while isolates obtained from the lungs of patients affected by cystic fibrosis contain a hexa-acylated form of LPS that possesses additional aminoarabinose and palmitate residues (Ernst et al., 1999). Importantly, it was found that clinical but not laboratory isolates were able to stimulate a robust inflammatory response in human endothelial (HUVEC) cells, evidenced by the induction of pro-inflammatory cytokines, thus providing further evidence that LPS derivatives can act as agonists or antagonists of the TLR4 receptor, and that this interaction may be governed by the acylation state of the molecule (Ernst et al., 1999; Somerville et al., 1996).

(Hajjar et al., 2002) further found that while human cells and TLR4 (hTLR4) were able to differentiate between penta- and hexa-acylated forms of LPS, murine cells and TLR4 receptors (mTLR4) were not. Because the interaction between LPS and the TLR4 receptor also requires coupling of the LPS molecule to MD2 via CD14, it was necessary to investigate which of these components contributed to differential LPS

recognition. Using endothelial cell leukocyte adhesion molecule (ELAM)-luciferase as a readout for NFκB activity in response to LPS stimulation, ectopic expression studies of murine and human TLR4, MD2 and CD14 components were carried out in transfected HEK-293 cells, demonstrating that variations between human and murine TLR4 receptors, and not the MD2 or CD14 components, contributed to differential sensitivity to LPS variation (Hajjar et al., 2002).

The region of the TLR4 receptor attributable to differences in NFκB activity was initially identified through sequence comparisons across a range of species, revealing an 82 amino acid hypervariable ecto-domain that lacked leucine-rich repeat regions characteristic of TLRs (Hajjar et al., 2002). Furthermore, this region is contained within a larger 330 amino acid region in the extracellular domain, where polymorphisms within the human population are known to reside and are reportedly responsible for hypo-responsiveness of certain individuals to endotoxin (Arbour et al., 2000).

The high degree of variation within this region, evidenced by the high ratio of non-synonymous to synonymous SNPs (Hajjar et al., 2002), suggests that this part of the receptor has been under species-specific environmental pressure in response to pathogen adaptation by LPS modifications, and may also be a contributing factor to inter-individual variation in disease outcome following infection by certain pathogenic bacteria. Furthermore, these observations highlight the caveats of using preclinical models to study the efficacy of LPS-based adjuvants without prior characterization and evaluation of immune responses in primary human cells. This is

of paramount importance for the future development of TLR4 agonists, where the degree of immunogenicity in mice may not necessarily reflect that in humans.

This species-specificity of LPS recognition using *P.aeruginosa* as a model organism is further corroborated by investigation of *N.meningitidis* LpxL1 LPS, where hexa-acylated but not penta-acylated structures elicit robust immune responses in human macrophages, whilst significant changes in the inflammatory response are indiscriminate between the two orthologs when administered as adjuvants in mice (Steeghs et al., 2008). This study was important, as the authors previously showed potent immune-stimulating properties of LpxL1 in murine models of *N.meningitidis* infection (Steeghs et al., 1999; van der Ley et al., 2001), evidenced by high levels of maturation of murine BMDCs *in vitro* (Fisseha et al., 2005), implying that LpxL1 may be incorporated as a candidate adjuvant in future vaccines. However, in the context of what is now known about species-specific differences in the TLR4-MD2-LPS interaction, validation of the translational potential of subsequent 'designer' adjuvants will require prior evaluation in a range of both human and murine APCs *in vitro*.

The recent 3D structural description of the molecular interactions of murine TL4 with both LPS and Lipid IVa, a precursor of *E.coli* LPS, has highlighted important structural design principles for future LPS derivatives as novel adjuvants (Ohto et al., 2012). It was previously shown that the lipid A moiety, with acyl chains of variable lengths attached to the diglucosamine backbone of LPS, was responsible for immunostimulatory activity (Schletter et al., 1995). In addition, the presence of two phosphate groups was further shown to be key for immuno-stimulatory properties, as

deletion of the either group diminished endotoxin potency (Rietschel et al., 1994; Rietschel et al., 1993).

Interestingly, binding of LPS induced the formation of M-shaped TLR4-MD2-LPS dimers (Ohto et al., 2012). Examination of the crystal structures of the TLR4-MD2-LPS interfaces revealed that during binding of hexa-acylated LPS, only one of the six acyl chains are exposed at the surface of MD2, and form hydrophobic interactions with phenylalanine residues of TLR4. However, the five other acyl chains of LPS remained buried within MD2, without changing the size of the binding pocket. This is in contrast to tetra-acylated LPS derivatives, where lipid IVa showed displacement of the di-glucosamine backbone by a 5Å upward shift towards the solvent area. It was further observed that this displacement aided dimerization through the formation of ionic interactions between the negatively charged phosphate groups and positively charged amino acid residues on TLR4 and MD2 (Ohto et al., 2012).

Interestingly, binding of LPS induced the formation of M-shaped TLR4-MD2-LPS dimers (Ohto et al., 2012). Examination of the crystal structures of the TLR4-MD2-LPS interfaces revealed that during binding of hexa-acylated LPS, only one of the six acyl chains are exposed at the surface of MD2, and exert hydrophobic interactions with phenylalanine residues of TLR4. However, the five other acyl chains of LPS remained buried within MD2, without changing the size of the binding pocket. This is in contrast to tetra-acylated LPS derivatives, where lipid IVa showed displacement of the di-glucosamine backbone by a 5Å upward shift towards the solvent area. It was further observed that this displacement aided dimerization through the formation of

ionic interactions between the negatively charged phosphate groups and positively charged amino acid residues on TLR4 and MD2 (Ohto et al., 2012).

Thus, it is clear that the differential activation of hTLR4 by structural modifications in LPS derivatives employed by certain pathogens offers a unique opportunity to tune TLR signaling, and hence modulate the ensuing innate immune response. In the context of the 3D description of the TLR4 structure, the ability to rationally design and test new adjuvants holds great potential for achieving a balance of pro-inflammatory immune signatures to initiate robust cell-mediated immunity, with therapeutic windows that may result in enhanced safety profiles in human clinical trials. This is important to avoid the risk of severe adverse events in clinical trials, as exposure to LPS can often amplify signaling through TLR4 resulting in localized inflammation or systemic septic shock (Angus et al., 2001). Importantly, these observations substantially guided the development of a glucopyranosyl lipid adjuvant (GLA) developed by IDRI, a precursor to the structurally designed second-generation lipid adjuvant (SLA) employed in our study. The design principles upon which these two adjuvants were developed will be discussed next.

6.1.3 Design of glucopyranosyl lipid adjuvant (GLA)

GLA was designed using previous knowledge on the variable potencies of different LPS analogues discussed above (Rietschel et al., 1993; Schletter et al., 1995). The structure of GLA is shown in **Fig.6.2** (Coler et al., 2011). Key differences between GLA and naturally occurring LPS derivatives are highlighted. These include: (i) the removal of sugar residues from the hydroxyl group proximal to the phosphate moiety

(ii) the removal of the second phosphate group on GLA (iii) the engineering of acyl chains of defined lengths.
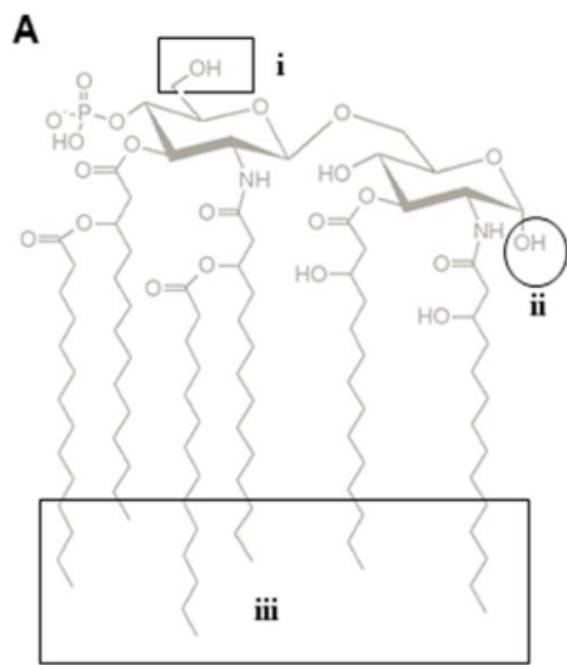
Figure 6.2: Structure of glucopyranosyl lipid adjuvant (GLA) (Coler et al., 2010). GLA was designed using modification of key moieties within the LPS molecule known to modulate interactions with the TLR4 receptor. Key differences between the LPS molecule and GLA include (i) the removal of sugar residues from the backbone (ii) the removal of the second phosphate group on LPS (iii) engineering of acyl chains of defined length

The immunostimulatory effects of GLA were investigated using mRNA and protein multiplex assays, flow cytometry and microarrays on both human and murine DCs (Coler et al., 2011). These responses were compared with the commercially approved MPL agonist, currently employed as part of the AS04 adjuvant system in the Cervarix vaccine (Didierlaurent et al., 2009). Specifically, following stimulation by each TLR4 agonist (GLA or MPL) formulated in an aqueous suspension, mouse bone-marrow derived dendritic cells (BMDCs) and human monocyte-derived DCs were assayed for an array of 23 genes implicated in the inflammatory response and the maturation of APCs, including the interleukin family (e.g. IL-1β, IL-6, IL-12p40, TNF) and an array of cellular expression markers (such as CD40, CD80, CD83 and CCR7) (Coler et al., 2011).

Interestingly, it was found that GLA and MPL both induced similar dose- and time-dependent immune responses in murine BMDCs. However, in human monocyte-derived DCs, GLA was found to be 10-100 times more potent than the commercial MPL agonist (Coler et al., 2011). Furthermore, the authors demonstrate the *in vivo* potency of GLA when paired with the ID83 *M.tuberculosis* vaccine antigen in a stable oil-in-water emulsion (GLA-SE), where robust systemic immune responses and Th1-bias were observed.

Thus, Coler et.al (2011) elucidated likely mechanistic correlates of protection elicited by previous preclinical vaccines incorporating GLA as an adjuvant in disease models of both leishmaniasis and tuberculosis (Baldwin et al., 2009;Bertholet et al., 2009). GLA-SE was previously shown to be safe and well-tolerated in Phase I trials (Coler et al., 2010), and clinical assessment of the immunogenicity of GLA-SE in humans was subsequently carried out with the purpose of evaluating different antigen-adjuvant combinations following vaccination of 12 young (20-30 years) and 15 older (>65 years) adults with subunit (SuV) or split-virus (SVV) influenza vaccines (Behzad et al., 2012).

Incorporation of GLA-SE with an influenza SVV showed enhanced cytotoxic T-lymphocyte (CTL) response to influenza virus challenge in *in vitro* stimulated PBMCs isolated from immunized subjects, evidenced by enhanced granzyme B (GrzB) activity, and was further associated with suppression of IL-10, as shown by elevated IFNγ:IL-10 ratios relative to control subjects (Behzad et al., 2012), indicating a Th1-biased response. Interestingly, these effects were significantly

enhanced when compared to GLA formulated in aqueous suspension (GLA-AF) or when compared to the TLR7/8 agonist R848, highlighting both the selective advantage of targeting TLR4 as well as the formulation-dependent variations in the efficacy and potency of adjuvants.

Immune senescence in the elderly, particularly in response to vaccines, has been shown to correlate with a variety of immunological parameters, including the variation of TLR expression with age (Grewe, 2001), reduced antigen presentation and diminished memory and effector T cell function (Haynes, 2005; Zhou and McElhaney, 2011). Specifically, reduced sterilizing immunity to influenza has further been demonstrated to correlate with an age-related shift in the immune response from a Th1- to a Th2-type bias (Shahid et al., 2010). Thus, reversing this bias through tailored adjuvant-antigen combinations is considered an effective way of contributing to improved protection against infectious diseases in the elderly population.

6.1.4   Second-generation lipid adjuvant (SLA)

The preclinical and clinical efficacy of GLA has subsequently prompted the tailored development of a novel second-generation lipid adjuvant (SLA), implemented by IDRI (Seattle). Adjuvant design was informed by ligand docking in to the previously solved 3D crystal structure of the TLR4-MD2 complex (**Fig.6.3(A)**) (Parket al., 2009). Molecular development in relation to the structure of GLA is shown in (**Fig.6.3(B)**). It was hypothesised that trimming of terminal carbon atoms from acyl chains protruding from the MD2 binding pocket may lead to a conformational difference in coupling, thus possibly modulating downstream TLR4 immune

signaling bias, as demonstrated in previous studies using modified LPS derivatives (Hajjar et al., 2002).

Design of SLA involved removal of methylene groups on the acyl chains of the GLA precursor. Although not currently determined experimentally, it was anticipated that overcrowding of the TLR4-MD2 interface with longer acyl chains results in energy
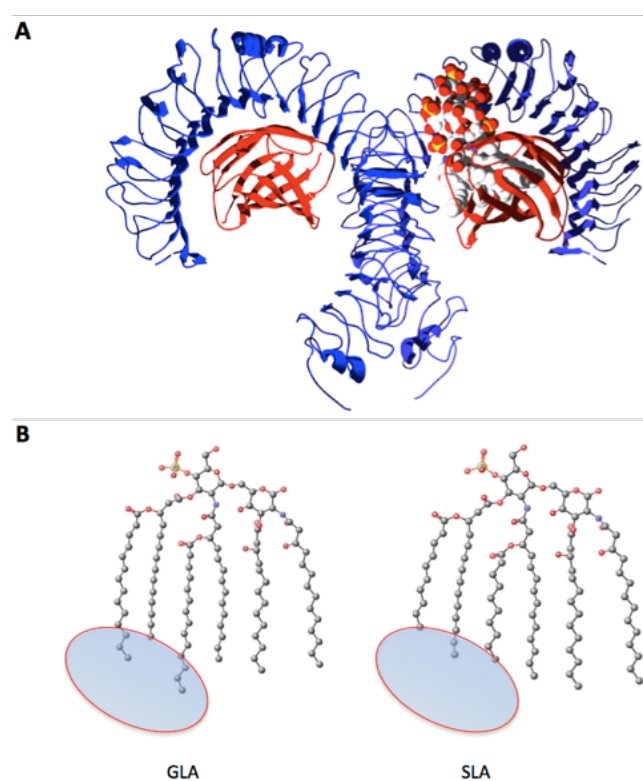
Figure 6.3: Molecular development of SLA in relation to the GLA precursor. (A) The structure of the TLR4 (blue) / MD2 (red) homodimer of heterodimers is depicted. The MD2 pocket accommodates the LPS molecule without a change in size. Increasing length of acyl chains causes the disaccharide head group to protrude further into the interstitial space between TLR4 and MD2 with displacement of the phosphate head groups. (B) Structural modifications were introduced to develop SLA from the GLA precursor (Fig.6.2). Removal of methylene groups at the terminal end of the acyl chains in GLA (groups highlighted by ovals) elicits a more compact fit into the MD2 binding pocket thus modifying the interaction between the TLR4/MD2 dimer. This was postulated to modulate downstream immune signaling.

penalties associated with binding, and may occur at the cost of diminished interaction of phosphate head groups by further upwards displacement of the molecule, that have previously been shown to be critical for endotoxin activity (Ohto et al., 2012;Rietschel et al., 1993). Further, it has been suggested that molecules with shorter acyl chains may result in a change in signaling pathway bias between the MyD88 and TRIF-dependent pathways (Bowen et al., 2012). Thus, removal of four carbon atoms of GLA maintained as large a hydrophobic surface area as possible to facilitate

energetically favourable binding kinetics between the new SLA molecule and the TLR4 interface as determined by the Avogadro software package (Hanwell et al., 2012).

In light of the aforementioned differences in murine and human TLR4 signaling and the impact of formulation on adjuvant efficacy and potency, both aqueous and oil-in-water emulsion formulations of the SLA molecule were tested *in vitro* in a human THP1 cell line and primary PBMCs isolated from healthy donors (IDRI, personal communication). As demonstrated in previous studies investigating TLR4-LPS interactions (Hajjar et al., 2002), the kinetics of NFκB activity were assessed using a reporter assay with GLA as a comparator. In HEK-293 cells expressing human TLR4, kinetics of NFκB phosphorylation were significantly enhanced with SLA relative to GLA, and were further found to plateau at lower concentrations than GLA, indicating a wider therapeutic window for SLA. SLA was also found to be 500 times more potent than GLA when added to transfected HEK cell lines expressing murine TLR4/MD2. As expected, this suggests that rational modification of TLR4 ligands can dramatically affect the kinetics and magnitude of inflammatory signaling pathways *in vitro*.

In addition to NFκB activity, cytokine and chemokine profiles were compared between SLA and its predecessor GLA. It was found that SLA induced a significantly more biased Th1-type immune response than GLA in primary human cells, evidenced by significantly lower levels of IL-10. The response was also less pro-inflammatory, with ten-fold lower levels of IL-1β and significantly less IL-6, while Th1-biasing cytokine and chemokine levels (IFNγ, GM-CSF and IP-10) remained unchanged. This

is further indicative of the differential ability of TLR4 agonists to tune innate immune signaling profiles, as it is known that TLR4 can signal through both the general MyD88 pathway shared by all other TLR receptors, but further possesses the ability to signal through the TRIF-dependent pathway (**Fig.6.4**) (Orr et al., 2013a). Based on the observation of significantly lower levels of pro-inflammatory IL-1β and IL-6 from *in vitro* studies, it was proposed that the altered binding interaction of SLA with TLR4 elicits a bias towards TRIF-dependent signaling (IDRI, personal communication).
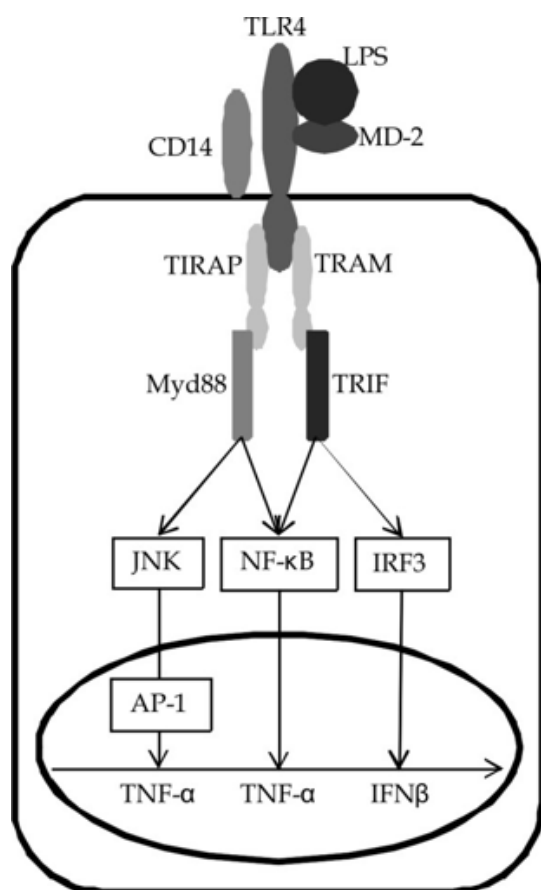
Figure 6.4: Signalling through TLR4 (Soares and Nunes, 2012). Activation of TLR4 induces two downstream signalling pathways, the MyD88-dependent and TRIF-dependent pathways. MyD88 recruitment to the TLR4 complex leads to activation of nuclear factor-κB (NF-κB) and subsequent induction of pro-inflammatory cytokines such as TNF-α, IL-6 and IL-1β. The TRIF-dependent pathway leads to induction of interferon regulatory factor 3 (IRF3) which leads to the transcription of IFN-β and other interferon-induced genes.

However, the *in vivo* efficacy of SLA has not been investigated in preclinical models of infectious disease, and these studies form the basis of this chapter, with particular focus on characterizing the efficacy of SLA in future *Ct* vaccine development. Our

data demonstrate formulation-dependent differences in the magnitude of the Th1-type immune response elicited by SLA within and between mouse strains, outlining the caveats of preclinical testing of adjuvants in different preclinical models. Although no significant differences in the enhancement of serum rPmpD-specific humoral IgG responses were detected using different adjuvant formulations, the magnitude of local rPmpD-specific cervico-vaginal IgG titres was significantly elevated with the SLA-SE formulation. Importantly, no correlation was observed between SLA formulation-specific differences in the magnitudes of Th1-biased immune responses and resistance or clearance of urogenital *Ct* infection, which seemed to correlate more with elevated serum IgG titres, although other non-specific innate immune mechanisms cannot be ruled out. Thus, our study is the first to provide evidence for the crucial role of the efficacy of rPmpD as an antigen that mediates protection against urogenital *Ct* infections *in vivo*, and further demonstrates the potency of a novel, TLR4 agonist for the first time *in vivo*, illustrating the importance of the application of structural design principles in the field of adjuvant biology.

6.2   Results

6.2.1   *In vivo* immunogenicity and challenge study design

The schematic for vaccination with monomeric 65kDa rPmpD passenger domain or *Ct* serovar E/Bour UVEBs and subsequent challenge with *Ct* serovar D/UW3/Cx is shown below (**Fig.6.5**). For assessment of vaccine-induced humoral and cell-mediated immunogenicity, mice from each group were sacrificed at day 56. For assessment of vaccine-induced protection, mice were administered a dose of DepoProvera (2.5mg/mouse) on day 56, and infected with *Ct* serovar D/UW3/Cx one week following final immunization. Bacterial shedding was monitored on days 1, 3, 7, 14

and 22 post challenge, and mice were sacrificed on day 104 of the study, 6 weeks post challenge.
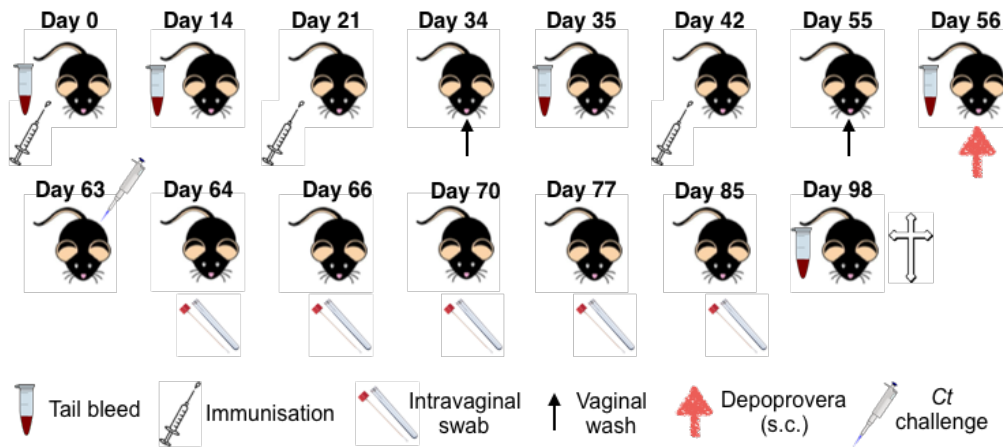
Figure 6.5: Schematic for immunogenicity and challenge studies *in vivo*. Immunogenicity studies were conducted until the day 56 time point, after which C57BL/6 or Balb/c mice were sacrificed and serum ELISAs and ELISpots conducted to determine humoral and cellular immune responses to each vaccine formulation. For challenge studies, C57BL/6 mice were given a subcutaneous administration of DepoProvera (2.5mg per mouse) on day 56 to synchronise oestrus cycles, and challenged with 4.5×10^8 IFU of *C.trachomatis* serovar D/UW3/ Cx. Swabbing of the vaginal vault was conducted on days 1, 3, 7, 14 and 22 post challenge for determination of chlamydial burden, and mice were sacrificed on day 98 of the study.

6.2.2 SLA in combination with rPmpD induces formulation-dependent antigen-specific Th1-type immune responses and significantly enhances systemic humoral antigen-specific titres in the C57BL/6 mouse strain

The magnitude and quality of systemic rPmpD-specific cellular immune responses elicited by each vaccine formulation were assessed in ELISpot assays to detect levels of IFNγ, IL-2, IL-5 and IL-10 cytokines following immunization (**Fig.6.6 (A-D)**). Very low levels of splenocytes secreting IL-5 and IL-10 were detected for all vaccine groups, and no significant difference in these populations relative to the control groups (PBS, SLA-LSQ or rPmpD only) was detected (**Fig.6.6 (C-D)**). In contrast,

mice immunized with rPmpD in combination with all SLA formulations showed significant increases in the populations of splenocytes secreting IFNγ and IL-2 relative to all control groups (p≤0.01), suggesting that this antigen-adjuvant combination elicits a robust Th1-biased immune response *in vivo* in C57BL/6 mice.

Interestingly, formulation-specific differences in the magnitude of the multifunctional T cell response were detected, with the SLA-SE formulation eliciting the most robust IFNγ response to rPmpD (>500 cells / 250,000) relative to the aqueous or liposomal formulations (SLA-AF and SLA-LSQ) (**Fig.6.6 (A)**). No significant difference between the IFNγ-secreting populations in SLA-AF-immunized (76 ± 38 cells / 250,000) or SLA-LSQ-immunized mice (145 ± 81/ 250,000) was detected (p=0.1739). IL-2-secreting splenocyte populations in vaccinated mice were found to largely mirror the anti-rPmpD IFNγ response (**Fig.6.6 (B)**).
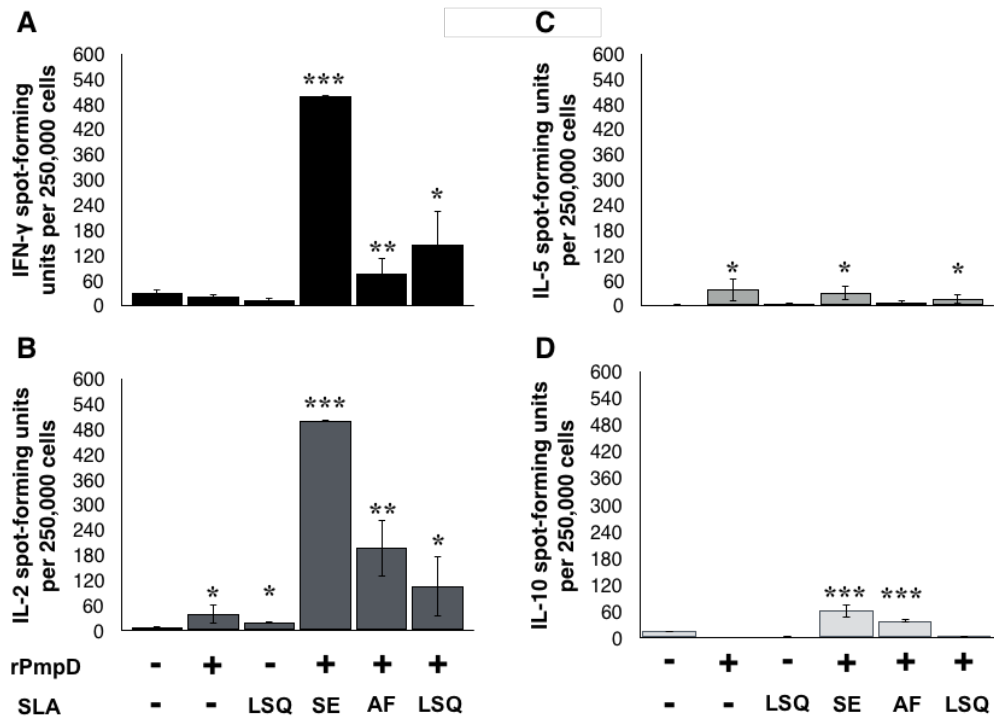
Figure 6.6: rPmpD in combination with SLA elicits a Th1-biased cellular immune response in vivo. Female C57BL/6 mice were immunized as described in the Materials and Methods, and splenocytes assessed for (**A**) IFN, (**B**) IL-2, (**C**) IL-5 and (**D**) IL-10 secretion after in vitro stimulation with rPmpD in an ELISpot assay. Data are from one experiment (n=5 animals per group). The mean $\pm$ the standard deviation is shown for each group (* = $p \leq 0.05$, ** $p \leq 0.01$, ***$p \leq 0.001$ relative to vehicle-immunized mice).

rPmpD-specific serum antibody responses were measured two weeks following the second (d35) and final (d56) boosts (**Fig.6.5**). The reciprocal titres at 50% maximal binding of anti-rPmpD IgG1 and IgG2c were measured (**Fig.6.7 (A-B)**). No detectable antigen-specific IgG was found in PBS- or SLA-LSQ only-immunized mice. All rPmpD-SLA formulations significantly boost systemic humoral anti-rPmpD IgG titres following successive boosts (d35 to d56), and no detectable differences in total IgG, IgG1 or IgG2c titres were observed at any time point between the three SLA formulations (p>0.05), despite formulation-dependent differences in the magnitudes of splenic Th1-biased cellular immune responses. Furthermore, no

increase in the ratio of systemic IgG2c:IgG1 titres (a surrogate measure for Th1 bias) was observed for any adjuvanted vaccine group, despite the significantly biased Th1-type cellular immune response elicited by the SLA-rPmpD combination (**Fig.6.6**).
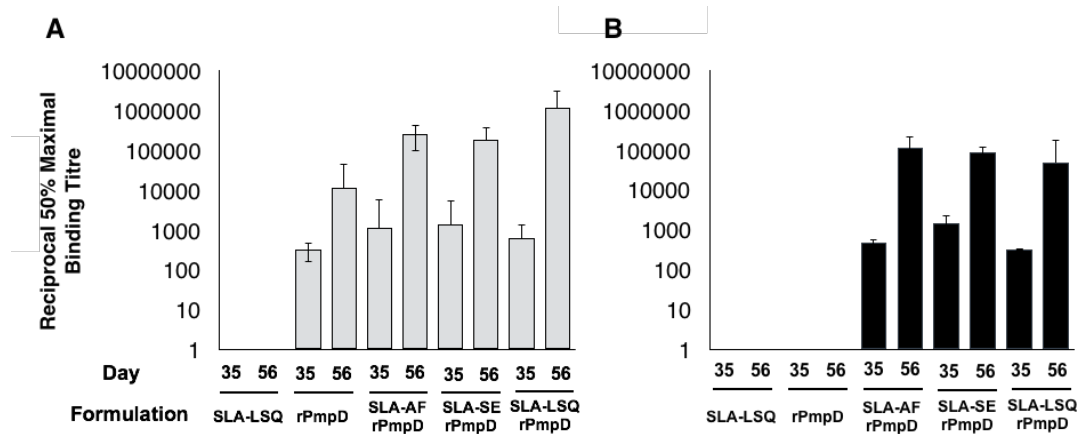
Figure 6.7: rPmpD in combination with all formulations of SLA boosts systemic antigen-specific IgG titres *in vivo* in the C57BL/6 strain. C57BL/6 mice immunised with all rPmpD-SLA formulations show an increase in anti rPmpD serum IgG1 and IgG2c titres following successive boosts (d35-d56). rPmpD administered without adjuvant also elicits robust rPmpD-specific IgG1 titres, however, no detectable anti-rPmpD IgG2c is detected in this group, suggesting SLA-mediated induction of Th1-bias, consistent with cytokine data (**Fig.6.6**). Quantitative data are derived from 1 experiment (n=4 animals per group).

Interestingly, rPmpD administered in the absence of SLA elicited strong systemic humoral immune responses, and showed detectable systemic immunoglobulin of the IgG1 but not IgG2c subclass. Only rPmpD in combination with SLA-AF elicited significantly greater total IgG and IgG1 ($p \leq 0.001$ and $p=0.012$, respectively) than rPmpD administered alone, and no detectable differences were observed in total systemic IgG or IgG1 titres between rPmpD alone and rPmpD in combination with SLA-SE ($p=0.0658$ and $p=0.1039$ respectively) and SLA-LSQ formulations ($p=0.267$ and $p=0.2495$ respectively). These data suggest that at concentrations used in this study (5μg/dose), rPmpD is sufficiently immunogenic in the absence of SLA to elicit robust titres of systemic antigen-specific IgG that may parallel that of certain adjuvanted rPmpD vaccine formulations. However, the presence of robust levels of

systemic IgG2c in adjuvanted rPmpD combinations, but not in mice receiving rPmpD alone is further evidence that SLA induces a Th1-type immune response.

6.2.3 SLA in combination with rPmpD enhances local cervico-vaginal mucosal IgG titres in a formulation-dependent manner in the C57BL/6 mouse strain

Cervico-vaginal washes were obtained at d34 and d55 of the study (**Fig.6.5**). The reciprocal titres at 50% maximal binding of anti-rPmpD IgG1 and IgG2c were measured (**Fig.6.8**). Detectable cervico-vaginal anti-rPmpD IgG, IgG1 and IgG2c were observed in all groups of C57BL/6 mice immunized with SLA formulations in combination with rPmpD. In contrast, no detectable levels of total IgG or IgG2c were observed in mice immunized with rPmpD alone in cervico-vaginal lavage, and only one mouse in this group had detectable antigen-specific IgG1. While SLA-AF and SLA-LSQ formulations do not boost anti-rPmpD cervico-vaginal anti-rPmpD IgG titres following successive immunizations, the SLA-SE formulation significantly augments cervico-vaginal IgG1 titres between the penultimate and final boosts (d34 to d55).

Interestingly, despite no significant formulation-dependent differences in systemic anti-rPmpD IgG titres between the vaccine groups, the SLA-SE formulation results in significantly elevated total anti-rPmpD IgG titres within the vaginal vault following the final boost (d55) relative to the control group (no detectable cervico-vaginal IgG), as well as SLA-AF (p=0.0425) and SLA-LSQ formulations (p=0.0386). No significant difference was observed in mucosal anti-rPmpD titres between SLA-AF and SLA-LSQ formulations combined with rPmpD (p=0.8721). As expected, no anti-rPmpD titres were detected in PBS- or SLA-only-immunized control groups.
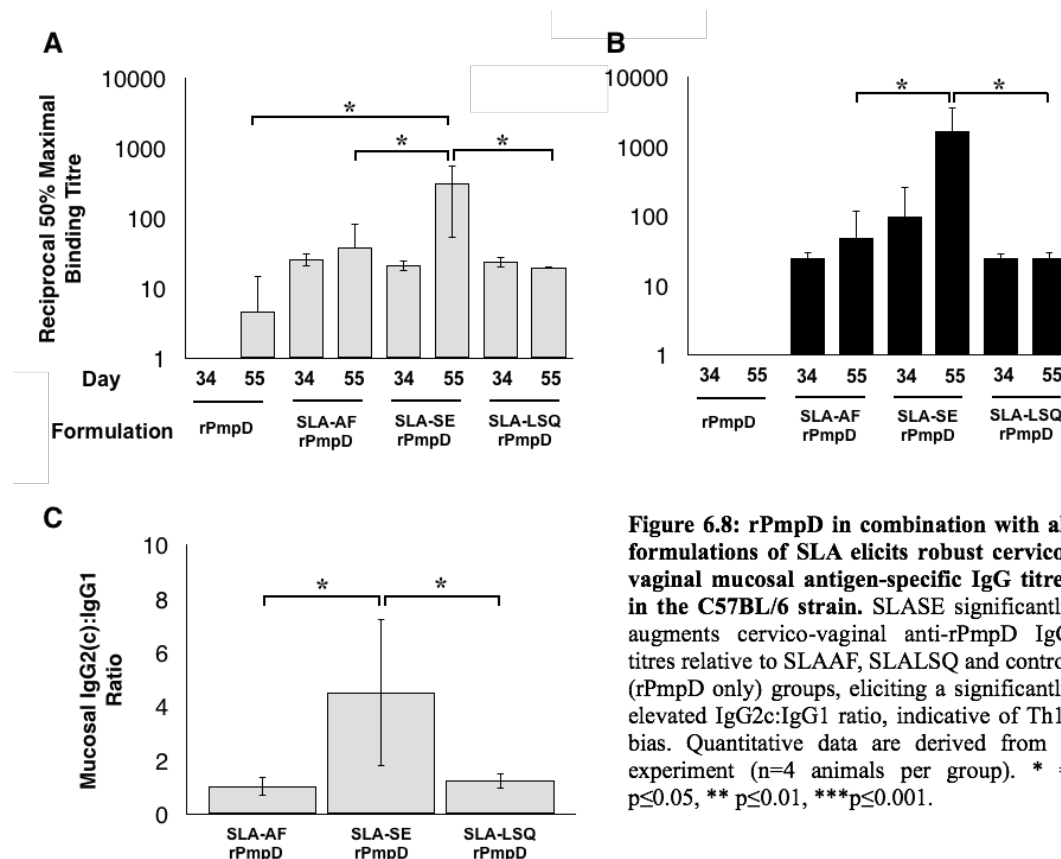
Figure 6.8: rPmpD in combination with all formulations of SLA elicits robust cervico-vaginal mucosal antigen-specific IgG titres in the C57BL/6 strain. SLASE significantly augments cervico-vaginal anti-rPmpD IgG titres relative to SLAAF, SLALSQ and control (rPmpD only) groups, eliciting a significantly elevated IgG2c:IgG1 ratio, indicative of Th1-bias. Quantitative data are derived from 1 experiment (n=4 animals per group). * = p≤0.05, ** p≤0.01, ***p≤0.001.

The anti-rPmpD IgG2c:IgG1 ratio within the vaginal vault was measured in cervico-vaginal lavage fluids on d55 following the final boost (**Fig.6.8 (C)**). This ratio was found to be significantly elevated in mice immunized with rPmpD in combination with the SLA-SE formulation (4.5 ± 2.7) relative to both SLA-AF (1.04 ± 0.34, p=0.0217) and SLA-LSQ (1.25 ± 0.28, p=0.0281) formulations. Often conventionally measured as a loose surrogate of Th1-type immunity, this observation may be indicative of a localized Th1-type immune response within the mucosal tissue elicited by the SLA-SE formulation. Although further work is required to confirm the trafficking of antigen-specific T cells to the reproductive mucosa, this observation may imply that adjuvant formulation may influence the recruitment of CD4^{+} T cells to the reproductive tract.

6.2.4 Reactivity of anti-rPmpD and anti-UVEB serum in Western Blot and ELISA

Mucosal washes obtained two weeks following the final boost from mice immunized with rPmpD in combination with SLA, were tested for reactivity against UVEBs in indirect ELISAs. Anti-rPmpD IgG from all rPmpD-adjuvant groups reacted with *Ct* serovar D/UW3/Cx UVEBs in ELISAs (**Fig.6.9 (C)**), suggesting recognition of native PmpD protein on *Ct* EB membranes, although it is possible immune recognition of similar motifs on other Pmps or COMC proteins may be elicited through adjuvant-induced antibody-response broadening, and further work is required to deduce whether cross-reactivity is detected against an array of chlamydial Pmps. Western Blots were conducted using heat-inactivated serum from PBS-, rPmpD- and UVEB-immunized mice following the final boost at day 56 (**Fig.6.9 (A-B)**). Anti-rPmpD serum recognizes rPmpD and associated proteolytic fragments, but fails to recognize antigens in UVEB lysates. Anti-UVEB serum does not recognize rPmpD protein, but shows predominant recognition of a 37kDa protein in UVEB lysates. Mass spectrometry of the 37kDa band confirmed this protein to be chlamydial MOMP. Immunodominance of MOMP in UVEB-immunized mice may preclude high-titre antibody responses to other antigens including PmpD, although the relatively low abundance of PmpD in the chlamydial outer membrane or specific conformational epitope recognition may also preclude recognition by anti-rPmpD serum in Western blots.
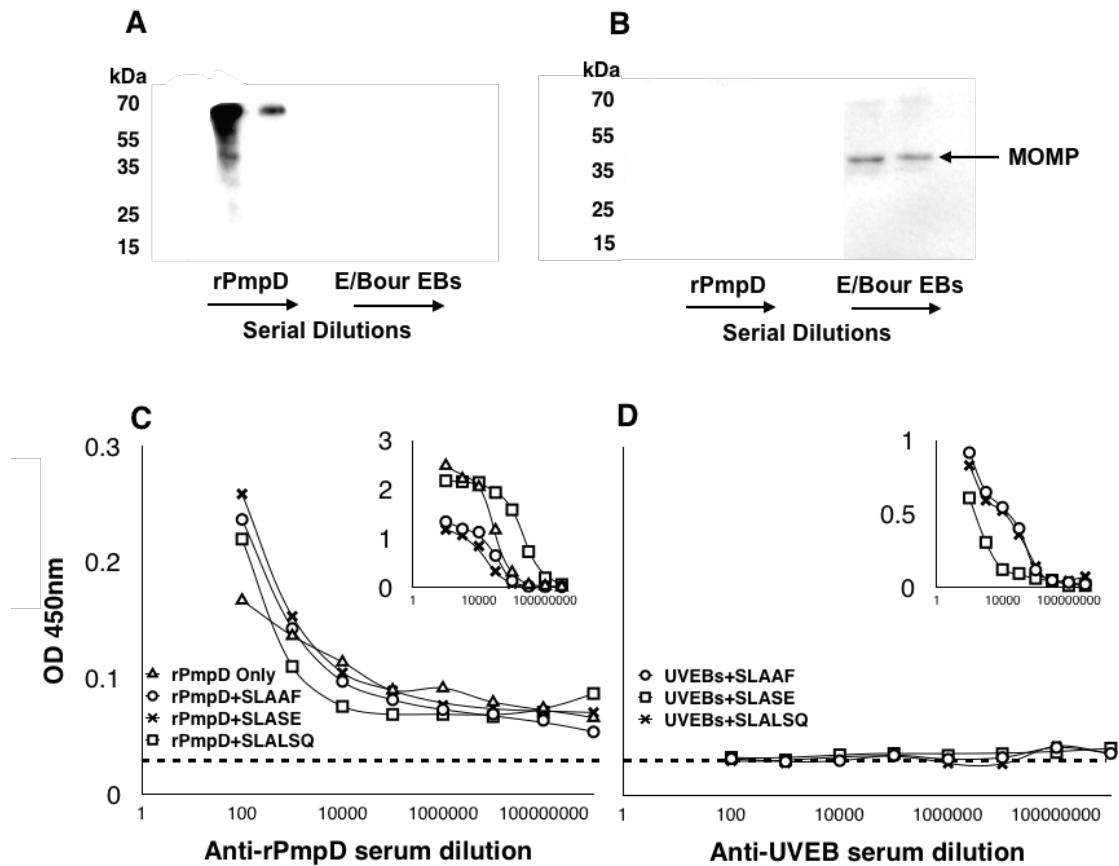
Figure 6.9: Reactivity of anti-rPmpD and anti-UVEB serum. Serum from mice immunized with rPmpD (**A**) or UVEBs (**B**) was tested for reactivity against UVEBs and rPmpD antigen in western blots. (**C**) Anti-rPmpD serum reacts with UVEBs in an indirect ELISA (inset shows reactivity against rPmpD). (**D**) Anti-UVEB serum failed to react with rPmpD (inset shows reactivity against UVEBs). Dotted lines represent the OD_{450} cut-off value equivalent to the mean plus two standard deviations of control pre-immune serum.

6.2.5 Vaccination with rPmpD or UV-inactivated EBs in combination with SLA significantly enhances resistance to *Ct* infection and reduces mean bacterial load independent of SLA formulation

Cervico-vaginal swabs were obtained from all 11 groups of immunized and control mice on days 1, 3, 7, 14 and 22 following intra-vaginal inoculation (day 0) of *Ct* serovar D/UW3/Cx (4.5×10^8 IFU per mouse). Intensity and duration of primary lower genital tract infection is shown for each group, with data points representing the mean ± standard deviations of the mean of each group of 5 mice (**Fig.6.11 (A-F)**). The

number of inclusions were visualized and enumerated on Hak cell monolayers using immunofluorescence (**Fig.6.10**).
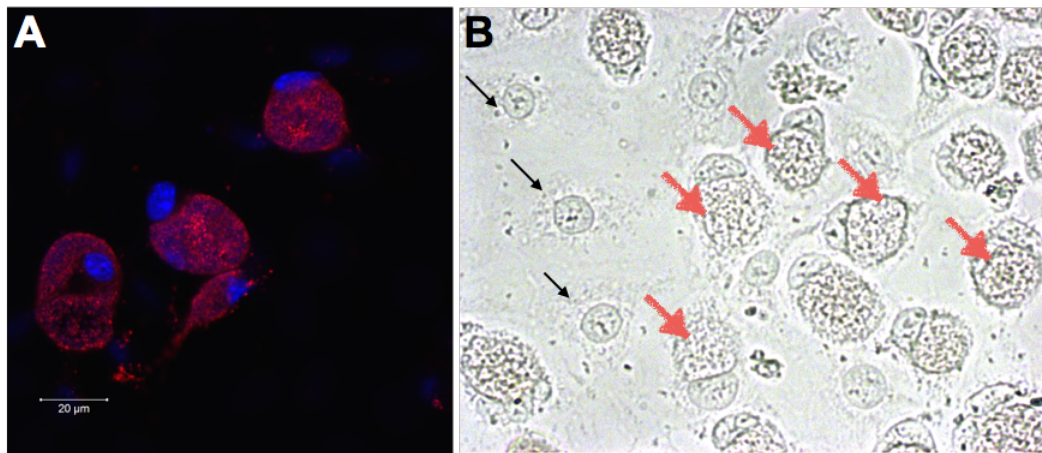
Figure 6.10: Confocal and phase contrast microscopy images showing chlamydial inclusions following infection of Hak cell monolayers. (**A**) Recoverable chlamydial inclusion forming units were enumerated following swabbing of C57BL/6 mice using immunofluorescence. Hak cell monolayers were infected with serial dilutions of swab samples in 96-well plates, cultured for 48hrs, fixed in methanol and stained as described in the Materials and Methods. Chlamydial EB and RB forms (red) and host cell nuclei (blue) can be visualised. Four infected Hak cells (inclusions) are shown in panel A. (**B**) Phase contrast microscopy of Hak cell monolayers infected with *Ct* serovar D/UW3/Cx. At 48-72hrs post infection, chlamydial RBs replicate through binary fission and occupy the entirety of the host cell cytosol. These are visualised as grainy spherical structures (red arrows) adjacent to compacted host cell nuclei. Uninfected cells are shown for comparison (black arrows).
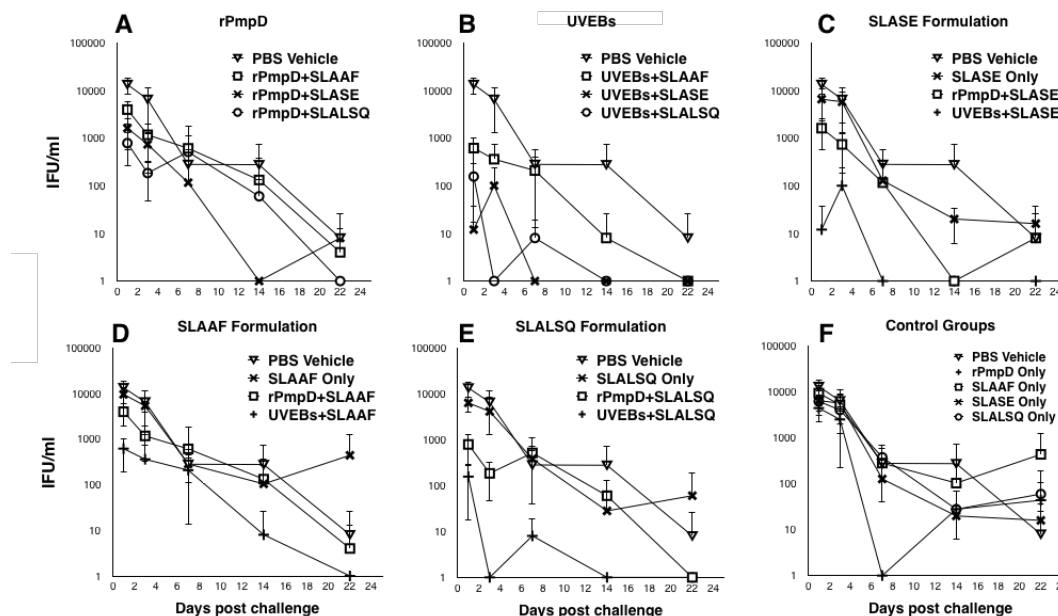
Figure 6.11: Monitoring of bacterial shedding following immunization in C57BL/6 mice. C57BL/6 mice were immunized and challenged intra-vaginally with 4.5×10^8 IFU *Ct* serovar D/UW3/Cx. Swabbing of the vaginal vault was performed on days 1, 3, 7, 14 and 22 (post challenge). Comparisons of bacterial clearance are made between the PBS control group and: (i) SLA formulations for a given antigen (**A** and **B**) (ii) rPmpD and UVEB antigens for a given SLA formulation (**C, D** and **E**) (iii) Control groups (**F**). Quantitative data are derived from 1 experiment (n=5 animals per group). The mean $\pm$ the standard deviation is shown for each group.

For quantification of resistance to infection, recoverable IFU at the day 1 time point were compared across each group using a one-way ANOVA (**Fig.6.12 (A)**). This is in contrast to an array of studies that typically use day 3 as the first sampling point in monitoring bacterial clearance. Thus, the number of organisms that are actually recoverable or able to establish infection following early vaccine-mediated protection is often unknown in the majority of preclinical studies. No significant differences were observed in recoverable IFU between PBS-immunized mice and the adjuvant only groups (SLA-AF only, SLA-SE only, SLA-LSQ only). All antigen-adjuvant combinations elicited enhanced resistance to infection relative to PBS-immunized mice, evidenced by significantly reduced recoverable IFU/ml relative to the control groups ($p \leq 0.01$). There were no detectable differences in the recoverable IFU obtained from rPmpD- and UVEB-immunized mice for a given adjuvant formulation, nor any formulation-specific differences in resistance to infection for a given antigen (**Fig.6.12 (A)**).

At this early time point during infection (day 1), these observations suggest pathogen-specific antibody-mediated neutralization of *Ct* infection within the vaginal mucosa in immunized mice, as fewer bacteria are able to establish infection when cultured *in vitro*, although other mechanisms of innate immune activation within the reproductive tract cannot be ruled out. Furthermore, antigen-specific T cells are usually found to occupy the site of infection 3-5 days following challenge (Roan et al., 2006). Interestingly, mice immunized with rPmpD alone also show significant resistance to infection relative to control mice ($p=0.026$).
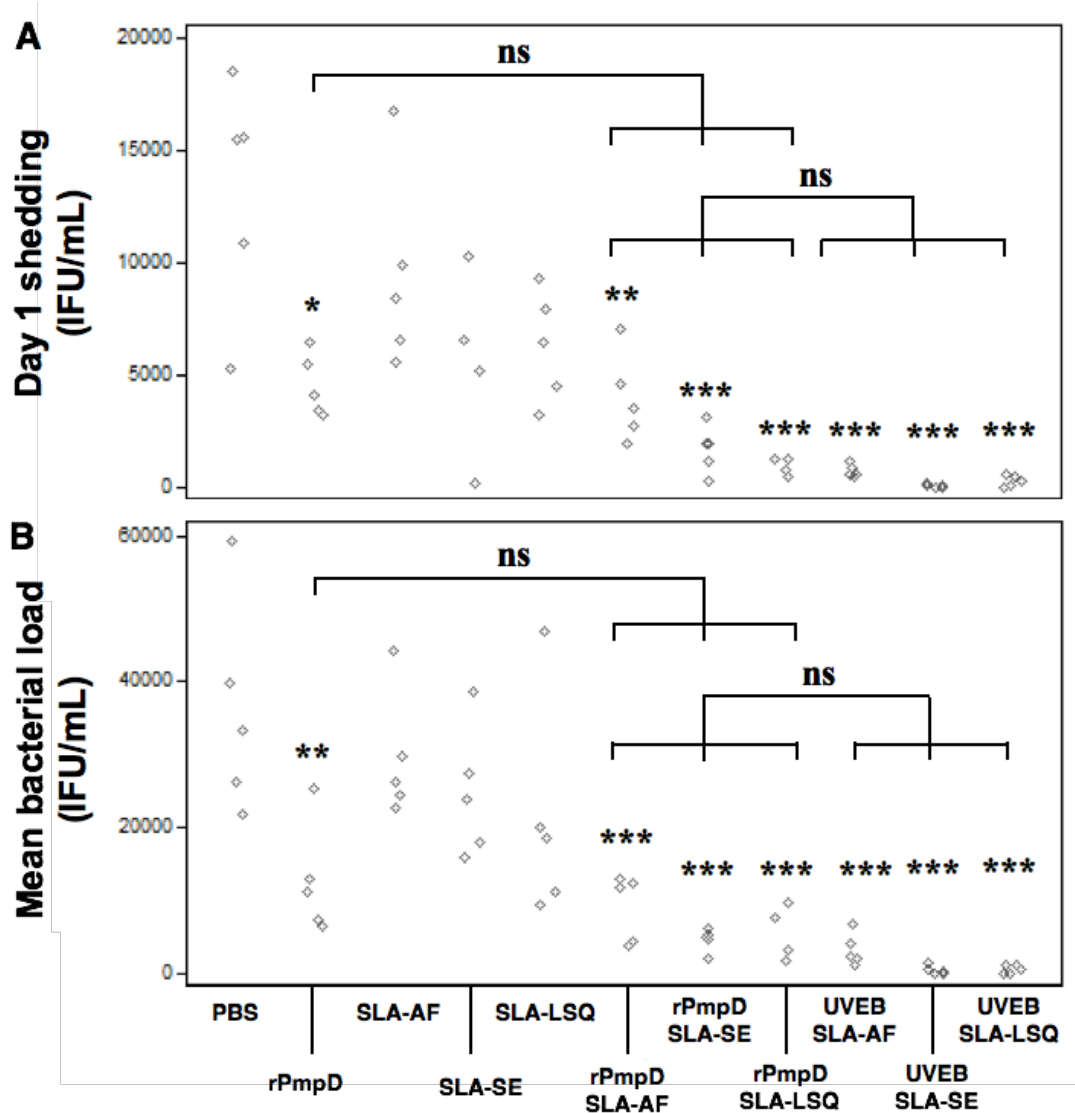
Figure 6.12: Vaccine-induced protection against *Ct* serovar D/UW3/Cx infection. C57BL/6 mice were immunized with either rPmpD or UVEBs in combination with all SLA formulations, challenged with 4.5×10^8 IFU of *Ct* serovar D/UW3/Cx EBs and swabbed on day 1 following infection to determine the recoverable IFU (**A**). Bacterial shedding was monitored on days 1, 3, 7, 14 and 22 post challenge. Mean bacterial load was quantified for individual mice in each group using an area under the curve (AUC) method (**B**). Data are shown for individual mice derived from one experiment (n=5 animals per group), and were analysed using a one-way analysis of variance (ANOVA). Significance values depicted are relative to PBS-immunized mice (* = p≤0.05, ** p≤0.01, ***p≤0.001) or between immunized groups (bars; ns=not significant).

rPmpD administered with or without adjuvant is able to elicit high-titre systemic anti-

rPmpD antibodies (**Fig.6.7 (A)**). It has previously been shown that IgG in the vaginal

194

vault originates from serum, likely through transudation mechanisms, and that protection against sexually transmitted pathogens such as SIV and HIV may be conferred through systemic administration of antibodies in passive protection experiments (Mascola et al., 2000; Mestecky, Moldoveanu and Russell, 2005). Thus, it is likely that circulating anti-rPmpD or anti-EB antibodies elicited by vaccination may mediate the observed neutralizing effects *in vivo*.

Mean bacterial load was quantified for each mouse in the 11 vaccine groups using an area under the curve (AUC) method (**Fig.6.12 (B)**). All groups immunized with either rPmpD or UVEBs showed a significant reduction ($p \leq 0.01$ or $p \leq 0.001$) in recoverable IFU over the course of infection relative to the PBS-immunized or SLA-immunized control groups. No significant differences were observed in mean recoverable bacterial load between PBS-immunized mice and the adjuvant only groups (SLA-AF only, SLA-SE only, SLA-LSQ only), suggesting non-specific innate immune activation by the TLR4 agonist does not play a role in resistance to or eradication of infection. For a given SLA formulation, no significant difference in mean bacterial load was detected irrespective of antigen (rPmpD or UVEBs), nor was any statistically significant difference in bacterial burden observed between groups immunized with any of the three SLA formulations in combination with a given antigen.

6.2.6   Humoral and cell-mediated immune responses following challenge of vaccinated mice

Spleens from immunized mice were obtained 42 days post challenge and stimulated with rPmpD antigen. Mice immunized with rPmpD + SLA-SE showed a very

significant Th1-biased immune profile, evidenced by a substantially higher population of splenocytes secreting IFNγ compared to all other vaccine groups (p≤0.01) (**Fig.6.13**).

Figure 6.13: Splenic T-cell response following challenge of immunized C57BL/6 mice. Spleens from vaccinated mice were obtained 42 days post challenge and stimulated with rPmpD antigen. Quantitative data are derived from 1 experiment (n=5 per group). The mean ± the standard deviation is shown for each group. * = p≤0.05, ** p≤0.01, ***p≤0.001.
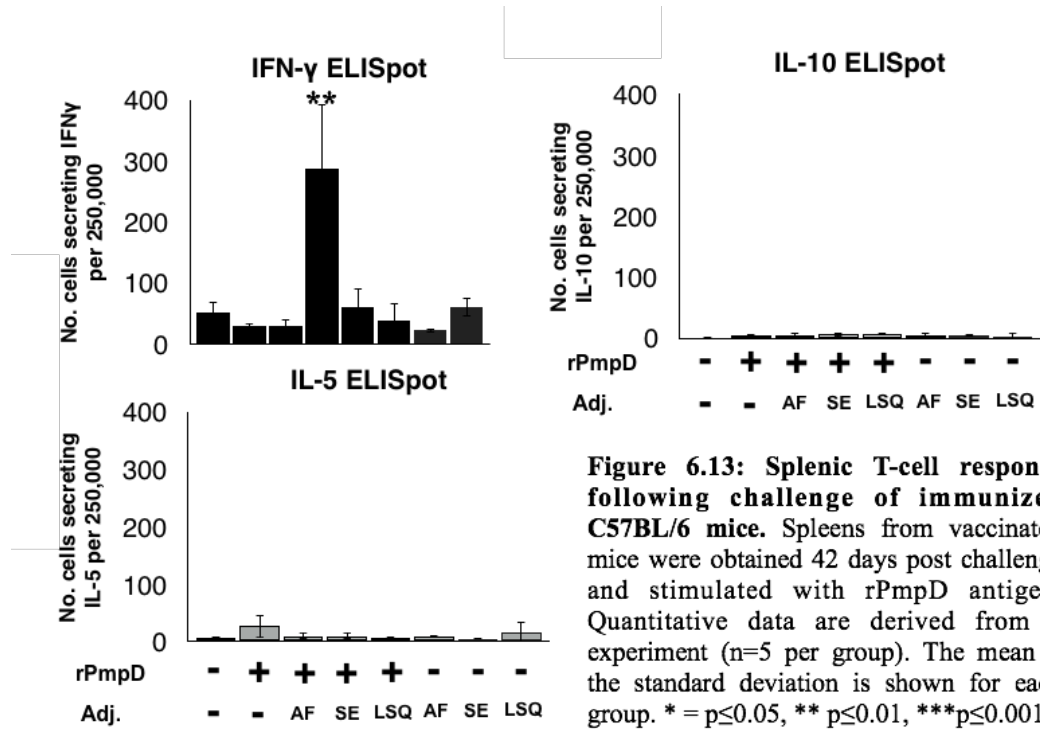
No significant difference in the IFNγ response in rPmpD + SLA-AF or rPmpD + SLA-LSQ groups was detected relative to control groups. Very low levels of IL-5 and IL-10 secreting cells were detected, and were similar to those observed prior to challenge. The observed T cell responses following challenge are likely composed of a proliferative memory recall response from circulating rPmpD-specific T cells, as well as an antigen-specific systemic T cell response elicited by *Ct* infection. Furthermore, at this time point following challenge, as the infection resolves, the population of circulating effector T cells is likely to wane. Thus, based on these observations, one cannot directly draw conclusions on SLA formulation-specific differences in the magnitudes of the antigen-specific memory T cell response, although it is likely that immunization with the SLA-SE oil-in-water formulation

results in a significantly more robust antigen-specific T cell memory response than the SLA-AF or SLA-LSQ formulations. In addition, serum from C57BL/6 mice in all vaccine groups was obtained 42 days post challenge. Mice immunized with SLA-SE in combination with rPmpD showed significant enhancement of systemic rPmpD-specific IgG1 and IgG2c titres following intra-vaginal challenge with *Ct* serovar D/UW3/Cx at this time point relative to all other groups (p≤0.05) (**Fig.6.14**).
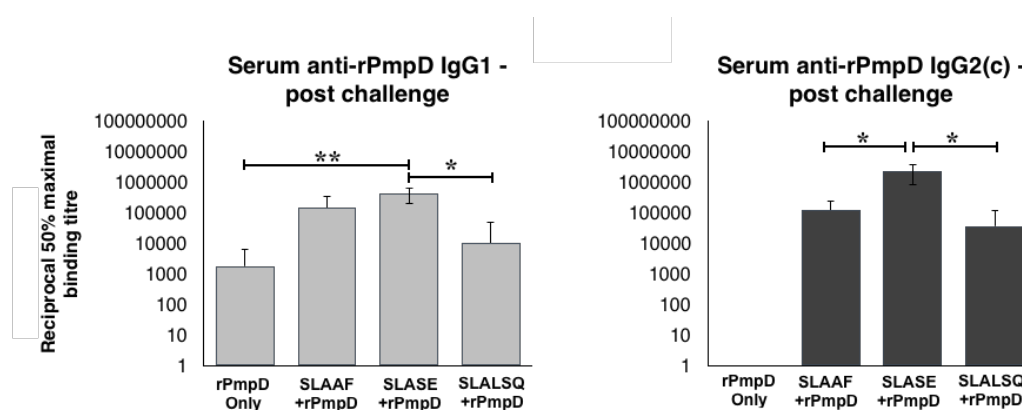
Figure 6.14: Systemic humoral immune response following challenge of immunized C57BL/6 mice. Groups of mice immunised with the respective rPmpD-SLA combinations show elevated anti-rPmpD serum titres 42 days post challenge. No detectable IgG2(c) is found for rPmpD-only immunised mice, suggesting the long-term induction of Th1-type immunity elicited by SLA, and further consistent with the cytokine data obtained at the same time point (**Fig.6.13**). Quantitative data are derived from 1 experiment (n=5 per group). The mean ± the standard deviation is shown for each group. * = p≤0.05, ** p≤0.01, ***p≤0.001.

6.2.7 SLA in combination with rPmpD induces formulation- and strain-dependent differences in the magnitude of the Th1-type immune response in different mouse strains

It has previously been shown that differences in cytokine profiles in response to chlamydial infection depend on the murine strain employed in the study, and this may also determine outcomes of pathogenesis *in vivo* in different mouse strains (Darville et al., 2001a; Darville et al., 2001b; Yang, HayGlass and Brunham, 1996). Thus, a comparison of the effects of different formulations of rPmpD combined with SLA-SE and SLA-AF was conducted to investigate potential formulation- and strain-specific

differences in immunogenicity in Balb/c mice. Splenocytes were stimulated *ex vivo* with rPmpD antigen as previously described. In the Balb/c strain, all adjuvants elicited enhanced antigen-specific Th1-type immune responses, evidenced by enhanced populations of splenocytes secreting the cytokines IFNγ and IL-2. As in the C57BL/6 strain, levels of IL-5 and IL-10 remained very low, and not significantly different from control (PBS-immunized) mice (**Fig.6.15**).
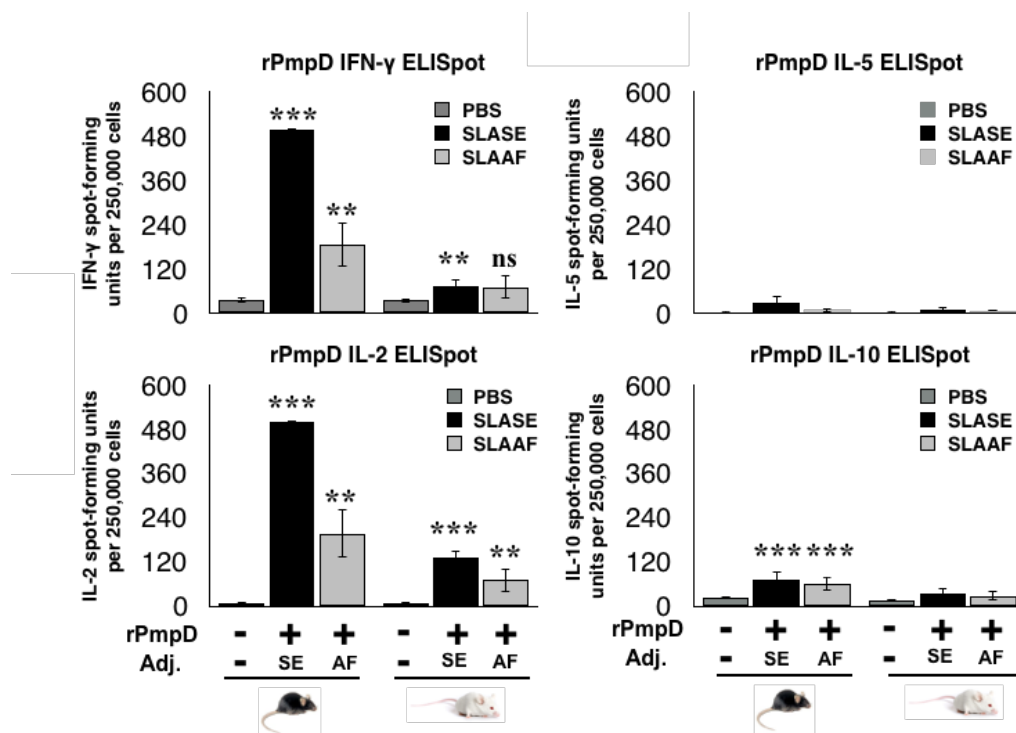
Figure 6.15: Strain-specific differences in cytokine profiles following immunization with rPmpD-SLA formulations *in vivo* in C57BL/6 and Balb/c strains. Mouse spleens were harvested 56 days following initial immunization and stimulated in the presence of rPmpD antigen. SLASE is a more potent Th1-biasing adjuvant than SLAAF in the C57BL/6 mouse strain, but not in the Balb/c strain, where no significant difference in the magnitude of IFNγ-secreting splenocyte populations are observed between the two adjuvant groups. Quantitative data are derived from 1 experiment (n=5 animals per group). * = p≤0.05, ** p≤0.01, ***p≤0.001 (relative to PBS-immunized mice).

Interestingly, it was found that in the Balb/c strain, the population of IFNγ-secreting splenocytes was significantly lower in mice immunized with rPmpD in combination with SLA-SE (p≤0.001) than in the corresponding group in the C57BL/6 murine

strain. However, no significance difference in the numbers of IFNγ-secreting splenocytes between mouse strains was observed when recombinant PmpD was paired with SLA-AF (**Fig.6.15**). Importantly, these observations suggest, that in addition to genetically predetermined strain-specific differences in cytokine profiles (Yang, HayGlass and Brunham, 1996), adjuvant formulation may also play a crucial role in the magnitude and quality of the cellular immune response in specific mouse strains. Interestingly, no strain- or formulation-specific differences in the magnitude of the systemic humoral immune response were observed following immunization (**Fig.6.7, Fig.6.16**).
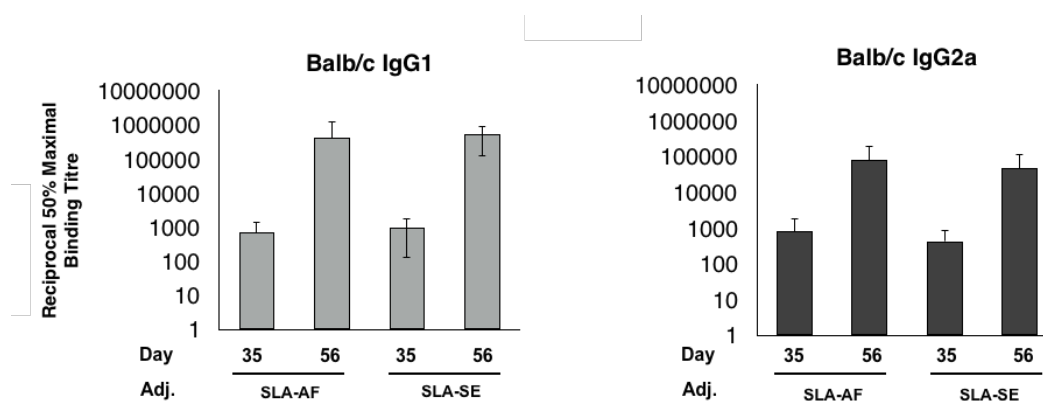
Figure 6.16: rPmpD in combination with all formulations of SLA significantly boosts systemic antigen-specific IgG titres *in vivo* in the Balb/c strain. Balb/c mice immunized with all SLA formulations in combination with rPmpD show significant enhancement of anti-rPmpD serum IgG1 and IgG2c titres following successive boosts (d35-d56). However, no significant differences in titres are observed at either d35 or d56 time points between each adjuvant formulation. Quantitative data are derived from 1 experiment (n=4 animals per group) and were analysed using an unpaired t-test. The mean ± the standard deviation is shown for each group.

6.2.8 Determination of kinetics of *Ct* serovar D/UW3/Cx bacterial shedding in the C57BL/6 and Balb/c mouse strains

To determine strain-specific differences in the kinetics of bacterial shedding, bacterial load was monitored on days 3, 7 and 10 following intra-vaginal chlamydial infection of C57BL/6 and Balb/c mice (**Fig.6.17**). Mice were challenged with 4×10^5 IFU of *Ct*

serovar D/UW3/Cx inoculated directly into the vaginal vault. No significant difference in bacterial load (quantified as recoverable IFU/ml) was recorded between each strain at any recorded time point. This is in accordance with previously observed kinetics of shedding between Balb/c and C57BL/6 strains (Darville et al., 2001b). Thus, the window for monitoring of vaccine efficacy through measuring bacterial shedding is similar between the two mouse strains.
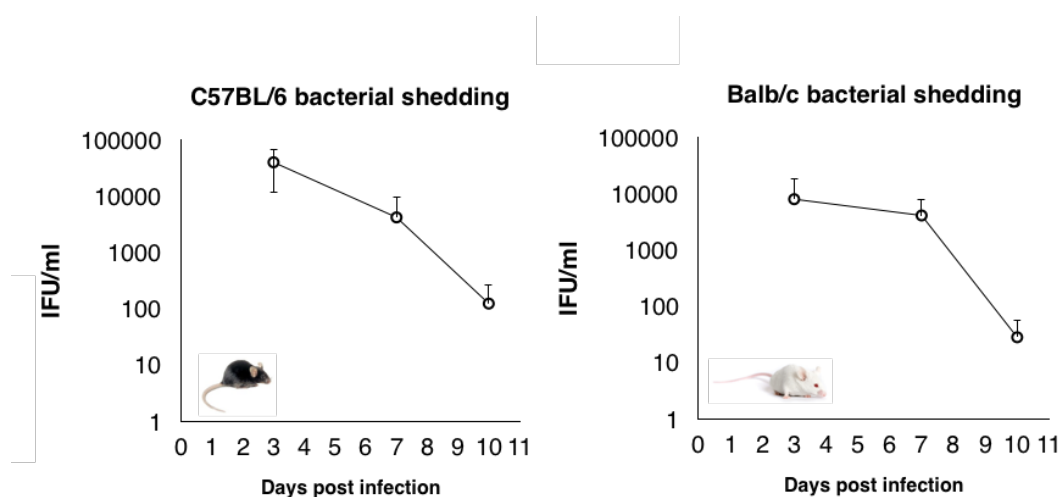
Figure 6.17: Bacterial shedding kinetics in C57BL/6 and Balb/c mouse strains. Naïve C57BL/6 and Balb/c mouse strains were challenged to determine strain-specific differences in shedding of *Ct* serovar D/UW3/Cx, and differences in the clearance window for monitoring vaccine efficacy. Swabbing of the vaginal vault was performed on days 3, 7 and 10 post challenge, and titred on Hak cell monolayers. No significant differences in bacterial load were detected between the two mouse strains. Quantitative data are derived from 1 experiment (n=5 animals per group). The mean ± the standard deviation is shown for each group.

6.3   Discussion

Our study is the first to investigate the efficacy of the recombinant chlamydial vaccine antigen PmpD, in addition to investigation of the potency and efficacy of a novel, rationally designed TLR4 agonist. PmpD was selected due to its highly conserved sequence (>99%) across all *Ct* strains (Swanson et al., 2009), constitutive expression throughout chlamydial biphasic development (Tan et al., 2010), surface exposure and proposed function as a putative chlamydial adhesin (Becker and Hegemann, 2014). In addition, we demonstrate that this antigen elicits significantly elevated Th1-biased immune responses in C57BL/6 and Balb/c strains when delivered subcutaneously

(s.c.) in combination with a novel, rationally designed TLR4 agonist (SLA), suggestive of a wide array of T cell epitopes and MHC class II presentation. Importantly, we also demonstrate significant protection against *Ct* serovar D/UW3/Cx challenge when rPmpD is administered in the absence of adjuvant, evidenced by enhanced resistance to infection and reduction in mean bacterial load in rPmpD-immunized mice relative to PBS- and SLA-only vaccinated control groups.

All SLA-rPmpD formulations elicit a Th1-biased cellular immune response, evidenced by very low IL-5 and IL-10 cytokine-secreting cells, and high levels of antigen-specific splenocytes secreting IFNγ and IL-2 (**Fig.6.6**). No significant SLA formulation-specific differences in the magnitude of rPmpD-specific IFNγ responses were found in the Balb/c strain. Interestingly, in the C57BL/6 mouse strain, significant formulation-specific differences in the magnitudes of Th1-bias are observed, with the stable oil-in-water emulsion (SLA-SE) formulation eliciting a significantly greater population of IFNγ-secreting rPmpD-specific splenocytes relative to the aqueous (SLA-AF) and QS21-liposomal (SLA-LSQ) formulations (p<0.001), indicative of likely differences in two mouse strains with different MHC haplotypes and antigen presentation, as well as differing sensitivities to antigen formulation and innate immune responses.

However, no correlation was observed between the relative magnitudes of the rPmpD-specific T cell responses elicited by the three formulations and protection against urogenital *Ct* challenge (**Fig.6.12**). Such observations are not uncommon, and the lack of correlation between distinct immunological phenotypes and protection has previously been documented for studies investigating vaccine development against

tuberculosis (TB) with a variety of antigen-adjuvant combinations. No distinct physico-chemical characteristics have been shown to be consistently reflective of the magnitude or efficacy of cell-mediated immune responses or bacterial clearance, and subtle differences in the type of oil in adjuvant formulations can affect the quality of the immune response (Fox et al., 2011), (Orr et al., 2013b).

Furthermore, the species used can significantly influence the observed potency of the adjuvant. (Vordermeier et al., 2009) employed the use of TB antigen Rv3019c in combination with either a oil-in-water emulsion or cationic liposome adjuvant, and demonstrate the generation of two distinct immunological phenotypes in cattle but not in mice. The oil-in-water emulsion elicited both an effector and a central memory T cell response, while the cationic liposomal formulation induced only the central memory response. Similar to *Ct* infections, the optimal immune correlates of protection against TB infections in humans are largely unknown. Indeed, although robust IFNγ responses have been postulated as essential for resolution of infection, it has been observed that transient total or T cell subset immune responses are not predictive of vaccine efficacy *in vivo* (Mittrucker et al., 2007). This suggests that memory rather than transient effector T cell responses may be more representative immune correlates of vaccine efficacy and protection. Thus, cultured rather than transient *ex vivo* ELISpots may be a more robust immunological assay for investigating correlates of protective immunity, as they provide a more definitive reflection of central memory responses. Interestingly, the development of malarial vaccines has provided further evidence of this (Keating et al., 2005; Reece et al., 2004).

Although formulation-specific differences in memory responses were not studied independent of *Ct* challenge in our study, it is likely that the magnitude of the rPmpD-specific IFNγ recall response to *Ct* infection (measured 6 weeks post-challenge) (**Fig.6.13**), represents a waning systemic population of a pool of activated circulating memory cells elicited by initial immunization, in addition to systemic pathogen-specific effector T cells following infection. Interestingly, we do observe significant formulation-specific differences in the recall response, with SLA-SE eliciting significantly higher levels of IFNγ-secreting antigen-specific splenocytes (p<0.001) in comparison to aqueous (SLA-AF) and liposomal (SLA-LSQ) formulations (**Fig.6.13**).

The robust effector and memory responses elicited by SLA-SE thus showcases the relative potency and durability of oil-in-water emulsions, corroborated by the findings of (Vordermeier et al., 2009) in a preclinical TB vaccine study in cattle. Furthermore, we detect significantly elevated mucosal cervico-vaginal anti-rPmpD titres following immunization with the SLA-SE adjuvant relative to both SLA-LSQ and SLA-AF adjuvants (p<0.05) (**Fig.6.8 (A,B)**). In contrast to systemic humoral responses, where similar titres of IgG1 and IgG2c subtypes were measured (**Fig.6.7**), we observe a significantly elevated (P<0.05) mucosal IgG2c:IgG1 ratio (4.5 ± 2.7) in mice immunized with rPmpD in combination with the SLA-SE adjuvant, relative to the SLA-AF (1.04 ± 0.3) or SLA-LSQ-immunized groups (1.25 ± 0.3) (**Fig.6.8 (C)**). This may be indicative of a locally induced Th1-type cellular immune response, although interestingly, this did not correlate with enhanced protection against *Ct* challenge relative to the other vaccine groups. These observations may suggest enhanced mucosal recruitment of systemic Th1-type memory effector cells, although further experimentation is required to establish this. Because *Ct* is an obligate intracellular

mucosatropic pathogen, it is widely anticipated that robust pathogen-specific cellular reproductive tract immune responses are required for optimal vaccine efficacy. This is elegantly described in perhaps the most informative and seminal experiments detailing the effector mechanisms of mucosal immunity in chlamydial vaccinology.

Importantly, the study by (Stary et al., 2015) elucidates the generation and contribution of uterine-resident *Ct*-specific memory T cells to protection against chlamydial infection. The vaccine employs intact UVEBs complemented with charge-switching synthetic adjuvant nanoparticles (cSAPs). Important advances that have facilitated the dissection of pathogen-specific T cells in the murine model of *Ct* infection used in this study stemmed largely from experiments conducted by (Roanet al., 2006), where the generation of NR1 T cell receptor (TCR) transgenic mice with specificity for the highly conserved *Ct* CD4$^+$ T cell antigen Cta1 were generated. Importantly, this enabled the tracking and differentiation of *Ct*-specific T cells from bystander T cells activated following intra-uterine infection. (Stary et al., 2015) define the mechanisms behind galvanization of mucosal *Ct*-specific effector and memory cellular immune responses using parabiosis experiments to track the movement and function of these *Ct*-specific CD4$^+$ transgenic T cells.

In addition, using UVEBs as antigens, they illustrate the importance of adjuvant selection and route of administration in the priming of tolerogenic versus immunogenic responses and effective T cell trafficking to the uterine mucosa. Interestingly, intrauterine or intranasal immunization with adjuvanted UVEB-*Ct*-cSAP but not UVEBs alone, was found to elicit protective CD4$^+$ T cell responses following intrauterine challenge with *Ct*, with time to clearance of 13 days which

paralleled that of live immunization (measured by recoverable IFU and qRTPCR of uterine bacterial load). Importantly, until now, no chlamydial vaccine study conducted in murine models of infection has demonstrated protective efficacy against *Ct* challenge comparable to that elicited by live *Ct* immunization, although the incorporation of native *Cm* MOMP as a vaccine candidate demonstrated similar protective efficacy to live immunization with *Cm* (Pal et al., 2001). UVEBs administered alone as a vaccine within the uterine mucosa elicited a more tolerogenic immune response with significantly elevated bacterial load relative to both naïve and UVEB-*Ct*-cSAP-immunized mice.

The mechanisms behind these observations were elegantly addressed in a series of experiments investigating the degree of uptake of live, UVEB and UVEB-*Ct*-cSAP vaccines in three subsets of MHC-II$^+$ uterine-resident antigen-presenting cells (APCs): F4/80 macrophages, CD11b$^+$CD103$^-$ and CD11b$^-$CD103$^+$ DCs. No differences were observed in uptake of all three vaccines in macrophages, but interestingly, live *Ct* EB and UVEB-*Ct*-cSAP vaccines preferentially accumulated in CD11b$^+$CD103$^-$ DCs while UVEBs accumulated in CD11b$^-$CD103$^+$ DCs. Furthermore, injection of CD11b$^+$CD103$^-$ DCs in murine footpads caused proliferation of NR1 T cells in the local draining lymph node (LDLN) of naïve mice, indicating effective priming of *Ct*-specific CD4$^+$ T cells *in vivo*, whereas CD11b$^-$CD103$^+$ DCs did not cause proliferation but instead provoked differentiation of NR1 cells to a regulatory (T$_{reg}$) phenotype *in vitro*. This seminal experiment provides a likely rationale behind the failure of the early trachoma vaccine trials of the 1960s, where ocular mucosal immunization with UV-inactivated EBs in the absence of any adjuvant caused exacerbation and prolonged infection following subsequent live

challenge in nonhuman primates and in patients (where protection was often short-lived) (Wang, Grayston and Alexander, 1967; Woolridge et al., 1967).

Because the density of pathogen-specific CD4^{+} T cells within the genital mucosa has been proposed to correlate with protection against chlamydial infection (Igietseme et al., 1993), it is postulated that the early recruitment of T cells is likely to offer optimal protection against establishment and proliferation of infection. Through tracking of *Ct*-specific NR1 cells, (Stary et al., 2015) further demonstrated that mucosal intranasal (i.n.) or intrauterine (i.u.) immunization with UVEB-*Ct*-cSAP vaccines elicited two waves of T cells (**Fig.6.18**). The first wave of effector T cells peaked at day 7 and then contracted reaching a plateau of similar numbers within the uterine mucosa for both routes of administration by day 9 post-immunization. This established a population of resident memory T cells that persisted for at least 6 months without the requirement for local antigen stimulation, and was postulated to provide early protection against subsequent challenge. The second wave of memory T cells was much larger, and found to reside in the blood and secondary lymphoid tissue (Stary et al., 2015). This circulating population is found to survey tissues for signs of inflammation and augment additional memory recall immune responses to pathogenic invasion (von Andrian and Mackay, 2000). Interestingly, systemic subcutaneous (s.c.) immunization elicited only the second wave of memory effector T cells, which was not found to correlate with enhanced protection relative to naïve mice (Stary et al., 2015).
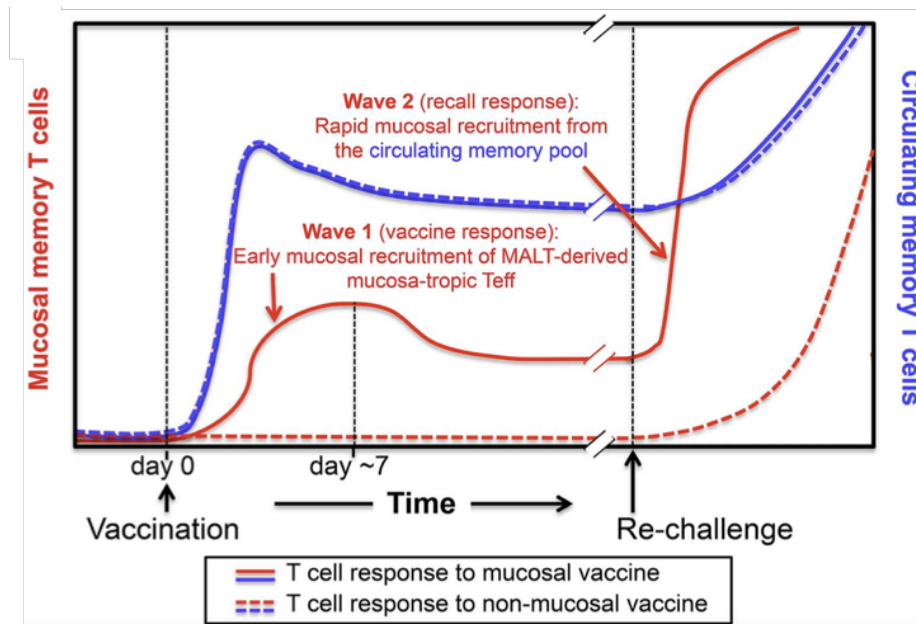
Figure 6.18: Differential waves of *Ct*-specific memory T-cells elicited by mucosal and systemic immunization routes elicit optimal protection. Optimal protection against *Ct* challenge is conferred by two waves of *Ct*-specific memory T cells. Mucosal vaccination with the UV-*Ct*-cSAP antigen-adjuvant combination elicits an early burst of circulating T cells (solid lines) that seed the uterine mucosa during the first week after immunization (wave 1) which result in long-lived resident memory T cells. In contrast, subcutaneous immunisation does not induce the first wave of mucosa-tropic memory cells (broken lines). However, both mucosal and subcutaneous immunisation routes result in circulating memory T cells. In mucosal vaccine recipients, uterine-resident memory T cells initiate the rapid recruitment of additional *Ct*-specific memory cells from the circulating pool (wave 2). Both waves are required for optimum protection.

Importantly, it was further found that the vaccination route selected elicits differences in mucosal homing pathways of systemic effector T cells. It has recently been shown that CD4$^+$ T cells require the $\alpha_4\beta_1$ integrin molecule to access uterine mucosal surfaces (Davila, Olive and Starnbach, 2014), although the full repertoire of infection-induced signals such as chemokines and other pro-inflammatory factors that recruit systemic T cells to mucosal sites is still not fully understood. Stary et al. (2015) showed that monoclonal antibodies to α_4 integrin prevented access of NR1 and endogenous CD4$^+$ T cells to the uterine mucosa following *Ct* challenge, correlating with increased chlamydial burden relative to mice that received control rat IgG. Thus, it is postulated that intrauterine but not systemic immunization results in 'imprinting' of homing mechanisms on effector T cells which mediate the differential trafficking

to these mucosal sites in response to infection. These 'imprinting' signals may be achieved by mucosal-specific APCs that are not found in skin-draining lymph nodes.

Thus, optimal protection in this study was achieved through intrauterine mucosal immunization with UVEB-*Ct*-cSAP, and was dependent upon both mucosal and systemic waves of *Ct*-specific CD4$^+$ T cells with the correct homing mechanisms that elicited seeding of and trafficking to the uterine mucosa. Unexpectedly, however, despite the generation of robust systemic *Ct*-specific antibodies following intrauterine immunization with UVEB-*Ct*-cSAP, (Stary et al., 2015) report no definitive role for antibody-mediated protection in this study, evidenced by no significant protection in non-vaccinated parabionts of conjoined immunized partners, as antibodies are expected to have fully equilibrated between individuals following immunization at the point of challenge.

However, we show that significantly elevated anti-rPmpD IgG cervico-vaginal and serum titres following immunization correlate with significantly enhanced resistance to infections and bacterial clearance in the absence of significantly elevated rPmpD-specific T-cell responses (**Figs. 6.7, 6.8** and **6.12 (A,B)**). Notably, in contrast to the bacterial shedding data presented by Stary et al. (2015), who demonstrate no difference in recoverable IFU between immunized groups and naïve mice at day 1 post challenge, we detect significant early reduction in bacterial burden on day 1 between all vaccine groups and the control PBS-immunized and SLA-immunized groups (**Fig.6.12 (A)**). Furthermore, we propose that this early neutralization is likely to be predominantly antibody-mediated, as the initiation of T cell priming occurs outside the genital mucosa in the absence of organized lymphoid epithelial structures

(e.g. Peyer's patches) within this environment (Cain and Rank, 1995). Thus, the kinetics of T cell priming and trafficking likely preclude antigen-specific T cell mediated effector function at this early time point, and it has further been shown that *Ct*-specific NR1 activation takes about 3-4 days to occur following intra-vaginal chlamydial infection (Roan et al., 2006).

Interestingly, we demonstrate that SLA formulation-specific differences in the relative magnitudes of the splenic rPmpD-specific Th1-type responses reflected by the population of IFNγ-secreting T cells (**Fig.6.6**) do not correlate with enhanced reduction in mean bacterial load over the 22-day period during which shedding was monitored, as no significant differences in reduction in bacterial load between the different rPmpD- or UVEB-adjuvanted groups were observed (p>0.05) (**Fig.6.12 (B)**), although all groups demonstrate significantly reduced burden relative to vehicle and corresponding adjuvant control groups (p<0.001). Even though the magnitude of the rPmpD-specific IFNγ T cell component of the systemic recall response to *Ct* challenge elicited by SLA-SE is significantly more robust than the SLA-AF or SLA-LSQ formulations (**Fig.6.13**), we observe no enhanced reduction in bacterial load between rPmpD-adjuvanted groups. Therefore, in our study, a consistently observed correlate of protection seems to be the sustained presence of elevated rPmpD- or UVEB-specific serum and cervico-vaginal antibody titres (**Fig.6.7, 6.8**).

In light of the established importance of CD4^{+} T cells in resolution of primary chlamydial infection in mice (Morrison, Feilzer and Tumas, 1995; Perry, Feilzer and Caldwell, 1997; Su and Caldwell, 1995; Yu et al., 2014), the majority of preclinical vaccine studies in murine models of infections seek to employ immunization

strategies (administration routes, adjuvant classes and antigens) that elicit robust pathogen-specific CD4$^+$ T cell effector responses. However, a body of evidence also points to a dispensable role of CD4$^+$ T cells in resolution of primary chlamydial infection and protective immunity (Morrison et al., 2011;Morrison and Morrison, 2001), and although the contribution of antibodies is often overlooked as a correlate of protection, accumulating evidence suggests that antibodies may play a more important role in the control of *Ct* infections than previously anticipated (Moore et al., 2003; Morrison and Morrison, 2005a; Morrison and Morrison, 2005b; Olsen et al., 2015). Most recently, (Olsen et al., 2015) have highlighted the importance of neutralizing antibodies in conferring heterotypic protection against highly prevalent urogenital *Ct* D, E and F strains, and provide a case for the importance of rational chlamydial vaccine design through generation of the first chimeric recombinant peptide vaccine. The authors revisit chlamydial MOMP as a target antigen, and focus on rational modifications of the VD4 region of the protein that is rich in neutralizing epitopes (Villeneuve et al., 1994).

Because optimal protection against *Ct* infection using MOMP as a vaccine candidate is known to be both dependent on antigen conformation (Pal et al., 2001) and is usually serovar specific due to extensive inter- and intra-serovar recombination, the strategy employed by (Olsen et al., 2015) sought to design a recombinant peptide vaccine to make use of the non-conformational but highly conserved species-specific LNPTIAG epitope of MOMP embedded within the VD4 region (Baehr et al., 1988;Stephens, Wagar and Schoolnik, 1988), that has been shown to confer neutralization against highly prevalent *Ct* serovars D, E, F and G (Su and Caldwell, 1993). In addition, multivalency and T cell epitopes were incorporated in to the

peptide through fusion of extended segments (either side of the conserved LNPTIAG epitope) from D, E and F serovars, and this fusion construct could also be incorporated in to full-length recombinant MOMP, increasing the array of neutralizing antibody and T cell epitopes.

Importantly, passive transfer of serum from chimeric peptide-immunized containing the extended VD4 domains from serovars D, E and F conferred early protection against infection, suggesting systemic neutralizing antibody is sufficient to mediate lower genital tract protection. Antibodies generated against this chimeric recombinant MOMP vaccine (CTH522) were further shown to confer significant heterologous neutralization of *Ct* serovars D, E, F and G relative to *Ct* recombinant MOMP *in vitro*. This is in accordance with observations in our study, where we report a correlation between early reduction in chlamydial load and enhanced serum antibody titres for rPmpD-immunized mice in both the presence (rPmpD + SLA-SE / SLA-AF / SLA-LSQ) and absence (rPmpD only) of enhanced rPmpD-specific Th1-type cellular immunity.

However, in contrast to our study, Olsen et al. (2015) utilize a simultaneous subcutaneous plus intranasal immunization regimen to boost local genital tract mucosal antibody responses. However, we demonstrate that subcutaneous immunization alone elicits high-titre antigen-specific systemic humoral responses that likely contribute to the presence of observed rPmpD-specific cervico-vaginal IgG. We thus postulate that significantly elevated pathogen-specific mucosal IgG titres are necessary and sufficient to mediate effective early neutralization against *Ct* challenge,

although the potential contribution of certain innate immune mechanisms to observed bacterial clearance could not be ruled out in our study.

Prior to our study, only two previous studies presented robust evidence of neutralizing antibodies effecting protection against chlamydial infection *in vivo*, both employing MOMP as a vaccine immunogen (Olsen et al., 2015; Pal et al., 2001). In order to further confirm the role of neutralizing antibodies to PmpD, current and ongoing experiments involve the passive transfer of immune serum to naïve mice prior to intra-vaginal *Ct* challenge, as well as the investigation of *in vivo* neutralization of *Ct* following pre-incubation of *Ct* EBs with immune or pre-immune serum.

Our findings illustrate the efficacy of using rPmpD as a *Ct* vaccine immunogen *in vivo*. rPmpD elicits significant protection against *Ct* serovar D/UW3/Cx challenge in both the presence and absence of adjuvant. While this protection correlates with the presence of anti-rPmpD serum IgG, further work is required to detail the underpinnings of other likely immunomodulatory properties of rPmpD. For instance, the *Leishmania major* hydrophilic acylated surface protein B (HASPB) elicited long-term protection and antigen-specific CD8^{+} T-cells in the absence of exogenous adjuvant or delivery vehicle (Stager et al., 2003) and the leishmanial vaccine candidate antigen LeIF was shown to have inherent IL-12 stimulating capacity (Skeiky et al., 1995; Skeiky et al., 1998). Similar to *Leishmania* HASPB (Alce et al., 1999), the passenger domains of rPmpD and a plethora of other chlamydial Pmps also possess highly repetitive GGA(I,L,V) and FXXN motifs (Swanson et al., 2009). Hence, in addition to extending the evaluation of preclinical *Ct* vaccine candidates to include antibody-mediated mechanisms of protection, our results highlight the need

for a more basic mechanistic understanding of vaccine antigens that may confer protection in the absence of Th1-bias.

Further experimentation using murine and nonhuman primate *in vivo* challenge models against other highly prevalent clinical serovars (D, E and F) will reliably confirm the previously postulated *in vitro* pan-neutralising abilities of anti-PmpD antibodies (Crane et al., 2006), and its potential efficacy as a future chlamydial vaccine antigen, particularly given its surface-exposure, constitutive expression during *Ct* biphasic development, and presence of multiple T cell epitopes (Swanson et al., 2009;Tan et al., 2010). Our study also demonstrates the efficacy of the novel, rationally designed adjuvant, SLA, in combination with rPmpD, at mediating robust protection against *Ct* infection. In light of previously observed differences in immunogenicity and protection of different antigen-adjuvant combinations, it may be prudent to investigate the applicability of SLA in combination with a wider array of chlamydial antigens. For instance, PmpG was found to be immunodominant and protective in C57BL/6 mice (Yu et al., 2014) when paired with the DDA/MPL TLR4 agonist adjuvant, but this was not found to be the case when paired with the CpG-ODN TLR9 agonist (Yu et al., 2010).

Importantly, a recently described caveat to the use of highly passaged laboratory strains in *in vitro* assays may impact future studies on *Ct* infection dynamics *in vivo*, as it has been demonstrated that key adaptive mechanisms occur during *in vivo* to *in vitro* transition following high passage of ocular, genital and LGV *Ct* strains (Borges et al., 2015). Most notably, non-invasive genital serovars were found to acquire inactivating CT135 mutations, not observed in ocular or LGV strains. Importantly,

RNA-seq analysis revealed that CT135 influences the expression of well-known chlamydial virulence factors such as CT694, TepP and Tarp (Borges et al., 2015), and such inactivating mutations are likely to lead to attenuation of virulence *in vivo*. Furthermore, (Borges et al., 2015) find that the CT166 gene, which encodes the putative chlamydial cytotoxin in *Ct* genital strains (but is truncated in ocular and LGV serovars), is potentially disrupted following high passage of noninvasive urogenital serovars.

Although a direct link to alterations in *pmp* expression following prolonged passage has not yet been elucidated, it may be likely that high passage rates lead to adaptation mechanisms that favour expression or phase variation of a particular Pmp or subset of Pmps *in vitro*, which do not reflect infection dynamics *in vivo*, and that these adaptive mechanisms may also be serovar-specific *in vitro*. For instance, the *pmpD* null mutant generated by (Kari et al., 2014) was derived from a non-invasive urogenital *Ct* serovar D/UW3/Cx laboratory parental strain. However, a significant caveat to the reported attenuation of the null mutant virulence *in vivo*, was the implementation of ocular infection studies conducted in cynomolgus macaques, for which this genital strain has no natural tropism. More representative studies should investigate genital tract infection and clearance kinetics of this *pmpD* mutant in nonhuman primates, or employ the use of a trachoma *pmpD* null mutant biovar in the macaque ocular challenge model. Furthermore, ocular serovars have not been documented to acquire CT135 mutations over successive passages during cell culture *in vitro*, unlike urogenital serovars, where this and other mutations are found to lead to attenuation of virulence *in vivo* (Borges et al., 2015).

Furthermore, (Kari et al., 2014) propose that the *Ct* D/UW3/Cx *pmpD* null mutant is significantly attenuated in an ocular infection model of nonhuman primates, yet show no statistically significant difference in the mean bacterial load, rate of bacterial clearance or recoverable IFU at any time point two weeks post infection. These findings call in to question the use of laboratory adapted strains for *in vivo* infection, and suggest that the use of low passage clinical strains for *in vivo* studies may be more representative models for deriving more robust conclusions about the pathogenesis of clinical infections as well as vaccine efficacy.

Chapter 7: General Discussion

7.1   Introduction

The immune correlates of protection and resolution of sexually transmitted *Ct* infections within an outbred human population remain poorly understood. In addition, the ancient origins, extreme phylogenetic divergence, and obligate intracellular adaptation of *Ct* preclude straightforward inference of gene or protein function by comparison with a wide array of more well investigated bacterial pathogens of humans. Our study has sought to address key structural, biochemical and immunological properties of PmpD, a putative *Ct* adhesin. The efficacy of this highly conserved chlamydial antigen as a preclinical vaccine candidate has been investigated for the first time. In addition, we have provided the first biophysical characterization of CT694, a *Ct*-specific early T3SS effector molecule.

Although no crystal structures were obtained, the importance and implications of adopting a structure-based approach to investigating the function of a plethora of chlamydial proteins will first be discussed in this chapter within the context of current knowledge in the field. This is followed by a brief discussion of the advantageous approach of structural vaccinology that may be applied to Pmps and other chlamydial antigens such as MOMP that display extensive inter-strain variation. With recent advances in the genetic manipulation of *Ct* as well as whole-genome sequencing, it is anticipated that a more rational approach may expedite the advent of a new chlamydial vaccine designed to elicit protection against a wider array of prevalent strains.

7.2   The impact of past and future structural biological approaches to the study of *Chlamydia trachomatis*

Although no rPmpD or CT694 crystals have yet been obtained that are amenable to X-ray diffraction studies, the importance of structural biological application in the chlamydial field is of primary importance for several reasons. Crucially, the few putative virulence factors and hypothetical proteins of *Chlamydia trachomatis* solved by X-ray crystallography have unveiled key pathogen-specific mechanisms of survival, and this is crucial for facilitating and expediting (i) functional genomic annotation and the elucidation of species- and strain-specific mechanisms of pathogenesis (ii) the development of novel drugs and vaccines. Since complete sequencing of the (relatively) small (~1.14Mbp) *Ct* serovar D/UW3/Cx genome in 1998 (Stephens et al., 1998), ~25% still comprises genes encoding 'hypothetical' proteins, while about 35% of the *C.pneumoniae* genome (another widespread and important pathogen of humans) still requires annotation (Kalman et al., 1999).

The extreme phylogenetic distance between *Chlamydiales* and more widely studied bacterial species (*E.coli*, *B.subtilis* and *S.enterica*) has largely precluded straightforward assignment of putative gene function through primary sequence homology comparisons (Pace, 1997). In addition, the obligate intracellular lifestyle and lack of known conjugative plasmids or bacteriophages for the *Chlamydiales* has prevented the use of conventional genetic techniques typically used to interrogate specific gene function in genetically tractable phyla. Thus, in the absence of a fully tractable genetic system for *Ct* until 2011, structural characterization has been the most reliable means of revealing a number of unique aspects of *Ct* pathogen biology in hypothetical proteins with no known sequence homology to a plethora of other

bacterial species. Key examples are subsequently discussed in this section, emphasizing the importance of future work in this area.

The first structure of a *Ct* hypothetical protein was solved in 2004, six years following publication of the genome. Since then, the structures of only 22 *Ct* proteins have been deposited in the PDB. A 3D description of CT610, a dimer of seven α-helical bundles, led to its functional assignment as CADD (Chlamydia protein associating with death domains) (Schwarzenbacher et al., 2004). Although CADD showed only 18% sequence identity with co-enzyme pyrrolo-quinoline-quinone synthesis protein C (PqqC) family members, the crystal structure did indicate fold similarity to heme-oxygenase and 'PqqC-like' enzymes. However, CADD enzymatic active sites were not conserved. Furthermore, ectopic expression of *Klebsiella pneumoniae* PqqC failed to elicit apoptosis in transfected cells (Stenner-Liewen et al., 2002).

This indicates the possible divergent evolution of proteins between two species adapted to different environmental niches, and informs subsequent study and rational design of inhibitors of this multi-domain 'orphan' protein unique to *Ct* pathogenesis. Interestingly, no orthologs of CADD were present in other *Chlamydia* species, further suggesting possible unique adaptations of *Ct* tailored towards host-specific intracellular survival. These studies emphasize important caveats inherent in genome annotation of pathogens that are phylogenetically distinct using sequence or even structural homology without a detailed examination of molecular mechanisms of substrate or ligand interactions. This is exemplified by the 3D molecular description of the CT296 hypothetical protein (Kemege et al., 2011).

CT296 was initially reported to display characteristics akin to that of the *E.coli* iron-responsive transcriptional repressor – Fur, leading to its functional assignment as a metal responsive transcriptional repressor. These data were obtained through cross-reactive antibodies, functional complementation in *E.coli* and electrophoretic mobility shift assays (Rau et al., 2005; Wyllie and Raulston, 2001). However, examination of the crystal structure revealed no divalent cations present within the active site, with no metal binding sites or DNA-binding motifs. Structural homology searches identified this protein as a member of the cupin superfamily of enzymes, which are known for their display of extensive diversity through subtle active site modifications despite the preservation of tertiary and quaternary structural homology (Khuri, Bakker and Dunwell, 2001). Proteins with structural homology to CT296 have been shown to possess a wide array of enzymatic functions (from halogenases to oxidoreductases), and despite significant structural homology to the cupin 2-oxoglutarate iron-dependent enzyme subclass, an incomplete double-stranded β–helix fold, the lack of an iron- or 2-oxoglutatarate binding site and poor conservation of key residues required in coordinating metal ions reveal that this may not be the case.

Importantly, this study showcases the utility of structural biology within the field of *Ct* research, particularly in challenging traditionally established paradigms obtained from established *in vitro* studies. Lack of experimental sensitivity, non-native growth conditions and other technical limitations in heterologous bacterial or ectopic expression systems may indeed preclude accurate functional annotation of *Ct* proteins, and hence, a structural approach for guiding functional assignment of 'hypothetical' *Ct* genes is crucial, and will almost certainly be required as an adjunct to complement nascent genetic techniques as they become more established.

Another application of structural biology is to facilitate guidance of rational drug development. Although an obligate intracellular lifestyle was initially thought to preclude extensive lateral gene transfer and likely acquisition of antibiotic resistance, recent evidence shows that there are no absolute barriers to recombination within and between *Ct* serovars despite this intracellular niche (Harris et al., 2012), and that these bacteria do possess the ability for the transfer of tetracycline resistance *in vitro* (Suchland et al., 2009). Furthermore, treatment failure has also been documented in clinical settings (Hocking et al., 2015), as well as instances of antibiotic resistance (Somani et al., 2000). Thus, the design of novel therapeutics for treating *Ct* and related veterinary and zoonotic chlamydioses may largely depend on a molecular and functional description of *Ct* proteins.

The characterization of the *Ct* LL-diaminopimelate aminotransferase (DAP-AT) epitomises evolutionary adaptation towards utilization of a broad array of substrates (Watanabe et al., 2011). This family of enzymes is responsible for providing an alternative route of lysine biosynthesis, and products of this pathway are important for cross-linking poly-glycan chains in the bacterial cell wall, thus maintaining structural integrity (van Heijenoort, 2001). However, because humans obtain lysine from their diet, and have no requirement for lysine biosynthesis, *Ct*DAP offers an attractive drug target for the rational design of novel inhibitors using modeling within the active site of the crystal structure.

Although the overall protein fold was found to be almost identical to that of the *Arabidopsis thaliana At*DAP, major differences in substrate specificity were

observed. Crystals of *At*DAP show strict substrate specificity for the L-isomer of DAP, whereas *Ct*DAP also recognizes the diastereoisomer in addition to a range of other substrates (McCoy et al., 2006). Examination of the crystal structure of *Ct*DAP revealed that the highly mobile loop lining the active site resulted due to the presence of the helices α_{10} and α_{11} forming a largely unstructured loop. In *At*DAP, the α_{11} helix is much larger and contains a sharp turn between α_{10}-α_{11} with a proline residue (Pro$_{325}$) that reduces mobility. This results in a 9.5 Å movement of the active site loop in *Ct*DAP relative to only a 3-4 Å movement typical of most DAP-ATs (Okamoto et al., 1994). Such insights are important in gaining insight on mechanisms of pathogenesis, but also in the design of novel inhibitors.

Structural approaches have further shed light on metabolic flexibility of the *Chlamydiaceae* through the 3D description of hypothetical protein CT263, which has been classified as a 5'-methylthioadenosine nucleosidase (Barta et al., 2014). This study describes the biosynthesis of menaquinone through the futalosine pathway; an alternative to the traditional pathway employed by numerous commensals to synthesis lipid-soluble electron carriers which support cellular respiration (Kurosu and Begari, 2010). Because humans do not synthesise menaquinone, this enzyme could represent another *Chlamydia*-specific candidate drug target that may be exploited for development using structural approaches, as it has further been hypothesized to play a role in the persistent state of *Chlamydiaceae* (Beatty, Morrison and Byrne, 1994; Bonner, Byrne and Jensen, 2014). Importantly, divergence in the use of metabolic pathways and associated enzymes utilized by pathogenic bacteria such as *Ct* may be comprise a judicious range of therapeutic targets that do not affect host commensal or non-pathogenic counterparts.

It is likely that the implementation of structure-based design of novel therapeutics will now need to be validated in tandem with newly emerging genetic techniques to assess the essential requirement of identified targets *in vitro* by generating and characterizing *Ct* null mutants using forward or reverse genetics approaches. However, if the target is essential for *Ct* intracellular survival, chromosomal mutagenesis resulting in loss-of-function mutations will inevitably result in lethality *in vitro*, making it impossible to phenotypically deduce targets crucial for novel drug development. In addition, the expense and labour-intensive nature of generating *Ct* null mutants may prohibit the widespread use of genetic manipulation, and structural approaches may thus still constitute an important tool within the field of therapeutic development for *Ct* infections.

7.3   Structural approaches to rational vaccinology

While the utility of structural biology in genome annotation and the development of small molecule inhibitors has been addressed, another key area in which it may be exploited is in the development of novel, rationally designed *Ct* vaccines. The development of Bexsero is the first example of a vaccine successfully designed using 'reverse vaccinology', which primarily focused on the use of genomic analysis to predict secreted or surface-localized proteins (**Fig.7.1**). Following shotgun sequencing of the *N.meningitidis* genome revealing ~2000 proteins, 91 proteins were tested for their potential to elicit bactericidal antibodies in mice, and further prioritized according to the ability of the antigens to confer broad protection following immunization and passive protection in infant rodent models of infection (Serruto et al., 2012). These selected antigens were called Genome-derived Neisseria Antigens

(GNA), consisting of GNA2132 (Neisserial Heparin Binding Antigen, or NHBA), GNA1870 (factor H binding protein, or fHbp) and GNA1994 (Neisseria adhesin A, or NadA), the latter of which is a trimeric T5AT. GNA2091 and GNA1030 were also included as fusion proteins in the final vaccine cocktail with fHbp and NHBA (respectively) in order to facilitate large-scale manufacturing.
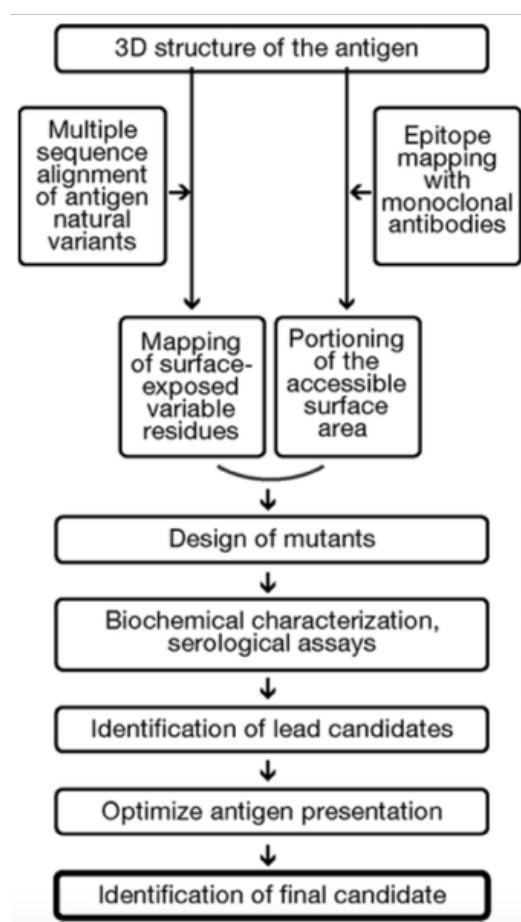
Figure 7.1: Schematic depicting a rational, structure-based approach to vaccine design (Scarselli et al., 2010). A 3D structure of the antigen of interest is prerequisite to facilitate rational vaccine design. This enables the identification of surface-exposed residues, in tandem with epitope mapping of monoclonal antibodies and sequence alignments to determine antigenic variability and allow mapping of point mutations on to the 3D surface. Expression, purification and experimental validation of protective efficacy and immunogenicity using relevant *in vivo* and *in vitro* assays is then implemented to assess relative chimeric antigen vaccine efficacy.

The design of Bexsero represents a paradigm shift in traditional vaccinology approaches where attenuated pathogens or recombinant antigens have conventionally been empirically tested for efficacy *in vivo*. Conjugate capsular polysaccharide vaccines resembling the decorated outer membrane of *N.menigitidis* strains were previously licensed against clinically prevalent serogroups A, C, W and Y, with the incorporation of outer membrane vesicle (OMV)-based vaccines used to combat

epidemic disease (Serruto et al., 2012). However, development of a similar vaccine against serogroup B using the same method was largely precluded by extensive structural similarity of the type B capsular polysaccharide to human N-CAM1 (Nedelec et al., 1990). The α_{2-8} linked polysialic acid type B serogroup capsule is hence poorly immunogenic, and incorporation in to an adjuvanted vaccine carries the risk of autoimmunity (Finne et al., 1987). In addition to this, extensive strain polymorphism of a key meningococcal surface antigen and virulence protein known as factor H binding protein (fHbp) limited the breadth of protective bactericidal antibodies elicited by specific strains. Such similarities are paralleled in *Ct* by widespread recombination of the key protective MOMP antigen and polymorphisms within the Pmp family leading to antigen variation (Harris et al., 2012; Nunes et al., 2015).

Thus, rational structural design of the fHbp antigen was employed in the attempt to elicit a broadly neutralising antibody repertoire (Scarselli et al., 2011). Bioinformatics analysis of over 2000 clinical strains of *N.meningitidis* serogroup B revealed the presence of 300 polymorphic variants of fHbp. These were divided in to three separate clades (V1-V3), representing ~65%, ~25% and ~10% prevalence rates in the global population (respectively) (Beernink et al., 2007; Murphy et al., 2009). Epitope mapping of monoclonal antibodies directed against these three fHbp variants revealed distinct epitopes for strain-specific mAbs, and regions of the protein where there was no overlap between antibodies directed against each clade (Giuliani et al., 2005; Scarselli et al., 2009). It was discovered that the C-terminal β–barrel of the V1 protein contained most of the amino acids recognized by V2 and V3 groups. However,

incorporation of up to three point mutations on the V1 backbone corresponding to the relevant epitopes in V2/V3 groups did not result in broadly neutralising antibodies (Scarselli et al., 2011).

Thus, a novel approach that involved the generation of a chimeric fHbp antigen based on the V1 group backbone that incorporated whole patches (instead of point mutations) of V2 and V3 group antigens was employed through examination of the crystal structure. Eleven partially overlapping areas that were large enough to incorporate at least one conformational epitope (based on the assumption that conformational epitopes of proteins typically range from 900 $Å^2$ -2000 $Å^2$ in surface area (Davies and Cohen, 1996; Rubinstein et al., 2008), were incorporated in to the V1 fHbp backbone to form chimeric antigens and used separately as vaccines in mice, adjuvanted with both aluminium hydroxide and IC31 (a TLR9 agonist recently used in clinical trials) (van Dissel et al., 2010).

Serum from immunized mice was used in *in vitro* bactericidal assays against 7 *N.meningitidis* serogroup B strains expressing divergent fHbp sequences. It was subsequently observed that only the engineered fHbp variant G1 elicited serum antibodies that killed all seven strains expressing divergent fHbp sequences. This is illustrated in **Fig.7.2**. Importantly, chimeric antigenic design also mimicked the native protein conformation, as verified by structural comparison to native fHbp protein, and was achieved without compromising the original antibody repertoire, structural integrity, or ability to bind factor H.
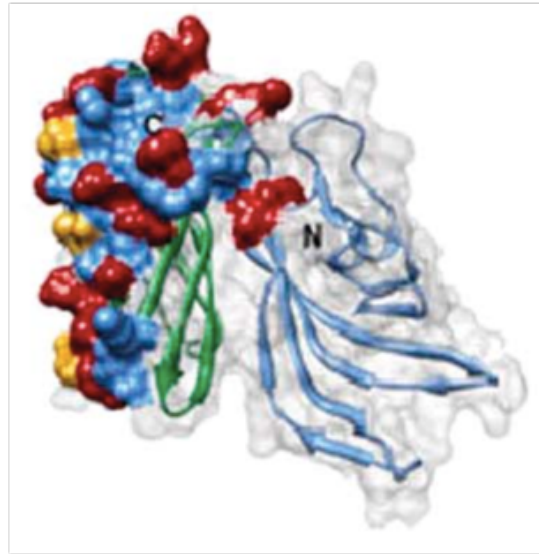
Figure 7.2: G1 variant of *N.meningitidis* fHbp (Scarselli et al., 2010). A 3D surface representation of the engineered G1 chimeric variant of fHbp showing N- and C-terminal domains (blue and green, respectively) with engineered surfaces represented as solid surfaces. Hypervariable residues are coloured yellow, residues common to all three main *N.meningitidis* serogroup B variants are coloured blue, while red residues represent those shared between the less widespread type 2 and 3 variant groups. It is likely that 3D structures of Pmps or MOMP may facilitate future rational design of these chimeric or polymorphic chlamydial vaccine candidate that have been shown to elicit protection in *in vivo* preclinical models.

The design of Bexsero neatly illustrates a paradigm shift in the field of traditional vaccinology, especially in light of the expansion of whole genome sequences of multiple strains of pathogenic bacteria. Previously, efforts to develop vaccines against antigens with large inter-strain variability (such as *Ct*) have focused on enhancing immunogenicity against the most conserved motifs of the protein. However, these strategies have met with limited success (Huang et al., 2005; Wu et al., 2010). A possible reason for this may be the fact that natural selection has shaped these regions to be weakly immunogenic.

For *N.meningitidis*, antibodies play a dominant role in vaccine-mediated immunity to infection, so the identification and incorporation of surface-exposed membrane antigens through bioinformatics is likely to yield a large proportion of key adhesins and virulence factors that may mediate protection. However, for *C.trachomatis*, an obligate intracellular, the task becomes more complex, as a combination of antibody and T cell responses may be required to eradicate persistent infections and achieve optimal bacterial clearance. Furthermore, the identification of key intracellularly expressed effector proteins is less straightforward. Recent whole genome sequencing of 52 clinical *C.trachomatis* strains from a collection of temporally and geographically diverse populations (Harris et al., 2012) will now spur the rational selection and design of antigens identified through a combination of *in vitro* and *in vivo* approaches which assess cell-mediated as well as humoral responses to chlamydial components.

Comparison of the 52 different ocular and urogenital strains revealed that the *ompA* gene (encoding MOMP) is an area of extensive recombination that undergoes replacement and chimerism, likely mechanisms for evading host immunity (Harris et al., 2012). Moreover, 24 recombination events were reconstructed between trachoma and LGV biovars, with 14 of these incorporated in to the *ompA* sequence. The L3 *ompA* sequence was very similar to trachoma serotypes Ia, J and K. Furthermore, recombination events were found to be much more frequent in the trachoma biovars, with a high degree of *ompA* swapping between strains. Interestingly, 43 recombination events were detected between ocular and urogenital branches, showing no absolute barriers to biovar recombination despite differences in tissue tropism.

MOMP comprises ~65% of the chlamydial outer membrane complex, and anti-MOMP antibodies show strain-specific neutralization *in vitro* (Caldwell, Kromhout and Schachter, 1981; Villeneuve et al., 1994). Furthermore, the recently developed multivalent vaccine construct incorporating the VD4 regions and proximal conserved segments of serovars D, E and F showed broadly neutralising protection against the three urogenital serovars (Olsen et al., 2015). However, this does not encompass several ocular and LGV strains that are also highly prevalent worldwide. Thus, MOMP represents a highly attractive chlamydial vaccine candidate that, akin to *N.meningitidis* fHbp, may be amenable to rational design if a 3D structural description and mapping of surface-exposed epitopes from antigenically diverse strains becomes available. This may also be applied to the most variable surface-exposed Pmps and antigens likely to be presented on MHC Class II and recognized by CD4$^+$ T-helper cells (Karunakaran et al., 2015; Nunes et al., 2015), so that a multicomponent vaccine may be able to elicit protection and enhanced bacterial clearance through both humoral and cellular arms of the immune response.

7.4 Concluding remarks

The development of a chlamydial vaccine is multi-factorial, and likely to require an interdisciplinary approach involving immunologists, geneticists, clinicians, epidemiologists and vaccinologists. Our study investigates the preclinical efficacy of a novel TLR4 agonist that elicits a robust Th1-biased immune response *in vivo*, a parameter that has been the major focus of *Ct* vaccine development in preclinical models to date. However, the predominant role of T cells is based upon an array of often conflicting evidence in different murine models of infection, and very few studies focus on the role of antibodies in vaccine-mediated protection *in vivo*. Indeed,

the only robust evidence provided thus far, highlighting the dominant role of antibodies in protection against *Ct* infection *in vivo* focuses on the antigenically variable MOMP antigen (Olsen et al., 2015).

We demonstrate that the highly conserved *Ct* rPmpD is a potent vaccine immunogen *in vivo*, eliciting high titre serum and cervico-vaginal mucosal antibodies that correlate with both resistance to *Ct* challenge and enhanced bacterial clearance *in vivo*. No correlation with the magnitude of the rPmpD-specific cellular immune response to resistance or bacterial load is observed. However, other mechanisms of vaccine-induced protection such as synergism between B cells and CD4^{+} T cells or innate immune responses stimulated by rPmpD independent of adjuvant cannot be ruled out. To further confirm the role of antibody-mediated protection, future experimentation will implement passive transfer of anti-rPmpD serum *in vivo* to assess levels of protection. In corroboration with the recent study by (Olsen et al., 2015), we propose that future preclinical vaccine studies focus more widely on the role of antibody-mediated protection mechanisms *in vivo*.

As mentioned previously, clinical studies investigating potential correlates of protective immunity in human urogenital chlamydial infections are scarce (Batteiger et al., 2010; Gottlieb et al., 2010; Kimani et al., 1996). A particularly pertinent question in the context of infection within the human population is how much time the host requires to clear or control natural infection, and whether genetic differences determine the resolution or pathogenesis of chlamydial infection. In several preclinical models such as mice and guinea pigs, clearance is typically achieved within a few weeks, although in humans, this can range from months to years.

Studies documenting *Ct* infections within the human population are limited. A long-term study of up to four years in women with untreated *Ct* cervical infections revealed that 54% spontaneously cleared infection within one year, 82% at two years and 95% at four years (Molano et al., 2005; Morre et al., 2002). However, without serotyping of strains, it is difficult to deduce whether the observed longer-term durations were due to unresolved infections or re-infection with different serovars. Typically, studies of natural infection and transmission within the human population are both ethically and logistically difficult to implement, but are nonetheless an important prerequisite to understanding immune correlates of protection and pathogenesis to guide development of safe and effective vaccines.

Moreover, a prospective vaccine would need to be readily synchronized with existing immunization regimens, in addition to fulfilling regulatory requirements and standardized, reproducible good manufacturing practice stipulations. These stringent regulatory hurdles generally preclude the straightforward incorporation of whole-cell or live-attenuated vaccines, and this is further complicated by the obligate intracellular life cycle of *Ct* and the associated labour-intensive maintenance and costs of bacterial culture. Thus, it is likely that a multicomponent subunit vaccine may be the most likely future candidate for development.

Ideally, a successful *Ct* vaccine would achieve sterilizing immunity while offering protection against adverse pathological sequelae. To date, no preclinical vaccine study conducted in any animal model of infection has demonstrated sterilizing immunity following challenge. If this is not achievable, potential strategies may include

targeting antigens that are constitutively expressed during the 'persistent' phase of infection to treat pathology associated with prolonged infection. However, it may be difficult to measure the efficacy of such therapeutic vaccines in clinical trials, as clinical endpoints of upper genital tract pathology may be subjective and difficult to assess practically.

Clinical trials of novel trachoma vaccines may thus prove useful surrogates of assessing clinical pathology, and knowledge gained in this setting may possibly be translated to the development of urogenital *Ct* vaccines. It is thought that the pathogenesis of urogenital chlamydial infections broadly mimics that of ocular infection, with the development of lymphoid follicles at infection sites and the subsequent initiation of fibrosis (Darville and Hiltke, 2010; Hu, Holland and Burton, 2013). Furthermore, ocular and genital serovars of *Ct* share >99% genetic identity (Carlson et al., 2005). Thus, because the natural history of infection, sampling and pathology are easier to examine in trachoma patients, it has been proposed that the study of trachoma may offer a more feasible means of obtaining more robust and geographically diverse, large-scale patient cohort data on links between chlamydial disease and the host immune response and genetics, which may subsequently be applied to the study of sexually transmitted urogenital infections.

Given the unique Cys-rich, disulphide linked complexity of the *Ct* COMC, it is likely that a key prerequisite to efficacious recombinant subunit vaccine development and structure-function relationships will be optimizing the expression and folding of antigenic components to mimic native conformation. In light of the phylogenetic divergence between *Chlamydiales* and more well-characterized Proteobacteria such as

E.coli, optimum production may necessitate the use of higher order baculovirus or mammalian expression systems that are able to more reliably incorporate a much wider array of intricate post-translational modifications, with an enhanced repertoire of chaperones that may facilitate correct folding of membrane proteins. Indeed, yeast and baculovirus expression systems have been used in the synthesis of virus-like particles in the manufacture of the licensed Cervarix (GSK) and Gardasil (Merck) vaccines (respectively), currently employed as prophylactic vaccines against a subset of HPV strains in women (Schiller, Day and Kines, 2010;Schiller and Lowy, 2012).

Crucially, following elucidation of widespread recombination within *Ct* in the human population (Harris et al., 2012), the design of a vaccine that is able to elicit immunity against a broad range of strains is perhaps most desirable. One way of achieving this may be the rational design of immunogenic and protective antigens such as a consensus MOMP or Pmp-based vaccine that may be guided by structural biological approaches. More emphasis must also be placed on elucidating the adhesion mechanisms of *Ct* to host cells, in order to identify putative adhesins that may be targeted as vaccine antigens. Finally, perhaps most importantly, recent novel advances in genetic manipulation of *Ct* will further help to interrogate the contribution of specific chlamydial virulence factors in *in vitro* and *in vivo* infection models, which will significantly enhance our knowledge of the infection biology of this obligate intracellular bacterium, and expedite the development of vaccines and novel therapeutics.

8. Appendix

I: DNA sequencing of 65kDa *pmpD*-encoding plasmid from T7 promoter

```
pmpd      GATCTATTCGTTGGGTCTAAAGATAGTCAGGCTGAAGGACAGTATAGGTTAATTGTAGGA
plasmid   ------------------ATGGATAGTCAGGCTGAAGGACAGTATAGGTTAATTGTAGGA
                           *:.************************************

pmpd      GATCCAAGTTCTTTCCAAGAGAAAGATGCGGATACTCTTCCCGGTAAGGTAGAGCAAAGT
plasmid   GATCCAAGTTCTTTCCAAGAGAAAGATGCGGATACTCTTCCCGGTAAGGTAGAGCAAAGT
          ************************************************************

pmpd      ACTTTGTTCTCAGTAACCAATCCCGTAGTTTTCCAAGGTGTGGACCAACAGGATCAAGTC
plasmid   ACTTTGTTCTCAGTAACCAATCCCGTAGTTTTCCAAGGTGTGGACCAACAGGATCAAGTC
          ************************************************************

pmpd      TCTTCCCAAGGGTTAATTTGTAGTTTTACGAGCAGCAACCTTGATTCTCCTCGTGACGGA
plasmid   TCTTCCCAAGGGTTAATTTGTAGTTTTACGAGCAGCAACCTTGATTCTCCTCGTGACGGA
          ************************************************************

pmpd      GAATCTTTTTTAGGTATTGCTTTTGTTGGGGATAGTAGTAAGGCTGGAATCACATTAACT
plasmid   GAATCTTTTTTAGGTATTGCTTTTGTTGGGGATAGTAGTAAGGCTGGAATCACATTAACT
          ************************************************************

pmpd      GACGTGAAAGCTTCTTTGTCTGGAGCGGCTTTATATTCTACAGAAGATCTTATCTTTGAA
plasmid   GACGTGAAAGCTTCTTTGTCTGGAGCGGCTTTATATTCTACAGAAGATCTTATCTTTGAA
          ************************************************************

pmpd      AAGATTAAGGGTGGATTGGAATTTGCATCATGTTCTTCTCTAGAACAGGGGGGGAGCTTGT
plasmid   AAGATTAAGGGTGGATTGGAATTTGCATCATGTTCTTCTCTAGAACAGGGGGGGAGCTTGT
          ************************************************************

pmpd      GCAGCTCAAAGTATTTTGATTCATGATTGTCAAGGATTGCAGGTTAAACACTGTACTACA
plasmid   GCAGCTCAAAGTATTTTGATTCATGATTGTCAAGGATTGCAGGTTAAACACTGTACTACA
          ************************************************************

pmpd      GCCGTGAATGCTGAGGGGTCTAGTGCGAATGATCATCTTGGATTTGGAGGAGGCGCTTTC
plasmid   GCCGTGAATGCTGAGGGGTCTAGTGCGAATGATCATCTTGGATTTGGAGGAGGCGCTTTC
          ************************************************************

pmpd      TTTGTTACGGGTTCTCTTTCTGGAGAGAAAAGTCTCTATATGCCTGCAGGAGATATGGTA
plasmid   TTTGTTACGGGTTCTCTTTCTGGAGAGAAAAGTCTCTATATGCCTGCAGGAGATATGGTA
          ************************************************************

pmpd      GTTGCGAATTGTGATGGGGCTATATCTTTTGAAGGAAACAGCGCGAACTTTGCTAATGGA
plasmid   GTTGCGAATTGTGATGGGGCTATATCTTTTGAAGGAAACAGCGCGAACTTTGCTAATGGA
          ************************************************************

pmpd      GGAGCGATTGCTGCCTCTGGGAAAGTGCTTTTTGTCGCTAATGATAAAAAGACTTCTTTT
plasmid   GGAGCGATTGCTGCCTCTGGGAAAGTGCTTTTTGTCGCTAATGATAAAAAGACTTCTTTT
          ************************************************************

pmpd      ATAGAGAACCGAGCTTTGTCTGGAGGAGCGATTGCAGCCTCTTCTGATATTGCCTTTCAA
plasmid   ATAGAGAACCGAGCTTTGTCTGGAGGAGCGATTGCAGCCTCTTCTGATATTGCCTTTCAA
          ************************************************************

pmpd      AACTGCGCAGAACTAGTTTTCAAAGGCAATTGTGCAATTGGAACAGAGGATAAAGGTTCT
plasmid   AACTGCGCAGAACTAGTTTTCAAAGGCAATTGTGCAATTGGAACAGAGGATAAAGGTTCT
          ************************************************************

pmpd      TTAGGTGGAGGGGCTATATCTTCTCTAGGCACCGTTCTTTTGCAAGGGAATCACGGGATA
plasmid   TTAGGTGGAGGGGCTATATCTTCTCTAGGCACCGTTCTTTTGCAAGGGAATCACGGGATA
          ************************************************************
```

II: DNA sequencing of 65kDa *pmpD*-encoding plasmid from T7 terminator

```
pmpd      ATTTCTGACAACGAGGGGCCAGTGGTTTTCAGAGATAGTACAGCTTGCTTAGGAGGAGGC
plasmid   ATTTCTGACAACGAGGGGCCAGTGGTTTTCAGAGATAGTACAGCTTGCTTAGGAGGAGGC
          ************************************************************

pmpd      GCTATTGCAGCTCAAGAAATTGTTTCTATTCAGAACAATCAGGCTGGGATTTCCTTCGAG
plasmid   GCTATTGCAGCTCAAGAAATTGTTTCTATTCAGAACAATCAGGCTGGGATTTCCTTCGAG
          ************************************************************

pmpd      GGAGGTAAGGCTAGTTTCGGAGGAGGTATTGCGTGTGAATCTTTTTCTTCCGCAGGTGGT
plasmid   GGAGGTAAGGCTAGTTTCGGAGGAGGTATTGCGTGTGAATCTTTTTCTTCCGCAGGTGGT
          ************************************************************

pmpd      GCTTCTGTTTTAGGGGCTATTGATATTTCGAAGAATTTAGGCGCGATTTCGTTCTCTCGT
plasmid   GCTTCTGTTTTAGGGGCTATTGATATTTCGAAGAATTTAGGCGCGATTTCGTTCTCTCGT
          ************************************************************

pmpd      ACTTTATGTACGACCTCAGATTTAGGACAAATGGAGTACCAGGGAGGAGGAGCTCTATTT
plasmid   ACTTTATGTACGACCTCAGATTTAGGACAAATGGAGTACCAGGGAGGAGGAGCTCTATTT
          ************************************************************

pmpd      GGTGAAAATATTTCTCTTTCTGAGAATGCTGGTGTGCTCACCTTTAAAGACAACATTGTG
plasmid   GGTGAAAATATTTCTCTTTCTGAGAATGCTGGTGTGCTCACCTTTAAAGACAACATTGTG
          ************************************************************

pmpd      AAGACTTTTGCTTCGAATGGGAAAATTCTGGGAGGAGGAGCGATTTTAGCTACTGGTAAG
plasmid   AAGACTTTTGCTTCGAATGGGAAAATTCTGGGAGGAGGAGCGATTTTAGCTACTGGTAAG
          ************************************************************

pmpd      GTGGAAATTACCAATAATTCCGGAGGAATTTCTTTTACAGGAAATGCGAGAGCTCCACAA
plasmid   GTGGAAATTACCAATAATTCCGGAGGAATTTCTTTTACAGGAAATGCGAGAGCTCCACAA
          ************************************************************

pmpd      GCTCTTCCAACTCAAGAGGAGTTTCCTTTATTCAGCAAAAAAGAAGGGCGGCCACTCTCT
plasmid   GCTCTTCCAACTCAAGAGGAGTTTCCTTTATTCAGCAAAAAAGAAGGGCGGCCACTCTCT
          ************************************************************

pmpd      TCAGGATATTCTGGGGGAGGAGCGATTTTAGGAAGAGAAGTAGCTATTCTCCACAACGCT
plasmid   TCAGGATATTCTGGGGGAGGAGCGATTTTAGGAAGAGAAGTAGCTATTCTCCACAACGCT
          ************************************************************

pmpd      GCAGTAGTATTTGAGCAAAATCGTTTGCAGTGCAGCGAAGAAGAAGCGACATTATTAGGT
plasmid   GCAGTAGTATTTGAGCAAAATCGTTTGCAGTGCAGCGAAGAAGAAGCGACATTATTAGGT
          ************************************************************

pmpd      TGTTGTGGAGGAGGCGCTGTTCATGGGATGGATAGCACTTCGATTGTTGGCAACTCTTCA
plasmid   TGTTGTGGAGGAGGCGCTGTTCATGGGATGGATAGCACTTCGATTGTTGGCAACTCTTCA
          ************************************************************

pmpd      GTAAGATTTGGTAATAATTACGCAATGGGACAAGGAGTCTCAGGAGGAGCTCTTTTATCT
plasmid   GTAAGATTTGGTAATAATTACGCAATGGGACAAGGAGTCTCAGGAGGAGCTCTTTTATCT
          ************************************************************

pmpd      AAAACAGTGCAGTTAGCTGGAAATGGAAGCGTCGATTTTTCTCGAAATATTGCTAGTTTG
plasmid   AAAACAGTGCAGTTAGCTGGAAATGGAAGCGTCGATTTTTCTCGAAATATTGCTAGTTTG
          ************************************************************

pmpd      GGAGGAGGAGCTCTTCAAGCTTCTGAAGGAAATTGTGAGCTAGTTGATAACGGCTATGTG
plasmid   GGAGGAGGAGCTCTTCAAGCTTCTGAAGGAAATTGTGAGCTAGTTGATAACGGCTATGTG
          ************************************************************

pmpd      CTATTCAGAGATAATCGAGGGAGGGTTTATGGGGGTGCTATTTCTTGCTTACGTGGAGAT
plasmid   CTATTCAGAGATAATCGAGGGAGGGTTTATGGGGGTGCTATTTCTTGCTTACGT------
          ********************************************************
```

III: *E.coli* rare codon usage for 65kDa PmpD fragment

gta gat ctt cat gct gga gga cag tct gta aat gag ctg gta tat gta ggc cct caa gcg gtt tta ttg tta gac caa att CGA gat CTA ttc gtt ggg tct aaa gat agt cag gct gaa gga cag tat AGG tta att gta gga gat cca agt tct ttc caa gag aaa gat gcg gat act ctt CCC ggt aag gta gag caa agt act ttg ttc tca gta acc aat CCC gta gtt ttc caa ggt gtg gac caa cag gat caa gtc tct tcc caa ggg tta att tgt agt ttt acg agc agc aac ctt gat tct cct cgt gac gga gaa tct ttt tta ggt att gct ttt gtt ggg gat agt agt aag gct gga atc aca tta act gac gtg aaa gct tct ttg tct gga gcg gct tta tat tct aca gaa gat ctt atc ttt gaa aag att aag ggt gga ttg gaa ttt gca tca tgt tct tct CTA gaa cag ggg gga gct tgt gca gct caa agt att ttg att cat gat tgt caa gga ttg cag gtt aaa cac tgt act aca gcc gtg aat gct gag ggg tct agt gcg aat gat cat ctt gga ttt gga gga ggc gct ttc ttt gtt acg ggt tct ctt tct gga gag aaa agt ctc tat atg cct gca gga gat atg gta gtt gcg aat tgt gat ggg gct ATA tct ttt gaa gga aac agc gcg aac ttt gct aat gga gga gcg att gct gcc tct ggg aaa gtg ctt ttt gtc gct aat gat aaa aag act tct ttt ATA gag aac CGA gct ttg tct gga gga gcg att gca gcc tct tct gat att gcc ttt caa aac tgc gca gaa CTA gtt ttc aaa ggc aat tgt gca att gga aca gag gat aaa ggt tct tta ggt gga ggg gct ATA tct tct CTA ggc acc gtt ctt ttg caa ggg aat cac ggg ATA act tgt gat aag aat gag tct gct tcg caa gga ggc gcc att ttt ggc aaa aat tgt cag att tct gac aac gag ggg cca gtg gtt ttc AGA gat agt aca gct tgc tta gga gga ggc gct att gca gct caa gaa att gtt tct att cag aac aat cag gct ggg att tcc ttc gag gga ggt aag gct agt ttc gga gga ggt att gcg tgt gaa tct ttt tct tcc gca ggt ggt gct tct gtt tta ggg gct att gat att tcg aag aat tta ggc gcg att tcg ttc tct cgt act tta tgt acg acc tca gat tta gga caa atg gag tac cag gga gga gga gct CTA ttt ggt gaa aat att tct ctt tct gag aat gct ggt gtg ctc acc ttt aaa gac aac att gtg aag act ttt gct tcg aat ggg aaa att ctg gga gga gga gcg att tta gct act ggt aag gtg gaa att acc aat aat tcc gga gga att tct ttt aca gga aat gcg AGA gct cca caa gct ctt cca act caa gag gag ttt cct tta ttc agc aaa aaa gaa ggg cgg cca ctc tct tca gga tat tct ggg gga gga gcg att tta gga AGA gaa gta gct att ctc cac aac gct gca gta gta ttt gag caa aat cgt ttg cag tgc agc gaa gaa gaa gcg aca tta tta ggt tgt tgt gga gga ggc gct gtt cat ggg atg gat agc act tcg att gtt ggc aac tct tca gta AGA ttt ggt aat aat tac gca atg gga caa gga gtc tca gga gga gct ctt tta tct aaa aca gtg cag tta gct gga aat gga agc gtc gat ttt tct CGA aat att gct agt ttg gga gga gga gct ctt caa gct tct gaa gga aat tgt gag CTA gtt gat aac ggc tat gtg CTA ttc AGA gat aat CGA ggg AGG gtt tat ggg ggt gct att tct tgc tta cgt

Red = rare Arg codons **AGG, AGA, CGA**
Green = rare Leu codon **CTA**
Blue = rare Ile codon **ATA**
Orange = rare Pro codon **CCC**

9. Abbreviations

4SP	0.4M sucrose-phosphate buffer
ANOVA	analysis of variance
APC	antigen presenting cell
BCG	Bacille-Calmette-Guerin
BMDC	bone-marrow derived dendritic cell
BSA	bovine serum albumin
CADD	Chlamydia protein associating with death domains
CCR	CC chemokine receptor
CD	circular dichroism
CD(X)	cluster of differentiation (X)
CHO	Chinese hamster ovary cell line
Cm	*Chlamydia muridarum*
COMC	chlamydial outer membrane complex
Cp	*Chlamydia pneumoniae*
CPAF	chlamydial protease-like activity factor
CRP	cysteine-rich protein
cSAPs	charge switching adjuvant particles
Ct	*Chlamydia trachomatis*
CTB	Cholera toxin B
CTL	cytotoxic T-lymphocytes
Cys	cysteine
DAP	di-amino palmitoyltransferase
DAPI	4', 6-diamino-2-phenylindole
DC	dendritic cell
DDA	dimethyl-dioctadecyl-ammonium bromide
DMEM	Dulbecco's modified Eagle's medium
DMPC	Dimyristoyl phosphatidylcholine
DNA	deoxyribonucleic acid
dNTP	deoxynucleotide triphosphate
DOPC	Dioleoyl phosphatidylcholine
DPPC	Dipalmitoyl phosphatidylcholine
DPT	Diphtheria-pertussis-tetanus (vaccine)
Dsb	disulphide-bonding enzyme
dsRNA	double stranded ribonucleic acid
DTNB	5,5'-dithiobis[2-nitrobenzoic acid]
DTT	dithiothreitol
EB	elementary body
EDAC	*N*-Ethyl-*N'*-(3-dimethylaminopropyl)carbodiimide
EDTA	ethylenediaminetetraacetate
EGFR	endothelial growth factor receptor
ELAM	endothelial cell leukocyte adhesion molecule
ELISA	enzyme-linked immunosorbent assay
ELISpot	enzyme-linked immunospot
FA	Freund's adjuvant

FCS	fetal calf serum
fHbp	Factor H binding protein
FPLC	fast protein liquid chromatography
FRT	female reproductive tract
GAG	glycosaminoglycan
GAP	GTPase activating protein
GNA	Genome-derived Neisserial antigen
HBM	heparin binding motif
HIV	human immunodeficiency virus
HPV	human pappilomavirus
HRP	horseradish peroxidase
HUVEC	lymphogranuloma venereum
i.n.	intranasal
i.u.	intrauterine
IDRI	Infectious Disease Research Institute
IFA	Incomplete Freund's adjuvant
IFN	interferon
IFU	inclusion forming units
Ig	immunoglobulin
IL	interleukin
IPTG	Isopropyl β-D-1-thiogalactopyranoside
IRF	interferon regulatory factor
IRG	interferon regulated gene
LAL	Limulus Amebocyte Lysate
LDLN	local draining lymph node
LGV	lymphogranuloma venereum
LPS	lipopolysaccharide
MALDI-MS	matrix-assisted laser desorption ionization mass spectrometry
MALT	mucosa-associated lymphoid tissue
MD2	myeloid differentiation factor 2
MHC	major histocompatibility complex
MIP	macrophage inflammatory protein
MLD	membrane localization domain
MOMP	major outer membrane protein
MPL	monophosphoryl lipid
MSM	men who have sex with men
Mtb	Mycobacterium tuberculosis
MYPT	myosin light chain phosphatase
N-CAM1	Neural cell adhesion molecule 1
NLS	nuclear localization sequence
OMV	outer-membrane vesicle
pAb	polyclonal antibody
Pam3CSK4	N-palmitoyl-S-[2,3-bis (palmitoyl)-(2RS)-propyl]-(R)cysteinyl-alanyl-glycine
PAMP	pathogen associated mmolecular pattern
PBMC	peripheral blood mononuclear cell
PBS	phosphate buffered saline

PCR	polymerase chain reaction
PDB	Protein Data Bank
PDI	protein disulphide isomerase
PDI	polydispersity index
Pet	plasmid encoded toxin
PID	pelvic inflammatory disease
Pmp	polymorphic membrane protein
PMSF	phenylmethylsulfonyl fluoride
PRR	pathogen recognition receptor
qPCR	quantitative polymerase chain reaction
RB	reticulate body
RGD	arginine-glycine-aspartic acid
RNA	ribonucleic acid
rpm	rotations per minute
RPMI	Roswell Park Memorial Institute
s.c.	subcutaneous
SDS-PAGE	sodium dodecyl sulphate polyacrylamide gel electrophoresis
sIgA	secretory immunoglobulin A
SIV	simian immunodeficiency virus
SLA	second-generation lipid adjuvant
SLT	Shiga-like toxin
SNP	single nucleotide polymorphism
SPATE	serine protease autotransporter of the *Enterobacteriaceae*
ssRNA	single-stranded ribonucleic acid
SuV	subunit vaccine
SVV	split viral vaccine
T3SS	type three secretion system
T5AT	type five autotransporter
TB	tuberculosis
TCEP	tris(2-carboxyethyl)phosphine
TCR	T-cell receptor
tg	transgenic
Th	T-helper cell
TLR	Toll-like receptor
TMB	3,3',5,5'-tetramethylbenzidine
TNF	tumour necrosis factor
Treg	regulatory T-cell
TRIF	TIR-domain-containing adapter-inducing interferon-β
UVEB	UV-inactivated elementary bodies
VCG	*Vibrio cholerae* ghost

10. References

Abell, B. A., and Brown, D. T. (1993). Sindbis virus membrane fusion is mediated by reduction of glycoprotein disulfide bridges at the cell surface. J Virol 67, 5496.

Abromaitis, S., and Stephens, R. S. (2009). Attachment and entry of Chlamydia have distinct requirements for host protein disulfide isomerase. PLoS Pathog 5, e1000357.

Agnandji, S. T., Lell, B., Soulanoudjingar, S. S., Fernandes, J. F., Abossolo, B. P., Conzelmann, C., Methogo, B. G., Doucka, Y., Flamen, A., Mordmuller, B., Issifou, S., Kremsner, P. G., Sacarlal, J., Aide, P., Lanaspa, M., Aponte, J. J., Nhamuave, A., Quelhas, D., Bassat, Q., Mandjate, S., Macete, E., Alonso, P., Abdulla, S., Salim, N., Juma, O., Shomari, M., Shubis, K., Machera, F., Hamad, A. S., Minja, R., Mtoro, A., Sykes, A., Ahmed, S., Urassa, A. M., Ali, A. M., Mwangoka, G., Tanner, M., Tinto, H., D'Alessandro, U., Sorgho, H., Valea, I., Tahita, M. C., Kabore, W., Ouedraogo, S., Sandrine, Y., Guiguemde, R. T., Ouedraogo, J. B., Hamel, M. J., Kariuki, S., Odero, C., Oneko, M., Otieno, K., Awino, N., Omoto, J., Williamson, J., Muturi-Kioi, V., Laserson, K. F., Slutsker, L., Otieno, W., Otieno, L., Nekoye, O., Gondi, S., Otieno, A., Ogutu, B., Wasuna, R., Owira, V., Jones, D., Onyango, A. A., Njuguna, P., Chilengi, R., Akoo, P., Kerubo, C., Gitaka, J., Maingi, C., Lang, T., Olotu, A., Tsofa, B., Bejon, P., Peshu, N., Marsh, K., Owusu-Agyei, S., Asante, K. P., Osei-Kwakye, K., Boahen, O., Ayamba, S., Kayan, K., Owusu-Ofori, R., Dosoo, D., Asante, I., Adjei, G., Adjei, G., Chandramohan, D., Greenwood, B., Lusingu, J., Gesase, S., Malabeja, A., Abdul, O., Kilavo, H., Mahende, C., Liheluka, E. (2011). First results of phase 3 trial of RTS,S/AS01 malaria vaccine in African children. N Engl J Med 365, 1863.

Alce, T. M., Gokool, S., McGhie, D., Stager, S., and Smith, D. F. (1999). Expression of hydrophilic surface proteins in infective stages of Leishmania donovani. Mol Biochem Parasitol 102, 191.

Anacker, R. L., Mann, R. E., and Gonzales, C. (1987). Reactivity of monoclonal antibodies to Rickettsia rickettsii with spotted fever and typhus group rickettsiae. J Clin Microbiol 25, 167.

Andersson, S. G., Zomorodipour, A., Andersson, J. O., Sicheritz-Ponten, T., Alsmark, U. C., Podowski, R. M., Naslund, A. K., Eriksson, A. S., Winkler, H. H., and Kurland, C. G. (1998). The genome sequence of Rickettsia prowazekii and the origin of mitochondria. Nature 396, 133.

Angus, D. C., Linde-Zwirble, W. T., Lidicker, J., Clermont, G., Carcillo, J., and Pinsky, M. R. (2001). Epidemiology of severe sepsis in the United States: analysis of incidence, outcome, and associated costs of care. Crit Care Med 29, 1303.

Arbour, N. C., Lorenz, E., Schutte, B. C., Zabner, J., Kline, J. N., Jones, M., Frees, K., Watt, J. L., and Schwartz, D. A. (2000). TLR4 mutations are associated with endotoxin hyporesponsiveness in humans. Nat Genet 25, 187.

Aspholm-Hurtig, M., Dailide, G., Lahmann, M., Kalia, A., Ilver, D., Roche, N., Vikstrom, S., Sjostrom, R., Linden, S., Backstrom, A., Lundberg, C., Arnqvist, A.,

Mahdavi, J., Nilsson, U. J., Velapatino, B., Gilman, R. H., Gerhard, M., Alarcon, T., Lopez-Brea, M., Nakazawa, T., Fox, J. G., Correa, P., Dominguez-Bello, M. G., Perez-Perez, G. I., Blaser, M. J., Normark, S., Carlstedt, I., Oscarson, S., Teneberg, S., Berg, D. E., and Boren, T. (2004). Functional adaptation of BabA, the H. pylori ABO blood group antigen binding adhesin. Science 305, 519.

Baba, T. W., Liska, V., Hofmann-Lehmann, R., Vlasak, J., Xu, W., Ayehunie, S., Cavacini, L. A., Posner, M. R., Katinger, H., Stiegler, G., Bernacky, B. J., Rizvi, T. A., Schmidt, R., Hill, L. R., Keeling, M. E., Lu, Y., Wright, J. E., Chou, T. C., and Ruprecht, R. M. (2000). Human neutralizing monoclonal antibodies of the IgG1 subtype protect against mucosal simian-human immunodeficiency virus infection. Nat Med 6, 200.

Bachmann, M. F., and Jennings, G. T. (2010). Vaccine delivery: a matter of size, geometry, kinetics and molecular patterns. Nat Rev Immunol 10, 787.

Baehr, W., Zhang, Y. X., Joseph, T., Su, H., Nano, F. E., Everett, K. D., and Caldwell, H. D. (1988). Mapping antigenic domains expressed by Chlamydia trachomatis major outer membrane protein genes. Proc Natl Acad Sci U S A 85, 4000.

Baldridge, J. R., McGowan, P., Evans, J. T., Cluff, C., Mossman, S., Johnson, D., and Persing, D. (2004). Taking a Toll on human disease: Toll-like receptor 4 agonists as vaccine adjuvants and monotherapeutic agents. Expert Opin Biol Ther 4, 1129.

Baldwin, S. L., Bertholet, S., Kahn, M., Zharkikh, I., Ireton, G. C., Vedvick, T. S., Reed, S. G., and Coler, R. N. (2009). Intradermal immunization improves protective efficacy of a novel TB vaccine candidate. Vaccine 27, 3063.

Banchereau, J., and Steinman, R. M. (1998). Dendritic cells and the control of immunity. Nature 392, 245.

Bantel, H., Sinha, B., Domschke, W., Peters, G., Schulze-Osthoff, K., and Janicke, R. U. (2001). alpha-Toxin is a mediator of Staphylococcus aureus-induced cell death and activates caspases via the intrinsic death pathway independently of death receptor signaling. J Cell Biol 155, 637.

Barron, A. L., White, H. J., Rank, R. G., Soloff, B. L., and Moses, E. B. (1981). A new animal model for the study of Chlamydia trachomatis genital infections: infection of mice with the agent of mouse pneumonitis. J Infect Dis 143, 63.

Barta, M. L., Thomas, K., Yuan, H., Lovell, S., Battaile, K. P., Schramm, V. L., and Hefty, P. S. (2014). Structural and biochemical characterization of Chlamydia trachomatis hypothetical protein CT263 supports that menaquinone synthesis occurs through the futalosine pathway. J Biol Chem 289, 32214.

Batteiger, B. E., Rank, R. G., Bavoil, P. M., and Soderberg, L. S. (1993). Partial protection against genital reinfection by immunization of guinea-pigs with isolated outer-membrane proteins of the chlamydial agent of guinea-pig inclusion conjunctivitis. J Gen Microbiol 139, 2965.

Batteiger, B. E., Xu, F., Johnson, R. E., and Rekart, M. L. (2010). Protective immunity to Chlamydia trachomatis genital infection: evidence from human studies. J Infect Dis 201 Suppl 2, S178.

Baudner, B. C., Ronconi, V., Casini, D., Tortoli, M., Kazzaz, J., Singh, M., Hawkins, L. D., Wack, A., and O'Hagan, D. T. (2009). MF59 emulsion is an effective delivery system for a synthetic TLR4 agonist (E6020). Pharm Res 26, 1477.

Bavoil, P., Ohlin, A., and Schachter, J. (1984). Role of disulfide bonding in outer membrane structure and permeability in Chlamydia trachomatis. Infect Immun 44, 479.

Beatty, W. L., Belanger, T. A., Desai, A. A., Morrison, R. P., and Byrne, G. I. (1994). Role of tryptophan in gamma interferon-mediated chlamydial persistence. Ann N Y Acad Sci 730, 304.

Beatty, W. L., Morrison, R. P., and Byrne, G. I. (1994). Persistent chlamydiae: from cell culture to a paradigm for chlamydial pathogenesis. Microbiol Rev 58, 686.

Becker, E., and Hegemann, J. H. (2014). All subtypes of the Pmp adhesin family are implicated in chlamydial virulence and show species-specific function. Microbiologyopen 3, 544.

Beeckman, D. S., and Vanrompay, D. C. (2010). Bacterial secretion systems with an emphasis on the chlamydial Type III secretion system. Curr Issues Mol Biol 12, 17.

Beernink, P. T., Welsch, J. A., Harrison, L. H., Leipus, A., Kaplan, S. L., and Granoff, D. M. (2007). Prevalence of factor H-binding protein variants and NadA among meningococcal group B isolates from the United States: implications for the development of a multicomponent group B vaccine. J Infect Dis 195, 1472.

Behzad, H., Huckriede, A. L., Haynes, L., Gentleman, B., Coyle, K., Wilschut, J. C., Kollmann, T. R., Reed, S. G., and McElhaney, J. E. (2012). GLA-SE, a synthetic toll-like receptor 4 agonist, enhances T-cell responses to influenza vaccine in older adults. J Infect Dis 205, 466.

Belland, R. J., Zhong, G., Crane, D. D., Hogan, D., Sturdevant, D., Sharma, J., Beatty, W. L., and Caldwell, H. D. (2003). Genomic transcriptional profiling of the developmental cycle of Chlamydia trachomatis. Proc Natl Acad Sci U S A 100, 8478.

Berger, I., Fitzgerald, D. J., and Richmond, T. J. (2004). Baculovirus expression system for heterologous multiprotein complexes. Nat Biotechnol 22, 1583.

Bertholet, S., Goto, Y., Carter, L., Bhatia, A., Howard, R. F., Carter, D., Coler, R. N., Vedvick, T. S., and Reed, S. G. (2009). Optimized subunit vaccine protects against experimental leishmaniasis. Vaccine 27, 7036.

Betts-Hampikian, H. J., and Fields, K. A. (2011). Disulfide bonding within components of the Chlamydia type III secretion apparatus correlates with development. J Bacteriol 193, 6950.

Beutler, B. (2000). Tlr4: central component of the sole mammalian LPS sensor. Curr Opin Immunol 12, 20.

Bidaisee, S., and Macpherson, C. N. (2014). Zoonoses and one health: a review of the literature. J Parasitol Res 2014, 874345.

Bieniossek, C., Papai, G., Schaffitzel, C., Garzoni, F., Chaillet, M., Scheer, E., Papadopoulos, P., Tora, L., Schultz, P., and Berger, I. (2013). The architecture of human general transcription factor TFIID core complex. Nature 493, 699.

Blanc, G., Ngwamidiba, M., Ogata, H., Fournier, P. E., Claverie, J. M., and Raoult, D. (2005). Molecular evolution of rickettsia surface antigens: evidence of positive selection. Mol Biol Evol 22, 2073.

Boncristiano, M., Paccani, S. R., Barone, S., Ulivieri, C., Patrussi, L., Ilver, D., Amedei, A., D'Elios, M. M., Telford, J. L., and Baldari, C. T. (2003). The Helicobacter pylori vacuolating toxin inhibits T cell activation by two independent mechanisms. J Exp Med 198, 1887.

Bonner, C. A., Byrne, G. I., and Jensen, R. A. (2014). Chlamydia exploit the mammalian tryptophan-depletion defense strategy as a counter-defensive cue to trigger a survival state of persistence. Front Cell Infect Microbiol 4, 17.

Borges, V., Pinheiro, M., Antelo, M., Sampaio, D. A., Vieira, L., Ferreira, R., Nunes, A., Almeida, F., Mota, L. J., Borrego, M. J., and Gomes, J. P. (2015). Chlamydia trachomatis In Vivo to In Vitro Transition Reveals Mechanisms of Phase Variation and Down-Regulation of Virulence Factors. PLoS One 10, e0133420.

Bouvet, J. P., Belec, L., Pires, R., and Pillot, J. (1994). Immunoglobulin G antibodies in human vaginal secretions after parenteral vaccination. Infect Immun 62, 3957.

Bowen, W. S., Minns, L. A., Johnson, D. A., Mitchell, T. C., Hutton, M. M., and Evans, J. T. (2012). Selective TRIF-dependent signaling by a synthetic toll-like receptor 4 agonist. Sci Signal 5, ra13.

Brayton, K. A., Knowles, D. P., McGuire, T. C., and Palmer, G. H. (2001). Efficient use of a small genome to generate antigenic diversity in tick-borne ehrlichial pathogens. Proc Natl Acad Sci U S A 98, 4130.

Brunham, R. C., Kimani, J., Bwayo, J., Maitha, G., Maclean, I., Yang, C., Shen, C., Roman, S., Nagelkerke, N. J., Cheang, M., and Plummer, F. A. (1996). The epidemiology of Chlamydia trachomatis within a sexually transmitted diseases core group. J Infect Dis 173, 950.

Brunham, R. C., and Rappuoli, R. (2013). Chlamydia trachomatis control requires a vaccine. Vaccine 31, 1892.

Brunham, R. C., and Rekart, M. L. (2008). The arrested immunity hypothesis and the epidemiology of chlamydia control. Sex Transm Dis 35, 53.

Brunham, R. C., and Rey-Ladino, J. (2005). Immunology of Chlamydia infection: implications for a Chlamydia trachomatis vaccine. Nat Rev Immunol 5, 149.

Brzuszkiewicz, E., Bruggemann, H., Liesegang, H., Emmerth, M., Olschlager, T., Nagy, G., Albermann, K., Wagner, C., Buchrieser, C., Emody, L., Gottschalk, G., Hacker, J., and Dobrindt, U. (2006). How to become a uropathogen: comparative genomic analysis of extraintestinal pathogenic Escherichia coli strains. Proc Natl Acad Sci U S A 103, 12879.

Budrys, N. M., Gong, S., Rodgers, A. K., Wang, J., Louden, C., Shain, R., Schenken, R. S., and Zhong, G. (2012). Chlamydia trachomatis antigens recognized in women with tubal factor infertility, normal fertility, and acute infection. Obstet Gynecol 119, 1009.

Bullock, H. D., Hower, S., and Fields, K. A. (2012). Domain analyses reveal that Chlamydia trachomatis CT694 protein belongs to the membrane-localized family of type III effector proteins. J Biol Chem 287, 28078.

Cacalano, G., Lee, J., Kikly, K., Ryan, A. M., Pitts-Meek, S., Hultgren, B., Wood, W. I., and Moore, M. W. (1994). Neutrophil and B cell expansion in mice that lack the murine IL-8 receptor homolog. Science 265, 682.

Cain, T. K., and Rank, R. G. (1995). Local Th1-like responses are induced by intravaginal infection of mice with the mouse pneumonitis biovar of Chlamydia trachomatis. Infect Immun 63, 1784.

Caldwell, H. D., Kromhout, J., and Schachter, J. (1981). Purification and partial characterization of the major outer membrane protein of Chlamydia trachomatis. Infect Immun 31, 1161.

Caldwell, H. D., Kuo, C. C., and Kenny, G. E. (1975). Antigenic analysis of Chlamydiae by two-dimensional immunoelectrophoresis. II. A trachoma-LGV-specific antigen. J Immunol 115, 969.

Capecchi, B., Adu-Bobie, J., Di Marcello, F., Ciucchi, L., Masignani, V., Taddei, A., Rappuoli, R., Pizza, M., and Arico, B. (2005). Neisseria meningitidis NadA is a new invasin which promotes bacterial adhesion to and penetration into human epithelial cells. Mol Microbiol 55, 687.

Carabeo, R. A., Grieshaber, S. S., Fischer, E., and Hackstadt, T. (2002). Chlamydia trachomatis induces remodeling of the actin cytoskeleton during attachment and entry into HeLa cells. Infect Immun 70, 3793.

Cardwell, M. M., and Martinez, J. J. (2009). The Sca2 autotransporter protein from Rickettsia conorii is sufficient to mediate adherence to and invasion of cultured mammalian cells. Infect Immun 77, 5272.

Carey, A. J., Cunningham, K. A., Hafner, L. M., Timms, P., and Beagley, K. W. (2009). Effects of inoculating dose on the kinetics of Chlamydia muridarum genital infection in female mice. Immunol Cell Biol 87, 337.

Carlson, J. H., Hughes, S., Hogan, D., Cieplak, G., Sturdevant, D. E., McClarty, G., Caldwell, H. D., and Belland, R. J. (2004). Polymorphisms in the Chlamydia trachomatis cytotoxin locus associated with ocular and genital isolates. Infect Immun 72, 7063.

Carlson, J. H., Porcella, S. F., McClarty, G., and Caldwell, H. D. (2005). Comparative genomic analysis of Chlamydia trachomatis oculotropic and genitotropic strains. Infect Immun 73, 6407.

Carmichael, J. R., Tifrea, D., Pal, S., and de la Maza, L. M. (2013). Differences in infectivity and induction of infertility: a comparative study of Chlamydia trachomatis strains in the murine model. Microbes Infect 15, 219.

Chan, Y. G., Cardwell, M. M., Hermanas, T. M., Uchiyama, T., and Martinez, J. J. (2009). Rickettsial outer-membrane protein B (rOmpB) mediates bacterial invasion through Ku70 in an actin, c-Cbl, clathrin and caveolin 2-dependent manner. Cell Microbiol 11, 629.

Charles, I. G., Li, J. L., Roberts, M., Beesley, K., Romanos, M., Pickard, D. J., Francis, M., Campbell, D., Dougan, G., Brennan, M. J., and et al. (1991). Identification and characterization of a protective immunodominant B cell epitope of pertactin (P.69) from Bordetella pertussis. Eur J Immunol 21, 1147.

Chen, Y. S., Bastidas, R. J., Saka, H. A., Carpenter, V. K., Richards, K. L., Plano, G. V., and Valdivia, R. H. (2014). The Chlamydia trachomatis type III secretion chaperone Slc1 engages multiple early effectors, including TepP, a tyrosine-phosphorylated protein required for the recruitment of CrkI-II to nascent inclusions and innate immune signaling. PLoS Pathog 10, e1003954.

Cheng, C., Pal, S., Tifrea, D., Jia, Z., and de la Maza, L. M. (2014). A vaccine formulated with a combination of TLR-2 and TLR-9 adjuvants and the recombinant major outer membrane protein elicits a robust immune response and significant protection against a Chlamydia muridarum challenge. Microbes Infect 16, 244.

Cherry, J. D., Gornbein, J., Heininger, U., and Stehr, K. (1998). A search for serologic correlates of immunity to Bordetella pertussis cough illnesses. Vaccine 16, 1901.

Clarke, I. N. (2011). Evolution of Chlamydia trachomatis. Ann N Y Acad Sci 1230, E11.

Coler, R. N., Baldwin, S. L., Shaverdian, N., Bertholet, S., Reed, S. J., Raman, V. S., Lu, X., DeVos, J., Hancock, K., Katz, J. M., Vedvick, T. S., Duthie, M. S., Clegg, C. H., Van Hoeven, N., and Reed, S. G. (2010). A synthetic adjuvant to enhance and expand immune responses to influenza vaccines. PLoS One 5, e13677.

Coler, R. N., Bertholet, S., Moutaftsi, M., Guderian, J. A., Windish, H. P., Baldwin, S. L., Laughlin, E. M., Duthie, M. S., Fox, C. B., Carter, D., Friede, M., Vedvick, T. S., and Reed, S. G. (2011). Development and characterization of synthetic glucopyranosyl lipid adjuvant system as a vaccine adjuvant. PLoS One 6, e16333.

Collier, L. H., Blyth, W. A., Larin, N. M., and Treharne, J. (1967). Immunogenicity of experimental trachoma vaccines in baboons: III. Experiments with inactivated vaccines. J Hyg (Lond) 65, 97.

Comanducci, M., Bambini, S., Brunelli, B., Adu-Bobie, J., Arico, B., Capecchi, B., Giuliani, M. M., Masignani, V., Santini, L., Savino, S., Granoff, D. M., Caugant, D. A., Pizza, M., Rappuoli, R., and Mora, M. (2002). NadA, a novel vaccine candidate of Neisseria meningitidis. J Exp Med 195, 1445.

Conant, C. G., and Stephens, R. S. (2007). Chlamydia attachment to mammalian cells requires protein disulfide isomerase. Cell Microbiol 9, 222.

Coombes, B. K., and Mahony, J. B. (2001). cDNA array analysis of altered gene expression in human endothelial cells in response to Chlamydia pneumoniae infection. Infect Immun 69, 1420.

Coombes, B. K., and Mahony, J. B. (2002). Identification of MEK- and phosphoinositide 3-kinase-dependent signalling as essential events during Chlamydia pneumoniae invasion of HEp2 cells. Cell Microbiol 4, 447.

Couet, J., de Bernard, S., Loosfelt, H., Saunier, B., Milgrom, E., and Misrahi, M. (1996). Cell surface protein disulfide-isomerase is involved in the shedding of human thyrotropin receptor ectodomain. Biochemistry 35, 14800.

Cover, T. L., and Blanke, S. R. (2005). Helicobacter pylori VacA, a paradigm for toxin multifunctionality. Nat Rev Microbiol 3, 320.

Cover, T. L., Hanson, P. I., and Heuser, J. E. (1997). Acid-induced dissociation of VacA, the Helicobacter pylori vacuolating cytotoxin, reveals its pattern of assembly. J Cell Biol 138, 759.

Crane, D. D., Carlson, J. H., Fischer, E. R., Bavoil, P., Hsia, R. C., Tan, C., Kuo, C. C., and Caldwell, H. D. (2006). Chlamydia trachomatis polymorphic membrane protein D is a species-common pan-neutralizing antigen. Proc Natl Acad Sci U S A 103, 1894.

Creagh, E. M., and O'Neill, L. A. (2006). TLRs, NLRs and RLRs: a trinity of pathogen sensors that co-operate in innate immunity. Trends Immunol 27, 352.

Crowley-Nowick, P. A., Bell, M. C., Brockwell, R., Edwards, R. P., Chen, S., Partridge, E. E., and Mestecky, J. (1997). Rectal immunization for induction of specific antibody in the genital tract of women. J Clin Immunol 17, 370.

Darville, T., Andrews, C. W., Jr., Laffoon, K. K., Shymasani, W., Kishen, L. R., and Rank, R. G. (1997). Mouse strain-dependent variation in the course and outcome

of chlamydial genital tract infection is associated with differences in host response. Infect Immun 65, 3065.

Darville, T., Andrews, C. W., Jr., Sikes, J. D., Fraley, P. L., Braswell, L., and Rank, R. G. (2001a). Mouse strain-dependent chemokine regulation of the genital tract T helper cell type 1 immune response. Infect Immun 69, 7419.

Darville, T., Andrews, C. W., Jr., Sikes, J. D., Fraley, P. L., and Rank, R. G. (2001b). Early local cytokine profiles in strains of mice with different outcomes from chlamydial genital tract infection. Infect Immun 69, 3556.

Darville, T., and Hiltke, T. J. (2010). Pathogenesis of genital tract disease due to Chlamydia trachomatis. J Infect Dis 201 Suppl 2, S114.

Dautry-Varsat, A., Subtil, A., and Hackstadt, T. (2005). Recent insights into the mechanisms of Chlamydia entry. Cell Microbiol 7, 1714.

Davies, D. R., and Cohen, G. H. (1996). Interactions of protein antigens with antibodies. Proc Natl Acad Sci U S A 93, 7.

Davila, S. J., Olive, A. J., and Starnbach, M. N. (2014). Integrin alpha4beta1 is necessary for CD4^{+} T cell-mediated protection against genital Chlamydia trachomatis infection. J Immunol 192, 4284.

Davis, C. H., Raulston, J. E., and Wyrick, P. B. (2002). Protein disulfide isomerase, a component of the estrogen receptor complex, is associated with Chlamydia trachomatis serovar E attached to human endometrial epithelial cells. Infect Immun 70, 3413.

Dawson, H. D., Loveland, J. E., Pascal, G., Gilbert, J. G., Uenishi, H., Mann, K. M., Sang, Y., Zhang, J., Carvalho-Silva, D., Hunt, T., Hardy, M., Hu, Z., Zhao, S. H., Anselmo, A., Shinkai, H., Chen, C., Badaoui, B., Berman, D., Amid, C., Kay, M., Lloyd, D., Snow, C., Morozumi, T., Cheng, R. P., Bystrom, M., Kapetanovic, R., Schwartz, J. C., Kataria, R., Astley, M., Fritz, E., Steward, C., Thomas, M., Wilming, L., Toki, D., Archibald, A. L., Bed'Hom, B., Beraldi, D., Huang, T. H., Ait-Ali, T., Blecha, F., Botti, S., Freeman, T. C., Giuffra, E., Hume, D. A., Lunney, J. K., Murtaugh, M. P., Reecy, J. M., Harrow, J. L., Rogel-Gaillard, C., and Tuggle, C. K. (2013). Structural and functional annotation of the porcine immunome. BMC Genomics 14, 332.

De Clercq, E., Kalmar, I., and Vanrompay, D. (2013). Animal models for studying female genital tract infection with Chlamydia trachomatis. Infect Immun 81, 3060.

De Haan, L., and Hirst, T. R. (2004). Cholera toxin: a paradigm for multi-functional engagement of cellular mechanisms (Review). Mol Membr Biol 21, 77.

de la Maza, L. M., Pal, S., Khamesipour, A., and Peterson, E. M. (1994). Intravaginal inoculation of mice with the Chlamydia trachomatis mouse pneumonitis biovar results in infertility. Infect Immun 62, 2094.

Dessus-Babus, S., Darville, T. L., Cuozzo, F. P., Ferguson, K., and Wyrick, P. B. (2002). Differences in innate immune responses (in vitro) to HeLa cells infected with nondisseminating serovar E and disseminating serovar L2 of Chlamydia trachomatis. Infect Immun 70, 3234.

Di Tommaso, A., Saletti, G., Pizza, M., Rappuoli, R., Dougan, G., Abrignani, S., Douce, G., and De Magistris, M. T. (1996). Induction of antigen-specific antibodies in vaginal secretions by using a nontoxic mutant of heat-labile enterotoxin as a mucosal adjuvant. Infect Immun 64, 974.

Didierlaurent, A. M., Morel, S., Lockman, L., Giannini, S. L., Bisteau, M., Carlsen, H., Kielland, A., Vosters, O., Vanderheyde, N., Schiavetti, F., Larocque, D., Van Mechelen, M., and Garcon, N. (2009). AS04, an aluminum salt- and TLR4 agonist-based adjuvant system, induces a transient localized innate immune response leading to enhanced adaptive immunity. J Immunol 183, 6186.

Dong-Ji, Z., Yang, X., Shen, C., Lu, H., Murdin, A., and Brunham, R. C. (2000). Priming with Chlamydia trachomatis major outer membrane protein (MOMP) DNA followed by MOMP ISCOM boosting enhances protection and is associated with increased immunoglobulin A and Th1 cellular immune responses. Infect Immun 68, 3074.

Donovan, P. (1997). Confronting a hidden epidemic: the Institute of Medicine's report on sexually transmitted diseases. Fam Plann Perspect 29, 87.

Draper, E., Bissett, S. L., Howell-Jones, R., Waight, P., Soldan, K., Jit, M., Andrews, N., Miller, E., and Beddows, S. (2013). A randomized, observer-blinded immunogenicity trial of Cervarix((R)) and Gardasil((R)) Human Papillomavirus vaccines in 12-15 year old girls. PLoS One 8, e61825.

Dutton, R. J., Boyd, D., Berkmen, M., and Beckwith, J. (2008). Bacterial species exhibit diversity in their mechanisms and capacity for protein disulfide bond formation. Proc Natl Acad Sci U S A 105, 11933.

Eko, F. O., He, Q., Brown, T., McMillan, L., Ifere, G. O., Ananaba, G. A., Lyn, D., Lubitz, W., Kellar, K. L., Black, C. M., and Igietseme, J. U. (2004). A novel recombinant multisubunit vaccine against Chlamydia. J Immunol 173, 3375.

El-Sayed, N. M., Hegde, P., Quackenbush, J., Melville, S. E., and Donelson, J. E. (2000). The African trypanosome genome. Int J Parasitol 30, 329.

Emsley, P., Charles, I. G., Fairweather, N. F., and Isaacs, N. W. (1996). Structure of Bordetella pertussis virulence factor P.69 pertactin. Nature 381, 90.

Eriks, I. S., Palmer, G. H., McGuire, T. C., Allred, D. R., and Barbet, A. F. (1989). Detection and quantitation of Anaplasma marginale in carrier cattle by using a nucleic acid probe. J Clin Microbiol 27, 279.

Eriksson, K., Quiding-Jarbrink, M., Osek, J., Moller, A., Bjork, S., Holmgren, J., and Czerkinsky, C. (1998). Specific-antibody-secreting cells in the rectums and

genital tracts of nonhuman primates following vaccination. Infect Immun 66, 5889.

Ernst, R. K., Yi, E. C., Guo, L., Lim, K. B., Burns, J. L., Hackett, M., and Miller, S. I. (1999). Specific lipopolysaccharide found in cystic fibrosis airway Pseudomonas aeruginosa. Science 286, 1561.

Everest, P., Li, J., Douce, G., Charles, I., De Azavedo, J., Chatfield, S., Dougan, G., and Roberts, M. (1996). Role of the Bordetella pertussis P.69/pertactin protein and the P.69/pertactin RGD motif in the adherence to and invasion of mammalian cells. Microbiology 142 (Pt 11), 3261.

Everett, K. D., and Hatch, T. P. (1995). Architecture of the cell envelope of Chlamydia psittaci 6BC. J Bacteriol 177, 877.

Feener, E. P., Shen, W. C., and Ryser, H. J. (1990). Cleavage of disulfide bonds in endocytosed macromolecules. A processing not associated with lysosomes or endosomes. J Biol Chem 265, 18780.

Feng, H. M., Whitworth, T., Olano, J. P., Popov, V. L., and Walker, D. H. (2004a). Fc-dependent polyclonal antibodies and antibodies to outer membrane proteins A and B, but not to lipopolysaccharide, protect SCID mice against fatal Rickettsia conorii infection. Infect Immun 72, 2222.

Feng, H. M., Whitworth, T., Popov, V., and Walker, D. H. (2004b). Effect of antibody on the rickettsia-host cell interaction. Infect Immun 72, 3524.

Fields, K. A., and Hackstadt, T. (2000). Evidence for the secretion of Chlamydia trachomatis CopN by a type III secretion mechanism. Mol Microbiol 38, 1048.

Fields, K. A., Mead, D. J., Dooley, C. A., and Hackstadt, T. (2003). Chlamydia trachomatis type III secretion: evidence for a functional apparatus during early-cycle development. Mol Microbiol 48, 671.

Finco, O., Frigimelica, E., Buricchi, F., Petracca, R., Galli, G., Faenzi, E., Meoni, E., Bonci, A., Agnusdei, M., Nardelli, F., Bartolini, E., Scarselli, M., Caproni, E., Laera, D., Zedda, L., Skibinski, D., Giovinazzi, S., Bastone, R., Ianni, E., Cevenini, R., Grandi, G., and Grifantini, R. (2011). Approach to discover T- and B cell antigens of intracellular pathogens applied to the design of Chlamydia trachomatis vaccines. Proc Natl Acad Sci U S A 108, 9969.

Finne, J., Bitter-Suermann, D., Goridis, C., and Finne, U. (1987). An IgG monoclonal antibody to group B meningococci cross-reacts with developmentally regulated polysialic acid units of glycoproteins in neural and extraneural tissues. J Immunol 138, 4402.

Fisseha, M., Chen, P., Brandt, B., Kijek, T., Moran, E., and Zollinger, W. (2005). Characterization of native outer membrane vesicles from lpxL mutant strains of Neisseria meningitidis for use in parenteral vaccination. Infect Immun 73, 4070.

Fox, C. B., Baldwin, S. L., Duthie, M. S., Reed, S. G., and Vedvick, T. S. (2011). Immunomodulatory and physical effects of oil composition in vaccine adjuvant emulsions. Vaccine 29, 9563.

Fraser, C. M., Norris, S. J., Weinstock, G. M., White, O., Sutton, G. G., Dodson, R., Gwinn, M., Hickey, E. K., Clayton, R., Ketchum, K. A., Sodergren, E., Hardham, J. M., McLeod, M. P., Salzberg, S., Peterson, J., Khalak, H., Richardson, D., Howell, J. K., Chidambaram, M., Utterback, T., McDonald, L., Artiach, P., Bowman, C., Cotton, M. D., Fujii, C., Garland, S., Hatch, B., Horst, K., Roberts, K., Sandusky, M., Weidman, J., Smith, H. O., and Venter, J. C. (1998). Complete genome sequence of Treponema pallidum, the syphilis spirochete. Science 281, 375.

Fujikawa, A., Shirasaka, D., Yamamoto, S., Ota, H., Yahiro, K., Fukada, M., Shintani, T., Wada, A., Aoyama, N., Hirayama, T., Fukamachi, H., and Noda, M. (2003). Mice deficient in protein tyrosine phosphatase receptor type Z are resistant to gastric ulcer induction by VacA of Helicobacter pylori. Nat Genet 33, 375.

Garner, J. A., and Cover, T. L. (1996). Binding and internalization of the Helicobacter pylori vacuolating cytotoxin by epithelial cells. Infect Immun 64, 4197.

Gebert, B., Fischer, W., Weiss, E., Hoffmann, R., and Haas, R. (2003). Helicobacter pylori vacuolating cytotoxin inhibits T lymphocyte activation. Science 301, 1099.

Gerhard, M., Lehn, N., Neumayer, N., Boren, T., Rad, R., Schepp, W., Miehlke, S., Classen, M., and Prinz, C. (1999). Clinical relevance of the Helicobacter pylori gene for blood-group antigen-binding adhesin. Proc Natl Acad Sci U S A 96, 12778.

Giannini, S. L., Hanon, E., Moris, P., Van Mechelen, M., Morel, S., Dessy, F., Fourneau, M. A., Colau, B., Suzich, J., Losonksy, G., Martin, M. T., Dubin, G., and Wettendorff, M. A. (2006). Enhanced humoral and memory B cellular immunity using HPV16/18 L1 VLP vaccine formulated with the MPL/aluminium salt combination (AS04) compared to aluminium salt only. Vaccine 24, 5937.

Giuliani, M. M., Santini, L., Brunelli, B., Biolchi, A., Arico, B., Di Marcello, F., Cartocci, E., Comanducci, M., Masignani, V., Lozzi, L., Savino, S., Scarselli, M., Rappuoli, R., and Pizza, M. (2005). The region comprising amino acids 100 to 255 of Neisseria meningitidis lipoprotein GNA 1870 elicits bactericidal antibodies. Infect Immun 73, 1151.

Gomes, J. P., Bruno, W. J., Nunes, A., Santos, N., Florindo, C., Borrego, M. J., and Dean, D. (2007). Evolution of Chlamydia trachomatis diversity occurs by widespread interstrain recombination involving hotspots. Genome Res 17, 50.

Gomes, J. P., Nunes, A., Bruno, W. J., Borrego, M. J., Florindo, C., and Dean, D. (2006). Polymorphisms in the nine polymorphic membrane proteins of Chlamydia trachomatis across all serovars: evidence for serovar Da recombination and correlation with tissue tropism. J Bacteriol 188, 275.

Goodall, J. C., Yeo, G., Huang, M., Raggiaschi, R., and Gaston, J. S. (2001). Identification of Chlamydia trachomatis antigens recognized by human CD4$^+$ T lymphocytes by screening an expression library. Eur J Immunol 31, 1513.

Goodhew, E. B., Priest, J. W., Moss, D. M., Zhong, G., Munoz, B., Mkocha, H., Martin, D. L., West, S. K., Gaydos, C., and Lammie, P. J. (2012). CT694 and pgp3 as serological tools for monitoring trachoma programs. PLoS Negl Trop Dis 6, e1873.

Gottlieb, S. L., Martin, D. H., Xu, F., Byrne, G. I., and Brunham, R. C. (2010). Summary: The natural history and immunobiology of Chlamydia trachomatis genital infection and implications for Chlamydia control. J Infect Dis 201 Suppl 2, S190.

Grewe, M. (2001). Chronological ageing and photoageing of dendritic cells. Clin Exp Dermatol 26, 608.

Grimwood, J., and Stephens, R. S. (1999). Computational analysis of the polymorphic membrane protein superfamily of Chlamydia trachomatis and Chlamydia pneumoniae. Microb Comp Genomics 4, 187.

Guo, L., Lim, K. B., Gunn, J. S., Bainbridge, B., Darveau, R. P., Hackett, M., and Miller, S. I. (1997). Regulation of lipid A modifications by Salmonella typhimurium virulence genes phoP-phoQ. Science 276, 250.

Haase, H., Pagel, I., Khalina, Y., Zacharzowsky, U., Person, V., Lutsch, G., Petzhold, D., Kott, M., Schaper, J., and Morano, I. (2004). The carboxyl-terminal ahnak domain induces actin bundling and stabilizes muscle contraction. FASEB J 18, 839.

Hackstadt, T., Scidmore-Carlson, M. A., Shaw, E. I., and Fischer, E. R. (1999). The Chlamydia trachomatis IncA protein is required for homotypic vesicle fusion. Cell Microbiol 1, 119.

Hackstadt, T., Todd, W. J., and Caldwell, H. D. (1985). Disulfide-mediated interactions of the chlamydial major outer membrane protein: role in the differentiation of chlamydiae? J Bacteriol 161, 25.

Hajjar, A. M., Ernst, R. K., Tsai, J. H., Wilson, C. B., and Miller, S. I. (2002). Human Toll-like receptor 4 recognizes host-specific LPS modifications. Nat Immunol 3, 354.

Hamburger, Z. A., Brown, M. S., Isberg, R. R., and Bjorkman, P. J. (1999). Crystal structure of invasin: a bacterial integrin-binding protein. Science 286, 291.

Hanwell, M. D., Curtis, D. E., Lonie, D. C., Vandermeersch, T., Zurek, E., and Hutchison, G. R. (2012). Avogadro: an advanced semantic chemical editor, visualization, and analysis platform. J Cheminform 4, 17.

Harris, S. R., Clarke, I. N., Seth-Smith, H. M., Solomon, A. W., Cutcliffe, L. T., Marsh, P., Skilton, R. J., Holland, M. J., Mabey, D., Peeling, R. W., Lewis, D. A., Spratt, B. G.,

Unemo, M., Persson, K., Bjartling, C., Brunham, R., de Vries, H. J., Morré, S. A., Speksnijder, A., Bébéar, C. M., Clerc, M., de Barbeyrac, B., Parkhill, J., and Thomson, N. R. (2012). Whole-genome analysis of diverse Chlamydia trachomatis strains identifies phylogenetic relationships masked by current clinical typing. Nat Genet 44, 413.

Hassell, A. B., Reynolds, D. J., Deacon, M., Gaston, J. S., and Pearce, J. H. (1993). Identification of T-cell stimulatory antigens of Chlamydia trachomatis using synovial fluid-derived T-cell clones. Immunology 79, 513.

Hatch, T. P. (1996). Disulfide cross-linked envelope proteins: the functional equivalent of peptidoglycan in chlamydiae? J Bacteriol 178, 1.

Hatch, T. P., Allan, I., and Pearce, J. H. (1984). Structural and polypeptide differences between envelopes of infective and reproductive life cycle forms of Chlamydia spp. J Bacteriol 157, 13.

Hatch, T. P., Miceli, M., and Sublett, J. E. (1986). Synthesis of disulfide-bonded outer membrane proteins during the developmental cycle of Chlamydia psittaci and Chlamydia trachomatis. J Bacteriol 165, 379.

Hauck, C. R., and Meyer, T. F. (1997). The lysosomal/phagosomal membrane protein h-lamp-1 is a target of the IgA1 protease of Neisseria gonorrhoeae. FEBS Lett 405, 86.

Hawkins, R. A., Rank, R. G., and Kelly, K. A. (2002). A Chlamydia trachomatis-specific Th2 clone does not provide protection against a genital infection and displays reduced trafficking to the infected genital mucosa. Infect Immun 70, 5132.

Haynes, L. (2005). The effect of aging on cognate function and development of immune memory. Curr Opin Immunol 17, 476.

Hedges, S. R., Mayo, M. S., Kallman, L., Mestecky, J., Hook, E. W., 3rd, and Russell, M. W. (1998). Evaluation of immunoglobulin A1 (IgA1) protease and IgA1 protease-inhibitory activity in human female genital infection with Neisseria gonorrhoeae. Infect Immun 66, 5826.

Hemmi, H., Kaisho, T., Takeuchi, O., Sato, S., Sanjo, H., Hoshino, K., Horiuchi, T., Tomizawa, H., Takeda, K., and Akira, S. (2002). Small anti-viral compounds activate immune cells via the TLR7 MyD88-dependent signaling pathway. Nat Immunol 3, 196.

Henderson, I. R., Navarro-Garcia, F., and Nataro, J. P. (1998). The great escape: structure and function of the autotransporter proteins. Trends Microbiol 6, 370.

Hess, S., Rheinheimer, C., Tidow, F., Bartling, G., Kaps, C., Lauber, J., Buer, J., and Klos, A. (2001). The reprogrammed host: Chlamydia trachomatis-induced up-regulation of glycoprotein 130 cytokines, transcription factors, and antiapoptotic genes. Arthritis Rheum 44, 2392.

Hewlett, E. L., and Halperin, S. A. (1998). Serological correlates of immunity to Bordetella pertussis. Vaccine 16, 1899.

Hillman, R. D., Jr., Baktash, Y. M., and Martinez, J. J. (2013). OmpA-mediated rickettsial adherence to and invasion of human endothelial cells is dependent upon interaction with alpha2beta1 integrin. Cell Microbiol 15, 727.

Hocking, J. S., Kong, F. Y., Timms, P., Huston, W. M., and Tabrizi, S. N. (2015). Treatment of rectal chlamydia infection may be more complicated than we originally thought. J Antimicrob Chemother 70, 961.

Hohaus, A., Person, V., Behlke, J., Schaper, J., Morano, I., and Haase, H. (2002). The carboxyl-terminal region of ahnak provides a link between cardiac L-type Ca2+ channels and the actin-based cytoskeleton. FASEB J 16, 1205.

Hoiczyk, E., Roggenkamp, A., Reichenbecher, M., Lupas, A., and Heesemann, J. (2000). Structure and sequence analysis of Yersinia YadA and Moraxella UspAs reveal a novel class of adhesins. EMBO J 19, 5989.

Holland, M. J., Bailey, R. L., Conway, D. J., Culley, F., Miranpuri, G., Byrne, G. I., Whittle, H. C., and Mabey, D. C. (1996). T helper type-1 (Th1)/Th2 profiles of peripheral blood mononuclear cells (PBMC); responses to antigens of Chlamydia trachomatis in subjects with severe trachomatous scarring. Clin Exp Immunol 105, 429.

Hoshino, K., Takeuchi, O., Kawai, T., Sanjo, H., Ogawa, T., Takeda, Y., Takeda, K., and Akira, S. (1999). Cutting edge: Toll-like receptor 4 (TLR4)-deficient mice are hyporesponsive to lipopolysaccharide: evidence for TLR4 as the Lps gene product. J Immunol 162, 3749.

Hower, S., Wolf, K., and Fields, K. A. (2009). Evidence that CT694 is a novel Chlamydia trachomatis T3S substrate capable of functioning during invasion or early cycle development. Mol Microbiol 72, 1423.

Hu, V. H., Holland, M. J., and Burton, M. J. (2013). Trachoma: protective and pathogenic ocular immune responses to Chlamydia trachomatis. PLoS Negl Trop Dis 7, e2020.

Huang, C. C., Tang, M., Zhang, M. Y., Majeed, S., Montabana, E., Stanfield, R. L., Dimitrov, D. S., Korber, B., Sodroski, J., Wilson, I. A., Wyatt, R., and Kwong, P. D. (2005). Structure of a V3-containing HIV-1 gp120 core. Science 310, 1025.

Hubbell, J. A., Thomas, S. N., and Swartz, M. A. (2009). Materials engineering for immunomodulation. Nature 462, 449.

Igietseme, J. U., Ananaba, G. A., Bolier, J., Bowers, S., Moore, T., Belay, T., Eko, F. O., Lyn, D., and Black, C. M. (2000). Suppression of endogenous IL-10 gene expression in dendritic cells enhances antigen presentation for specific Th1 induction: potential for cellular vaccine development. J Immunol 164, 4212.

Igietseme, J. U., Eko, F. O., He, Q., and Black, C. M. (2004). Antibody regulation of Tcell immunity: implications for vaccine strategies against intracellular pathogens. Expert Rev Vaccines 3, 23.

Igietseme, J. U., Ramsey, K. H., Magee, D. M., Williams, D. M., Kincy, T. J., and Rank, R. G. (1993). Resolution of murine chlamydial genital infection by the adoptive transfer of a biovar-specific, Th1 lymphocyte clone. Reg Immunol 5, 317.

Inaba, K., Takahashi, Y. H., Ito, K., and Hayashi, S. (2006). Critical role of a thiolate-quinone charge transfer complex and its adduct form in de novo disulfide bond generation by DsbB. Proc Natl Acad Sci U S A 103, 287.

Jacob, C. O., Lee, S. K., and Strassmann, G. (1996). Mutational analysis of TNF-alpha gene reveals a regulatory role for the 3'-untranslated region in the genetic predisposition to lupus-like autoimmune disease. J Immunol 156, 3043.

Jain, S., McGinnes, L. W., and Morrison, T. G. (2007). Thiol/disulfide exchange is required for membrane fusion directed by the Newcastle disease virus fusion protein. J Virol 81, 2328.

Jansen, C., Wiese, A., Reubsaet, L., Dekker, N., de Cock, H., Seydel, U., and Tommassen, J. (2000). Biochemical and biophysical characterization of in vitro folded outer membrane porin PorA of Neisseria meningitidis. Biochim Biophys Acta 1464, 284.

Jewett, T. J., Dooley, C. A., Mead, D. J., and Hackstadt, T. (2008). Chlamydia trachomatis tarp is phosphorylated by src family tyrosine kinases. Biochem Biophys Res Commun 371, 339.

Jewett, T. J., Fischer, E. R., Mead, D. J., and Hackstadt, T. (2006). Chlamydial TARP is a bacterial nucleator of actin. Proc Natl Acad Sci U S A 103, 15599.

Jewett, T. J., Miller, N. J., Dooley, C. A., and Hackstadt, T. (2010). The conserved Tarp actin binding domain is important for chlamydial invasion. PLoS Pathog 6, e1000997.

Johannsen, D. B., Johnston, D. M., Koymen, H. O., Cohen, M. S., and Cannon, J. G. (1999). A Neisseria gonorrhoeae immunoglobulin A1 protease mutant is infectious in the human challenge model of urethral infection. Infect Immun 67, 3009.

Johansson, E. L., Rask, C., Fredriksson, M., Eriksson, K., Czerkinsky, C., and Holmgren, J. (1998). Antibodies and antibody-secreting cells in the female genital tract after vaginal or intranasal immunization with cholera toxin B subunit or conjugates. Infect Immun 66, 514.

Johansson, E. L., Rudin, A., Wassen, L., and Holmgren, J. (1999). Distribution of lymphocytes and adhesion molecules in human cervix and vagina. Immunology 96, 272.

Johansson, E. L., Wassen, L., Holmgren, J., Jertborn, M., and Rudin, A. (2001). Nasal and vaginal vaccinations have differential effects on antibody responses in vaginal and cervical secretions in humans. Infect Immun 69, 7481.

Johansson, M., Schon, K., Ward, M., and Lycke, N. (1997). Genital tract infection with Chlamydia trachomatis fails to induce protective immunity in gamma interferon receptor-deficient mice despite a strong local immunoglobulin A response. Infect Immun 65, 1032.

Johnson, C. M., and Fisher, D. J. (2013). Site-specific, insertional inactivation of incA in Chlamydia trachomatis using a group II intron. PLoS One 8, e83989.

Johnson, R. M., Yu, H., Kerr, M. S., Slaven, J. E., Karunakaran, K. P., and Brunham, R. C. (2012). PmpG303-311, a protective vaccine epitope that elicits persistent cellular immune responses in Chlamydia muridarum-immune mice. Infect Immun 80, 2204.

Jurk, M., Heil, F., Vollmer, J., Schetter, C., Krieg, A. M., Wagner, H., Lipford, G., and Bauer, S. (2002). Human TLR7 or TLR8 independently confer responsiveness to the antiviral compound R-848. Nat Immunol 3, 499.

Kalman, S., Mitchell, W., Marathe, R., Lammel, C., Fan, J., Hyman, R. W., Olinger, L., Grimwood, J., Davis, R. W., and Stephens, R. S. (1999). Comparative genomes of Chlamydia pneumoniae and C. trachomatis. Nat Genet 21, 385.

Kang, H. J., Coulibaly, F., Clow, F., Proft, T., and Baker, E. N. (2007). Stabilizing isopeptide bonds revealed in gram-positive bacterial pilus structure. Science 318, 1625.

Kantele, A., Hakkinen, M., Moldoveanu, Z., Lu, A., Savilahti, E., Alvarez, R. D., Michalek, S., and Mestecky, J. (1998). Differences in immune responses induced by oral and rectal immunizations with Salmonella typhi Ty21a: evidence for compartmentalization within the common mucosal immune system in humans. Infect Immun 66, 5630.

Kari, L., Bakios, L. E., Goheen, M. M., Bess, L. N., Watkins, H. S., Southern, T. R., Song, L., Whitmire, W. M., Olivares-Zavaleta, N., and Caldwell, H. D. (2013). Antibody signature of spontaneous clearance of Chlamydia trachomatis ocular infection and partial resistance against re-challenge in a nonhuman primate trachoma model. PLoS Negl Trop Dis 7, e2248.

Kari, L., Goheen, M. M., Randall, L. B., Taylor, L. D., Carlson, J. H., Whitmire, W. M., Virok, D., Rajaram, K., Endresz, V., McClarty, G., Nelson, D. E., and Caldwell, H. D. (2011). Generation of targeted Chlamydia trachomatis null mutants. Proc Natl Acad Sci U S A 108, 7189.

Kari, L., Southern, T. R., Downey, C. J., Watkins, H. S., Randall, L. B., Taylor, L. D., Sturdevant, G. L., Whitmire, W. M., and Caldwell, H. D. (2014). Chlamydia trachomatis polymorphic membrane protein D is a virulence factor involved in early host-cell interactions. Infect Immun 82, 2756.

Karunakaran, K. P., Rey-Ladino, J., Stoynov, N., Berg, K., Shen, C., Jiang, X., Gabel, B. R., Yu, H., Foster, L. J., and Brunham, R. C. (2008). Immunoproteomic discovery of novel T cell antigens from the obligate intracellular pathogen Chlamydia. J Immunol 180, 2459.

Karunakaran, K. P., Yu, H., Jiang, X., Chan, Q., Moon, K. M., Foster, L. J., and Brunham, R. C. (2015). Outer membrane proteins preferentially load MHC class II peptides: implications for a Chlamydia trachomatis T cell vaccine. Vaccine 33, 2159.

Kasturi, S. P., Skountzou, I., Albrecht, R. A., Koutsonanos, D., Hua, T., Nakaya, H. I., Ravindran, R., Stewart, S., Alam, M., Kwissa, M., Villinger, F., Murthy, N., Steel, J., Jacob, J., Hogan, R. J., Garcia-Sastre, A., Compans, R., and Pulendran, B. (2011). Programming the magnitude and persistence of antibody responses with innate immunity. Nature 470, 543.

Keating, S. M., Bejon, P., Berthoud, T., Vuola, J. M., Todryk, S., Webster, D. P., Dunachie, S. J., Moorthy, V. S., McConkey, S. J., Gilbert, S. C., and Hill, A. V. (2005). Durable human memory T cells quantifiable by cultured enzyme-linked immunospot assays are induced by heterologous prime boost immunization and correlate with protection against malaria. J Immunol 175, 5675.

Kemege, K. E., Hickey, J. M., Lovell, S., Battaile, K. P., Zhang, Y., and Hefty, P. S. (2011). Ab initio structural modeling of and experimental validation for Chlamydia trachomatis protein CT296 reveal structural similarity to Fe(II) 2-oxoglutarate-dependent enzymes. J Bacteriol 193, 6517.

Kester, K. E., Cummings, J. F., Ofori-Anyinam, O., Ockenhouse, C. F., Krzych, U., Moris, P., Schwenk, R., Nielsen, R. A., Debebe, Z., Pinelis, E., Juompan, L., Williams, J., Dowler, M., Stewart, V. A., Wirtz, R. A., Dubois, M. C., Lievens, M., Cohen, J., Ballou, W. R., Heppner, D. G., Jr., and Rts, S. V. E. G. (2009). Randomized, double-blind, phase 2a trial of falciparum malaria vaccines RTS,S/AS01B and RTS,S/AS02A in malaria-naive adults: safety, efficacy, and immunologic associates of protection. J Infect Dis 200, 337.

Khuri, S., Bakker, F. T., and Dunwell, J. M. (2001). Phylogeny, function, and evolution of the cupins, a structurally conserved, functionally diverse superfamily of proteins. Mol Biol Evol 18, 593.

Kieser, S. T., Eriks, I. S., and Palmer, G. H. (1990). Cyclic rickettsemia during persistent Anaplasma marginale infection of cattle. Infect Immun 58, 1117.

Kilian, M., Reinholdt, J., Lomholt, H., Poulsen, K., and Frandsen, E. V. (1996). Biological significance of IgA1 proteases in bacterial colonization and pathogenesis: critical evaluation of experimental evidence. APMIS 104, 321.

Kimani, J., Maclean, I. W., Bwayo, J. J., MacDonald, K., Oyugi, J., Maitha, G. M., Peeling, R. W., Cheang, M., Nagelkerke, N. J., Plummer, F. A., and Brunham, R. C. (1996). Risk factors for Chlamydia trachomatis pelvic inflammatory disease among sex workers in Nairobi, Kenya. J Infect Dis 173, 1437.

Kiselev, A. O., Skinner, M. C., and Lampe, M. F. (2009). Analysis of pmpD expression and PmpD post-translational processing during the life cycle of Chlamydia trachomatis serovars A, D, and L2. PLoS One 4, e5191.

Klappa, P., Hawkins, H. C., and Freedman, R. B. (1997). Interactions between protein disulphide isomerase and peptides. Eur J Biochem 248, 37.

Klemm, P., Hjerrild, L., Gjermansen, M., and Schembri, M. A. (2004). Structure-function analysis of the self-recognizing Antigen 43 autotransporter protein from Escherichia coli. Mol Microbiol 51, 283.

Klinman, D. M., Currie, D., Gursel, I., and Verthelyi, D. (2004). Use of CpG oligodeoxynucleotides as immune adjuvants. Immunol Rev 199, 201.

Kobayashi, J., and Matsuura, Y. (2013). Structural basis for cell-cycle-dependent nuclear import mediated by the karyopherin Kap121p. J Mol Biol 425, 1852.

Kong, F. Y., Tabrizi, S. N., Fairley, C. K., Vodstrcil, L. A., Huston, W. M., Chen, M., Bradshaw, C., and Hocking, J. S. (2015). The efficacy of azithromycin and doxycycline for the treatment of rectal chlamydia infection: a systematic review and meta-analysis. J Antimicrob Chemother 70, 1290.

Koretke, K. K., Szczesny, P., Gruber, M., and Lupas, A. N. (2006). Model structure of the prototypical non-fimbrial adhesin YadA of Yersinia enterocolitica. J Struct Biol 155, 154.

Kozlowski, P. A., Williams, S. B., Lynch, R. M., Flanigan, T. P., Patterson, R. R., Cu-Uvin, S., and Neutra, M. R. (2002). Differential induction of mucosal and systemic antibody responses in women after nasal, rectal, or vaginal immunization: influence of the menstrual cycle. J Immunol 169, 566.

Kuipers, E. J., Uyterlinde, A. M., Pena, A. S., Roosendaal, R., Pals, G., Nelis, G. F., Festen, H. P., and Meuwissen, S. G. (1995). Long-term sequelae of Helicobacter pylori gastritis. Lancet 345, 1525.

Kurosu, M., and Begari, E. (2010). Vitamin K2 in electron transport system: are enzymes involved in vitamin K2 biosynthesis promising drug targets? Molecules 15, 1531.

Landel, C. C., Kushner, P. J., and Greene, G. L. (1995). Estrogen receptor accessory proteins: effects on receptor-DNA interactions. Environ Health Perspect 103 Suppl 7, 23.

Lee, B. J., Cansizoglu, A. E., Suel, K. E., Louis, T. H., Zhang, Z., and Chook, Y. M. (2006). Rules for nuclear localization sequence recognition by karyopherin beta 2. Cell 126, 543.

Levie, K., Gjorup, I., Skinhoj, P., and Stoffel, M. (2002). A 2-dose regimen of a recombinant hepatitis B vaccine with the immune stimulant AS04 compared with the standard 3-dose regimen of Engerix-B in healthy young adults. Scand J Infect Dis 34, 610.

Leyton, D. L., Sevastsyanovich, Y. R., Browning, D. F., Rossiter, A. E., Wells, T. J., Fitzpatrick, R. E., Overduin, M., Cunningham, A. F., and Henderson, I. R. (2011). Size and conformation limits to secretion of disulfide-bonded loops in autotransporter proteins. J Biol Chem 286, 42283.

Li, L., Saade, F., and Petrovsky, N. (2012). The future of human DNA vaccines. J Biotechnol 162, 171.

Li, L. X., and McSorley, S. J. (2013). B cells enhance antigen-specific CD4 T cell priming and prevent bacteria dissemination following Chlamydia muridarum genital tract infection. PLoS Pathog 9, e1003707.

Lichtenwalner, A. B., Patton, D. L., Van Voorhis, W. C., Sweeney, Y. T., and Kuo, C. C. (2004). Heat shock protein 60 is the major antigen which stimulates delayed-type hypersensitivity reaction in the macaque model of Chlamydia trachomatis salpingitis. Infect Immun 72, 1159.

Liechti, G. W., Kuru, E., Hall, E., Kalinda, A., Brun, Y. V., VanNieuwenhze, M., and Maurelli, A. T. (2014). A new metabolic cell-wall labelling method reveals peptidoglycan in Chlamydia trachomatis. Nature 506, 507.

Lin, H. S., and Moulder, J. W. (1966). Patterns of response to sulfadiazine, D-cycloserine and D-alanine in members of the psittacosis group. J Infect Dis 116, 372.

Lin, L., Ayala, P., Larson, J., Mulks, M., Fukuda, M., Carlsson, S. R., Enns, C., and So, M. (1997). The Neisseria type 2 IgA1 protease cleaves LAMP1 and promotes survival of bacteria within epithelial cells. Mol Microbiol 24, 1083.

Ling, H., Boodhoo, A., Hazes, B., Cummings, M. D., Armstrong, G. D., Brunton, J. L., and Read, R. J. (1998). Structure of the shiga-like toxin I B-pentamer complexed with an analogue of its receptor Gb3. Biochemistry 37, 1777.

Lo, C. C., Xie, G., Bonner, C. A., and Jensen, R. A. (2012). The alternative translational profile that underlies the immune-evasive state of persistence in Chlamydiaceae exploits differential tryptophan contents of the protein repertoire. Microbiol Mol Biol Rev 76, 405.

Longbottom, D., and Coulter, L. J. (2003). Animal chlamydioses and zoonotic implications. J Comp Pathol 128, 217.

Lorenzen, D. R., Dux, F., Wolk, U., Tsirpouchtsidis, A., Haas, G., and Meyer, T. F. (1999). Immunoglobulin A1 protease, an exoenzyme of pathogenic Neisseriae, is a potent inducer of proinflammatory cytokines. J Exp Med 190, 1049.

Lu, Y. C., Yeh, W. C., and Ohashi, P. S. (2008). LPS/TLR4 signal transduction pathway. Cytokine 42, 145.

Lutter, E. I., Barger, A. C., Nair, V., and Hackstadt, T. (2013). Chlamydia trachomatis inclusion membrane protein CT228 recruits elements of the myosin phosphatase pathway to regulate release mechanisms. Cell Rep 3, 1921.

Mac, T. T., von Hacht, A., Hung, K. C., Dutton, R. J., Boyd, D., Bardwell, J. C., and Ulmer, T. S. (2008). Insight into disulfide bond catalysis in Chlamydia from the structure and function of DsbH, a novel oxidoreductase. J Biol Chem 283, 824.

Marrack, P., McKee, A. S., and Munks, M. W. (2009). Towards an understanding of the adjuvant action of aluminium. Nat Rev Immunol 9, 287.

Marrazzo, J., and Suchland, R. (2014). Recent advances in understanding and managing Chlamydia trachomatis infections. F1000Prime Rep 6, 120.

Martin, D. L., Bid, R., Sandi, F., Goodhew, E. B., Massae, P. A., Lasway, A., Philippin, H., Makupa, W., Molina, S., Holland, M. J., Mabey, D. C., Drakeley, C., Lammie, P. J., and Solomon, A. W. (2015). Serology for trachoma surveillance after cessation of mass drug administration. PLoS Negl Trop Dis 9, e0003555.

Mascola, J. R., Stiegler, G., VanCott, T. C., Katinger, H., Carpenter, C. B., Hanson, C. E., Beary, H., Hayes, D., Frankel, S. S., Birx, D. L., and Lewis, M. G. (2000). Protection of macaques against vaginal transmission of a pathogenic HIV-1/SIV chimeric virus by passive infusion of neutralizing antibodies. Nat Med 6, 207.

McCoy, A. J., Adams, N. E., Hudson, A. O., Gilvarg, C., Leustek, T., and Maurelli, A. T. (2006). L,L-diaminopimelate aminotransferase, a trans-kingdom enzyme shared by Chlamydia and plants for synthesis of diaminopimelate/lysine. Proc Natl Acad Sci U S A 103, 17909.

McCoy, A. J., and Maurelli, A. T. (2006). Building the invisible wall: updating the chlamydial peptidoglycan anomaly. Trends Microbiol 14, 70.

Mestecky, J., Moldoveanu, Z., and Russell, M. W. (2005). Immunologic uniqueness of the genital tract: challenge for vaccine development. Am J Reprod Immunol 53, 208.

Mettens, P., Dubois, P. M., Demoitie, M. A., Bayat, B., Donner, M. N., Bourguignon, P., Stewart, V. A., Heppner, D. G., Jr., Garcon, N., and Cohen, J. (2008). Improved T cell responses to Plasmodium falciparum circumsporozoite protein in mice and monkeys induced by a novel formulation of RTS,S vaccine antigen. Vaccine 26, 1072.

Miller, E., Andrews, N., Stellitano, L., Stowe, J., Winstone, A. M., Shneerson, J., and Verity, C. (2013). Risk of narcolepsy in children and young people receiving AS03 adjuvanted pandemic A/H1N1 2009 influenza vaccine: retrospective analysis. BMJ 346, f794.

Millman, K. L., Tavare, S., and Dean, D. (2001). Recombination in the ompA gene but not the omcB gene of Chlamydia contributes to serovar-specific differences in tissue tropism, immune surveillance, and persistence of the organism. J Bacteriol 183, 5997.

Mittrucker, H. W., Steinhoff, U., Kohler, A., Krause, M., Lazar, D., Mex, P., Miekley, D., and Kaufmann, S. H. (2007). Poor correlation between BCG vaccination-

induced T cell responses and protection against tuberculosis. Proc Natl Acad Sci U S A 104, 12434.

Moelleken, K., and Hegemann, J. H. (2008). The Chlamydia outer membrane protein OmcB is required for adhesion and exhibits biovar-specific differences in glycosaminoglycan binding. Mol Microbiol 67, 403.

Molano, M., Meijer, C. J., Weiderpass, E., Arslan, A., Posso, H., Franceschi, S., Ronderos, M., Munoz, N., and van den Brule, A. J. (2005). The natural course of Chlamydia trachomatis infection in asymptomatic Colombian women: a 5-year follow-up study. J Infect Dis 191, 907.

Molestina, R. E., Miller, R. D., Ramirez, J. A., and Summersgill, J. T. (1999). Infection of human endothelial cells with Chlamydia pneumoniae stimulates transendothelial migration of neutrophils and monocytes. Infect Immun 67, 1323.

Molleken, K., Becker, E., and Hegemann, J. H. (2013). The Chlamydia pneumoniae invasin protein Pmp21 recruits the EGF receptor for host cell entry. PLoS Pathog 9, e1003325.

Molleken, K., Schmidt, E., and Hegemann, J. H. (2010). Members of the Pmp protein family of Chlamydia pneumoniae mediate adhesion to human cells via short repetitive peptide motifs. Mol Microbiol 78, 1004.

Moore, T., Ananaba, G. A., Bolier, J., Bowers, S., Belay, T., Eko, F. O., and Igietseme, J. U. (2002). Fc receptor regulation of protective immunity against Chlamydia trachomatis. Immunology 105, 213.

Moore, T., Ekworomadu, C. O., Eko, F. O., MacMillan, L., Ramey, K., Ananaba, G. A., Patrickson, J. W., Nagappan, P. R., Lyn, D., Black, C. M., and Igietseme, J. U. (2003). Fc receptor-mediated antibody regulation of T cell immunity against intracellular pathogens. J Infect Dis 188, 617.

Morre, S. A., van den Brule, A. J., Rozendaal, L., Boeke, A. J., Voorhorst, F. J., de Blok, S., and Meijer, C. J. (2002). The natural course of asymptomatic Chlamydia trachomatis infections: 45% clearance and no development of clinical PID after one-year follow-up. Int J STD AIDS 13 Suppl 2, 12.

Morrison, R. P., Feilzer, K., and Tumas, D. B. (1995). Gene knockout mice establish a primary protective role for major histocompatibility complex class II-restricted responses in Chlamydia trachomatis genital tract infection. Infect Immun 63, 4661.

Morrison, S. G., Farris, C. M., Sturdevant, G. L., Whitmire, W. M., and Morrison, R. P. (2011). Murine Chlamydia trachomatis genital infection is unaltered by depletion of CD4$^+$ T cells and diminished adaptive immunity. J Infect Dis 203, 1120.

Morrison, S. G., and Morrison, R. P. (2001). Resolution of secondary Chlamydia trachomatis genital tract infection in immune mice with depletion of both CD4$^+$ and CD8$^+$ T cells. Infect Immun 69, 2643.

Morrison, S. G., and Morrison, R. P. (2005a). A predominant role for antibody in acquired immunity to chlamydial genital tract reinfection. J Immunol 175, 7536.

Morrison, S. G., and Morrison, R. P. (2005b). The protective effect of antibody in immunity to murine chlamydial genital tract reinfection is independent of immunoglobulin A. Infect Immun 73, 6183.

Morrison, S. G., Su, H., Caldwell, H. D., and Morrison, R. P. (2000). Immunity to murine Chlamydia trachomatis genital tract reinfection involves B cells and CD4(+) T cells but not CD8 (+) T cells. Infect Immun 68, 6979.

Mougous, J. D., Cuff, M. E., Raunser, S., Shen, A., Zhou, M., Gifford, C. A., Goodman, A. L., Joachimiak, G., Ordonez, C. L., Lory, S., Walz, T., Joachimiak, A., and Mekalanos, J. J. (2006). A virulence locus of Pseudomonas aeruginosa encodes a protein secretion apparatus. Science 312, 1526.

Moulder, J. W. (1966). The relation of the psittacosis group (Chlamydiae) to bacteria and viruses. Annu Rev Microbiol 20, 107.

Mount, D. T., Bigazzi, P. E., and Barron, A. L. (1972). Infection of genital tract and transmission of ocular infection to newborns by the agent of guinea pig inclusion conjunctivitis. Infect Immun 5, 921.

Mount, D. T., Bigazzi, P. E., and Barron, A. L. (1973). Experimental genital infection of male guinea pigs with the agent of guinea pig inclusion conjunctivitis and transmission to females. Infect Immun 8, 925.

Murphy, E., Andrew, L., Lee, K. L., Dilts, D. A., Nunez, L., Fink, P. S., Ambrose, K., Borrow, R., Findlow, J., Taha, M. K., Deghmane, A. E., Kriz, P., Musilek, M., Kalmusova, J., Caugant, D. A., Alvestad, T., Mayer, L. W., Sacchi, C. T., Wang, X., Martin, D., von Gottberg, A., du Plessis, M., Klugman, K. P., Anderson, A. S., Jansen, K. U., Zlotnick, G. W., and Hoiseth, S. K. (2009). Sequence diversity of the factor H binding protein vaccine candidate in epidemiologically relevant strains of serogroup B Neisseria meningitidis. J Infect Dis 200, 379.

Murray, E. S. (1964). Guinea Pig Inclusion Conjunctivitis Virus. I. Isolation and Identification as a Member of the Psittacosis-Lymphogranuloma-Trachoma Group. J Infect Dis 114, 1.

Muschiol, S., Bailey, L., Gylfe, A., Sundin, C., Hultenby, K., Bergstrom, S., Elofsson, M., Wolf-Watz, H., Normark, S., and Henriques-Normark, B. (2006). A small-molecule inhibitor of type III secretion inhibits different stages of the infectious cycle of Chlamydia trachomatis. Proc Natl Acad Sci U S A 103, 14566.

Mutsch, M., Zhou, W., Rhodes, P., Bopp, M., Chen, R. T., Linder, T., Spyr, C., and Steffen, R. (2004). Use of the inactivated intranasal influenza vaccine and the risk of Bell's palsy in Switzerland. N Engl J Med 350, 896.

Nagele, V., Heesemann, J., Schielke, S., Jimenez-Soto, L. F., Kurzai, O., and Ackermann, N. (2011). Neisseria meningitidis adhesin NadA targets beta1 integrins: functional similarity to Yersinia invasin. J Biol Chem 286, 20536.

Nakamoto, H., and Bardwell, J. C. (2004). Catalysis of disulfide bond formation and isomerization in the Escherichia coli periplasm. Biochim Biophys Acta 1694, 111.

Nakayama, M., Kimura, M., Wada, A., Yahiro, K., Ogushi, K., Niidome, T., Fujikawa, A., Shirasaka, D., Aoyama, N., Kurazono, H., Noda, M., Moss, J., and Hirayama, T. (2004). Helicobacter pylori VacA activates the p38/activating transcription factor 2-mediated signal pathway in AZ-521 cells. J Biol Chem 279, 7024.

Nardelli-Haefliger, D., Kraehenbuhl, J. P., Curtiss, R., 3rd, Schodel, F., Potts, A., Kelly, S., and De Grandi, P. (1996). Oral and rectal immunization of adult female volunteers with a recombinant attenuated Salmonella typhi vaccine strain. Infect Immun 64, 5219.

Nedelec, J., Boucraut, J., Garnier, J. M., Bernard, D., and Rougon, G. (1990). Evidence for autoimmune antibodies directed against embryonic neural cell adhesion molecules (N-CAM) in patients with group B meningitis. J Neuroimmunol 29, 49.

Nelson, D. E., Virok, D. P., Wood, H., Roshick, C., Johnson, R. M., Whitmire, W. M., Crane, D. D., Steele-Mortimer, O., Kari, L., McClarty, G., and Caldwell, H. D. (2005). Chlamydial IFN-gamma immune evasion is linked to host infection tropism. Proc Natl Acad Sci U S A 102, 10658.

Nguyen, B. D., and Valdivia, R. H. (2012). Virulence determinants in the obligate intracellular pathogen Chlamydia trachomatis revealed by forward genetic approaches. Proc Natl Acad Sci U S A 109, 1263.

Nguyen, V. Q., Caprioli, R. M., and Cover, T. L. (2001). Carboxy-terminal proteolytic processing of Helicobacter pylori vacuolating toxin. Infect Immun 69, 543.

Nigg, C. (1942). An Unidentified Virus Which Produces Pneumonia and Systemic Infection in Mice. Science 95, 49.

Nishimura, K., Tajima, N., Yoon, Y. H., Park, S. Y., and Tame, J. R. (2010). Autotransporter passenger proteins: virulence factors with common structural themes. J Mol Med (Berl) 88, 451.

Nunes, A., Gomes, J. P., Karunakaran, K. P., and Brunham, R. C. (2015). Bioinformatic Analysis of Chlamydia trachomatis Polymorphic Membrane Proteins PmpE, PmpF, PmpG and PmpH as Potential Vaccine Antigens. PLoS One 10, e0131695.

Nunes, A., Gomes, J. P., Mead, S., Florindo, C., Correia, H., Borrego, M. J., and Dean, D. (2007). Comparative expression profiling of the Chlamydia trachomatis pmp gene family for clinical and reference strains. PLoS One 2, e878.

O'Hagan, D. T., Ott, G. S., De Gregorio, E., and Seubert, A. (2012). The mechanism of action of MF59 - an innately attractive adjuvant formulation. Vaccine 30, 4341.

O'Meara, C. P., Andrew, D. W., and Beagley, K. W. (2014). The mouse model of Chlamydia genital tract infection: a review of infection, disease, immunity and vaccine development. Curr Mol Med 14, 396.

Ohto, U., Fukase, K., Miyake, K., and Shimizu, T. (2012). Structural basis of species-specific endotoxin sensing by innate immune receptor TLR4/MD-2. Proc Natl Acad Sci U S A 109, 7421.

Okamoto, A., Higuchi, T., Hirotsu, K., Kuramitsu, S., and Kagamiyama, H. (1994). X-ray crystallographic study of pyridoxal 5'-phosphate-type aspartate aminotransferases from Escherichia coli in open and closed form. J Biochem 116, 95.

Olsen, A. W., Follmann, F., Erneholm, K., Rosenkrands, I., and Andersen, P. (2015). Protection Against Chlamydia trachomatis Infection and Upper Genital Tract Pathological Changes by Vaccine-Promoted Neutralizing Antibodies Directed to the VD4 of the Major Outer Membrane Protein. J Infect Dis.

Orr, M. T., Duthie, M. S., Windish, H. P., Lucas, E. A., Guderian, J. A., Hudson, T. E., Shaverdian, N., O'Donnell, J., Desbien, A. L., Reed, S. G., and Coler, R. N. (2013a). MyD88 and TRIF synergistic interaction is required for TH1-cell polarization with a synthetic TLR4 agonist adjuvant. Eur J Immunol 43, 2398.

Orr, M. T., Fox, C. B., Baldwin, S. L., Sivananthan, S. J., Lucas, E., Lin, S., Phan, T., Moon, J. J., Vedvick, T. S., Reed, S. G., and Coler, R. N. (2013b). Adjuvant formulation structure and composition are critical for the development of an effective vaccine against tuberculosis. J Control Release 172, 190.

Ou, W., and Silver, J. (2006). Role of protein disulfide isomerase and other thiol-reactive proteins in HIV-1 envelope protein-mediated fusion. Virology 350, 406.

Owusu-Agyei, S., Ansong, D., Asante, K., Kwarteng Owusu, S., Owusu, R., Wireko Brobby, N. A., Dosoo, D., Osei Akoto, A., Osei-Kwakye, K., Adjei, E. A., Boahen, K. O., Sylverken, J., Adjei, G., Sambian, D., Apanga, S., Kayan, K., Vekemans, J., Ofori-Anyinam, O., Leach, A., Lievens, M., Demoitie, M. A., Dubois, M. C., Cohen, J., Ballou, W. R., Savarese, B., Chandramohan, D., Gyapong, J. O., Milligan, P., Antwi, S., Agbenyega, T., Greenwood, B., and Evans, J. (2009). Randomized controlled trial of RTS,S/AS02D and RTS,S/AS01E malaria candidate vaccines given according to different schedules in Ghanaian children. PLoS One 4, e7302.

Oyewumi, M. O., Kumar, A., and Cui, Z. (2010). Nano-microparticles as immune adjuvants: correlating particle sizes and the resultant immune responses. Expert Rev Vaccines 9, 1095.

Pace, N. R. (1997). A molecular view of microbial diversity and the biosphere. Science 276, 734.

Pagliaccia, C., de Bernard, M., Lupetti, P., Ji, X., Burroni, D., Cover, T. L., Papini, E., Rappuoli, R., Telford, J. L., and Reyrat, J. M. (1998). The m2 form of the Helicobacter pylori cytotoxin has cell type-specific vacuolating activity. Proc Natl Acad Sci U S A 95, 10212.

Pais, S. V., Milho, C., Almeida, F., and Mota, L. J. (2013). Identification of novel type III secretion chaperone-substrate complexes of Chlamydia trachomatis. PLoS One 8, e56292.

Pal, S., Theodor, I., Peterson, E. M., and de la Maza, L. M. (2001). Immunization with the Chlamydia trachomatis mouse pneumonitis major outer membrane protein can elicit a protective immune response against a genital challenge. Infect Immun 69, 6240.

Palm, N. W., and Medzhitov, R. (2009). Pattern recognition receptors and control of adaptive immunity. Immunol Rev 227, 221.

Palmer, G. H. (2002). The highest priority: what microbial genomes are telling us about immunity. Vet Immunol Immunopathol 85, 1.

Palmer, G. H., Brown, W. C., and Rurangirwa, F. R. (2000). Antigenic variation in the persistence and transmission of the ehrlichia Anaplasma marginale. Microbes Infect 2, 167.

Palmer, G. H., Eid, G., Barbet, A. F., McGuire, T. C., and McElwain, T. F. (1994). The immunoprotective Anaplasma marginale major surface protein 2 is encoded by a polymorphic multigene family. Infect Immun 62, 3808.

Papini, E., Satin, B., Norais, N., de Bernard, M., Telford, J. L., Rappuoli, R., and Montecucco, C. (1998). Selective increase of the permeability of polarized epithelial cell monolayers by Helicobacter pylori vacuolating toxin. J Clin Invest 102, 813.

Park, B. S., Song, D. H., Kim, H. M., Choi, B. S., Lee, H., and Lee, J. O. (2009). The structural basis of lipopolysaccharide recognition by the TLR4-MD-2 complex. Nature 458, 1191.

Parsonnet, J., Friedman, G. D., Vandersteen, D. P., Chang, Y., Vogelman, J. H., Orentreich, N., and Sibley, R. K. (1991). Helicobacter pylori infection and the risk of gastric carcinoma. N Engl J Med 325, 1127.

Partinen, M., Saarenpaa-Heikkila, O., Ilveskoski, I., Hublin, C., Linna, M., Olsen, P., Nokelainen, P., Alen, R., Wallden, T., Espo, M., Rusanen, H., Olme, J., Satila, H., Arikka, H., Kaipainen, P., Julkunen, I., and Kirjavainen, T. (2012). Increased incidence and clinical picture of childhood narcolepsy following the 2009 H1N1 pandemic vaccination campaign in Finland. PLoS One 7, e33723.

Patton, D. L., Halbert, S. A., Kuo, C. C., Wang, S. P., and Holmes, K. K. (1983). Host response to primary Chlamydia trachomatis infection of the fallopian tube in pig-tailed monkeys. Fertil Steril 40, 829.

Patton, D. L., Kuo, C. C., Wang, S. P., Brenner, R. M., Sternfeld, M. D., Morse, S. A., and Barnes, R. C. (1987). Chlamydial infection of subcutaneous fimbrial transplants in cynomolgus and rhesus monkeys. J Infect Dis 155, 229.

Patton, D. L., Sweeney, Y. C., Rabe, L. K., and Hillier, S. L. (1996). The vaginal microflora of pig-tailed macaques and the effects of chlorhexidine and benzalkonium on this ecosystem. Sex Transm Dis 23, 489.

Patton, D. L., Sweeney, Y. T., and Paul, K. J. (2009). A summary of preclinical topical microbicide rectal safety and efficacy evaluations in a pigtailed macaque model. Sex Transm Dis 36, 350.

Peeling, R. W., Kimani, J., Plummer, F., Maclean, I., Cheang, M., Bwayo, J., and Brunham, R. C. (1997). Antibody to chlamydial hsp60 predicts an increased risk for chlamydial pelvic inflammatory disease. J Infect Dis 175, 1153.

Peipert, J. F. (2003). Clinical practice. Genital chlamydial infections. N Engl J Med 349, 2424.

Perry, L. L., Feilzer, K., and Caldwell, H. D. (1997). Immunity to Chlamydia trachomatis is mediated by T helper 1 cells through IFN-gamma-dependent and -independent pathways. J Immunol 158, 3344.

Perry, L. L., Feilzer, K., Hughes, S., and Caldwell, H. D. (1999). Clearance of Chlamydia trachomatis from the murine genital mucosa does not require perforin-mediated cytolysis or Fas-mediated apoptosis. Infect Immun 67, 1379.

Peter, N. G., Clark, L. R., and Jaeger, J. R. (2004). Fitz-Hugh-Curtis syndrome: a diagnosis to consider in women with right upper quadrant pain. Cleve Clin J Med 71, 233.

Pohlner, J., Halter, R., Beyreuther, K., and Meyer, T. F. (1987). Gene structure and extracellular secretion of Neisseria gonorrhoeae IgA protease. Nature 325, 458.

Polhemus, M. E., Remich, S. A., Ogutu, B. R., Waitumbi, J. N., Otieno, L., Apollo, S., Cummings, J. F., Kester, K. E., Ockenhouse, C. F., Stewart, A., Ofori-Anyinam, O., Ramboer, I., Cahill, C. P., Lievens, M., Dubois, M. C., Demoitie, M. A., Leach, A., Cohen, J., Ballou, W. R., and Heppner, D. G., Jr. (2009). Evaluation of RTS,S/AS02A and RTS,S/AS01B in adults in a high malaria transmission area. PLoS One 4, e6465.

Poltorak, A., He, X., Smirnova, I., Liu, M. Y., Van Huffel, C., Du, X., Birdwell, D., Alejos, E., Silva, M., Galanos, C., Freudenberg, M., Ricciardi-Castagnoli, P., Layton, B., and Beutler, B. (1998). Defective LPS signaling in C3H/HeJ and C57BL/10ScCr mice: mutations in Tlr4 gene. Science 282, 2085.

Quash, G., Roch, A. M., Niveleau, A., Grange, J., Keolouangkhot, T., and Huppert, J. (1978). The preparation of latex particles with covalently bound polyamines, IgG and measles agglutinins and their use in visual agglutination tests. J Immunol Methods 22, 165.

Querec, T. D., Akondy, R. S., Lee, E. K., Cao, W., Nakaya, H. I., Teuwen, D., Pirani, A., Gernert, K., Deng, J., Marzolf, B., Kennedy, K., Wu, H., Bennouna, S., Oluoch, H., Miller, J., Vencio, R. Z., Mulligan, M., Aderem, A., Ahmed, R., and Pulendran, B. (2009). Systems biology approach predicts immunogenicity of the yellow fever vaccine in humans. Nat Immunol 10, 116.

Ramsey, K. H., Cotter, T. W., Salyer, R. D., Miranpuri, G. S., Yanez, M. A., Poulsen, C. E., DeWolfe, J. L., and Byrne, G. I. (1999). Prior genital tract infection with a murine or human biovar of Chlamydia trachomatis protects mice against heterotypic challenge infection. Infect Immun 67, 3019.

Ramsey, K. H., and Rank, R. G. (1991). Resolution of chlamydial genital infection with antigen-specific T-lymphocyte lines. Infect Immun 59, 925.

Ramsey, K. H., Soderberg, L. S., and Rank, R. G. (1988). Resolution of chlamydial genital infection in B cell-deficient mice and immunity to reinfection. Infect Immun 56, 1320.

Rank, R. G., Soderberg, L. S., and Barron, A. L. (1985). Chronic chlamydial genital infection in congenitally athymic nude mice. Infect Immun 48, 847.

Rasmussen, S. G., Choi, H. J., Rosenbaum, D. M., Kobilka, T. S., Thian, F. S., Edwards, P. C., Burghammer, M., Ratnala, V. R., Sanishvili, R., Fischetti, R. F., Schertler, G. F., Weis, W. I., and Kobilka, B. K. (2007). Crystal structure of the human beta2 adrenergic G-protein-coupled receptor. Nature 450, 383.

Rasmussen, S. J., Eckmann, L., Quayle, A. J., Shen, L., Zhang, Y. X., Anderson, D. J., Fierer, J., Stephens, R. S., and Kagnoff, M. F. (1997). Secretion of proinflammatory cytokines by epithelial cells in response to Chlamydia infection suggests a central role for epithelial cells in chlamydial pathogenesis. J Clin Invest 99, 77.

Rau, A., Wyllie, S., Whittimore, J., and Raulston, J. E. (2005). Identification of Chlamydia trachomatis genomic sequences recognized by chlamydial divalent cation-dependent regulator A (DcrA). J Bacteriol 187, 443.

Reece, W. H., Pinder, M., Gothard, P. K., Milligan, P., Bojang, K., Doherty, T., Plebanski, M., Akinwunmi, P., Everaere, S., Watkins, K. R., Voss, G., Tornieporth, N., Alloueche, A., Greenwood, B. M., Kester, K. E., McAdam, K. P., Cohen, J., and Hill, A. V. (2004). A CD4(+) T-cell immune response to a conserved epitope in the circumsporozoite protein correlates with protection from natural Plasmodium falciparum infection and disease. Nat Med 10, 406.

Reed, S. G., Orr, M. T., and Fox, C. B. (2013). Key roles of adjuvants in modern vaccines. Nat Med 19, 1597.

Rekart, M. L., Gilbert, M., Meza, R., Kim, P. H., Chang, M., Money, D. M., and Brunham, R. C. (2013). Chlamydia public health programs and the epidemiology of pelvic inflammatory disease and ectopic pregnancy. J Infect Dis 207, 30.

Rietschel, E. T., Kirikae, T., Schade, F. U., Mamat, U., Schmidt, G., Loppnow, H., Ulmer, A. J., Zahringer, U., Seydel, U., Di Padova, F., and et al. (1994). Bacterial

endotoxin: molecular relationships of structure to activity and function. FASEB J 8, 217.

Rietschel, E. T., Kirikae, T., Schade, F. U., Ulmer, A. J., Holst, O., Brade, H., Schmidt, G., Mamat, U., Grimmecke, H. D., Kusumoto, S., and et al. (1993). The chemical structure of bacterial endotoxin in relation to bioactivity. Immunobiology 187, 169.

Riha, J., Mercer, C. H., Soldan, K., French, C. E., and Macintosh, M. (2011). Who is being tested by the English National Chlamydia Screening Programme? A comparison with national probability survey data. Sex Transm Infect 87, 306.

Riley, S. P., Goh, K. C., Hermanas, T. M., Cardwell, M. M., Chan, Y. G., and Martinez, J. J. (2010). The Rickettsia conorii autotransporter protein Sca1 promotes adherence to nonphagocytic mammalian cells. Infect Immun 78, 1895.

Roan, N. R., Gierahn, T. M., Higgins, D. E., and Starnbach, M. N. (2006). Monitoring the T cell response to genital tract infection. Proc Natl Acad Sci U S A 103, 12069.

Rockey, D. D., Scidmore, M. A., Bannantine, J. P., and Brown, W. J. (2002). Proteins in the chlamydial inclusion membrane. Microbes Infect 4, 333.

Rodgers, A. K., Budrys, N. M., Gong, S., Wang, J., Holden, A., Schenken, R. S., and Zhong, G. (2011). Genome-wide identification of Chlamydia trachomatis antigens associated with tubal factor infertility. Fertil Steril 96, 715.

Rosenbusch, J. P. (1974). Characterization of the major envelope protein from Escherichia coli. Regular arrangement on the peptidoglycan and unusual dodecyl sulfate binding. J Biol Chem 249, 8019.

Roux, K. J., Kim, D. I., Raida, M., and Burke, B. (2012). A promiscuous biotin ligase fusion protein identifies proximal and interacting proteins in mammalian cells. J Cell Biol 196, 801.

Roy, A., Kucukural, A., and Zhang, Y. (2010). I-TASSER: a unified platform for automated protein structure and function prediction. Nat Protoc 5, 725.

Rubinstein, N. D., Mayrose, I., Halperin, D., Yekutieli, D., Gershoni, J. M., and Pupko, T. (2008). Computational characterization of B cell epitopes. Mol Immunol 45, 3477.

Rumke, H. C., Richardus, J. H., Rombo, L., Pauksens, K., Plassmann, G., Durand, C., Devaster, J. M., Dewe, W., and Oostvogels, L. (2013). Selection of an adjuvant for seasonal influenza vaccine in elderly people: modelling immunogenicity from a randomized trial. BMC Infect Dis 13, 348.

Russell, M. W., and Mestecky, J. (2002). Humoral immune responses to microbial infections in the genital tract. Microbes Infect 4, 667.

Russell, M. W., Moldoveanu, Z., White, P. L., Sibert, G. J., Mestecky, J., and Michalek, S. M. (1996). Salivary, nasal, genital, and systemic antibody responses in

monkeys immunized intranasally with a bacterial protein antigen and the Cholera toxin B subunit. Infect Immun 64, 1272.

Ryser, H. J., Levy, E. M., Mandel, R., and DiSciullo, G. J. (1994). Inhibition of human immunodeficiency virus infection by agents that interfere with thiol-disulfide interchange upon virus-receptor interaction. Proc Natl Acad Sci U S A 91, 4559.

Ryser, H. J., Mandel, R., and Ghani, F. (1991). Cell surface sulfhydryls are required for the cytotoxicity of diphtheria toxin but not of ricin in Chinese hamster ovary cells. J Biol Chem 266, 18439.

Saka, H. A., Thompson, J. W., Chen, Y. S., Kumar, Y., Dubois, L. G., Moseley, M. A., and Valdivia, R. H. (2011). Quantitative proteomics reveals metabolic and pathogenic properties of Chlamydia trachomatis developmental forms. Mol Microbiol 82, 1185.

Sargent, F., Bogsch, E. G., Stanley, N. R., Wexler, M., Robinson, C., Berks, B. C., and Palmer, T. (1998). Overlapping functions of components of a bacterial Sec-independent protein export pathway. EMBO J 17, 3640.

Saxena, M., Van, T. T., Baird, F. J., Coloe, P. J., and Smooker, P. M. (2013). Pre-existing immunity against vaccine vectors--friend or foe? Microbiology 159, 1.

Scarselli, M., Arico, B., Brunelli, B., Savino, S., Di Marcello, F., Palumbo, E., Veggi, D., Ciucchi, L., Cartocci, E., Bottomley, M. J., Malito, E., Lo Surdo, P., Comanducci, M., Giuliani, M. M., Cantini, F., Dragonetti, S., Colaprico, A., Doro, F., Giannetti, P., Pallaoro, M., Brogioni, B., Tontini, M., Hilleringmann, M., Nardi-Dei, V., Banci, L., Pizza, M., and Rappuoli, R. (2011). Rational design of a meningococcal antigen inducing broad protective immunity. Sci Transl Med 3, 91ra62.

Scarselli, M., Cantini, F., Santini, L., Veggi, D., Dragonetti, S., Donati, C., Savino, S., Giuliani, M. M., Comanducci, M., Di Marcello, F., Romagnoli, G., Pizza, M., Banci, L., and Rappuoli, R. (2009). Epitope mapping of a bactericidal monoclonal antibody against the factor H binding protein of Neisseria meningitidis. J Mol Biol 386, 97.

Schautteet, K., Stuyven, E., Cox, E., and Vanrompay, D. (2011). Validation of the Chlamydia trachomatis genital challenge pig model for testing recombinant protein vaccines. J Med Microbiol 60, 117.

Schiller, J. T., Day, P. M., and Kines, R. C. (2010). Current understanding of the mechanism of HPV infection. Gynecol Oncol 118, S12.

Schiller, J. T., and Lowy, D. R. (2012). Understanding and learning from the success of prophylactic human papillomavirus vaccines. Nat Rev Microbiol 10, 681.

Schletter, J., Heine, H., Ulmer, A. J., and Rietschel, E. T. (1995). Molecular mechanisms of endotoxin activity. Arch Microbiol 164, 383.

Schwarzenbacher, R., Stenner-Liewen, F., Liewen, H., Robinson, H., Yuan, H., Bossy-Wetzel, E., Reed, J. C., and Liddington, R. C. (2004). Structure of the

Chlamydia protein CADD reveals a redox enzyme that modulates host cell apoptosis. J Biol Chem 279, 29320.

Serruto, D., Bottomley, M. J., Ram, S., Giuliani, M. M., and Rappuoli, R. (2012). The new multicomponent vaccine against meningococcal serogroup B, 4CMenB: immunological, functional and structural characterization of the antigens. Vaccine 30 Suppl 2, B87.

Shah, A. A., Schripsema, J. H., Imtiaz, M. T., Sigar, I. M., Kasimos, J., Matos, P. G., Inouye, S., and Ramsey, K. H. (2005). Histopathologic changes related to fibrotic oviduct occlusion after genital tract infection of mice with Chlamydia muridarum. Sex Transm Dis 32, 49.

Shahid, Z., Kleppinger, A., Gentleman, B., Falsey, A. R., and McElhaney, J. E. (2010). Clinical and immunologic predictors of influenza illness among vaccinated older adults. Vaccine 28, 6145.

Singh, M., Kazzaz, J., Ugozzoli, M., Baudner, B., Pizza, M., Giuliani, M., Hawkins, L. D., Otten, G., and O'Hagan, D. T. (2012). MF59 oil-in-water emulsion in combination with a synthetic TLR4 agonist (E6020) is a potent adjuvant for a combination Meningococcus vaccine. Hum Vaccin Immunother 8, 486.

Skeiky, Y. A., Guderian, J. A., Benson, D. R., Bacelar, O., Carvalho, E. M., Kubin, M., Badaro, R., Trinchieri, G., and Reed, S. G. (1995). A recombinant Leishmania antigen that stimulates human peripheral blood mononuclear cells to express a Th1-type cytokine profile and to produce interleukin 12. J Exp Med 181, 1527.

Skeiky, Y. A., Kennedy, M., Kaufman, D., Borges, M. M., Guderian, J. A., Scholler, J. K., Ovendale, P. J., Picha, K. S., Morrissey, P. J., Grabstein, K. H., Campos-Neto, A., and Reed, S. G. (1998). LeIF: a recombinant Leishmania protein that induces an IL-12-mediated Th1 cytokine profile. J Immunol 161, 6171.

Skilton, R. J., Cutcliffen, L. T., Barlow, D., Wang, Y., Salim, O., Lambden, P. R., and Clarke, I. N. (2009). Penicillin induced persistence in Chlamydia trachomatis: high quality time lapse video analysis of the developmental cycle. PLoS One 4, e7723.

Snavely, E. A., Kokes, M., Dunn, J. D., Saka, H. A., Nguyen, B. D., Bastidas, R. J., McCafferty, D. G., and Valdivia, R. H. (2014). Reassessing the role of the secreted protease CPAF in Chlamydia trachomatis infection through genetic approaches. Pathog Dis 71, 336.

Somani, J., Bhullar, V. B., Workowski, K. A., Farshy, C. E., and Black, C. M. (2000). Multiple drug-resistant Chlamydia trachomatis associated with clinical treatment failure. J Infect Dis 181, 1421.

Somerville, J. E., Jr., Cassiano, L., Bainbridge, B., Cunningham, M. D., and Darveau, R. P. (1996). A novel Escherichia coli lipid A mutant that produces an antiinflammatory lipopolysaccharide. J Clin Invest 97, 359.

Stager, S., Alexander, J., Kirby, A. C., Botto, M., Rooijen, N. V., Smith, D. F., Brombacher, F., and Kaye, P. M. (2003). Natural antibodies and complement are endogenous adjuvants for vaccine-induced CD8$^+$ T-cell responses. Nat Med 9, 1287.

Stary, G., Olive, A., Radovic-Moreno, A. F., Gondek, D., Alvarez, D., Basto, P. A., Perro, M., Vrbanac, V. D., Tager, A. M., Shi, J., Yethon, J. A., Farokhzad, O. C., Langer, R., Starnbach, M. N., and von Andrian, U. H. (2015). VACCINES. A mucosal vaccine against Chlamydia trachomatis generates two waves of protective memory T cells. Science 348, aaa8205.

Steeghs, L., Keestra, A. M., van Mourik, A., Uronen-Hansson, H., van der Ley, P., Callard, R., Klein, N., and van Putten, J. P. (2008). Differential activation of human and mouse Toll-like receptor 4 by the adjuvant candidate LpxL1 of Neisseria meningitidis. Infect Immun 76, 3801.

Steeghs, L., Kuipers, B., Hamstra, H. J., Kersten, G., van Alphen, L., and van der Ley, P. (1999). Immunogenicity of outer membrane proteins in a lipopolysaccharide-deficient mutant of Neisseria meningitidis: influence of adjuvants on the immune response. Infect Immun 67, 4988.

Stenner-Liewen, F., Liewen, H., Zapata, J. M., Pawlowski, K., Godzik, A., and Reed, J. C. (2002). CADD, a Chlamydia protein that interacts with death receptors. J Biol Chem 277, 9633.

Stephens, R. S. (2003). The cellular paradigm of chlamydial pathogenesis. Trends Microbiol 11, 44.

Stephens, R. S., Kalman, S., Lammel, C., Fan, J., Marathe, R., Aravind, L., Mitchell, W., Olinger, L., Tatusov, R. L., Zhao, Q., Koonin, E. V., and Davis, R. W. (1998). Genome sequence of an obligate intracellular pathogen of humans: Chlamydia trachomatis. Science 282, 754.

Stephens, R. S., Wagar, E. A., and Schoolnik, G. K. (1988). High-resolution mapping of serovar-specific and common antigenic determinants of the major outer membrane protein of Chlamydia trachomatis. J Exp Med 167, 817.

Stephenson, K. (2005). Sec-dependent protein translocation across biological membranes: evolutionary conservation of an essential protein transport pathway (review). Mol Membr Biol 22, 17.

Storsaeter, J., Hallander, H. O., Gustafsson, L., and Olin, P. (1998). Levels of anti-pertussis antibodies related to protection after household exposure to Bordetella pertussis. Vaccine 16, 1907.

Stoute, J. A., Slaoui, M., Heppner, D. G., Momin, P., Kester, K. E., Desmons, P., Wellde, B. T., Garcon, N., Krzych, U., and Marchand, M. (1997). A preliminary evaluation of a recombinant circumsporozoite protein vaccine against Plasmodium falciparum malaria. RTS,S Malaria Vaccine Evaluation Group. N Engl J Med 336, 86.

Sturdevant, G. L., Kari, L., Gardner, D. J., Olivares-Zavaleta, N., Randall, L. B., Whitmire, W. M., Carlson, J. H., Goheen, M. M., Selleck, E. M., Martens, C., and Caldwell, H. D. (2010). Frameshift mutations in a single novel virulence factor alter the in vivo pathogenicity of Chlamydia trachomatis for the female murine genital tract. Infect Immun 78, 3660.

Su, H., and Caldwell, H. D. (1993). Immunogenicity of a synthetic oligopeptide corresponding to antigenically common T-helper and B cell neutralizing epitopes of the major outer membrane protein of Chlamydia trachomatis. Vaccine 11, 1159.

Su, H., and Caldwell, H. D. (1995). CD4$^+$ T cells play a significant role in adoptive immunity to Chlamydia trachomatis infection of the mouse genital tract. Infect Immun 63, 3302.

Su, H., Morrison, R., Messer, R., Whitmire, W., Hughes, S., and Caldwell, H. D. (1999). The effect of doxycycline treatment on the development of protective immunity in a murine model of chlamydial genital infection. J Infect Dis 180, 1252.

Su, H., Parnell, M., and Caldwell, H. D. (1995). Protective efficacy of a parenterally administered MOMP-derived synthetic oligopeptide vaccine in a murine model of Chlamydia trachomatis genital tract infection: serum neutralizing IgG antibodies do not protect against chlamydial genital tract infection. Vaccine 13, 1023.

Subtil, A., Parsot, C., and Dautry-Varsat, A. (2001). Secretion of predicted Inc proteins of Chlamydia pneumoniae by a heterologous type III machinery. Mol Microbiol 39, 792.

Suchland, R. J., Sandoz, K. M., Jeffrey, B. M., Stamm, W. E., and Rockey, D. D. (2009). Horizontal transfer of tetracycline resistance among Chlamydia spp. in vitro. Antimicrob Agents Chemother 53, 4604.

Sun, G., Pal, S., Sarcon, A. K., Kim, S., Sugawara, E., Nikaido, H., Cocco, M. J., Peterson, E. M., and de la Maza, L. M. (2007). Structural and functional analyses of the major outer membrane protein of Chlamydia trachomatis. J Bacteriol 189, 6222.

Supajatura, V., Ushio, H., Wada, A., Yahiro, K., Okumura, K., Ogawa, H., Hirayama, T., and Ra, C. (2002). Cutting edge: VacA, a vacuolating cytotoxin of Helicobacter pylori, directly activates mast cells for migration and production of proinflammatory cytokines. J Immunol 168, 2603.

Swanson, K. A., Taylor, L. D., Frank, S. D., Sturdevant, G. L., Fischer, E. R., Carlson, J. H., Whitmire, W. M., and Caldwell, H. D. (2009). Chlamydia trachomatis polymorphic membrane protein D is an oligomeric autotransporter with a higher-order structure. Infect Immun 77, 508.

Tamura, M., Nogimori, K., Yajima, M., Ase, K., and Ui, M. (1983). A role of the B-oligomer moiety of islet-activating protein, pertussis toxin, in development of the biological effects on intact cells. J Biol Chem 258, 6756.

Tan, C., Hsia, R. C., Shou, H., Carrasco, J. A., Rank, R. G., and Bavoil, P. M. (2010). Variable expression of surface-exposed polymorphic membrane proteins in in vitro-grown Chlamydia trachomatis. Cell Microbiol 12, 174.

Tan, C., Hsia, R. C., Shou, H., Haggerty, C. L., Ness, R. B., Gaydos, C. A., Dean, D., Scurlock, A. M., Wilson, D. P., and Bavoil, P. M. (2009). Chlamydia trachomatis-infected patients display variable antibody profiles against the nine-member polymorphic membrane protein family. Infect Immun 77, 3218.

Tan, T. W., Herring, A. J., Anderson, I. E., and Jones, G. E. (1990). Protection of sheep against Chlamydia psittaci infection with a subcellular vaccine containing the major outer membrane protein. Infect Immun 58, 3101.

Tanzer, R. J., Longbottom, D., and Hatch, T. P. (2001). Identification of polymorphic outer membrane proteins of Chlamydia psittaci 6BC. Infect Immun 69, 2428.

Taylor, H. R., Whittum-Hudson, J., Schachter, J., Caldwell, H. D., and Prendergast, R. A. (1988). Oral immunization with chlamydial major outer membrane protein (MOMP). Invest Ophthalmol Vis Sci 29, 1847.

Thanassi, D. G., and Hultgren, S. J. (2000). Multiple pathways allow protein secretion across the bacterial outer membrane. Curr Opin Cell Biol 12, 420.

Theunissen, J. J., van Heijst, B. Y., Wagenvoort, J. H., Stolz, E., and Michel, M. F. (1992). Factors influencing the infectivity of Chlamydia pneumoniae elementary bodies on HL cells. J Clin Microbiol 30, 1388.

Thomson, N. R., Holden, M. T., Carder, C., Lennard, N., Lockey, S. J., Marsh, P., Skipp, P., O'Connor, C. D., Goodhead, I., Norbertzcak, H., Harris, B., Ormond, D., Rance, R., Quail, M. A., Parkhill, J., Stephens, R. S., and Clarke, I. N. (2008). Chlamydia trachomatis: genome sequence analysis of lymphogranuloma venereum isolates. Genome Res 18, 161.

Tuffrey, M., Alexander, F., Conlan, W., Woods, C., and Ward, M. (1992). Heterotypic protection of mice against chlamydial salpingitis and colonization of the lower genital tract with a human serovar F isolate of Chlamydia trachomatis by prior immunization with recombinant serovar L1 major outer-membrane protein. J Gen Microbiol 138 Pt 8, 1707.

Tuffrey, M., Falder, P., and Taylor-Robinson, D. (1982). Genital-tract infection and disease in nude and immunologically competent mice after inoculation of a human strain of Chlamydia trachomatis. Br J Exp Pathol 63, 539.

Ueno, H., Klechevsky, E., Schmitt, N., Ni, L., Flamar, A. L., Zurawski, S., Zurawski, G., Palucka, K., Banchereau, J., and Oh, S. (2011). Targeting human dendritic cell subsets for improved vaccines. Semin Immunol 23, 21.

Ulrich, J. T., and Myers, K. R. (1995). Monophosphoryl lipid A as an adjuvant. Past experiences and new directions. Pharm Biotechnol 6, 495.

van den Berg, B. M., Beekhuizen, H., Willems, R. J., Mooi, F. R., and van Furth, R. (1999). Role of Bordetella pertussis virulence factors in adherence to epithelial cell lines derived from the human respiratory tract. Infect Immun 67, 1056.

van der Ley, P., Steeghs, L., Hamstra, H. J., ten Hove, J., Zomer, B., and van Alphen, L. (2001). Modification of lipid A biosynthesis in Neisseria meningitidis lpxL mutants: influence on lipopolysaccharide structure, toxicity, and adjuvant activity. Infect Immun 69, 5981.

van Dissel, J. T., Arend, S. M., Prins, C., Bang, P., Tingskov, P. N., Lingnau, K., Nouta, J., Klein, M. R., Rosenkrands, I., Ottenhoff, T. H., Kromann, I., Doherty, T. M., and Andersen, P. (2010). Ag85B-ESAT-6 adjuvanted with IC31 promotes strong and long-lived Mycobacterium tuberculosis specific T cell responses in naive human volunteers. Vaccine 28, 3571.

van Ginkel, F. W., Jackson, R. J., Yuki, Y., and McGhee, J. R. (2000). Cutting edge: the mucosal adjuvant cholera toxin redirects vaccine proteins into olfactory tissues. J Immunol 165, 4778.

van Heijenoort, J. (2001). Recent advances in the formation of the bacterial peptidoglycan monomer unit. Nat Prod Rep 18, 503.

Van Voorhis, W. C., Barrett, L. K., Sweeney, Y. T., Kuo, C. C., and Patton, D. L. (1997). Repeated Chlamydia trachomatis infection of Macaca nemestrina fallopian tubes produces a Th1-like cytokine response associated with fibrosis and scarring. Infect Immun 65, 2175.

Vandahl, B. B., Pedersen, A. S., Gevaert, K., Holm, A., Vandekerckhove, J., Christiansen, G., and Birkelund, S. (2002). The expression, processing and localization of polymorphic membrane proteins in Chlamydia pneumoniae strain CWL029. BMC Microbiol 2, 36.

Vanrompay, D., Hoang, T. Q., De Vos, L., Verminnen, K., Harkinezhad, T., Chiers, K., Morre, S. A., and Cox, E. (2005). Specific-pathogen-free pigs as an animal model for studying Chlamydia trachomatis genital infection. Infect Immun 73, 8317.

Vanrompay, D., Lyons, J. M., and Morre, S. A. (2006). Animal models for the study of Chlamydia trachomatis infections in the female genital infection. Drugs Today (Barc) 42 Suppl A, 55.

Villeneuve, A., Brossay, L., Paradis, G., and Hebert, J. (1994). Determination of neutralizing epitopes in variable domains I and IV of the major outer-membrane protein from Chlamydia trachomatis serovar K. Microbiology 140 (Pt 9), 2481.

Visser, L. G., Annema, A., and van Furth, R. (1995). Role of Yops in inhibition of phagocytosis and killing of opsonized Yersinia enterocolitica by human granulocytes. Infect Immun 63, 2570.

Voigt, A., Schofl, G., and Saluz, H. P. (2012). The Chlamydia psittaci genome: a comparative analysis of intracellular pathogens. PLoS One 7, e35097.

von Andrian, U. H., and Mackay, C. R. (2000). T-cell function and migration. Two sides of the same coin. N Engl J Med 343, 1020.

Vordermeier, H. M., Dean, G. S., Rosenkrands, I., Agger, E. M., Andersen, P., Kaveh, D. A., Hewinson, R. G., and Hogarth, P. J. (2009). Adjuvants induce distinct immunological phenotypes in a bovine tuberculosis vaccine model. Clin Vaccine Immunol 16, 1443.

Wang, S., Fan, Y., Brunham, R. C., and Yang, X. (1999). IFN-gamma knockout mice show Th2-associated delayed-type hypersensitivity and the inflammatory cells fail to localize and control chlamydial infection. Eur J Immunol 29, 3782.

Wang, S. P., Grayston, J. T., and Alexander, E. R. (1967). Trachoma vaccine studies in monkeys. Am J Ophthalmol 63, Suppl:1615.

Wang, Y., Kahane, S., Cutcliffe, L. T., Skilton, R. J., Lambden, P. R., and Clarke, I. N. (2011). Development of a transformation system for Chlamydia trachomatis: restoration of glycogen biosynthesis by acquisition of a plasmid shuttle vector. PLoS Pathog 7, e1002258.

Watanabe, N., Clay, M. D., van Belkum, M. J., Fan, C., Vederas, J. C., and James, M. N. (2011). The structure of LL-diaminopimelate aminotransferase from Chlamydia trachomatis: implications for its broad substrate specificity. J Mol Biol 411, 649.

Wehrl, W., Brinkmann, V., Jungblut, P. R., Meyer, T. F., and Szczepek, A. J. (2004). From the inside out--processing of the Chlamydial autotransporter PmpD and its role in bacterial adhesion and activation of human host cells. Mol Microbiol 51, 319.

Wells, T. J., Tree, J. J., Ulett, G. C., and Schembri, M. A. (2007). Autotransporter proteins: novel targets at the bacterial cell surface. FEMS Microbiol Lett 274, 163.

Wetten, S., Mohammed, H., Yung, M., Mercer, C. H., Cassell, J. A., and Hughes, G. (2015). Diagnosis and treatment of chlamydia and gonorrhoea in general practice in England 2000-2011: a population-based study using data from the UK Clinical Practice Research Datalink. BMJ Open 5, e007776.

Wheelhouse, N., Aitchison, K., Laroucau, K., Thomson, J., and Longbottom, D. (2010). Evidence of Chlamydophila abortus vaccine strain 1B as a possible cause of ovine enzootic abortion. Vaccine 28, 5657.

Wheelhouse, N. M., Sait, M., Aitchison, K., Livingstone, M., Wright, F., McLean, K., Inglis, N. F., Smith, D. G., and Longbottom, D. (2012). Processing of Chlamydia abortus polymorphic membrane protein 18D during the chlamydial developmental cycle. PLoS One 7, e49190.

Wijnans, L., Lecomte, C., de Vries, C., Weibel, D., Sammon, C., Hviid, A., Svanstrom, H., Molgaard-Nielsen, D., Heijbel, H., Dahlstrom, L. A., Hallgren, J., Sparen, P.,

Jennum, P., Mosseveld, M., Schuemie, M., van der Maas, N., Partinen, M., Romio, S., Trotta, F., Santuccio, C., Menna, A., Plazzi, G., Moghadam, K. K., Ferro, S., Lammers, G. J., Overeem, S., Johansen, K., Kramarz, P., Bonhoeffer, J., and Sturkenboom, M. C. (2013). The incidence of narcolepsy in Europe: before, during, and after the influenza A(H1N1)pdm09 pandemic and vaccination campaigns. Vaccine 31, 1246.

Wiley, S. R., Raman, V. S., Desbien, A., Bailor, H. R., Bhardwaj, R., Shakri, A. R., Reed, S. G., Chitnis, C. E., and Carter, D. (2011). Targeting TLRs expands the antibody repertoire in response to a malaria vaccine. Sci Transl Med 3, 93ra69.

Willhite, D. C., and Blanke, S. R. (2004). Helicobacter pylori vacuolating cytotoxin enters cells, localizes to the mitochondria, and induces mitochondrial membrane permeability changes correlated to toxin channel activity. Cell Microbiol 6, 143.

Wolf, K., Betts, H. J., Chellas-Gery, B., Hower, S., Linton, C. N., and Fields, K. A. (2006). Treatment of Chlamydia trachomatis with a small molecule inhibitor of the Yersinia type III secretion system disrupts progression of the chlamydial developmental cycle. Mol Microbiol 61, 1543.

Woolridge, R. L., Grayston, J. T., Chang, I. H., Yang, C. Y., and Cheng, K. H. (1967). Long-term follow-up of the initial (1959-1960) trachoma vaccine field trial on Taiwan. Am J Ophthalmol 63, Suppl:1650.

Wotherspoon, A. C., Ortiz-Hidalgo, C., Falzon, M. R., and Isaacson, P. G. (1991). Helicobacter pylori-associated gastritis and primary B cell gastric lymphoma. Lancet 338, 1175.

Wu, X., Yang, Z. Y., Li, Y., Hogerkorp, C. M., Schief, W. R., Seaman, M. S., Zhou, T., Schmidt, S. D., Wu, L., Xu, L., Longo, N. S., McKee, K., O'Dell, S., Louder, M. K., Wycuff, D. L., Feng, Y., Nason, M., Doria-Rose, N., Connors, M., Kwong, P. D., Roederer, M., Wyatt, R. T., Nabel, G. J., and Mascola, J. R. (2010). Rational design of envelope identifies broadly neutralizing human monoclonal antibodies to HIV-1. Science 329, 856.

Wuppermann, F. N., Hegemann, J. H., and Jantos, C. A. (2001). Heparan sulfate-like glycosaminoglycan is a cellular receptor for Chlamydia pneumoniae. J Infect Dis 184, 181.

Wyllie, S., and Raulston, J. E. (2001). Identifying regulators of transcription in an obligate intracellular pathogen: a metal-dependent repressor in Chlamydia trachomatis. Mol Microbiol 40, 1027.

Yang, X., Gartner, J., Zhu, L., Wang, S., and Brunham, R. C. (1999). IL-10 gene knockout mice show enhanced Th1-like protective immunity and absent granuloma formation following Chlamydia trachomatis lung infection. J Immunol 162, 1010.

Yang, X., HayGlass, K. T., and Brunham, R. C. (1996). Genetically determined differences in IL-10 and IFN-gamma responses correlate with clearance of Chlamydia trachomatis mouse pneumonitis infection. J Immunol 156, 4338.

Yeaman, G. R., Guyre, P. M., Fanger, M. W., Collins, J. E., White, H. D., Rathbun, W., Orndorff, K. A., Gonzalez, J., Stern, J. E., and Wira, C. R. (1997). Unique CD8$^+$ T cell-rich lymphoid aggregates in human uterine endometrium. J Leukoc Biol 61, 427.

Yen, T. Y., Pal, S., and de la Maza, L. M. (2005). Characterization of the disulfide bonds and free cysteine residues of the Chlamydia trachomatis mouse pneumonitis major outer membrane protein. Biochemistry 44, 6250.

Yi, Y., Yang, X., and Brunham, R. C. (1997). Autoimmunity to heat shock protein 60 and antigen-specific production of interleukin-10. Infect Immun 65, 1669.

Yu, H., Jiang, X., Shen, C., Karunakaran, K. P., Jiang, J., Rosin, N. L., and Brunham, R. C. (2010). Chlamydia muridarum T-cell antigens formulated with the adjuvant DDA/TDB induce immunity against infection that correlates with a high frequency of gamma interferon (IFN-gamma)/tumor necrosis factor alpha and IFN-gamma/interleukin-17 double-positive CD4$^+$ T cells. Infect Immun 78, 2272.

Yu, H., Karunakaran, K. P., Jiang, X., and Brunham, R. C. (2014). Evaluation of a multisubunit recombinant polymorphic membrane protein and major outer membrane protein T cell vaccine against Chlamydia muridarum genital infection in three strains of mice. Vaccine 32, 4672.

Yu, H., Karunakaran, K. P., Kelly, I., Shen, C., Jiang, X., Foster, L. J., and Brunham, R. C. (2011). Immunization with live and dead Chlamydia muridarum induces different levels of protective immunity in a murine genital tract model: correlation with MHC class II peptide presentation and multifunctional Th1 cells. J Immunol 186, 3615.

Zeng, H., Gong, S., Hou, S., Zou, Q., and Zhong, G. (2012). Identification of antigen-specific antibody responses associated with upper genital tract pathology in mice infected with Chlamydia muridarum. Infect Immun 80, 1098.

Zhi, N., Ohashi, N., and Rikihisa, Y. (1999). Multiple p44 genes encoding major outer membrane proteins are expressed in the human granulocytic ehrlichiosis agent. J Biol Chem 274, 17828.

Zhou, X., and McElhaney, J. E. (2011). Age-related changes in memory and effector T cells responding to influenza A/H3N2 and pandemic A/H1N1 strains in humans. Vaccine 29, 2169.